



INTERNATIONAL DOCTORAL SCHOOL OF THE  
USC

María  
Díaz Urbano

PhD Thesis

ENDOPHYTIC FUNGI AS NATURAL  
AGENTS FOR ENHANCING  
AGRICULTURAL RESILIENCE IN  
GALICIA

Lugo, 2025





ESCOLA DE DOUTORAMENTO  
INTERNACIONAL DA USC

## DOCTORAL THESIS

### **ENDOPHYTIC FUNGI AS NATURAL AGENTS FOR ENHANCING AGRICULTURAL RESILIENCE IN GALICIA**

María Díaz Urbano

Supervisor/s: Víctor Manuel Rodríguez Graña and Pablo Velasco Pazos

Tutor: Cristina Cabaleiro Sobrino

**PHD PROGRAMME IN AGRICULTURAL AND FORESTRY RESEARCH**



LUGO 2025



El doctorando declara no tener ningún conflicto de interés en relación con la tesis doctoral.

A mi madre, mi padre y mi hermana,  
que siempre estuvieron ahí.

Gracias.

Sin vosotros, hubiese sido impensable.



## AGRADECIMIENTOS

En primer lugar, me gustaría dar las gracias a mis directores de tesis, Pablo Velasco Pazos y Víctor Manuel Rodríguez Graña, por haberme dado el espacio y la oportunidad de realizar este trabajo. Por todas las horas invertidas en hacerme pensar, por escucharme, por valorar mi opinión y por discutir conmigo. Por los pinchos de tortilla de los viernes. Porque siempre fuisteis compasivos y humanos antes que jefes.

Debo destacar las infinitas horas frente al ordenador discutiendo con Víctor sobre algún texto que podía mejorar, una figura o cualquier experimento. Gracias por haberme enseñado tanto; sin ti no habría podido (ni querido) transitar esta etapa.

Y a Pablo, por pensar siempre en lo mejor para mi futuro: por preocuparse de dónde iba a hacer mi estancia, de dónde dormiría en Estados Unidos o por ser un foco de buen rollo y debates irresolubles. Por incluirme en cada nuevo proyecto que surgía. Lástima que la levadura negra no nos sacara de pobres.

También quiero agradecer a Jorge Poveda, por su constante disponibilidad, sus ideas siempre oportunas y sus protocolos para casi todo, así como por su incansable dedicación como científico. Del mismo modo, agradezco a Iñigo Zabalgogezcoa su ayuda, su claridad para resolver dudas y su disponibilidad siempre que la necesité.

Debo hacer especial mención a todas las personas que hicieron posible que mi tesis fuese viable a nivel económico. Su apoyo fue esencial para que este proyecto pudiera llevarse a cabo. En particular, quiero agradecer a M<sup>a</sup> Elena Cartea y Pilar Soengas, cuya confianza hizo posible que pudiera terminar la tesis. Gracias por creer en este proyecto y por apoyarme en cada etapa.

Además, sin muchas otras personas este trabajo no habría sido posible. A Rosaura, por su incansable esfuerzo y por llevar sobre sus hombros toda la memoria experimental de los últimos veinte años. Por enseñarme trucos, a organizarme y por ser la persona a la que todos acudimos cuando no sabemos cómo proceder.

Y a quienes me salvaron tantas veces entre plantas y hongos:

a Donata, por ayudarme con el procesamiento de mil y una raíces y experimentos de sequía;

a Chiara, por poner todo su empeño y cariño en que los ensayos de antibiosis salieran bien;

a Gresheen, por echar una mano siempre que pudo;

y a Diego y Ainhoa, por ayudarme incansablemente con los experimentos de sequía.

Sin vuestro trabajo, aún estaría contando hojas.

Tampoco puedo olvidar a todos los agricultores que me permitieron acceder a sus fincas, por su hospitalidad, su paciencia y por confiar en que sus cultivos formasen parte de este trabajo. Del

mismo modo, agradezco a todas las personas de campo que me acompañaron en los muestreos y contribuyeron a mantener mis experimentos con vida.

Agradezco también al resto de mis compañeros de grupo:

a Taciana, siempre tan observadora y resolutiva;

a Juan Carlos, fiel vigilante de todas nuestras plantas;

a Marta, por amenizar los ratos de café;

a Luis, cuyos locos consejos casi me llevan al infarto, pero que tantas comidas y tardes me ha alegrado junto con Lina, siempre atenta a nuestro bienestar y fuente de infinitas charlas;

a Carmen y Ángela, por tener siempre una palabra amable, por preocuparse y por todas las tardes y noches compartidas.

Y, por supuesto, a Sonia, sin quien no habría llegado hasta aquí. Por ser compañera de aventuras y de penas, por haberse convertido en parte de mi día a día, porque ya no concibo pasar una semana sin hablar contigo y porque espero que sigas siendo soporte y amiga durante muchos años más.

A Lucía, que me acogió como una hermana, con quien he recorrido festivales y los rincones más insospechados de Galicia y Yucatán. Por todas esas excursiones a pie, en bus o en furgó. Por contar siempre conmigo y por ser referente, junto con Fani y Carla.

Y a Héctor, que llegó a tu vida y, por extensión, a la mía. Por ser fuente de debate y diversión.

A Gemma, por ser la voz de la razón, por pensar a lo grande y por estar siempre ahí. No sé qué sería de mí sin la aliada perfecta.

A mis compis de piso, Antía, Saúl, Víctor y Lucía, porque lo que une la precariedad y las cañas no lo separe un casero. Gracias por vuestra paciencia y cariño.

A mis amigos de siempre, Nina, Manu, Pili y Leire, por acogerme, por estar ahí, por permitirme volver como si no pasase el tiempo y por cuidar vínculos que son indispensables para mí.

A mi familia, porque sin ellos estaría perdida. Gracias a vuestro infinito esfuerzo, dedicación, cariño y apoyo estoy aquí. Por entenderme, por respetar mis decisiones y por acompañarme en todo momento. Por restaurarme cada vez que vuelvo a casa, por recordarme que con vosotros siempre tendré un hogar al que regresar y porque sé que vendrías a la otra punta del mundo a visitarme si fuera necesario. Sin vosotros, nada de esto habría sido posible.

Y, por último, a Edo, por ver siempre más allá.

Por sostenerme, cuidarme, escucharme y quererme.

## INDEX OF CONTENT

RESUMEN.....	1
RESUMO .....	10
SUMMARY .....	19
INTRODUCTION.....	27
1.MICROBIAL SYMBIOSIS IN PLANTS.....	28
1.1.Plant–microbiome interactions: a dynamic continuum.....	30
1.2.Compatibility Mechanisms and Specialization .....	30
1.3.Lifestyle Plasticity and Host Specificity .....	31
2.EVOLUTION OF FUNGAL TAXONOMY: FROM MORPHOLOGICAL APPROACHES TO INTEGRATIVE SYSTEMATICS.....	32
2.1.Classification of endophytic fungi: phylogeny .....	36
2.2.Classification of endophytic fungi: Ecological perspective.....	37
2.3.Taxonomic evolution of the genus <i>Pseudopyrenochaeta</i> .....	39
2.4. <i>Pseudopyrenochaeta</i> and its interaction with plants: From pathogenesis to endophytic plasticity .....	40
3.FUNGAL SECONDARY METABOLITES AND METABOLOMICS: FROM CHEMICAL DIVERSITY TO BIOTECHNOLOGICAL POTENTIAL .....	42
4.FUNGAL ENDOPHYTES IN THE MODULATION OF PLANT STRESS TOLERANCE .....	43
4.1.Fungal endophytes and pathogen control.....	45
4.2.Fungal endophytes and abiotic stress.....	47
5.AGRICULTURE CONTEXT .....	50
5.1. <i>Brassica rapa</i> : origin, diversity and agricultural relevance .....	50
5.2. <i>Capsicum annuum</i> : origin, diversity and agricultural relevance.....	51
5.3. <i>Current knowledge of root-associated endophytes in B. rapa and C. annuum</i> ....	53
HYPOTHESIS AND OBJECTIVES .....	55
GENERAL METHODOLOGY .....	55
1.ESTABLISHMENT OF THE ENDOPHYTIC FUNGI COLLECTION .....	56
1.1.Sampling, isolation and identification of culturable endophytic fungi .....	56
1.2.Analysis of the fungal diversity .....	57
2.FUNGAL ENDOPHYTE EVALUATION AGAINST ABIOTIC STRESS.....	58
2.1.Drought stress testing: <i>in planta</i> evaluation.....	58
2.1.1.Plant material and growth conditions .....	58
2.1.2.Physiological measurements.....	60
2.1.3.Statistical analysis.....	60

2.2.Drought stress testing: <i>In vitro</i> evaluation .....	61
2.2.1.Solid media assays with PEG 8000 .....	62
2.2.2.Liquid media assays with PEG 8000 .....	62
2.2.3.Culture on cellophane membranes with PEG 8000.....	62
2.2.4.PDA with increased agar concentration .....	63
3.FUNGAL ENDOPHYTE EVALUATION AGAINST BIOTIC STRESS.....	63
3.1. <i>In vitro</i> evaluation of antifungal activity.....	63
3.2. <i>In planta</i> evaluation of antifungal activity.....	64
3.2.1.Plant material.....	64
3.2.2.Endophytic fungi inoculation .....	64
3.2.3.Pathogen inoculation .....	65
3.2.4.Endophyte colonization.....	65
3.2.5.Experimental design for <i>in planta</i> assays.....	65
3.2.6.Infection evaluation and statistical analysis .....	66
3.2.7.Plant growth evaluation.....	66
4.FUNCTIONAL AND METABOLOMIC CHARACTERIZATION OF <i>PSEUDOPYRENOCHAETA</i> ISOLATES WITH ANTIFUNGAL ACTIVITY .....	66
4.1.Molecular identification of selected fungal isolates.....	66
4.2. <i>In vitro</i> evaluation of selected endophytes with antifungal activity.....	67
4.2.1.Dual-culture assays.....	67
4.2.2.Extract-based inhibition assays (disc diffusion method).....	68
4.2.3.Medium effect on antifungal activity .....	68
4.3.Untargeted metabolomic analysis and compound identification .....	68
4.3.1.Sample Preparation and chromatography.....	69
4.3.2.Mass Spectrometry Acquisition.....	70
4.3.3.Data Processing and Quality Control .....	70
4.3.4.Statistical Analysis .....	70
4.3.5.Tentative Metabolite Identification .....	71
4.3.6.Molecular Formula Assignment and Feature Curation .....	71
RESULTS AND DISCUSSION .....	71
1.TAXONOMIC CHARACTERIZATION OF ENDOPHYTIC FUNGI IN <i>Brassica rapa</i> AND <i>Capsicum annuum</i> .....	72
1.1.Comparative analysis of fungal community composition.....	73
1.2.Diversity patterns and community analysis .....	75
1.3.Ecological Drivers of Community Structure.....	76
2.FUNGAL ENDOPHYTE EVALUATION AGAINST ABIOTIC STRESS.....	77

2.1. <i>In planta</i> results.....	77
2.1.1. Relative water content (RWC) .....	77
2.2. <i>In vitro</i> results.....	81
3. FUNGAL ENDOPHYTE EVALUATION AGAINST BIOTIC STRESS.....	88
3.1. <i>In vitro</i> antagonistic activity against <i>Rhizoctonia solani</i> .....	88
3.2. <i>In planta</i> evaluation of antifungal activity .....	92
3.3. Effect of endophytic fungi on plant growth and physiology.....	93
4. FUNCTIONAL AND METABOLOMIC CHARACTERIZATION OF <i>PSEUDOPYRENOCHAETA</i> ISOLATES WITH ANTIFUNGAL ACTIVITY .....	95
4.1. Molecular identification of fungal isolates.....	95
4.2. <i>In vitro</i> evaluation of antifungal activity.....	96
4.2.1. Dual-culture assays.....	96
4.2.2. Extract-based inhibition assays (disc diffusion method).....	97
4.2.3. Medium effect on antifungal activity .....	99
4.3. Untargeted metabolomic analysis and compound identification .....	101
4.3.1. Tentative identification and annotation.....	103
4.3.1.1. <i>Group 1: Features 1 y 2 – Tentative annotation and fragmentation analysis</i> .....	105
4.3.1.2. <i>Group 2: Features 3, 4 y 5. Tentative annotation and fragmentation analysis</i> .....	107
4.3.1.3. <i>Group 3: Features 6 y 7 (m/z , RT min) – Tentative annotation and fragmentation analysis</i> .....	111
4.3.1.4. <i>Feature 8 (m/z 565.1703, RT 24.08 min) – Tentative annotation and fragmentation analysis</i> .....	116
4.3.1.5. <i>Feature 9 (m/z 365.067, RT 20.27 min) – Tentative annotation and fragmentation analysis</i> .....	119
GENERAL CONCLUSIONS .....	123
FUTURE PERSPECTIVES .....	124
REFERENCES.....	126
APPENDIX .....	141

## **FIGURE INDEX**

- Figure 1:** Macroscopic characteristics of endophytic colonies isolated in this study. Variations in texture, topography, pigmentation, exudate production, colony shape, and margin type are observable..... 33
- Figure 2:** Schematic representation of gene segment of eukaryotic rDNA contains 18S (small subunit rDNA gene), 5.8S, and 28S (Large subunit rDNA gene). ITS, internal transcribed spacers 1 and 2..... 35
- Figure 3:** Sampling site locations. The plots where *B. rapa* samples were collected are shown within the white rectangle (1B, 2B, 3B, 4B, 5B, and 6B), while the sampling sites for *C. annuum* are indicated within the yellow rectangle (1P, 2P, 3P, and 4P). ..... 56
- Figure 4:** Two-week-old *Arabidopsis thaliana* plants being inoculated with endophytic fungal suspensions. Inoculation was performed by submerging the roots into reservoirs containing the fungal solution, allowing direct contact between the root system and the inoculum..... 59
- Figure 5:** Schematic representation of the spatial arrangement of pots within a shelving unit, following a randomized block design. The diagram illustrates a simplified subset of eight treatments plus the control. Each colour corresponds to a different fungal inoculation treatment, while white represents the non-inoculated control. Each pot contained three *Arabidopsis thaliana* plants. .... 60
- Figure 6:** Taxonomic distribution of endophytic fungi isolated from *C. annuum* (A) and *B. rapa* (B). Percentages indicate the proportion of distinct genera within each order. The outer ring represents: Ascomycota (blue), Mucoromycota (orange), Basidiomycota (green), and Oomycota (purple). ..... 73
- Figure 7:** Total number of endophytic fungi isolated from *C. annuum* and *B. rapa* across the different sampling spots (1–6)..... 74
- Figure 8:** Representation of the proportion of identified fungal genera and orders isolated from each sampling event in *B. rapa* and *C. annuum*. Only taxonomically identified isolates are shown. .... 74
- Figure 9:** Rarefaction curves of endophytic fungal isolates from *C. annuum* (red) and *B. rapa* (blue). ..... 75
- Figure 10:** Relative water content (RWC) in *A. thaliana* inoculated with endophytic fungi under drought stress. Only the 18 treatments that showed significant differences from the uninoculated control ( $p < 0.05$ ; ANOVA) are displayed, with data normalized and arcsine-transformed. Bars show mean RWC per treatment, ranked from highest to lowest. The horizontal line indicates the mean control value (1), blue shading represents the control's standard error. Error bars show standard error per treatment..... 78
- Figure 11:** Fresh (black bars) and dry (white bars) biomass of *A. thaliana* inoculated with endophytic fungi under drought stress. Only the 14 treatments with significant differences from the control ( $p < 0.05$ ; ANOVA) are shown. Bars represent the normalized mean biomass per treatment, ranked by fresh weight. The horizontal line marks the mean

control value (normalized to 1), blue shading indicates control standard error. Error bars indicate standard error for each treatment. .... 79

**Figure 12:** Average growth of the endophytic fungi Bo441, Bo690, Bo890 and Bo421 at three time points ( $t_1$ : light gray,  $t_2$ : dark gray, and  $t_3$ : black) and under three PEG concentrations (0, 400, and 550 g/L). Asterisks indicate statistically significant differences compared to the control (0g/L). .... 82

**Figure 13:** Left: Eight membranes containing fungal hyphae retained after filtration of cultures grown under different PEG concentrations. The top four membranes correspond to *Trichoderma* isolate, while the bottom four correspond to *Fusarium*. Right: Three tubes showing the formation of compact spherical aggregates by different fungal isolates grown in liquid media supplemented with PEG. .... 83

**Figure 14:** The first row shows cellophane membranes on a black background, each corresponding to one of three replicates of the same fungal isolate. In the first two replicates, growth appears homogeneous and circular, whereas in the third, the fungus exhibits irregular development. The second row displays three different fungal isolates growing on cellophane membranes. .... 84

**Figure 15:** Growth area of endophytic fungi on control medium (100% agar; black bars) and drought-simulating medium (125% agar; white bars), based on three replicate plates per isolate. Asterisks indicate statistically significant differences ( $P < 0.05$ ). Error bars represent standard error. .... 86

**Figure 16:** Infographic illustrating the challenges associated with in vitro drought stress testing..... 87

**Figure 17:** Dual culture assays on PDA plates showing antagonistic interactions between endophytic fungi isolated from *B. rapa* and phytopathogens. The top row shows individual growth of endophytic fungi, the left column displays individual growth of phytopathogens, and the central panel shows dual confrontations between each pathogen and endophyte 15 days after inoculation. .... 88

**Figure 18:** Dual culture assays on PDA plates showing antagonistic interactions between endophytic fungi isolated from *C. annuum* and phytopathogens. The top row shows individual growth of endophytic fungi, the left column displays individual growth of phytopathogens, and the central panel shows dual confrontations between each pathogen and endophyte 15 days after inoculation. .... 89

**Figure 19:** Summary of antibiosis effect represented by the mean percentage of inhibition for all pathogens (left y-axis, shown as white bars). The right y-axis (black bars) shows the mean inhibition halo radius in centimeters, averaged across all pathogens. The x-axis displays the different endophytic isolates selected. Error bars represent the standard error. .... 90

**Figure 20:** Boxplots representing the lesion area caused by *S. sclerotiorum* in plants pre-inoculated with endophytic fungi (BrT4.01, P20.11, P23.03) or with PBS 1× (control; CTRL). Panels A and C correspond to *C. annuum*, and panels B and D to *B. rapa*. Panels A and B show results from the first experiment, while panels C and D present data from

the second experiment. Statistically significant differences ( $p < 0.05$ ) are indicated with an asterisk. .... 93

**Figure 21:** Bar chart showing the fresh weight of plants inoculated with different endophytic fungi (BrT4.01, P20.11, P23.03) or with PBS 1× (control; CTRL). Error bars represent the standard error. Panels A and C correspond to *C. annuum* plants, and panels B and D to *B. rapa* plants. Panels A and B show data from the first experiment, while panels C and D show data from the second experiment. Statistically significant differences ( $p < 0.05$ ) are indicated with an asterisk. .... 94

**Figure 22:** Agarose gel electrophoresis showing PCR amplification of fungal isolates P20.08, P23.10, P23.03, P22.09, P27.24, P24.08, P27.06, and P30.06 using species-specific primers Plyc1-F/R (lane 1) and Plyc2-F/R (lane 2). Isolates were classified as *P. terrestris* or *P. lycopersici* based on the presence of a ~147 bp band in lane 1 or a 209 bp band in lane 2, respectively. A 100 bp DNA ladder (Thermo Fisher Scientific) was included as a molecular size reference. The final lane shows the negative controls..... 95

**Figure 23:** Representative replicate of dual-culture assays between *Pseudopyrenochaeta* isolates and *R. solani* on PDA Sigma-Aldrich medium (St. Louis, MO, USA), 15 days post-inoculation (dpi). Each plate shows the antagonist inoculated at the center and *R. solani* as four plugs arranged in a square. .... 97

**Figure 24:** Disc diffusion assays assessing the effect of species identity on antifungal activity against *R. solani*. Each PDA Sigma-Aldrich (St. Louis, MO, USA) plate was inoculated with *R. solani* at the center and surrounded by eight cotton discs containing fungal culture extracts. (A) *R. solani* without extracts; (B) extracts from *P. terrestris* (1) and *P. lycopersici* (2) grown on PDA Sigma-Aldrich (St. Louis, MO, USA). Unnumbered discs are negative controls. .... 98

**Figure 25:** Comparative growth of *P. terrestris* and *R. solani* on PDA prepared with the two commercial media. The top row shows plates containing PDA from Dinkelberg Analytics (Budapest, Hungary), while the bottom row corresponds to PDA from Sigma-Aldrich (St. Louis, MO, USA). Within each row: column 1 shows dual-culture assays, column 2 shows *P. terrestris* in monoculture, and column 3 shows *R. solani* alone. The images highlight how fungal morphology and inhibitory capacity vary depending on the culture medium, after six weeks of incubation. .... 99

**Figure 26:** Disc diffusion assays evaluating the effect of culture medium on antifungal activity against *R. solani*, after four weeks of incubation. Each PDA Sigma-Aldrich (St. Louis, MO, USA) plate was inoculated with *R. solani* at the center and surrounded by eight cotton discs containing *P. terrestris* fungal extracts: (A) extracts from isolates grown on PDA Dinkelberg Analytics (Budapest, Hungary); (B) extracts from the same isolates grown on PDA Sigma-Aldrich (St. Louis, MO, USA). Numbers correspond to isolates: 1 = P23.10, 2 = P24.08, 3 = P20.08, 4 = P22.09, 5 = P30.06, 6 = P23.03. Unnumbered discs represent negative controls. .... 100

**Figure 27:** Volcano plots (A and C; FDR = 0.1) showing differences in the metabolomic profiles between the compared groups. A: Comparison between *P. terrestris* (isolate P23.03) and *P. lycopersici* (P27.24 and P27.06). C: Comparison of endophytic fungi grown on PDA medium from two different suppliers (Dinkelberg Analytics (Budapest, Hungary) and Sigma-Aldrich (St. Louis, MO, USA)). B and D: PLS-DA Score plots

illustrate the separation between groups corresponding to the comparisons shown in A and C, respectively. In the plots, green triangles represent *P. lycopersici*, red circles correspond to *P. terrestris* (P23.03), blue squares indicate isolates grown on Dinkelberg Analytics (Budapest, Hungary) PDA (P23.03, P30.06, P20.08, P23.10, P22.09, and P24.08), and yellow diamonds represent the same isolates grown on Sigma-Aldrich (St. Louis, MO, USA) PDA. .... 102

**Figure 28:** MS/MS spectrum showing the fragmentation pattern of feature 1 (left) and feature 2 (right), with a precursor ion at  $m/z$  162.113 and  $m/z$  204.123, respectively. 105

**Figure 29:** Proposed fragmentation scheme for features 1 (A,  $m/z$  162.113,  $[M+H]^+$ ) and 2 (B,  $m/z$  204.123,  $[M+H]^+$ ), tentatively annotated as carnitine and acetylcarnitine, respectively. The main MS/MS fragment ions are shown, with their corresponding chemical formulas, theoretical  $m/z$  values (to three decimal places). Arrows indicate inferred neutral losses between fragments..... 106

**Figure 30:** MS/MS spectra displaying the fragmentation patterns of: (A) the correlated feature at  $m/z$  530.12; (B) feature 3 with  $m/z$  513.099; (C) feature 4 with  $m/z$  283.093; and (D) feature 5 with  $m/z$  495.089..... 108

**Figure 31:** Proposed fragmentation scheme, highlighting the precursor ions (white boxes), major fragments (blue), and neutral losses (orange). The ion  $m/z$  283.09 appears both as the precursor of F4 and as a fragment of F3. The correlated precursor  $m/z$  530.12 is indicated in green. Arrows represent proposed relationships between features and their main fragments, and molecular formulas are shown for each species. .... 109

**Figure 32:** Proposed fragmentation scheme for features 3, 4, and 5 ( $[M+H]^+$ ), tentatively annotated as thiodiketopiperazine alkaloids. The diagram displays the main MS/MS fragment ions, along with their corresponding chemical formulas, theoretical  $m/z$  values (to three decimal places). Arrows indicate inferred neutral losses between fragments.110

**Figure 33:** Summary of the detected molecular features. The molecular formula and molecular weight of the compound are shown. The image includes three ion species observed: (i) the deprotonated ion ( $[M-H]^-$ ), (ii) the deprotonated dimer ( $[2M-H]^-$ ), and (iii) the doubly deprotonated dimer with a sodium adduct ( $[2M-2H+Na]^-$ ). .... 111

**Figure 34:** MS/MS spectrum showing the fragmentation pattern of feature 7  $m/z$  681.413 (A), MS/MS spectrum of feature 6 (B) and MS/MS the  $m/z$  329.213 (C)..... 112

**Figure 35:** Proposed fragmentation scheme for the ion at  $m/z$  329.212. The diagram shows the  $m/z$  values and the proposed molecular formulas of the fragments detected by MS/MS (in blue). Arrows indicate the relationships between fragments, and neutral losses are represented in orange..... 113

**Figure 36:** Proposed fragmentation scheme for the ion at  $m/z$  329.212 ( $[M-H]^-$ ), tentatively annotated as hydroxyretinoic acid methyl ester. The diagram displays the fragments detected by MS/MS, indicating for each its chemical formula, theoretical  $m/z$  value (to three decimal places). Arrows represent inferred neutral losses between fragments. .... 115

**Figure 37:** MS/MS spectrum showing the fragmentation pattern of feature 8,  $m/z$  565.1703. .... 116

**Figure 38:** Proposed fragmentation scheme for the ion at  $m/z$  565.17. The diagram shows the  $m/z$  values and the proposed molecular formulas of the fragments detected by MS/MS (in blue). Arrows indicate the relationships between fragments, and neutral losses are represented in orange..... 117

**Figure 39:** Proposed fragmentation scheme for the feature 8 at  $m/z$  565.171 ( $[M-H]^-$ ), tentatively annotated as polyphenol. The diagram displays the fragments detected by MS/MS, indicating for each its chemical formula, theoretical  $m/z$  value (to three decimal places). Arrows represent inferred neutral losses between fragments..... 118

**Figure 40:** MS/MS spectrum showing the fragmentation pattern of feature 8,  $m/z$  565.1703. .... 119

**Figure 41:** Proposed fragmentation scheme for the feature 9,  $m/z$  365.067 ( $[M-H]^-$ ), tentatively annotated as a pentahydroxyflavone. The diagram displays the fragments detected by MS/MS, indicating for each its chemical formula, theoretical  $m/z$  value (to three decimal places). Arrows represent inferred neutral losses between fragments... 121

## **TABLE INDEX**

**Table 1.** Alpha (Shannon and Simpson) and beta diversity (Jaccard) index of endophytic fungal culturable communities isolated from *C. annuum* (A, B) and *B. rapa* (C, D).....76

**Table 2.** Summary of the 9 key metabolic features (F) consistently overrepresented in *P. terrestris* and Sigma-Aldrich (St. Louis, MO, USA) medium extracts. The table includes the group in which they are classified (G), exact mass (M), ionization mode (I), retention time (RT, minutes), the fragments with highest intensity, the putative chemical formula and the putative compound identification.....104

## **APPENDIX**

**Supplementary Table 1.** Climate variables and soil characteristics at sampling points. The soil section includes pH, organic matter content (%), and texture class. The climate section includes annual averages for temperature (MAT, °C) and precipitation (MAP, mm). Data retrieved from the RGIS portal (<http://rgis.cesga.es/>).....141

**Supplementary Table 2.** Table showing the GenBank accession codes of the fungal isolates, the internal code assigned in this thesis (isolate), and the name given to each isolate (organism). The table also includes the closest match obtained using the BLAST tool, the query cover (QC, %), percentage identity (PI, %), and the phylogenetic classification at the phylum, order, family, and genus levels.....142

**Supplementary Table 3.** Table showing the percentage of pathogen inhibition during in vitro co-cultivation with endophytes, as well as the inhibition halo (cm) generated with the corresponding standard deviations.....154



## RESUMEN

La agricultura gallega se sustenta sobre cultivos que, además de su relevancia económica, conforman una parte esencial del patrimonio cultural y social del territorio. Estos cultivos tradicionales no solo aportan valor económico a las comunidades rurales, sino que reflejan un conocimiento agrario transmitido entre generaciones y un modelo de producción profundamente enraizado en el paisaje y la identidad gallega. Entre ellos destacan dos especies emblemáticas: *Brassica rapa*, base de la Indicación Geográfica Protegida (IGP) Grelos de Galicia, y *Capsicum annuum*, asociado a la Denominación de Origen Protegida (DOP) Pemento de Herbón. Ambos sistemas hortícolas constituyen auténticos pilares del patrimonio agroalimentario de Galicia, donde la calidad diferenciada y el arraigo territorial se combinan con prácticas agrícolas sostenidas históricamente por la experiencia campesina. En este sentido, representan un modelo singular dentro de la agricultura española: productos locales de alta calidad vinculados a su origen, respaldados por certificaciones que garantizan su trazabilidad, autenticidad y valor añadido.

La sostenibilidad de estos sistemas resulta, por tanto, esencial para el futuro de la agricultura gallega. Mantener su productividad y su viabilidad social exige estrategias que fortalezcan la capacidad adaptativa de los cultivos frente a los desafíos emergentes del siglo XXI. Entre dichos desafíos, el cambio climático ocupa un lugar central. Este fenómeno, de alcance global, constituye una amenaza creciente para la estabilidad de la producción agrícola, ya que modifica las condiciones climáticas que sustentan el rendimiento de los cultivos y altera la distribución e incidencia de plagas y enfermedades. El incremento de las temperaturas, la irregularidad en las precipitaciones y la mayor frecuencia de eventos extremos como sequías o lluvias torrenciales repercuten directamente en la fisiología vegetal, la disponibilidad hídrica y la dinámica del suelo. Estas perturbaciones pueden comprometer tanto el rendimiento como la calidad de los productos certificados, afectando de manera particular a aquellos sistemas agrícolas que dependen de recursos locales limitados o que se desarrollan en pequeñas explotaciones familiares, como es el caso gallego.

A este escenario se suma otro factor determinante: la progresiva limitación en el uso de fitosanitarios de síntesis química, derivada de la aplicación de políticas europeas orientadas hacia la reducción del impacto ambiental de la agricultura. Normativas cada

vez más estrictas restringen el uso de compuestos perjudiciales para la salud humana, la biodiversidad y la calidad del agua y del suelo. Esta reducción del arsenal químico disponible para el control de plagas y enfermedades ha dejado a muchos productores con pocas herramientas eficaces, lo que ha impulsado la necesidad de desarrollar alternativas sostenibles. La búsqueda de soluciones biológicas que mantengan la productividad y la sanidad vegetal, sin comprometer los objetivos ambientales y sociales de la política agraria común, se ha convertido en una prioridad estratégica dentro del marco de la transición agroecológica europea. En este contexto, la innovación basada en la biotecnología microbiana aparece como una de las líneas prometedoras para lograr sistemas agrícolas más resilientes y de bajo impacto ambiental.

Entre las aproximaciones más relevantes se encuentra la manipulación y aprovechamiento del microbioma vegetal, entendido como el conjunto de microorganismos que habitan en los tejidos y superficies de las plantas, incluyendo rizosfera, filósfera y endosfera. Este microbioma, complejo y dinámico, desempeña un papel crucial en la salud de las plantas, actuando como una extensión funcional de su fisiología. Dentro de este conjunto microbiano, los hongos endófitos filamentosos merecen especial atención. Estos microorganismos colonizan los tejidos internos de las plantas sanas sin causar síntomas visibles de enfermedad, y su modo de vida íntimamente asociado al hospedador les permite establecer relaciones que pueden oscilar desde el comensalismo hasta el mutualismo. En numerosos casos, estas interacciones resultan beneficiosas, traducándose en mejoras tangibles del crecimiento vegetal, del estado hídrico, de la tolerancia a estreses bióticos y abióticos, o en la supresión de patógenos mediante mecanismos de competencia, micoparasitismo o producción de metabolitos antibióticos.

No obstante, la acción de los endófitos no es uniforme ni universal. Su efecto depende de una compleja red de factores interrelacionados que incluyen la compatibilidad específica entre planta y hongo, las condiciones ambientales, la composición del microbioma de fondo y las características fisiológicas y metabólicas propias de cada cepa. De hecho, un mismo taxón endofítico puede comportarse como mutualista, neutro o incluso como patógeno latente según el contexto ecológico o fisiológico en que se encuentre. Esta plasticidad funcional explica la elevada variabilidad de resultados reportados entre estudios y evidencia la necesidad de avanzar desde la mera observación de fenómenos beneficiosos hacia una validación sistemática de las interacciones planta–endófito. Solo

mediante enfoques integradores se podrá discernir qué cepas poseen un efecto estable y reproducible, y en qué condiciones y hospedadores ese efecto se expresa.

La traslación de los resultados experimentales al campo representa actualmente uno de los principales cuellos de botella en el desarrollo de bioinoculantes fúngicos. A pesar de su potencial, los hongos endófitos suelen mostrar tasas de colonización variables en condiciones reales de cultivo, y su eficacia puede verse atenuada por la competencia con las comunidades microbianas nativas o por las características físico-químicas del suelo y del clima. Además, las formulaciones comerciales deben asegurar la viabilidad del inoculante y su capacidad de establecerse de forma duradera, aspectos que dependen de factores aún poco comprendidos. Por ello, el camino que conduce desde la identificación de un aislado prometedor hasta su uso práctico como herramienta biotecnológica requiere un itinerario coherente de selección, caracterización y validación, que contemple tanto la diversidad natural como la funcionalidad y la estabilidad ecológica de los candidatos.

Desde esta perspectiva, el estudio de la micobiota endofítica asociada a cultivos gallegos ofrece una oportunidad doble. En primer lugar, permite realizar una descripción inicial de la diversidad fúngica cultivable autóctona que coevoluciona con sistemas agrícolas tradicionales, adaptados históricamente a las condiciones climáticas y edáficas de la región. Estos hongos locales podrían representar una fuente privilegiada de adaptaciones funcionales y genéticas de interés biotecnológico, especialmente por su compatibilidad con los cultivos de referencia. En segundo lugar, el conocimiento de esta micobiota puede revelar cepas con potencial agronómico capaces de contribuir tanto al control biológico de patógenos como al fortalecimiento de la tolerancia a estreses abióticos como la sequía, un factor cada vez más determinante en el rendimiento de los cultivos gallegos. Así, la exploración de estos microorganismos endófitos no solo amplía el conocimiento básico sobre la biodiversidad microbiana regional, sino que también proporciona las bases científicas para su aprovechamiento en estrategias de sostenibilidad agrícola y conservación del patrimonio agroalimentario de Galicia.

Con ese propósito, esta tesis partió de la hipótesis de que las raíces de *B. rapa* y *C. annuum* albergan una fracción cultivable de hongos endófitos con potencial para mitigar el daño causado por patógenos relevantes y/o para mejorar la tolerancia de la planta a la sequía. Asimismo, se planteó que es posible identificar candidatos de interés biotecnológico

mediante la combinación de prospección en campo, ensayos funcionales y caracterización metabolómica.

La investigación se estructuró en cuatro ejes complementarios. El primero se centró en el aislamiento e identificación de la diversidad cultivable de endófitos radiculares en parcelas comerciales certificadas bajo figuras de calidad IGP/DOP en Galicia, con el objetivo de describir su composición y estructura comunitaria. El segundo eje abordó la función biológica de los aislados, mediante un cribado antifúngico frente a patógenos clave, tanto *in vitro* como en condiciones controladas *in planta*. El tercero profundizó en la base química de la antibiosis a través del estudio metabolómico del género *Pseudopyrenochaeta*, que destacó en los ensayos de biocontrol. Finalmente, se evaluó el papel potencial de estos endófitos bajo estrés hídrico, comparando diferentes metodologías *in vitro* y priorizando la validación fisiológica *in planta*.

Estos objetivos se articularon en un itinerario metodológico secuencial, concebido para avanzar desde el aislamiento microbiano hasta la validación funcional de los candidatos. En la primera fase se realizaron muestreos de raíces de *B. rapa* y *C. annuum* durante la recolección comercial. Tras la esterilización superficial, los fragmentos radiculares se sembraron en medio PDA suplementado con cloranfenicol, recuperándose la fracción cultivable de la microbiota fúngica endófito. Los aislados se agruparon por morfotipos y se identificaron mediante barcoding ITS (ITS1/ITS4), complementado con análisis filogenético cuando fue necesario.

En total se obtuvieron 842 aislados, 203 procedentes de *B. rapa* y 644 de *C. annuum*, agrupados en decenas de morfotipos. La asignación taxonómica reveló una notable riqueza: 28 taxones (23 géneros) asociados a *B. rapa* y 24 (20 géneros) a *C. annuum*, pertenecientes a 12 y 10 órdenes respectivamente. En ambos cultivos predominó el filo *Ascomycota*, aunque también se detectaron representantes de *Basidiomycota*, *Mucoromycota* y, en menor medida, *Oomycota*. Entre los géneros recurrentes se identificaron *Chaetomium*, *Cladosporium*, *Fusarium*, *Penicillium*, *Talaromyces* y *Trichoderma*, conformando un núcleo de endófitos radiculares generalistas compartido por ambas especies.

El análisis de diversidad reveló diferencias estructurales marcadas entre cultivos. Las comunidades de *C. annuum* presentaron mayor densidad de aislados por planta y una

composición más uniforme entre parcelas, mientras que las de *B. rapa* mostraron elevada heterogeneidad espacial, con numerosos taxones *singleton* (aislados representados por una única observación) y una beta-diversidad considerable. Las curvas de rarefacción sugirieron un muestreo relativamente completo en pimiento, pero subrepresentado en brásica, probablemente debido a la alta recuperación de levaduras (p. ej. *Cyberlindnera*, *Rhodotorula*), que en placa pueden competir con hongos filamentosos de crecimiento más lento. Estos resultados fueron inesperados, ya que se partía de la hipótesis de que la presencia de glucosinolatos en *B. rapa* podría modular la estructura de su comunidad endofítica y favorecer un grupo de hongos adaptados a estos compuestos. No obstante, los datos no apuntan a una comunidad especializada, sino más bien a un conjunto de endófitos generalistas. Al mismo tiempo, ponen de relieve las limitaciones de los enfoques dependientes de cultivo para caracterizar comunidades fúngicas complejas y señalan la necesidad de un muestreo más exhaustivo en *B. rapa* para obtener una visión más completa de su diversidad endofítica.

Sobre esta base se exploró el potencial de biocontrol. Un cribado de 146 aislados frente a *Rhizoctonia solani* mediante confrontación dual permitió distinguir dos mecanismos principales de antagonismo: (i) la competencia por sobrecrecimiento, en la que el endófito ocupa rápidamente el espacio e impide el avance del patógeno, y (ii) la antibiosis difusible, observable como halos claros de inhibición alrededor de la colonia endofítica. Dentro del primer grupo destacaron cepas de *Trichoderma* capaces de suprimir con firmeza el crecimiento del patógeno sin formar halos visibles; en el segundo, *Talaromyces*, *Chaetomium* y especialmente *Pseudopyrenochaeta* produjeron halos consistentes frente a un panel ampliado de patógenos fitotóxicos (*Fusarium oxysporum*, *Alternaria alternata*, *Botrytis cinerea*, *Sclerotinia sclerotiorum*, *Fusarium solani*, *Colletotrichum acutatum*, *Phytophthora capsici*, entre otros).

A partir de estos resultados se seleccionaron tres candidatos representativos, dos de antibiosis (*Pseudopyrenochaeta* y *Talaromyces*) y uno de competencia (*Trichoderma*) para ensayos *in planta* en *Capsicum annuum* y *Brassica* sp. La estrategia consistió en preinocular las raíces con el endófito y, tras un periodo de establecimiento, inocular el patógeno en hojas para evaluar la progresión de la enfermedad. En un primer experimento, las cepas *Pseudopyrenochaeta* (P23.03) y *Talaromyces* (BrT4.01) redujeron significativamente el área necrótica causada por *S. sclerotiorum* sin

comprometer el crecimiento vegetal. No obstante, en un segundo ensayo independiente el efecto no se reprodujo con la misma consistencia.

El análisis de causas identificó dos principales limitaciones metodológicas. Por un lado, la verificación de colonización mediante el aislamiento se vio obstaculizada por el sobrecrecimiento de contaminantes oportunistas no inoculados; por otro, la detección molecular del endófito también en los controles indicó posibles contaminaciones cruzadas. Este contraste entre resultados iniciales prometedores y la dificultad para reproducirlos de forma robusta pone de manifiesto la complejidad de trasladar la actividad antifúngica observada *in vitro* al contexto *in planta*. Asimismo, resalta la necesidad de optimizar los protocolos de inoculación y verificación de colonización, incorporando cuantificación molecular (por ejemplo, qPCR) y controles de contaminación estrictos, que permitan evaluar de manera más precisa la persistencia y el impacto real del endófito en el hospedador.

La singularidad del comportamiento de *Pseudopyrenochaeta* motivó un estudio específico que integró aspectos biológicos, taxonómicos y químicos. Mediante PCR con cebadores específicos se logró discriminar entre *P. terrestris* y *P. lycopersici*, observándose que la actividad antifúngica consistente correspondía a varios aislados de *P. terrestris*. Los ensayos con extractos confirmaron que el antagonismo dependía de metabolitos extracelulares difusibles y, de manera reveladora, que la bioactividad variaba en función del medio de cultivo: los extractos obtenidos de *P. terrestris* cultivada en PDA de un proveedor mantenían la inhibición, mientras que en el medio equivalente de otro proveedor desaparecía por completo.

Esta plasticidad metabólica ofreció una oportunidad para abordar un análisis metabolómico no dirigido mediante LC-MS/MS, orientado a identificar señales químicas asociadas con la bioactividad. La comparación entre especies, cepas y condiciones de cultivo permitió detectar un conjunto de metabolitos enriquecidos simultáneamente en las muestras de *P. terrestris* activas frente a aquellas inactivas. Entre las señales más destacadas, algunas correspondían con alta probabilidad a derivados de carnitina, lo que sugiere una reprogramación del metabolismo energético más que un efecto antifúngico directo; otras mostraron fragmentaciones compatibles con núcleos flavonoides, compuestos azufrados o fracciones lipofílicas, si bien las asignaciones siguen siendo provisionales. Destacan las tiodicetopiperazinas (TDKP) que se perfilan como los

principales candidatos para explicar la actividad inhibidora contra *R. solani* y constituyen un punto de partida para estudios destinados a la caracterización química y funcional de estas moléculas. Estos resultados son la base para estudios posteriores de elucidación estructural mediante técnicas complementarias (NMR, comparación con estándares) y evidencian que los determinantes químicos de la antibiosis pueden depender tanto de la cepa como de las condiciones de cultivo.

En términos ecológicos, *Pseudopyrenochaeta* emerge como un taxón de estilo de vida flexible: conocido por su papel patogénico en la raíz corchosa del tomate, en este trabajo fue aislado de raíces sanas de pimiento, lo que sugiere que algunas cepas podrían comportarse como endófitos mutualistas capaces de competir con patógenos. Esta plasticidad plantea la necesidad de validar experimentalmente la dualidad de su comportamiento mediante ensayos de patogenicidad, perfiles de seguridad y pruebas de eficacia en las especies hospedadoras de interés.

Para evaluar el efecto de hongos endófitos en condiciones de estrés hídrico, se desarrollaron aproximaciones tanto *in planta* como *in vitro*. En los ensayos *in planta*, se realizó un cribado en la planta modelo *Arabidopsis thaliana*, comparando sus respuestas fisiológicas a la sequía cuando estaba inoculada con hongos endófitos frente a plantas no inoculadas. Las raíces de plántulas se inocularon con 45 aislados representativos de 36 taxones, que posteriormente se trasplantaron a sustrato y se sometieron a una sequía progresiva de cuatro semanas. Las variables evaluadas incluyeron conductancia estomática, contenido relativo de agua (RWC) y biomasa fresca y seca, todas normalizadas respecto a controles del mismo bloque experimental para minimizar la varianza ambiental.

En paralelo, se exploraron distintas metodologías *in vitro* para simular déficit hídrico. Se evaluó (i) la suplementación de medios con polietilenglicol (PEG 8000) en formatos sólido, líquido y sobre membranas de celofán para reducir el potencial hídrico, y (ii) el aumento de la concentración de agar para limitar la disponibilidad de agua. Entre estos enfoques, los ensayos basados en el incremento de agar resultaron ser los más informativos y se presentan como una herramienta de cribado inicial especialmente prometedora.

Los resultados del cribado *in planta* mostraron que las plantas inoculadas presentaron diferencias significativas en su RWC respecto al control en dieciocho tratamientos: en cinco de ellos, las plantas inoculadas alcanzaron valores más altos de RWC, mientras que en trece mostraron valores inferiores. En términos de biomasa, las plantas inoculadas en catorce tratamientos difirieron significativamente del control, y en ocho de ellos registraron un mayor peso seco. Entre estos, las plantas inoculadas con dos de los aislados pertenecientes a *Humicola* sp. y Pseudeurotiaceae también mostraron un aumento del peso fresco, una combinación que sugiere un posible equilibrio entre el mantenimiento del contenido hídrico y el crecimiento vegetativo.

No se observó ningún tratamiento en el que las plantas inoculadas presentaran mejoras simultáneas y consistentes tanto en RWC como en biomasa. Este patrón es coherente con la idea de que los procesos que contribuyen al mantenimiento del agua tisular (como el ajuste osmótico, la regulación estomática o cambios en la arquitectura radicular) no necesariamente coinciden con aquellos asociados al aumento de masa vegetal. Asimismo, la progresión del estrés, moderado al inicio y más severo en etapas posteriores, podría favorecer inicialmente a hongos que estimulan el crecimiento bajo recursos limitados y, en fases críticas, a aquellos que mejoran la retención hídrica.

En conjunto, de estos hallazgos se derivan líneas claras de trabajo futuro. La validación en los hospedadores diana, tanto en condiciones de invernadero como de campo, permitirá evaluar la estabilidad del efecto y su impacto en el rendimiento y la calidad comercial. La estandarización de los procedimientos de inoculación, incluyendo formulaciones y *carriers* que favorezcan la implantación, junto con la cuantificación molecular de la colonización debería incorporarse como parte esencial del flujo de desarrollo de cualquier inoculante.

Paralelamente, se requiere la confirmación estructural de los metabolitos antifúngicos identificados mediante técnicas complementarias y la caracterización de sus modos de acción tanto sobre patógenos como sobre las plantas hospedadoras. La integración de enfoques genómicos, transcriptómicos y metabolómicos en aislados clave permitirá mapear clústeres biosintéticos y explicar por qué cepas estrechamente relacionadas pueden mostrar comportamientos tan dispares. Asimismo, campañas de muestreo en diferentes anualidades facilitarán evaluar la estabilidad interanual de la micobiota y su

respuesta a eventos reales de sequía, contribuyendo al diseño de estrategias de selección más robustas y ajustadas a las condiciones de los sistemas IGP/DOP gallegos.

Por último, el desarrollo de comunidades sintéticas de endófitos con funciones complementarias se perfila como una vía prometedora para generar inoculantes más estables y eficaces que las cepas individuales, aprovechando la cooperación metabólica y la partición de nichos.

En conjunto, esta tesis demuestra que la diversidad endofítica cultivable en raíces de *B. rapa* y *C. annuum* en Galicia encierra un potencial funcional tangible. Su aprovechamiento práctico exige combinar evidencia ecológica, fisiológica y química, garantizando colonización, reproducibilidad y seguridad. Solo a través de este enfoque integrado será posible trasladar las cepas más prometedoras al campo como inoculantes microbianos capaces de compatibilizar productividad, resiliencia climática y conservación del patrimonio agroalimentario gallego.

## RESUMO

A agricultura galega susténtase en cultivos que, ademais da súa relevancia económica, constitúen unha parte esencial do patrimonio cultural e social do territorio. Estes cultivos tradicionais non só achegan valor económico ás comunidades rurais, senón que reflicten un coñecemento agrario transmitido entre xeracións e un modelo de produción profundamente enraizado na paisaxe e na identidade galega. Entre eles destacan dúas especies emblemáticas: *Brassica rapa*, base da Indicación Xeográfica Protexida (IXP) *Grelos de Galicia*, e *Capsicum annuum*, asociado á Denominación de Orixe Protexida (DOP) *Pemento de Herbón*. Ambos sistemas hortícolas constitúen auténticos piares do patrimonio agroalimentario de Galicia, onde a calidade diferenciada e o arraigamento territorial se combinan con prácticas agrícolas sostidas historicamente pola experiencia campesiña. Neste sentido, representan un modelo singular dentro da agricultura española: produtos locais de alta calidade vinculados á súa orixe, respaldados por certificacións que garantizan a súa trazabilidade, autenticidade e valor engadido.

A sustentabilidade destes sistemas resulta, por tanto, esencial para o futuro da agricultura galega. Manter a súa produtividade e a súa viabilidade social esixe estratexias que fortalezcan a capacidade adaptativa dos cultivos fronte aos desafíos emerxentes do século XXI. Entre estes desafíos, o cambio climático ocupa un lugar central. Este fenómeno, de alcance global, constitúe unha ameaza crecente para a estabilidade da produción agrícola, xa que modifica as condicións climáticas que sustentan o rendemento dos cultivos e altera a distribución e incidencia de pragas e enfermidades. O incremento das temperaturas, a irregularidade das precipitacións e a maior frecuencia de eventos extremos como secas ou choivas torrenciais repercuten directamente na fisioloxía vexetal, na dispoñibilidade hídrica e na dinámica do solo. Estas perturbacións poden comprometer tanto o rendemento como a calidade dos produtos certificados, afectando de maneira particular aqueles sistemas agrícolas que dependen de recursos locais limitados ou que se desenvolven en pequenas explotacións familiares, como é o caso galego.

A este escenario súmase outro factor determinante: a progresiva restrición do uso de fitosanitarios de síntese química, derivada da aplicación de políticas europeas orientadas á redución do impacto ambiental da agricultura. Normativas cada vez máis estritas limitan o uso de compostos prexudiciais para a saúde humana, a biodiversidade e a calidade da auga e do solo. Esta redución do arsenal químico dispoñible para o control de pragas e

enfermidades deixou a moitos produtores con poucas ferramentas eficaces, o que impulsou a necesidade de desenvolver alternativas sostibles. A busca de solucións biolóxicas que manteñan a produtividade e a sanidade vexetal, sen comprometer os obxectivos ambientais e sociais da política agraria común, converteuse nunha prioridade estratéxica no marco da transición agroecolóxica europea. Neste contexto, a innovación baseada na biotecnoloxía microbiana aparece como unha das liñas máis prometedoras para acadar sistemas agrícolas máis resilientes e de baixo impacto ambiental.

Entre as aproximacións máis relevantes atópase a manipulación e aproveitamento do microbioma vexetal, entendido como o conxunto de microorganismos que habitan nos tecidos e superficies das plantas, incluíndo rizosfera, filósfera e endosfera. Este microbioma, complexo e dinámico, desempeña un papel crucial na saúde das plantas, actuando como unha extensión funcional da súa fisioloxía. Dentro deste conxunto microbiano, os fungos endófitos filamentosos merecen especial atención. Estes microorganismos colonizan os tecidos internos de plantas sas sen causar síntomas visibles de enfermidade, e o seu modo de vida intimamente asociado ao hospedador permítelles establecer relacións que poden oscilar desde o comensalismo até o mutualismo. En numerosos casos, estas interaccións resultan beneficiosas, traducíndose en melloras tanxibles do crecemento vexetal, do estado hídrico, da tolerancia a estreses bióticos e abióticos, ou na supresión de patóxenos mediante mecanismos de competencia, micoparasitismo ou produción de metabolitos antibióticos.

Non obstante, a acción dos endófitos non é uniforme nin universal. O seu efecto depende dunha complexa rede de factores interrelacionados que inclúen a compatibilidade específica entre planta e fungo, as condicións ambientais, a composición do microbioma de fondo e as características fisiolóxicas e metabólicas propias de cada cepa. De feito, un mesmo taxon endófito pode comportarse como mutualista, neutro ou incluso como patóxeno latente segundo o contexto ecolóxico ou fisiolóxico en que se atope. Esta plasticidade funcional explica a elevada variabilidade de resultados reportados entre estudos e evidencia a necesidade de avanzar desde a mera observación de fenómenos beneficiosos cara a unha validación sistemática das interaccións planta–endófito. Só mediante enfoques integradores se poderá discernir que cepas posúen un efecto estable e reproducible, e en que condicións e hospedadores ese efecto se expresa.

A traslación dos resultados experimentais ao campo representa actualmente un dos principais atrancos no desenvolvemento de bioinoculantes fúngicos. A pesar do seu potencial, os fungos endófitos adoitan mostrar taxas de colonización variables en condicións reais de cultivo, e a súa eficacia pode verse atenuada pola competencia coas comunidades microbianas nativas ou polas características físico-químicas do solo e do clima. Ademais, as formulacións comerciais deben asegurar a viabilidade do inoculante e a súa capacidade para establecerse de forma duradeira, aspectos que dependen de factores aínda pouco comprendidos. Por iso, o camiño que conduce desde a identificación dun illado prometedor até o seu uso práctico como ferramenta biotecnolóxica require un itinerario coherente de selección, caracterización e validación, que contemple tanto a diversidade natural como a funcionalidade e a estabilidade ecolóxica dos candidatos.

Desde esta perspectiva, o estudo da microbiota endofítica asociada a cultivos galegos ofrece unha dobre oportunidade. En primeiro lugar, permite realizar unha descrición inicial da diversidade fúngica cultivable autóctona que coevoluciona con sistemas agrícolas tradicionais, adaptados historicamente ás condicións climáticas e edáficas da rexión. Estes fungos locais poderían representar unha fonte privilexiada de adaptacións funcionais e xenéticas de interese biotecnolóxico, especialmente pola súa compatibilidade cos cultivos de referencia. En segundo lugar, o coñecemento desta microbiota pode revelar cepas con potencial agronómico capaces de contribuír tanto ao control biolóxico de patóxenos como ao fortalecemento da tolerancia a estreses abióticos como a seca, un factor cada vez máis determinante no rendemento dos cultivos galegos. Así, a exploración destes microorganismos endófitos non só amplía o coñecemento básico sobre a biodiversidade microbiana rexional, senón que tamén proporciona as bases científicas para o seu aproveitamento en estratexias de sustentabilidade agrícola e conservación do patrimonio agroalimentario de Galicia.

Con ese propósito, esta tese partiu da hipótese de que as raíces de *B. rapa* e *C. annuum* albergan unha fracción cultivable de fungos endófitos con potencial para mitigar o dano causado por patóxenos relevantes e/ou para mellorar a tolerancia da planta á seca. Así mesmo, plantexouse que é posible identificar candidatos de interese biotecnolóxico mediante a combinación de prospección en campo, ensaios funcionais e caracterización metabólica.

A investigación estruturouse en catro eixos complementarios. O primeiro centrouse no illamento e identificación da diversidade cultivable de endófitos radiculares en parcelas comerciais certificadas baixo figuras de calidade Indicación Xeográfica Protexida (IXP) e Denominación de Orixe Protexida (DOP) en Galicia, co obxectivo de describir a súa composición e estrutura comunitaria. O segundo eixo abordou a función biolóxica dos illados, mediante un cribado antifúnxico fronte a patóxenos clave, tanto *in vitro* como en condicións controladas *in planta*. O terceiro profundizou na base química da antibiose a través do estudo metabolómico do xénero *Pseudopyrenochaeta*, empregado como modelo de caso paradigmático. Finalmente, avalíase o papel potencial destes endófitos baixo estrés hídrico, comparando diferentes metodoloxías *in vitro* e priorizando a validación fisiolóxica *in planta*.

Estes obxectivos articuláronse nun itinerario metodolóxico secuencial, concibido para avanzar desde o illamento microbiano até a validación funcional dos candidatos. Na primeira fase realizáronse mostreos de raíces de *B. rapa* e *C. annuum* durante a recolección comercial. Despois da esterilización superficial, os fragmentos radiculares colocáronse en medio agar pataca-dextrosa (PDA) suplementado con cloranfenicol, permitindo a recuperación da fracción cultivable da microbiota fúngica endófito. Os illados agrupáronse por morfotipos e identificáronse mediante barcoding ITS. Utilizando os cebadores descritos como ITS1 e ITS4, complementando a identificación con análises filoxenéticas cando foi necesario. O ITS, ou Espazo Transcrito Interno (*Internal Transcribed Spacer* en inglés), é unha rexión do ADN ribosómico situada entre os xenes do ARNr 18S, 5,8S e 28S nos fungos, e a súa alta variabilidade entre especies permite a súa utilización como marcador molecular para a identificación taxonómica.

En total obtivéronse 842 illados, 203 procedentes de *B. rapa* e 644 de *C. annuum*, agrupados en ducias de morfotipos. A asignación taxonómica revelou unha notable riqueza: 28 taxóns (23 xéneros) asociados a *B. rapa* e 24 taxóns (20 xéneros) a *C. annuum*, pertencentes a 12 e 10 ordes respectivamente. En ambos cultivos predominou o filo Ascomycota, aínda que tamén se detectaron representantes de Basidiomycota, Mucoromycota e, en menor medida, Oomycota. Entre os xéneros recorrentes identificáronse *Chaetomium*, *Cladosporium*, *Fusarium*, *Penicillium*, *Talaromyces* e *Trichoderma*, conformando un núcleo de endófitos radiculares generalistas compartido por ambas especies.

A análise de diversidade revelou diferenzas estruturais marcadas entre cultivos. As comunidades de *C. annuum* presentaron maior densidade de illados por planta e unha composición máis uniforme entre parcelas, mentres que as de *B. rapa* mostraron elevada heteroxeneidade espacial, con numerosos taxóns *singleton* (taxón ou illado que aparece unha única vez nun conxunto de mostraxes ou nunha comunidade) e unha beta-diversidade considerable. As curvas de rarefacción suxeriron un mostreo relativamente completo en pemento, pero subrepresentado en brásica, probablemente debido á alta recuperación de levaduras (p. ex. *Cyberlindnera*, *Rhodotorula*), que en placa poden competir con fungos filamentosos de crecemento máis lento. Estes resultados foron inesperados, xa que se partía da hipótese de que a presenza de glucosinolatos en *B. rapa* podería modular a estrutura da súa comunidade endofítica e favorecer un grupo de fungos adaptados a estes compostos. Non obstante, os datos non apuntan a unha comunidade especializada, senón máis ben a un conxunto de endófitos generalistas. Ao mesmo tempo, poñen de relevo as limitacións dos enfoques dependentes de cultivo para caracterizar comunidades fúngicas complexas e sinalan a necesidade de realizar un mostreo máis exhaustivo en *B. rapa* para obter unha visión máis completa da súa diversidade endofítica.

Sobre esta base explorouse o potencial de biocontrol. Un cribado de 146 illados fronte a *Rhizoctonia solani* mediante confrontación dual permitiu distinguir dous mecanismos principais de antagonismo: (i) a competencia por sobrecrecemento, na que o endófito ocupa rapidamente o espazo e impide o avance do patóxeno, e (ii) a antibiose difusible, observable como halos claros de inhibición arredor da colonia endofítica. Dentro do primeiro grupo destacaron cepas de *Trichoderma* capaces de suprimir con firmeza o crecemento do patóxeno sen formar halos visibles; no segundo, *Talaromyces*, *Chaetomium* e especialmente *Pseudopyrenochaeta* produciron halos consistentes fronte a un panel ampliado de patóxenos fitotóxicos (*Fusarium oxysporum*, *Alternaria alternata*, *Botrytis cinerea*, *Sclerotinia sclerotiorum*, *Fusarium solani*, *Colletotrichum acutatum*, *Phytophthora capsici*, entre outros).

A partir destes resultados seleccionáronse tres candidatos representativos, dous de antibiose (*Pseudopyrenochaeta* e *Talaromyces*) e un de competencia (*Trichoderma*) para ensaios *in planta* en *Capsicum annuum* e *Brassica* sp. A estratexia consistiu en preinocular as raíces co endófito e, tras un período de establecemento, inocular o patóxeno en follas para avaliar a progresión da enfermidade. Nun primeiro experimento, as cepas

*Pseudopyrenochaeta* (P23.03) e *Talaromyces* (BrT4.01) reduciron significativamente a área necrótica causada por *S. sclerotiorum* sen comprometer o crecemento vexetal. Non obstante, nun segundo ensaio independente o efecto non se reproduciu coa mesma consistencia.

A análise das causas identificou dúas principais limitacións metodolóxicas. Por unha banda, a verificación da colonización mediante illamento viuse obstaculizada polo sobrecrecemento de contaminantes oportunistas non inoculados; por outra, a detección molecular do endófito tamén nos controis indicou posibles contaminacións cruzadas. Este contraste entre resultados iniciais prometedores e a dificultade para reproducilos de forma robusta pon de manifesto a complexidade de trasladar a actividade antifúngica observada *in vitro* ao contexto *in planta*. Así mesmo, resáltase a importancia de optimizar os protocolos de inoculación e de verificación da colonización, incorporando cuantificación molecular (por exemplo, mediante a reacción en cadea da polimerase cuantitativa en tempo real, qPCR) e controis estritos de contaminación, co obxectivo de avaliar de forma máis precisa a persistencia e o efecto real do endófito sobre o hospedador.

A singularidade do comportamento de *Pseudopyrenochaeta* motivou un estudo específico que integrou aspectos biolóxicos, taxonómicos e químicos. Mediante PCR con cebadores específicos logrouse discriminar entre *P. terrestris* e *P. lycopersici*, observándose que a actividade antifúngica consistente correspondía a varios illados de *P. terrestris*. Os ensaios con extractos confirmaron que o antagonismo dependía de metabolitos extracelulares difusibles e, de maneira reveladora, que a bioactividade variaba en función do medio de cultivo: os extractos obtidos de *P. terrestris* cultivada en PDA dun provedor mantiveron a inhibición, mentres que no medio equivalente doutro provedor desaparecía por completo.

Esta plasticidade metabólica ofreceu unha oportunidade para abordar unha análise metabolómica non dirixida mediante cromatografía líquida con espectrometría de masas en tándem (LC-MS/MS), orientada a identificar sinais químicas asociadas á bioactividade. A comparación entre especies, cepas e condicións de cultivo permitiu detectar un conxunto de metabolitos enriquecidos simultaneamente nas mostras de *P. terrestris* activas fronte a aquelas inactivas. Entre as sinais máis destacadas, algunhas correspondían con alta probabilidade a derivados de carnitina, o que suxire unha reprogramación do metabolismo enerxético máis que un efecto antifúngico directo; outras

mostraron fragmentacións compatibles con núcleos flavonoides, compostos sulfurados ou fraccións lipofílicas, se ben as asignacións seguen sendo tentativas. Destacan as tiodicetopiperacinas (TDKP), que se perfilan como os principais candidatos para explicar a actividade inhibidora contra *R. solani* e constitúen un punto de partida para estudos destinados á caracterización química e funcional destas moléculas. Estes resultados serven como fundamento para estudos posteriores de elucidación estrutural utilizando técnicas complementarias, como a resonancia magnética nuclear ou a comparación con estándares, e evidencian que os compoñentes químicos responsables da antibiose poden variar segundo a cepa e as condicións de cultivo.

En termos ecolóxicos, *Pseudopyrenochaeta* emerxe como un taxon de estilo de vida flexible: coñecido polo seu papel patoxénico na raíz cortizada do tomate, neste traballo foi illado de raíces sas de pemento, o que suxire que algunhas cepas poderían comportarse como endófitos mutualistas capaces de competir con patóxenos. Esta plasticidade formula a necesidade de validar experimentalmente a dualidade do seu comportamento mediante ensaios de patoxenicidade, perfís de seguridade e probas de eficacia nas especies hospedadoras de interese.

Para avaliar o efecto de fungos endófitos en condicións de estrés hídrico, desenvóléronse aproximacións tanto *in planta* como *in vitro*. Nos ensaios *in planta*, realizouse un cribado na planta modelo *Arabidopsis thaliana*, comparando as súas respostas fisiolóxicas á seca cando estaba inoculada con fungos endófitos fronte a plantas non inoculadas. As raíces de plántulas inoculáronse con 45 illados representativos de 36 taxóns, que posteriormente se trasplantaron a substrato e se someteron a unha seca progresiva de catro semanas. As variables avaliadas incluíron conductancia estomática, contido relativo de auga (RWC) e biomasa fresca e seca, todas normalizadas respecto dos controis do mesmo bloque experimental para minimizar a varianza ambiental.

En paralelo, exploráronse distintas metodoloxías *in vitro* para simular déficit hídrico. Avaliouse (i) a suplementación de medios con polietilenglicol (PEG 8000) en formatos sólido, líquido e sobre membranas de celofán para reducir o potencial hídrico, e (ii) o aumento da concentración de agar para limitar a dispoñibilidade de auga. Entre estes enfoques, os ensaios baseados no incremento de agar resultaron ser os máis informativos e preséntanse como unha ferramenta de cribado inicial especialmente prometedora.

Os resultados do cribado *in planta* mostraron que dezaoito illados modificaron de maneira significativa o RWC en comparación co control: cinco incrementárono, o que suxire posibles efectos beneficiosos sobre o estatus hídrico da planta e mesmo unha certa capacidade para mitigar o impacto inicial da seca, mentres que trece o reduciron, probablemente reflectindo interaccións incompatibles ou respostas fisiolóxicas subóptimas do hospedador. En termos de biomasa, catorce tratamentos diferiron significativamente do control e oito promoveron aumentos do peso seco. Entre eles, dous illados pertencentes a *Humicola* sp. e á familia Pseudeurotiaceae incrementaron tamén o peso fresco, unha combinación de efectos pouco frecuente que apunta a un equilibrio entre conservación da auga, mantemento da turgencia e promoción do crecemento vexetativo.

Non se identificou ningún illado que mellorase simultaneamente e de forma robusta tanto o RWC como a biomasa, un resultado coherente coa hipótese de que os mecanismos que preservan a auga tisular (como o axuste osmótico, a regulación estomática ou modificacións profundas na arquitectura radicular) poden non coincidir cos procesos que promoven a división ou elongación celular e, polo tanto, a acumulación de biomasa. Así mesmo, a progresión do estrés, moderado ao inicio e máis severo en fases posteriores, podería favorecer inicialmente aqueles fungos capaces de estimular o crecemento baixo recursos limitados e, en etapas máis críticas, os que contribúen a mellorar a retención hídrica e a estabilidade fisiolóxica. En conxunto, estes resultados non só identifican candidatos prometedores senón que tamén destacan a necesidade de que futuros estudos verifiquen a colonización efectiva e avalíen o seu comportamento en cultivos agrícolas reais, co fin de determinar o potencial destes fungos en contextos produtivos onde as interaccións planta-solo-microbiota son máis complexas.

Destas observacións despréndense liñas claras de traballo futuro. A validación nos hospedadores diana, tanto en condicións de invernadoiro como de campo, permitirá avaliar a estabilidade do efecto, a súa reproducibilidade en distintos escenarios ambientais e o seu impacto no rendemento e na calidade comercial. A estandarización dos procedementos de inoculación, incluíndo formulacións e *carriers* que favorezan o establecemento do endófito, xunto coa cuantificación molecular da colonización, debería incorporarse como parte esencial do fluxo de desenvolvemento de calquera inoculante de nova xeración.

En paralelo, requírese a confirmación estrutural dos metabolitos antifúnxicos identificados mediante técnicas complementarias, así como a caracterización detallada dos seus modos de acción tanto sobre patóxenos como sobre as plantas hospedadoras. A integración de enfoques xenómicos, transcriptómicos e metabolómicos en illados clave permitirá mapear clústeres biosintéticos, reconstruír rutas metabólicas e explicar por que cepas estreitamente relacionadas poden mostrar comportamentos tan dispares no que atinxe á promoción do crecemento, á tolerancia á seca ou á actividade antifúnxica. Así mesmo, campañas de mostraxe realizadas en diferentes anualidades facilitarán avaliar a estabilidade interanual da micobiota e a súa resposta a eventos reais de seca, contribuíndo ao deseño de estratexias de selección máis robustas e mellor adaptadas ás condicións dos sistemas IXP/DOP galegos.

Por último, o desenvolvemento de comunidades sintéticas de endófitos con funcións complementarias perfílase como unha vía particularmente prometedora para xerar inoculantes máis estables, resilientes e eficaces que as cepas individuais, ao aproveitar a cooperación metabólica, a partición de nichos e a redución das interferencias competitivas.

En conxunto, esta tese demostra que a diversidade endofítica cultivable en raíces de *B. rapa* e *C. annuum* en Galicia encerra un potencial funcional tanxible e subliña que o seu aproveitamento práctico esixe combinar evidencia ecolóxica, fisiolóxica e química, garantindo colonización, reproducibilidade e seguridade. Só a través deste enfoque integrado será posible trasladar ao campo as cepas máis prometedoras como inoculantes microbianos capaces de compatibilizar produtividade, resiliencia climática e conservación do patrimonio agroalimentario galego.

## SUMMARY

Galician agriculture is sustained by crops that, in addition to their economic relevance, constitute an essential part of the cultural and social heritage of the region. These traditional crops not only provide economic value to rural communities but also embody agricultural knowledge passed down through generations and a production model deeply rooted in the Galician landscape and identity. Among them, two emblematic species stand out: *Brassica rapa*, the basis of the Protected Geographical Indication (PGI) *Grelos de Galicia*, and *Capsicum annuum*, associated with the Protected Designation of Origin (PDO) *Pemento de Herbón*. Both horticultural systems represent true pillars of Galicia's agri-food heritage, where differentiated quality and territorial rootedness are combined with agricultural practices historically sustained by farming experience. In this sense, they represent a distinctive model within Spanish agriculture: high-quality local products tied to their origin and supported by certifications that guarantee their traceability, authenticity, and added value.

The sustainability of these systems is therefore essential for the future of Galician agriculture. Maintaining their productivity and social viability requires strategies that strengthen the adaptive capacity of crops against the emerging challenges of the twenty-first century. Among these challenges, climate change occupies a central place. This global phenomenon poses an increasing threat to the stability of agricultural production, as it alters the climatic conditions that sustain crop performance and affects the distribution and incidence of pests and diseases. Rising temperatures, irregular rainfall patterns, and the increasing frequency of extreme events such as droughts or torrential rains directly impact plant physiology, water availability, and soil dynamics. These disturbances may compromise both the yield and the quality of certified products, particularly in agricultural systems that depend on limited local resources or are managed in small family farms, as is generally the case in Galicia.

This scenario is compounded by another decisive factor: the progressive restriction of chemically synthesised plant protection products, driven by European policies aimed at reducing the environmental impact of agriculture. Increasingly stringent regulations limit the use of compounds harmful to human health, biodiversity, and water and soil quality. This reduction in the chemical arsenal available for pest and disease control has left many growers with few effective tools, prompting the need to develop sustainable alternatives.

The search for biological solutions capable of maintaining productivity and plant health without compromising the environmental and social objectives of the Common Agricultural Policy has therefore become a strategic priority within the European agroecological transition. In this context, innovation based on microbial biotechnology emerges as one of the most promising avenues for achieving more resilient and environmentally friendly agricultural systems.

Among the most relevant approaches is the manipulation and exploitation of the plant microbiome, understood as the community of microorganisms inhabiting plant tissues and surfaces, including the rhizosphere, phyllosphere, and endosphere. This complex and dynamic microbiome plays a crucial role in plant health, acting as a functional extension of plant physiology. Within this microbial assemblage, filamentous endophytic fungi merit particular attention. These microorganisms colonise the internal tissues of healthy plants without causing visible disease symptoms, and their intimate association with the host allows them to establish relationships that may range from commensalism to mutualism. In many cases, these interactions are beneficial, resulting in improvements in plant growth, water status, tolerance to biotic and abiotic stresses, or the suppression of pathogens through mechanisms such as competition, mycoparasitism, or the production of antibiotic metabolites.

However, the activity of endophytes is neither uniform nor universal. Their effect depends on a complex network of interrelated factors that include the specific compatibility between plant and fungus, environmental conditions, the background microbiome, and the physiological and metabolic traits of each strain. In fact, a single endophytic taxon may behave as a mutualist, a neutral partner, or even a latent pathogen depending on the ecological or physiological context. This functional plasticity explains the high variability of results reported across studies and highlights the need to move beyond the mere observation of beneficial phenomena towards a systematic validation of plant–endophyte interactions. Only through integrative approaches can we determine which strains exhibit stable and reproducible effects, and under what conditions and in which hosts such effects are expressed.

The translation of experimental results to field conditions currently represents one of the major bottlenecks in the development of fungal bioinoculants. Despite their potential, endophytic fungi often display variable colonization rates under real cultivation

conditions, and their efficacy may be weakened by competition with native microbial communities or by the physicochemical characteristics of soil and climate. Moreover, commercial formulations must ensure inoculant viability and its ability to establish long-lasting associations, aspects that depend on factors that are still poorly understood. For this reason, the pathway from identifying a promising isolate to its practical deployment as a biotechnological tool requires a coherent itinerary encompassing selection, characterization, and validation, considering both natural diversity and the functional and ecological stability of potential candidates.

From this perspective, studying the endophytic mycobiota associated with Galician crops offers a double opportunity. First, it enables an initial description of the cultivable native fungal diversity that coevolves with traditional agricultural systems historically adapted to the climatic and edaphic conditions of the region. These local fungi may represent a privileged source of functional and genetic traits of biotechnological interest, particularly due to their compatibility with the reference crops. Second, knowledge of this mycobiota may reveal strains with agronomic potential capable of contributing to both the biological control of pathogens and the enhancement of tolerance to abiotic stresses such as drought, an increasingly decisive factor for the performance of Galician crops. Thus, exploring these endophytic microorganisms not only expands fundamental knowledge about regional microbial biodiversity but also provides the scientific basis for their use in strategies aimed at agricultural sustainability and the preservation of Galicia's agri-food heritage.

With this goal, the working hypothesis of this thesis was that the roots of *B. rapa* and *C. annuum* host a cultivable fraction of endophytic fungi with the potential to mitigate damage caused by relevant pathogens and/or to improve plant tolerance to drought. It was also hypothesised that candidates of biotechnological interest could be identified through a combination of field prospection, functional assays, and metabolomic characterization.

The research was structured into four complementary axes. The first focused on the isolation and identification of the cultivable diversity of root endophytes in commercial plots certified under PGI/PDO schemes in Galicia, with the aim of describing their community structure and composition. The second axis addressed the biological function of the isolates through antifungal screening against key pathogens, both *in vitro* and under controlled *in planta* conditions. The third investigated the chemical basis of antibiosis via

a metabolomic study of the genus *Pseudopyrenochaeta*, used as a paradigm case study. Finally, the potential role of these endophytes under water stress was assessed by comparing different *in vitro* methodologies and prioritizing physiological validation *in planta*.

These objectives were implemented through a sequential methodological itinerary designed to advance from microbial isolation to the functional validation of candidate strains. In the first phase, root samples of *B. rapa* and *C. annuum* were collected during commercial harvesting. After surface sterilization, root fragments were plated on PDA supplemented with chloramphenicol, enabling recovery of the cultivable fraction of the endophytic fungal microbiota. Isolates were grouped by morphotype and identified via ITS barcoding (ITS1/ITS4), complemented by phylogenetic analyses when necessary.

In total, 842 isolates were obtained: 203 from *B. rapa* and 644 from *C. annuum*, grouped into dozens of morphotypes. Taxonomic assignment revealed remarkable richness: 28 taxa (23 genera) associated with *B. rapa* and 24 taxa (20 genera) with *C. annuum*, belonging to 12 and 10 orders, respectively. In both crops, the phylum Ascomycota predominated, although representatives of Basidiomycota, Mucoromycota, and, to a lesser extent, Oomycota were also detected. Recurrent genera included *Chaetomium*, *Cladosporium*, *Fusarium*, *Penicillium*, *Talaromyces*, and *Trichoderma*, forming a core of generalist root endophytes shared by both species.

Diversity analyses revealed marked structural differences between crops. The *C. annuum* communities showed a higher density of isolates per plant and a more uniform composition across plots, while *B. rapa* displayed substantial spatial heterogeneity, with numerous singleton taxa and considerable beta diversity. Rarefaction curves suggested relatively complete sampling in pepper but underrepresentation in *Brassica*, likely due to the high recovery of yeasts (e.g., *Cyberlindnera*, *Rhodotorula*), which can outcompete more slowly growing filamentous fungi on plates. These results were unexpected, as the initial hypothesis posited that the presence of glucosinolates in *B. rapa* might modulate its endophytic community structure and favor fungi adapted to these compounds. However, the data do not point towards a specialized community but rather a set of generalist endophytes. At the same time, they highlight the limitations of culture-dependent approaches for characterizing complex fungal communities and indicate the

need for more exhaustive sampling in *B. rapa* to obtain a comprehensive view of its endophytic diversity.

Building on this basis, the biocontrol potential of the isolates was explored. A screening of 146 isolates against *Rhizoctonia solani* via dual confrontation revealed two main mechanisms of antagonism: (i) overgrowth-based competition, in which the endophyte rapidly occupies space and prevents pathogen advancement; and (ii) diffusible antibiosis, visible as clear inhibition halos around the endophytic colony. Within the first group, *Trichoderma* strains strongly suppressed pathogen growth without visible halo formation; in the second, *Talaromyces*, *Chaetomium*, and particularly *Pseudopyrenochaeta* produced consistent halos against an extended panel of phytopathogens (*Fusarium oxysporum*, *Alternaria alternata*, *Botrytis cinerea*, *Sclerotinia sclerotiorum*, *Fusarium solani*, *Colletotrichum acutatum*, *Phytophthora capsici*, among others).

Based on these results, three representative candidates: two from the antibiosis group (*Pseudopyrenochaeta* and *Talaromyces*) and one from the competition group (*Trichoderma*), were selected for *in planta* assays in *Capsicum annuum* and *Brassica* sp. The strategy consisted of pre-inoculating roots with the endophyte and, after an establishment period, inoculating the pathogen onto leaves to assess disease progression. In the first experiment, strains *Pseudopyrenochaeta* (P23.03) and *Talaromyces* (BrT4.01) significantly reduced the necrotic area caused by *S. sclerotiorum* without compromising plant growth. However, in a second independent assay, the effect was not reproduced with the same consistency.

Cause analysis revealed two main methodological constraints. On the one hand, verification of colonization by re-isolation was hindered by the overgrowth of opportunistic, non-inoculated contaminants; on the other hand, molecular detection of the endophyte even in control samples indicated possible cross-contamination. This contrast between promising initial results and the difficulty in achieving robust reproducibility highlights the complexity of transferring *in vitro* antifungal activity to the *in planta* context. It also underscores the need to optimize inoculation and colonization verification protocols, incorporating molecular quantification (e.g., qPCR) and stringent contamination controls to more accurately assess endophyte persistence and its actual impact on the host.

The unique behavior of *Pseudopyrenochaeta* motivated a dedicated study integrating biological, taxonomic, and chemical aspects. With species-specific PCR primers, it was possible to discriminate *P. terrestris* from *P. lycopersici*, revealing that consistent antifungal activity corresponded to several isolates of *P. terrestris*. Extract assays confirmed that antagonism depended on diffusible extracellular metabolites and, notably, that bioactivity varied according to culture medium: extracts of *P. terrestris* grown on PDA from one supplier retained inhibition, whereas those grown on an equivalent medium from another supplier completely lost it.

This metabolic plasticity provided an opportunity for an untargeted LC–MS/MS metabolomic analysis aimed at identifying chemical signals associated with bioactivity. Comparisons across species, strains, and growth conditions revealed a set of metabolites simultaneously enriched in active *P. terrestris* samples compared with inactive ones. Among the most prominent signals, some likely corresponded to carnitine derivatives, suggesting a reprogramming of energy metabolism rather than direct antifungal action; others showed fragmentation patterns compatible with flavonoid-like scaffolds, sulphur-containing compounds, or lipophilic fractions, although the assignments remain tentative. Thioketopiperazines (TDKPs) stood out as the main candidates explaining the inhibitory activity against *R. solani* and represent a starting point for studies aimed at the chemical and functional characterization of these molecules. These results provide the basis for future structural elucidation via complementary techniques (NMR, comparison with standards) and demonstrate that the chemical determinants of antibiosis may depend on both the strain and the growth conditions.

From an ecological perspective, *Pseudopyrenochaeta* emerges as a taxon with a flexible lifestyle: known for its pathogenic role in tomato corky root, in this work it was isolated from healthy pepper roots, suggesting that some strains may behave as mutualistic endophytes capable of competing with pathogens. This plasticity highlights the need to experimentally validate the duality of its behaviour through pathogenicity assays, safety profiles, and efficacy tests in the relevant host species.

To evaluate the effect of endophytic fungi under water stress conditions, both *in planta* and *in vitro* approaches were developed. In the *in planta* assays, a screening was performed in the model plant *Arabidopsis thaliana*, comparing its physiological responses to drought when inoculated with endophytes versus non-inoculated controls.

Roots of seedlings were inoculated with 45 isolates representing 36 taxa, which were then transplanted into substrate and subjected to progressive drought over four weeks. The variables measured included stomatal conductance, relative water content (RWC), and fresh and dry biomass, all normalised to controls within the same experimental block to minimise environmental variance.

In parallel, different *in vitro* methodologies were explored to simulate water deficit. These included (i) supplementing media with polyethylene glycol (PEG 8000) in solid, liquid, and cellophane-overlay formats to reduce water potential, and (ii) increasing agar concentration to limit water availability. Among these approaches, assays based on increasing agar concentration proved the most informative and show promise as a particularly useful initial screening tool.

The *in planta* screening results showed that eighteen isolates significantly altered RWC compared with controls: five increased it, suggesting potential beneficial effects on plant water status, while thirteen reduced it. Regarding biomass, fourteen treatments differed significantly from the control, and eight promoted increases in dry weight. Among these, two isolates belonging to *Humicola* sp. and the family Pseudeurotiaceae also increased fresh weight, a combination that suggests a balance between water conservation and growth promotion.

No isolate simultaneously and robustly improved both RWC and biomass, a finding consistent with the hypothesis that mechanisms preserving tissue water (osmotic adjustment, stomatal regulation, or changes in root architecture) may not coincide with those promoting cell division or elongation. Likewise, the progression of stress, from moderate at the onset to severe at later stages, may initially favor fungi that stimulate growth under limited resources and, in more critical phases, those that improve water retention. Overall, these results identify promising candidates and underscore the need for future studies to verify effective colonization and evaluate their behavior in crop species, in order to determine the real potential of these fungi in productive contexts.

Clear lines of future work emerge from these findings. Validation in the target host plants, both under greenhouse and field conditions, will make it possible to assess the stability of the effects and their impact on yield and commercial quality. Standardizing inoculation procedures, including formulations and carriers that enhance establishment, together with

molecular quantification of colonization should be incorporated as essential components of the development pipeline for any inoculant.

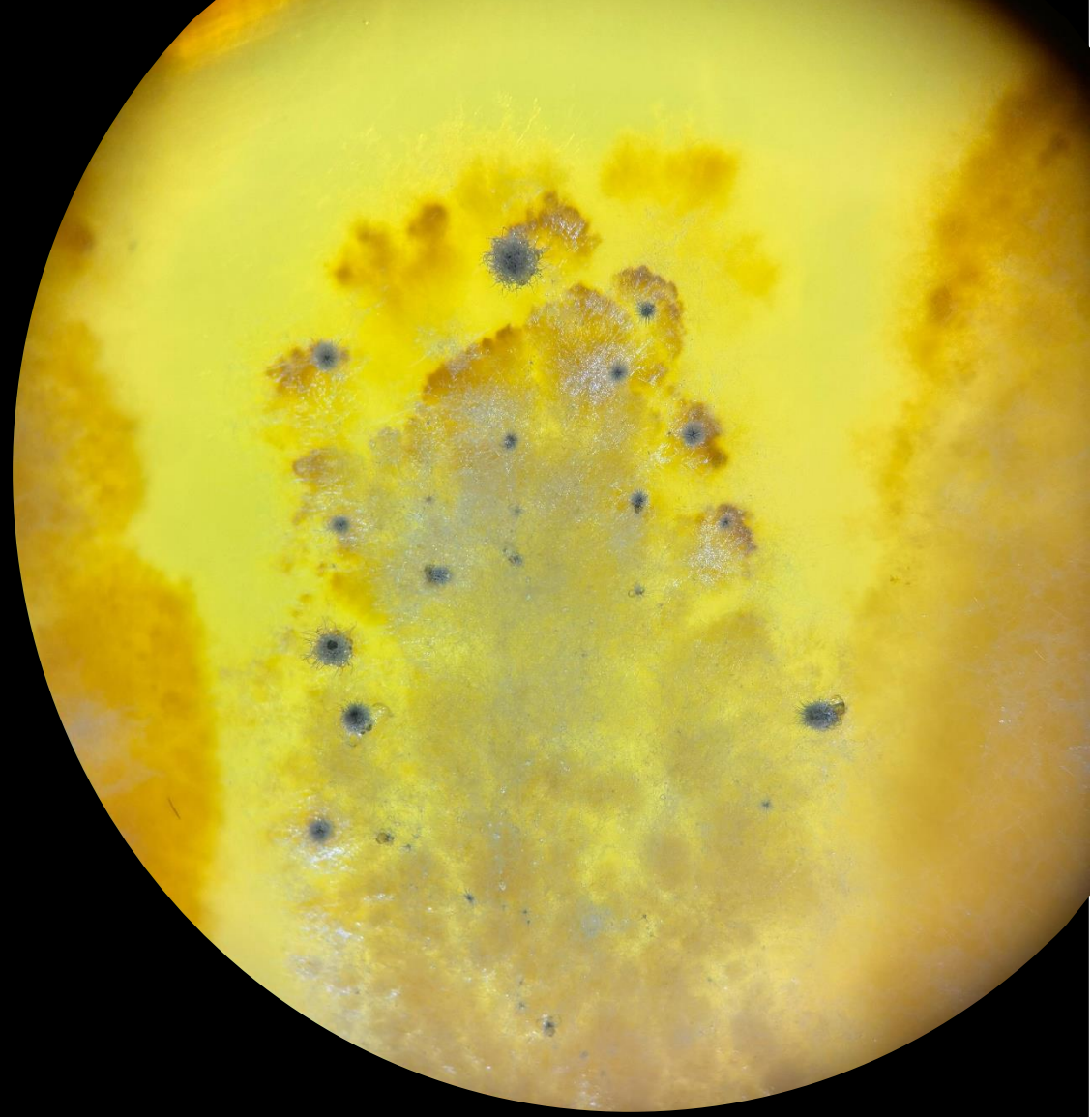
In parallel, structural confirmation of the antifungal metabolites identified via complementary techniques is required, together with characterization of their modes of action on both pathogens and host plants. Integrating genomic, transcriptomic, and metabolomic approaches for key isolates will allow the mapping of biosynthetic clusters and help explain why closely related strains can exhibit such divergent behaviors. Likewise, sampling campaigns across multiple years will facilitate evaluation of the interannual stability of the mycobiota and its response to real drought events, contributing to the design of more robust selection strategies tailored to the conditions of the Galician PGI/PDO systems.

Finally, the development of synthetic endophyte communities with complementary functions emerges as a promising avenue to generate more stable and effective inoculants than individual strains, taking advantage of metabolic cooperation and niche partitioning.

Taken together, this thesis demonstrates that the cultivable endophytic diversity present in the roots of *B. rapa* and *C. annuum* in Galicia host tangible functional potential. Its practical deployment requires combining ecological, physiological, and chemical evidence, ensuring colonization, reproducibility, and safety. Only through such an integrated approach will it be possible to transfer the most promising strains to the field as microbial inoculants capable of reconciling productivity, climate resilience, and the conservation of Galicia's agri-food heritage.







# INTRODUCTION

---

Modern agriculture faces complex challenges that threaten global food security, environmental sustainability, and the socio-economic resilience of rural communities. Addressing these issues requires a fundamental shift in productivity strategies, which involves redesigning current models to harmonize agricultural efficiency with ecological responsibility. Historically, the Green Revolution of the mid-20th century marked a turning point in agricultural development, particularly in the developing countries. The widespread adoption of high-yielding crop varieties and technological innovations, significantly boosted food production, helping to meet the demands of a rapidly growing population. However, this productivity-focused model came at a cost: the intensive use of irrigation, fertilizers, and pesticides, combined with the genetic selection of elite cultivars, led to reduced genetic diversity and diminished adaptive capacity. Crops bred for optimal conditions often sacrificed stress tolerance, making modern cultivars more vulnerable to environmental fluctuations (Gao et al., 2023). In response to emerging challenges, a new generation of strategies is being developed to improve crop adaptation. These strategies can be grouped into two main domains: genetic and microbiome-based approaches.

Genetic approaches encompass a wide range of technologies aimed at enhancing crop resilience and productivity. Genetic engineering and precision editing tools, such as CRISPR, have expanded the possibilities for introducing complex traits with high accuracy. In parallel, researchers are developing novel crops (such as perennial species or re-domesticated neglected plants) to diversify agricultural systems and promote sustainability (Gao et al., 2023). Speed breeding accelerates generation cycles under controlled conditions, while genomic selection enables the prediction of phenotypes based on molecular markers, streamlining the selection process. Additionally, the use of crop wild relatives provides a valuable genetic reservoir for traits such as drought, salinity, and heat tolerance. These traits can be introgressed through pre-breeding or advanced gene editing techniques.

Microbiome-based approaches focus on the manipulation of the plant microbiome to improve crop performance. Beneficial microbial consortia can enhance stress tolerance, nutrient uptake, and overall plant health, offering a rapid and low-input strategy to support resilience under adverse environmental conditions.

These technological advances are unfolding within a shifting regulatory landscape. In regions like Europe, legislation is increasingly restricting the use of synthetic pesticides due to their documented impacts on human health (Parrón et al., 2014), animal welfare, and ecosystem integrity (Mari et al., 2014). Compliance with stricter environmental and safety standards is reshaping agricultural practices, prompting the adoption of more sustainable inputs. Among these, plant biostimulants: substances or microorganisms applied to plants to enhance nutrient-use efficiency, abiotic stress tolerance, and crop quality traits, are gaining prominence. Integrated into modern management strategies, biostimulants offer a viable pathway to reduce chemical inputs, improve productivity, and strengthen agroecosystem resilience.

Together, these approaches reflect a multifaceted transformation in agriculture, combining ecological insight, genetic innovation, and regulatory adaptation to build more resilient and sustainable food systems.

## **1. MICROBIAL SYMBIOSIS IN PLANTS**

Plants establish complex and dynamic interactions with a wide range of microorganisms that colonize both the rhizosphere and internal plant tissues. These include fungi, bacteria, archaea, and algae (Wilson, 1995; Sánchez-Fernández et al., 2013; Hardoim et al., 2015). Depending on their location and relationship with the host, they can be classified as endophytes—organisms that inhabit internal plant tissues without causing disease—or epiphytes, which reside on the surface of plant organs such as leaves, stems, or roots. Among these groups, endophytes have received particular attention due to their intimate association with plant tissues and their potential functional roles. The definition of an endophyte has varied throughout history and remains elusive, although new proposals continue to refine the term to reduce ambiguity. Currently, the concept has evolved into a more integrative perspective that emphasizes the functional plasticity and dynamic nature of these interactions. Liao et al. (2025) define endophytes as “asymptomatic microbial partners that are intimately associated and co-inhabit within healthy internal plant tissues with the ability to confer benefits, co-evolve and alter their lifestyle depending upon plant life stages and adverse conditions” This definition emphasizes the flexible and context-dependent nature of endophytic symbiosis, which can shift according to the host's developmental stage and environmental conditions.

Within the endophyte group, fungi and bacteria are the most frequently reported. Fungal endophytes, in particular, exhibit a wide diversity of lifestyles and symbiotic relationships with plants. Among symbiotic fungi, two major types are commonly distinguished: mycorrhizal fungi and non-mycorrhizal endophytes, which include both yeasts and filamentous fungi. Mycorrhizae are mutualistic associations between specific soil fungi and plant roots, characterized by the formation of specialized structures (such as arbuscules, Hartig nets, or mantles) that facilitate nutrient exchange—particularly phosphorus and nitrogen—and improve water uptake. Notably, mycorrhizal fungi are obligate symbionts that require association with a host plant to complete their life cycle, as they depend entirely on the host for survival. In contrast, endophytic fungi colonize healthy plant tissues asymptotically and are not necessarily host-dependent. Many endophytes can survive independently in the soil or other environmental niches (Stone et al., 2000).

Beyond mycorrhizal associations, endophytic fungi encompass both yeasts and filamentous fungi, each with distinct ecological roles and functional contributions. Yeast endophytes are unicellular fungi that inhabit both intercellular and intracellular spaces of plant tissues (Isaeva et al., 2010). They are particularly abundant in the rhizosphere, where they assimilate simple organic compounds secreted through root exudates (Botha, 2006, 2011). Although yeasts are generally less abundant than bacteria or filamentous fungi in soils (Poveda et al., 2021), they can also be directly isolated from plant tissues. The most frequently reported genera include *Rhodotorula*, *Pichia*, *Candida*, and *Debaryomyces* (Madbouly et al., 2020). Beyond direct growth promotion, yeast endophytes have been shown to provide additional benefits such as protection against pathogens and improved tolerance to abiotic stress (Joubert & Doty, 2018; Poveda et al., 2021). Despite these contributions, yeast endophytes have been less extensively studied than filamentous endophytes.

Filamentous fungi are particularly relevant in agriculture due to their proven ability to stimulate plant growth, enhance resistance to environmental stress, and activate plant defense responses (Fite et al., 2023). Their taxonomic and functional diversity is extensive and shaped by factors such as host species, colonized tissue, environmental conditions, and seasonal variation. Several strains have already been formulated and are commercially available for crop protection. These fungi are phylogenetically diverse, encompassing multiple fungal lineages, with most representatives belonging to the

phylum Ascomycota. Given their agricultural relevance and broader functional characterization, from this point forward, the term “endophytic fungi” will specifically refer to filamentous endophytes.

### **1.1. PLANT–MICROBIOME INTERACTIONS: A DYNAMIC CONTINUUM**

The interaction between plants and fungi is one of the most diverse and decisive forces shaping terrestrial ecosystems, with profound ecological and agricultural implications. These associations span a continuum from mutualism to parasitism, and their outcome depends on a complex molecular dialogue between both partners.

This molecular dialogue begins with the initial recognition between plant and fungus. At the cellular level, this process involves the reciprocal detection of molecular signals on their surfaces. A central component of this process is the plant’s pattern recognition receptors (PRRs), which perceive conserved fungal structures and allow the plant to distinguish between beneficial microorganisms and potential pathogens. For symbiosis to be established, fungi must overcome the plant’s structural and chemical barriers without triggering strong immune responses, requiring mechanisms capable of modulating or temporarily suppressing basal immunity (Liao et al., 2025).

Rather than acting as passive hosts, plants influence the outcome of the interaction. Through root exudates, including sugars, amino acids, and organic acids, they can attract or select beneficial microorganisms, actively shaping the composition of their microbiome. In this way, roots function as dynamic interfaces where chemical signaling, molecular recognition, and resource exchange converge.

### **1.2. COMPATIBILITY MECHANISMS AND SPECIALIZATION**

A paradigmatic example of this dialogue is the interaction with arbuscular mycorrhizal fungi (AMF). Under nutrient-deficient conditions, especially phosphorus limitation, plants release strigolactones that stimulate spore germination and hyphal growth. In response, fungi secrete Myc factors (lipochitooligosaccharides), which are recognized by specific plant receptors, activating the common symbiosis signaling pathway (CSSP). This molecular cascade, characterized by calcium oscillations, kinases, and transcription factors, attenuates immunity and induces cellular changes that allow colonization. The process culminates in the formation of arbuscules, specialized intracellular structures that

facilitate nutrient exchange: the plant provides carbohydrates, while the fungus supplies water and minerals. However, the convergent loss of CSSP-associated genes in plant lineages such as Brassicaceae, Cyperaceae, and Proteaceae reflects the evolution of alternative nutrient acquisition strategies.

Endophytic fungi employ partially comparable mechanisms. Some secrete compatibility factors recognized by LysM-type receptor-like kinases (LysM-RLKs), which modulate immunity and facilitate colonization. In certain cases, CSSP components are also involved, although more flexibly than in mycorrhizal interactions, reflecting the functional heterogeneity of endophytic associations. These interactions, far from being neutral, can enhance plant tolerance to abiotic stress or resistance to pathogens, underscoring their ecological and agricultural relevance.

At the opposite end of the continuum, pathogenic fungi shift the balance toward defense activation. The detection of pathogen-associated molecular patterns (PAMPs) by PRRs triggers pattern-triggered immunity (PTI), characterized by the production of reactive oxygen species, phytoalexin synthesis, and programmed cell death. Pathogens counteract these responses by secreting effector proteins that suppress PTI, but plants possess intracellular receptors with NLR domains capable of detecting these effectors and activating effector-triggered immunity (ETI), typically associated with the hypersensitive response (Hou & Tsuda, 2022). The type of defense activated depends on the fungal lifestyle and the balance between jasmonic acid (JA) and salicylic acid (SA) hormonal pathways.

### **1.3. LIFESTYLE PLASTICITY AND HOST SPECIFICITY**

Beyond compatibility mechanisms, fungal lifestyle plasticity and host specificity are key aspects for understanding plant–fungus interactions. Endophytes can establish highly specific associations or generalist relationships. For example, *Epichloë* shows high specificity toward grasses, while genera such as *Colletotrichum*, *Diaporthe*, and *Fusarium* have broad host ranges. This specificity can manifest at two levels: establishment, when a fungus colonizes only certain hosts, and expression, when it colonizes several but completes its life cycle or produces reproductive structures only in a restricted group of species. Tissue chemistry, anatomical traits, and environmental conditions act as additional filters determining the degree of compatibility.

The plasticity of these interactions allows a single fungus to adopt different behaviors depending on the context. Some endophytes may behave as pathogens in certain species or under host stress conditions. For instance, *Colletotrichum magna* acts as an endophyte in non-cucurbit species but causes anthracnose in cucurbits (Sharma & Singh, 2021; Liao et al., 2025). Similarly, *Fusarium solani* can shift from endophyte to pathogen in rice (*Oryza sativa*) under high salinity (Eydoux & Farrer, 2020; Liao et al., 2025).

This behavioral shift can also extend beyond the host's lifespan. After tissue senescence, some endophytes adopt a saprotrophic lifestyle, producing degradative enzymes such as cellulases, ligninases, or chitinases that allow them to recycle nutrients. Promputtha et al. (2010) demonstrated that endophytes cultured in the lab develop enzymatic capabilities equivalent to those of saprotrophic fungi. Recent studies have confirmed that some foliar endophytes can colonize woody substrates through direct contact with leaves, evidencing their ability to alternate between endophytic and saprotrophic phases (Nelson et al., 2020; Liao et al., 2025).

Taken together, plant–fungus interactions depend on a dynamic balance between compatibility-promoting signals (symbiotic factors, CSSP, immune suppression) and defense mechanisms (PTI, ETI, SAR, JA–SA hormonal regulation). This balance is continuously adjusted according to the plant's physiological and nutritional status, the fungal lifestyle, and their shared evolutionary history. Ultimately, this molecular dialogue determines the type of relationship established, optimizing the cost–benefit of maintaining a diverse microbiota in changing environments.

## **2. EVOLUTION OF FUNGAL TAXONOMY: FROM MORPHOLOGICAL APPROACHES TO INTEGRATIVE SYSTEMATICS**

Fungal taxonomy has undergone a remarkable evolution over time, reflecting advances in the tools and concepts used to study this extraordinarily diverse kingdom. For decades, fungal classification relied almost exclusively on morphological traits, both macroscopic and microscopic. At the macroscopic level, features such as colony texture and topography (cottony, velvety, woolly, granular, flat or furrowed), pigmentation, the presence of exudates, and margin shape were considered (Figure 1). Microscopically, the observation of hyphae (septate or coenocytic, hyaline or melanized) and reproductive structures such as conidiophores, phialides, and spores provided finer taxonomic

resolution. Spore morphology, in terms of size, shape, pigmentation, and septation, was for a long time the central criterion for species identification.

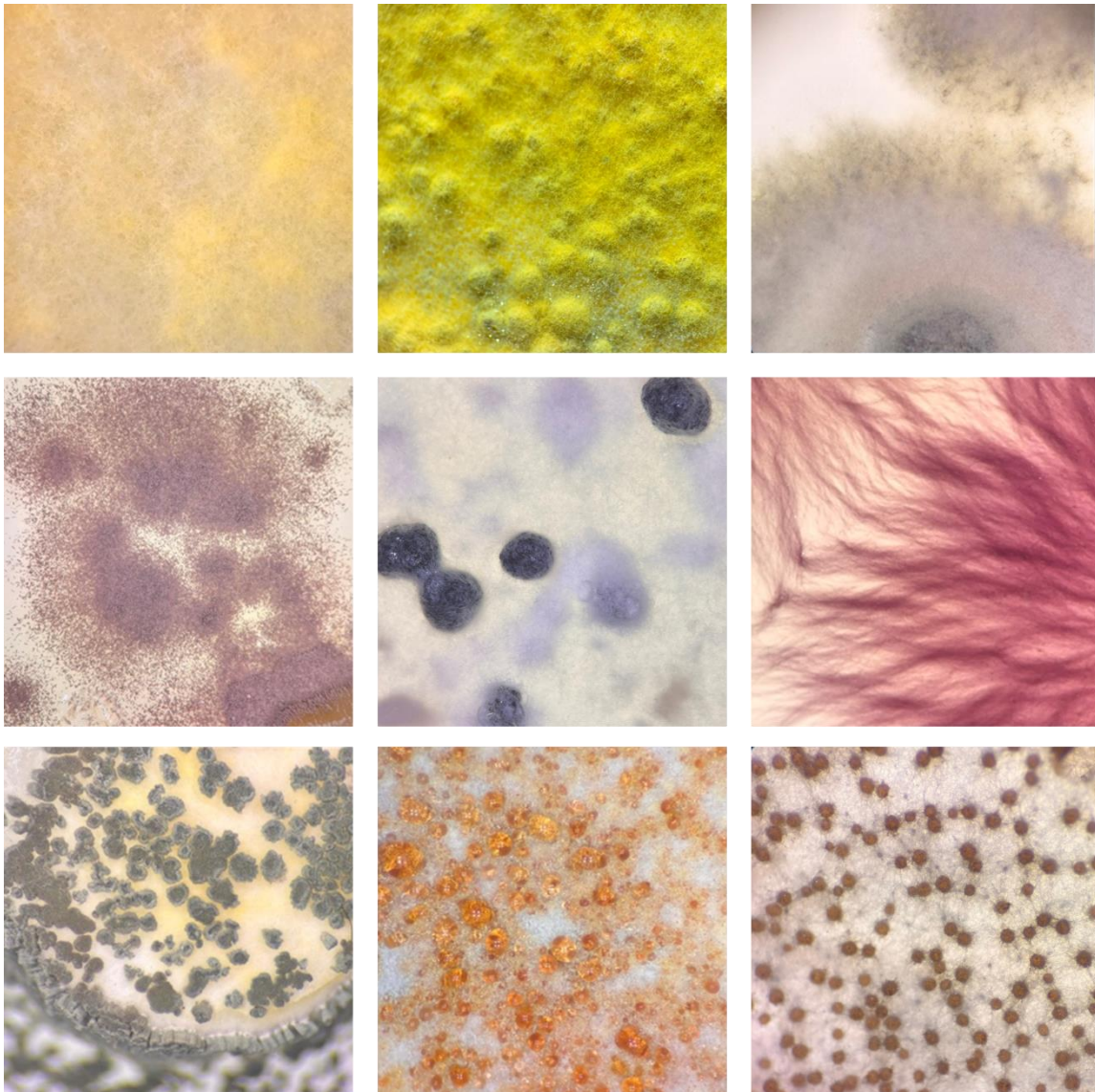


**Figure 1:** Macroscopic characteristics of endophytic colonies isolated in this study. Variations in texture, topography, pigmentation, exudate production, colony shape, and margin type are observable.

However, this approach presented significant limitations. Evolutionary convergence could result in similar structures in phylogenetically distant species, leading to misclassifications. Moreover, morphological plasticity, influenced by factors such as culture conditions, temperature, or nutrient availability, compromised the reproducibility of observed traits. Additionally, many fungi do not develop reproductive structures under *in vitro* conditions, which hinders species-level identification. These limitations are

particularly evident in cryptic species complexes, such as *Phialocephala fortinii*, which encompasses numerous genetically distinct but morphologically indistinguishable taxa.

Another historical challenge has been pleomorphism, a phenomenon in which a single organism can exhibit different morphological phases throughout its life cycle. In the asexual phase (anamorph), conidia are produced, while in the sexual phase (teleomorph), sexual spores such as ascospores or basidiospores are formed. These forms can differ so markedly that, for decades, they were classified as separate species or even genera, as seen in *Colletotrichum gloeosporioides* and *Glomerella cingulata*, or *Fusarium spp.* and its teleomorph *Gibberella spp.* This taxonomic duality prompted the “One fungus, one name” initiative, which aimed to unify fungal nomenclature and reduce confusion arising from the simultaneous use of anamorphic and teleomorphic names (Taylor, 2011).

To overcome these limitations, fungal taxonomy has progressively adopted a polyphasic or integrative approach, combining morphological traits with molecular and phylogenetic data. The development of sequencing technologies and the availability of genomic databases have revolutionized fungal systematics, enabling the resolution of cryptic and pleomorphic species and providing a more robust phylogenetic framework. Multilocus analyses have been particularly useful in clarifying evolutionary relationships. Highly conserved ribosomal sequences such as SSU (18S) and LSU (28S) help establish connections between distant lineages, while the more variable Internal Transcribed Spacer (ITS) region offers suitable resolution for distinguishing closely related species. Other coding genes, such as *TEF1- $\alpha$* , *RPB1*, *RPB2*, and  *$\beta$ -tubulin*, provide complementary information that contributes to building more consistent phylogenies. Among the available molecular markers, ITS has become established as the universal “barcode” for fungal identification. This non-coding region of ribosomal DNA is located between the genes encoding the 18S, 5.8S, and 28S ribosomal RNA subunits, and consists of two main segments: ITS1 (between 18S and 5.8S) and ITS2 (between 5.8S and 28S) (Figure 2). Because it does not encode proteins, mutations in this region do not affect organism viability, allowing for greater accumulation of interspecific variability. This high variability makes ITS a key tool for species identification, phylogenetic inference, and biodiversity analysis. In practice, ITS regions are amplified via PCR and compared against curated public databases to determine the taxonomic identity of isolates.

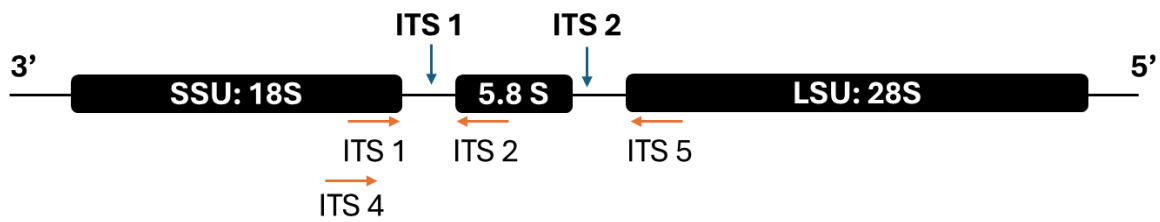


**Figure 2:** Schematic representation of gene segment of eukaryotic rDNA contains 18S (small subunit rDNA gene), 5.8S, and 28S (Large subunit rDNA gene). ITS, internal transcribed spacers 1 and 2.

In the study of endophytic fungi, the choice of taxonomic tools largely depends on the research objective. For large-scale community studies, culture-independent approaches based on high-throughput sequencing have become widely adopted, including DNA metabarcoding and shotgun metagenomics. The former, more accessible and cost-effective, relies on the amplification of a marker gene (typically the ITS region) to analyze community structure. The latter, more complex and expensive, sequences all DNA present in a sample, offering deeper insights into both taxonomic diversity and functional potential. On the other hand, culture-dependent studies remain essential when the goal is to isolate and functionally characterize cultivable endophytes. In this context, morphological grouping into “morphotypes” serves as a practical strategy for managing the large number of isolates typically recovered from a single plant. This preliminary classification is then refined through molecular identification of representative isolates, allowing for precise taxonomic resolution.

Despite the remarkable progress achieved in recent years through the application of molecular and phylogenomic tools, fungal taxonomy continues to face significant challenges. The use of whole genomes and large gene blocks has enabled the redefinition of numerous lineages, yet many fungal families still suffer from very limited or even nonexistent genetic sampling. This lack of data results in incomplete phylogenetic trees with poorly supported relationships, hindering the development of a stable and coherent view of fungal evolution.

In most cases, the available sequences for certain taxa are restricted to the ITS region.

Exclusive reliance on ITS can lead to misinterpretations. In some instances, identifications based solely on this marker have resulted in lumping (merging distinct species under a single name) or excessive splitting (dividing a single species into multiple

invalid entities). These issues are particularly common in species complexes such as *Fusarium* or *Colletotrichum*, where ITS sequences are highly similar or even identical across species. Additionally, the quality and reliability of public databases pose another major obstacle: many sequences lack a physical voucher, are not linked to viable cultures, or lack morphological descriptions and complete ecological metadata, making verification and rigorous use of these data in phylogenetic analyses difficult.

As a consequence of these limitations, numerous fungal lineages remain under revision or are undergoing reclassification. A representative example is the *Sordariomycetes*, a group in which multiple families are being redefined as multigene or whole-genome data are incorporated. Similarly, orders such as *Xylariales* have undergone significant taxonomic adjustments, with families being relocated or restructured based on molecular evidence. In parallel, there is a growing number of “dark taxa,” that is, lineages known only from environmental or ITS sequences, without associated physical specimens. These taxa cannot be formally described under the current International Code of Nomenclature for algae, fungi, and plants (ICN), creating a gap in classification and sparking ongoing debate about the need to allow sequence-based descriptions.

Fungal taxonomy faces several challenges, including insufficient genetic sampling, poor quality of some databases, technical and economic limitations in obtaining biological material and reliable sequences, and restrictions imposed by the nomenclatural system. These obstacles hinder species delimitation and the reconstruction of fungal evolutionary history. To overcome them, an integrative approach is proposed, combining molecular, morphological, ecological, and chemical evidence. The use of multigene sequences and whole genomes can improve phylogenetic resolution. Moreover, it is crucial to strengthen public databases through verified identifications, physical vouchers, complete metadata, and regular updates, in order to build a robust and representative fungal phylogeny.

## **2.1. CLASSIFICATION OF ENDOPHYTIC FUNGI: PHYLOGENY**

Endophytic fungi are found across several fungal phyla, but the vast majority belong to Ascomycota and, to a lesser extent, Basidiomycota. Ascomycota constitutes the largest fungal phylum and accounts for up to 90% of endophytic fungi reported in most studies. Members of this group are characterized by septate hyphae and the production of endogenous ascospores within asci. Three main subphyla are recognized within

Ascomycota: Taphrinomycotina, Saccharomycotina, and Pezizomycotina. The first represents an early-diverging lineage with limited relevance to filamentous endophytes, whereas Saccharomycotina is primarily composed of yeasts. By contrast, Pezizomycotina harbors the majority of filamentous endophytes and is therefore the main focus of taxonomic and ecological research. Within this subphylum, several classes concentrate the most representative endophytes. Sordariomycetes includes the orders Diaporthales, Hypocreales, Microascales, and Sordariales, encompassing emblematic genera such as *Pestalotiopsis* and *Colletotrichum*. Within Hypocreales, *Epichloë* and *Neotyphodium* (Clavicipitaceae) are particularly important as grass symbionts, while entomopathogenic fungi such as *Beauveria bassiana* and *Metarhizium brunneum* have also been reported as endophytes with potential applications in biological control. Dothideomycetes represents another major class, including orders such as Capnodiales and Pleosporales, and genera like *Alternaria*, *Phialocephala*, and *Neodidymelliopsis*. The class Leotiomycetes is especially relevant for containing the order Helotiales, which harbors numerous dark septate endophytes, whereas Eurotiomycetes includes the order Eurotiales, with genera such as *Aspergillus* and *Penicillium*, of great industrial and ecological importance. The taxonomy of these latter groups is being progressively clarified through multi-locus phylogenetic analyses involving markers such as RPB1, RPB2, and CaM.

Although less diverse than Ascomycota in this ecological niche, Basidiomycota also contributes relevant endophytes, particularly within the orders Sebaciniales and Tremellales. It is also worth mentioning the Mucoromycota phyla, as they fulfil specialised ecological roles and can play important functions in plant–fungus symbiosis. In particular, the Glomeromycotina subdivision forms arbuscular mycorrhizae known for their role in nutrition and stress tolerance in most terrestrial plants.

## 2.2. CLASSIFICATION OF ENDOPHYTIC FUNGI: ECOLOGICAL PERSPECTIVE

The ecological dimension has gained significant relevance in the taxonomy of endophytic fungi, highlighting that their classification is not solely based on morphological criteria, but also on functional and evolutionary aspects. A widely accepted framework in this field was proposed by Rodríguez et al. (2009), who established two major functional categories: clavicipitaceous endophytes (C-endophytes) and non-clavicipitaceous endophytes (NC-endophytes). This distinction is based on transmission mode, host range, and colonization patterns.

Clavicipitaceous endophytes, grouped under Class 1, belong to the family Clavicipitaceae (order Hypocreales, Ascomycota) and include genera such as *Balansia*, *Claviceps*, and *Epichloë*. These fungi form highly specialized and stable associations with grasses, characterized by systemic colonization of leaves, stems, and rhizomes, such that each plant typically harbors a single dominant genotype. Their transmission is primarily vertical, via seeds, although in some cases it may be complemented by horizontal mechanisms. Within this class, three functional types are recognized: Type I, associated with symptomatic relationships, sexual reproduction, and dispersal via ascospores (horizontal transmission); Type II, which combines sexual and asexual reproduction with mixed transmission; and Type III, characterized by asymptomatic relationships, asexual reproduction, and vertical transmission.

In contrast, non-clavicipitaceous endophytes encompass Classes 2, 3, and 4. This group includes cultivable fungi with broad phylogenetic diversity, mainly within Ascomycota, such as *Colletotrichum*, *Fusarium*, and *Diaporthe*, as well as some Basidiomycota representatives. Unlike clavicipitaceous fungi, they exhibit a much wider host range, including angiosperms, gymnosperms, ferns, and even non-vascular plants. Their transmission is predominantly horizontal, through spores, although vertical mechanisms may also occur. Class 2 includes endophytes that colonize both aerial and subterranean tissues (roots and rhizomes), with mixed transmission; Class 3 is restricted to aerial tissues, mainly leaves and stems, and is characterized by high diversity and horizontal transmission; while Class 4 corresponds to dark septate endophytes (DSE), associated with roots and distinguished by melanized hyphae.

This classification underscores the diversity of evolutionary and ecological strategies that endophytic fungi have developed to interact with plants, ranging from specific and stable associations, such as those between clavicipitaceous fungi and grasses, to opportunistic and generalist interactions typical of non-clavicipitaceous fungi. However, the origin and boundaries of these groups remain ambiguous, casting doubt on the validity of the proposed framework, as many isolated endophytes cannot be clearly assigned to these categories, and molecular data do not always support this division.

### 2.3. TAXONOMIC EVOLUTION OF THE GENUS *PSEUDOPYRENOCHAETA*

The transition from classical morphological identification to integrative, multi-locus systematics has fundamentally reshaped our understanding of many fungal lineages. The historical challenges such as morphological ambiguity, the presence of cryptic species complexes, and the limitations of defining strict ecological categories, are perfectly illustrated by specific taxa that have undergone continuous reclassification. A paradigmatic case of this taxonomic evolution, and a focal organism of this study, is the genus *Pseudopyrenochaeta*.

*Pseudopyrenochaeta* is taxonomically classified within the phylum Ascomycota, class Dothideomycetes, and order Pleosporales. This order is the largest within the class, encompassing over 4,700 species across 332 genera and 53 families. Delving into its taxonomy is complex, as it remains a subject of debate (Valenzuela-López et al., 2018). The genus *Pseudopyrenochaeta* emerged because of the profound revision of the coelomycetous fungi. These fungi constituted an artificial group, considered anamorphic (those lacking a known sexual stage), characterized by the production of conidia within closed structures called conidiomata, typically pycnidia (spherical, ostiolate) or acervuli (flattened).

The taxonomy of this group was considered imprecise due to limited morphological differentiation, the rarity of sexual states, and the rapid loss of fertility in culture. For decades, the term “coelomycetes” was used as a broad category to group fungi with similar morphological features, many of which are important phytopathogens. Among the most representative genera were *Phoma*, *Ascochyta*, *Coniothyrium*, and *Pyrenochaeta*, all characterized by ostiolate pycnidia and hyaline conidia.

The advent of molecular phylogenetics clarified the evolutionary relationships within this group, revealing that coelomycetes form a polyphyletic assemblage, meaning that they are composed of organisms that do not share an exclusive common ancestor. As a result, the concept of coelomycetes has been relegated to a morphological description, while current taxonomic classification is based on more precise molecular criteria (de Gruyter et al., 2010; de Gruyter et al., 2013; Wanasinghe et al., 2017). This shift led to the reassignment of many species to new families and orders, and the establishment of several

new genera within *Pleosporales*, such as *Didymellaceae*, *Leptosphaeriaceae*, *Phaeosphaeriaceae*, and *Cucurbitariaceae*.

Within this context, certain species with *Pyrenochaeta*-like morphology (setose pycnidia, hyaline conidia, phialidic conidiogenesis), previously classified under *Phoma* sect. *Paraphoma* or even *Pyrenochaeta*, were reassigned (Gruyter et al., 2013). Some of these did not fit phylogenetically within *Pyrenochaeta sensu stricto* or *Pyrenochaetopsis*, leading to the creation of new families and genera to accommodate them. Among these, *Pseudopyrenochaetaceae*, including the genus *Pseudopyrenochaeta*, was established (Valenzuela-López et al., 2018).

Prior to its reclassification, the genus *Pseudopyrenochaeta* was known under the name *Pyrenochaeta lycopersici*. The two species described by Valenzuela et al. (2018), currently recognized as *Pseudopyrenochaeta terrestris* and *Pseudopyrenochaeta lycopersici*, were delineated based on differences in four loci: LSU, ITS, tub2, and rpb2. Until then, both had been considered variants of *Pyrenochaeta lycopersici*, referred to as Type 1 and Type 2, respectively.

These two types were defined using ITS-rDNA, RAPD (Random Amplified Polymorphic DNA), and AFLP (Amplified Fragment Length Polymorphism) analyses (Sugiura et al., 2003; Infantino et al., 2003). Later, in 2005, Infantino & Pucci developed a PCR-based assay for the detection and identification of the two *Pyrenochaeta lycopersici* types. The primers were designed based on ITS sequence differences between the two types: Plyc1-F/Plyc1-R, which amplified a specific 147 bp band only in Type 1 isolates, and Plyc2-F/Plyc2-R, which produced a 209 bp band in Type 2 isolates. This tool enabled rapid differentiation of both types in the laboratory. However, it was not until the work of Testen et al. (2023) that *P. terrestris* and *P. lycopersici* were explicitly linked to the former Type 1 and Type 2 of *Pyrenochaeta lycopersici*, respectively.

#### **2.4. PSEUDOPYRENOCHAETA AND ITS INTERACTION WITH PLANTS: FROM PATHOGENESIS TO ENDOPHYTIC PLASTICITY**

Having clarified the taxonomic boundaries and evolutionary history of *Pseudopyrenochaeta*, it is equally important to address its functional ecology and the nature of its associations with plant hosts. As discussed in previous sections, plant–fungal interactions span a highly dynamic continuum. Historically, however, knowledge about

the genus *Pseudopyrenochaeta* has focused mainly on its role as a soilborne pathogen, particularly as the causal agent of tomato corky root rot, a disease that severely affects greenhouse production. In this context, most studies have been carried out using tomato as the host (Aragona et al., 2014; Infantino et al., 2015; Infantino & Pucci, 2005; Testen et al., 2023). However, this view is partial and limits our understanding of the range of interactions that this fungus can establish with different plants.

A turning point in the study of *Pseudopyrenochaeta* was the genome assembly performed by Aragona et al. (2014). Their analysis revealed that *P. lycopersici* is phylogenetically more closely related to hemibiotrophic and necrotrophic fungi, such as *Leptosphaeria*, *Pyrenophora* and *Stagonospora*, than to obligate biotrophs such as *Blumeria* or *Ustilago*. In addition, gene families associated with host–pathogen interactions were identified, including genes involved in nutrient uptake, fungicide detoxification, and plant cell wall degradation, confirming that a substantial portion of its genome is oriented toward pathogenic activity. On this basis, it was proposed that *P. lycopersici* displays a hemibiotrophic lifestyle (Aragona et al., 2014).

However, as established previously regarding fungal lifestyle plasticity, these behaviors depend on host genetic compatibility and immune responses, on the environmental context (available nutrients, microbiome composition) and on the regulation of key effectors (Redkar et al., 2022; De Silva et al., 2016). Accordingly, current evidence indicates that *Pseudopyrenochaeta* cannot be understood exclusively as a tomato pathogen. Although it has been reported in multiple solanaceous and cucurbitaceous hosts, symptom expression is highly host-dependent. In tomato, melon, and safflower, infection typically leads to the development of corky roots, whereas in tobacco, spinach, and pepper it results only in root darkening. Notably, in pepper there is no recent evidence identifying *Pseudopyrenochaeta* as a significant phytosanitary concern (Clergeot et al., 2012; Infantino et al., 2015; Testen 2023). Moreover, *Pseudopyrenochaeta* has been described in beneficial contexts: as an endophyte improving cadmium tolerance in *Pinus* (Zhou et al., 2024) or as an antagonist of *Phytophthora infestans* in potato (El-Hasan et al., 2022).

Taken together, these findings highlight the remarkable ecological plasticity of *Pseudopyrenochaeta*, whose lifestyle can encompass endophytism and parasitism depending on the identity of the host.

### 3. FUNGAL SECONDARY METABOLITES AND METABOLOMICS: FROM CHEMICAL DIVERSITY TO BIOTECHNOLOGICAL POTENTIAL

Fungi are among the most prolific sources of secondary metabolites, compounds that, while not essential for growth or development, play key ecological roles in communication, competition, host colonization, and nutrient acquisition. It is estimated that over 70,000 microbial secondary metabolites have been described, with approximately 33,500 exhibiting bioactive properties. Notably, nearly half of these (47%) are of fungal origin (Bills & Gloer, 2017).

The pharmaceutical significance of these compounds is profound, as exemplified by molecules that have transformed human medicine, including penicillin (*Penicillium chrysogenum*), cephalosporins (*Acremonium*), lovastatin (*Aspergillus terreus*), and cordycepin (*Cordyceps militaris*). In an agricultural context, fungal secondary metabolites offer a sustainable alternative to synthetic pesticides. Compounds such as gliotoxin (*Trichoderma*), beauvericin, and destruxins (*Beauveria*, *Metarhizium*) have demonstrated significant potential as biocontrol agents against phytopathogens and insect pests (Wu et al., 2018; Zaid et al., 2022). Furthermore, recent evidence suggests these metabolites can also enhance plant tolerance to abiotic stresses, such as drought (Díaz-Urbano et al., 2025). Beyond their biological efficacy, fungi present distinct industrial advantages as production platforms: they are amenable to large-scale cultivation in bioreactors, accessible for genetic manipulation, and exhibit remarkable metabolic plasticity.

Within this framework, metabolomics has emerged as a powerful tool for exploring fungal chemical diversity and identifying metabolites with ecological functions and biotechnological applications. Metabolomics is defined as the comprehensive study of the complete set of metabolites present in an organism at a given time, representing the closest molecular signature to the cellular phenotype. It provides a direct readout of biochemical activity in response to internal or environmental conditions.

Two main approaches are employed: targeted metabolomics, which focuses on the precise quantification of known metabolites using reference standards, and untargeted metabolomics, which aims to globally characterize the metabolome and identify novel compounds. While both approaches are complementary, untargeted metabolomics is

particularly valuable in discovery-driven studies, as it enables the elucidation of chemical diversity and the exploration of unexpected metabolic pathways (Allwood et al., 2021).

Metabolomic characterization relies primarily on analytical platforms that combine chromatography with mass spectrometry (MS). Liquid chromatography coupled with mass spectrometry (LC-MS) is the most widely used technique, suitable for detecting a broad range of polar and thermolabile compounds. Gas chromatography-mass spectrometry (GC-MS), on the other hand, is ideal for small, volatile metabolites. These techniques are often used in tandem to provide complementary coverage of the metabolome.

One of the main challenges in metabolomics is the unequivocal identification of detected metabolites, which requires additional structural information obtained through tandem mass spectrometry (MS/MS). This technique selectively fragments precursor ions and analyzes their characteristic fragmentation patterns, generating spectra that serve as structural “fingerprints.” These data allow for molecular identification with varying levels of confidence: from confirmation using pure standards (Level 1), to putative identification via spectral libraries (Level 2), and tentative classification based on molecular formulas (Levels 3–4).

Thanks to these approaches, untargeted metabolomics based on HPLC-MS/MS has become an essential method for investigating the chemical diversity of endophytic fungi and uncovering compounds with antifungal or biocontrol potential. The integration of high-resolution analytical techniques with advanced bioinformatic workflows enables not only the identification of known metabolites, but also the discovery of novel analogs with promising applications in agriculture

#### **4. FUNGAL ENDOPHYTES IN THE MODULATION OF PLANT STRESS TOLERANCE**

Throughout their development, plants are continuously exposed to environmental fluctuations that influence their life cycles. Optimal growth occurs within relatively narrow ranges of environmental conditions, beyond which physiological damage may arise. Environmental stresses are thus defined as any alteration in external conditions that negatively affects plant development. Broadly, these stresses can be classified into two categories: abiotic and biotic. Within an agricultural context, the potential yield of a crop

refers to the maximum productivity achievable under conditions for which the crop is adapted, assuming no limitations in water or nutrients and effective control of pests and diseases. In practice, however, average yields typically fall short of this potential due to the combined effects of abiotic and biotic stresses, a phenomenon known as the yield gap. On average, biotic stresses are estimated to reduce production by 20–40%, while abiotic stresses generally have a greater impact, accounting for 30–60% of losses (Zhang et al., 2022).

Today, agriculture faces an additional and increasingly pressing challenge: climate change. It threatens agricultural systems by altering farming structures, degrading agroclimatic resources, and increasing the frequency and severity of agrometeorological disasters. Numerous studies indicate that rising temperatures, shifts in precipitation patterns, and extreme climatic events (such as droughts and soil salinization) are likely to adversely affect crop yields. Virtually, all climatic parameters have experienced significant changes in recent decades. Global temperatures increased by 0.87 °C between 1850 and 2015, with projections suggesting a further rise of 0.2 °C per decade during the current century. Atmospheric CO<sub>2</sub> concentrations have risen by 40% since the pre-industrial era, currently reaching 410 ppm, compared with the previously optimal range of 280–300 ppm. These changes are already impacting agriculture, leading to reduced productivity and the migration of crops toward higher latitudes and elevations.

Moreover, climate change is expected to significantly alter the dynamics of crop pests and diseases, while contributing to pollinator losses. Shifts in environmental conditions are generating new ecological niches, allowing pests and pathogens to establish in regions previously unsuitable for their survival. To compensate for yield reductions caused by climatic events and increasing pest and disease pressures, farmers often intensify input use. However, this approach reduces the economic profitability of harvests and simultaneously increases the environmental footprint of agricultural production. These trends highlight the urgent need to enhance crop resilience and adapt production systems to increasingly adverse environmental conditions.

In this context, manipulation of the plant microbiome has emerged as a promising strategy to support development and enhance resilience against both biotic and abiotic stresses. These symbiotic microorganisms can improve plant growth and resilience by promoting nutrient acquisition, modulating hormone levels, and inducing systemic resistance against

pathogens and pests. By harnessing these natural interactions, endophytes offer a sustainable strategy to improve crop performance and stability in increasingly stressful agricultural environments.

#### **4.1. FUNGAL ENDOPHYTES AND PATHOGEN CONTROL**

Soilborne plant pathogens, including fungi and oomycetes, represent a major threat to horticultural production worldwide, causing substantial yield losses and compromising crop quality. It is estimated that plant diseases account for more than 20% of yield losses in key food and commercial crops worldwide (Hossain et al., 2024). Their persistence in soil, broad host range, and adaptability to diverse environmental conditions make them particularly difficult to manage. In addition to field losses, fungal pathogens are responsible for significant postharvest deterioration in grains, fruits, and vegetables, and can produce mycotoxins that are harmful to both human and animal health (Pelaez et al., 2000).

In response to these persistent agricultural challenges, endophytic fungi are increasingly recognized as key biocontrol agents in sustainable agricultural systems. Their ability to colonize plant tissues without causing apparent damage, combined with their potential to inhibit pathogen development, makes them promising allies in the fight against plant diseases. Unlike chemical fungicides, endophytes offer an ecological and long-lasting alternative that aligns with integrated pest management (IPM) strategies (Mousa & Raizada, 2013; Lugtenberg et al., 2016).

The biocontrol activity of endophytic fungi is based on a wide range of mechanisms that restrict or suppress pathogen development within the host plant, which can be broadly divided into direct and indirect mechanisms. Direct mechanisms involve an immediate action on the biotic threat, including competition for space and nutrients, colonization of plant tissues that prevents pathogen establishment, or the secretion of antimicrobial metabolites and lytic enzymes. The nature of these antimicrobial metabolites is diverse and includes bioactive secondary metabolites such as alkaloids, flavonoids, terpenoids, polyketides, phenolic compounds, and peptides that directly inhibit pathogen growth, sporulation, or viability (Liarzi et al., 2016; Macías-Rubalcava et al., 2018; Fontana et al., 2021; Khruengsai et al., 2021). Additionally, certain endophytes exert antagonistic effects through mycoparasitism, actively attacking pathogenic fungi by producing toxins and

hydrolytic enzymes, as well as through antibiosis, releasing volatile or soluble compounds that suppress pathogen development (Latz et al., 2018; Fontana et al., 2021).

Indirect mechanisms, by contrast, involve the modulation of plant defenses and physiological responses rather than direct inhibition of the pathogen. Endophytic fungi can induce systemic resistance, either as systemic acquired resistance (SAR) or induced systemic resistance (ISR), by modulating key hormonal pathways such as salicylic acid (SA), jasmonic acid (JA) or ethylene (ET). These responses lead to the accumulation of pathogenesis-related proteins, phytoalexins, and lignin, as well as the generation of reactive oxygen species (ROS) and the reinforcement of structural barriers (Latz et al., 2018; Fontana et al., 2021; Adeleke et al., 2022). Activation of these defense pathways is mediated by fungal molecules, including effectors (cell wall components such as chitin and  $\beta$ -glucans, and hydrolytic enzymes like xylanase, cellulase, and chitinase) that are recognized by plant pattern recognition receptors (PRRs) and trigger basal immunity (PTI) (Latz et al., 2018; Druzhinina et al., 2011). Beyond defense priming, endophytes can also improve nutrient uptake and assimilation, indirectly strengthening plant vigor and its capacity to withstand biotic stress.

Direct and indirect strategies often operate simultaneously, generating synergistic effects that enhance plant health and resilience against infection (Adeleke et al., 2022). Numerous studies in agricultural systems have demonstrated the role of endophytic fungi in enhancing disease resistance in specific crops. *Trichoderma*, *Fusarium*, and *Piriformospora* are among the most studied genera which have shown efficacy against pathogens such as *Sclerotinia sclerotiorum*, *Rhizoctonia solani*, *Phytophthora* spp., *Meloidogyne* spp., and *Fusarium oxysporum* (Fontana et al., 2021; Adeleke et al., 2022). For instance, *Trichoderma* spp. can parasitize fungal pathogens, nematodes or/and induce systemic resistance in crops like tomato, cucumber, maize and turnip (Shoreh et al., 2007; Ibrahim et al., 2012; Latz et al., 2018). In pepper, reports remain relatively scarce; nevertheless, Paul et al. (2012) demonstrated that endophytic isolates of *Colletotrichum acutatum*, *Fusarium oxysporum*, and *Penicillium* spp. significantly inhibited the mycelial growth of pathogenic fungi in dual culture assays. Non-pathogenic strains of *Fusarium* spp. have demonstrated the ability to compete for root niches and activate hormonal defense responses (Fontana et al., 2021). *Piriformospora indica*, meanwhile, has been extensively studied for its capacity to induce systemic resistance and abiotic stress

tolerance in crops such as barley, wheat, rice, and banana (Kumar et al., 2012; Waller et al., 2005; Cheng et al., 2022).

Currently, commercial products based on these endophytic fungi are available, underscoring their applied potential in integrated management programs. However, their efficacy can vary depending on the pathosystem, environmental conditions, and host genotype, highlighting the need for precise strain characterization and understanding of their modes of action. The integration of molecular tools such as transcriptomics, proteomics, and metabolomics is advancing our knowledge of these complex interactions and facilitating the selection of strains with high biotechnological potential (Fontana et al., 2021). In this context, endophytic fungi are emerging as essential tools for developing agriculture that is more resilient, sustainable, and adapted to the challenges of climate change.

#### **4.2. FUNGAL ENDOPHYTES AND ABIOTIC STRESS**

Abiotic stress factors, such as drought, salinity, and extreme temperatures, pose major challenges to contemporary agricultural systems. Their impact is expected to intensify due to climate change and global warming (Cramer et al., 2022). In response to abiotic stress, plants have developed a variety of strategies that can be broadly categorized into escape, avoidance, and tolerance mechanisms.

Escape involves completing the life cycle before the onset of stress, allowing sensitive developmental stages to occur under favorable conditions. This strategy is common in annual species and typically applies to recurrent stressors; however, it is far less effective under irregular or sporadic extreme events, conditions expected to become more frequent with climate change. Avoidance refers to the ability to maintain favorable internal conditions despite external stress, achieved through morphological and physiological adaptations like deep root systems, reduced leaf area, altered stomatal behavior, or selective ion exclusion. Tolerance, on the other hand, enables plants to sustain metabolic and physiological functions under adverse conditions. This includes mechanisms such as osmotic adjustment, antioxidant defense, membrane stability, and hormonal regulation.

Among these stressors, drought is one of the most pervasive and damaging factors affecting modern agricultural systems. The expected intensification of drought events due to climate change, characterized by increased temperatures and irregular precipitation

patterns, poses a growing threat to crop productivity (IPCC, 2023). Plants exposed to water deficit experience a cascade of physiological and biochemical disturbances. Visible symptoms include wilting due to turgor loss, leaf rolling, chlorosis, reduced growth, and impaired yield. At the physiological level, water stress triggers stomatal closure, restricting CO<sub>2</sub> uptake and photosynthesis, and inducing the accumulation of compatible solutes to maintain osmotic balance. Concurrently, the imbalance in cellular homeostasis leads to the generation of reactive oxygen species (ROS), causing oxidative damage to membranes and organelles (Hardoim et al., 2015; Sharma & Singh, 2021).

Given this vulnerability, endophytic fungi have emerged as promising allies for improving plant resilience. Beyond the plant's intrinsic responses, studies demonstrate that endophytes can mitigate the deleterious effects of drought by inducing systemic tolerance mechanisms in their hosts (Dastogeer & Wylie, 2017; Pratap et al., 2016). These beneficial effects arise through several complementary pathways acting at morphological, biochemical, and molecular levels.

Hormonal modulation represents a fundamental mechanism. Endophytes can produce phytohormones or modulate plant endogenous levels to regulate growth and stress responses. Many endophytes produce indole-3-acetic acid (IAA) or gibberellins (GAs), stimulating root system development and thereby improving water uptake (Waqas et al., 2012; Khan et al., 2012). Others alter levels of abscisic acid (ABA), salicylic acid (SA), or jasmonic acid (JA), fine-tuning the plant's response to stress. For instance, *Penicillium resedanum* enhances the growth of *Capsicum annuum* under drought and salinity specifically by regulating ABA and GA levels (Khan et al., 2013; Sharma et al., 2021).

Beyond hormonal signaling, endophytes also regulate osmotic adjustment, thereby ensuring the maintenance of cellular turgor. This is achieved via the accumulation of compatible solutes such as proline, soluble sugars, and amino acids, which stabilize proteins and membranes under dehydration (Pratap et al., 2016; Sharma & Singh, 2021). This effect has been documented in cereals and legumes inoculated with *Chaetomium globosum*, *Trichoderma hamatum*, or *Neotyphodium coenophialum* (Cong et al., 2015; Bae et al., 2009). In barley inoculated with *P. indica*, differential accumulation of amino acids such as phenylalanine, tyrosine, isoleucine, and glutamine suggests a reconfiguration of nitrogen metabolism aimed at cellular protection (Ghaffari et al., 2019).

Complementing osmotic adjustment, endophytes can interact with plant's defense against oxidative stress. They boost the activities of enzymes such as superoxide dismutase (SOD), catalase (CAT), and peroxidases (POD), which neutralize the ROS generated during stress (Marulanda et al., 2009; Johnson et al., 2014; Yan et al., 2019; Sadeghi et al., 2022). For example, in barley, colonization by *Piriformospora indica* has been associated with increased expression of ferredoxins, thioredoxins, and glutathione-S-transferases, contributing to redox homeostasis. Additionally, some endophytes produce bioactive metabolites with osmoprotective or antioxidant properties that may act systemically within the plant (Rodriguez et al., 2009; Hardoim et al., 2015). Such compounds can stabilize membranes, scavenge free radicals, or function as chemical signals triggering plant defense responses.

In addition to preserving cellular integrity, fungal endophytes play a crucial role in sustaining primary physiological functions, particularly photosynthesis. As reported in wheat and Chinese cabbage, endophytes increase chlorophyll content and protect photosynthetic enzymes from oxidative damage (Sun et al., 2010; Qiang et al., 2019). Furthermore, many species enhance nutrient availability by solubilizing phosphorus or mobilizing iron (siderophores) under limiting conditions, supporting overall plant fitness (Hardoim et al., 2015; Dastogeer & Wylie, 2017).

Notably, endophytes often exhibit multi-layered modes of action. For example, in tomato, *Diaporthe atlantica* enhances photosynthetic efficiency, nutrient uptake, proline accumulation, and antioxidant responses under drought and salt stress (Pereira et al., 2023). Similarly, in barley, colonization by *P. indica* reprograms photosynthetic and energy metabolism, maintaining photosystem II activity under severe drought and heat stress (Reza et al., 2019). Finally, novel survival strategies such as the induction of autophagy and cellular recycling have been proposed. In barley colonized by *P. indica*, positive regulation of exocyst complex components such as EXO70B1 has been observed, which are involved in autophagosome formation and adaptive stress responses (Reza et al., 2019).

Altogether, the plant–endophyte symbiosis represents a promising biotechnological strategy to improve plant resilience to abiotic stress. Understanding the underlying mechanisms, from cellular signaling to metabolic reprogramming, is essential for developing sustainable agronomic applications in the context of climate change.

## 5. AGRICULTURE CONTEXT

Galician agriculture plays a fundamental role in the region's economy and cultural identity, characterized by a strong connection to high-quality local products. Among these emblematic crops, two stand out for their agronomic, economic, and cultural importance: *Grelos de Galicia* (*Brassica rapa*) and *Pementos de Herbón* (*Capsicum annuum*), both protected by European quality labels, the Protected Geographical Indication (PGI) and the Protected Designation of Origin (PDO), respectively. These crops not only have significant economic value but are also deeply rooted in Galician culinary tradition, representing a bridge between biodiversity, local knowledge, and regional identity.

### 5.1. *BRASSICA RAPA*: ORIGIN, DIVERSITY AND AGRICULTURAL RELEVANCE

The family Brassicaceae constitutes one of the largest and most diverse botanical groups, encompassing over 321 genera and approximately 3,660 species distributed worldwide (Raza et al., 2020). It includes species of major scientific interest, such as *Arabidopsis thaliana*, and numerous crops of high economic value for human and animal nutrition as well as for industrial applications (Warwick, 2011). Among these, *Brassica* crops (including cabbage, broccoli, cauliflower, kale, brussels sprouts, and turnips) are particularly prominent. Their global production in 2024 exceeded 70 million tons, positioning Europe as the second largest producer worldwide, after Asia (FAOSTAT, 2025). Beyond its agronomic and cultural value, Brassicaceae also attracts considerable scientific attention for its phytochemical composition. Members of the family are characterized by their richness in glucosinolates (GSLs), amino acid-derived secondary metabolites that, upon hydrolysis, yield biologically active compounds such as isothiocyanates (ITCs). These molecules play a pivotal role in plant defence against herbivores and pathogens and have been extensively studied for their insecticidal, antimicrobial, anti-inflammatory, and anticancer activities.

Within this family, the genus *Brassica* occupies a central position due to its exceptional agricultural, nutritional, and economic importance. It comprises around 37 species cultivated for diverse purposes, including vegetable, oilseed, and forage production. The most representative species: *B. oleracea*, *B. rapa*, *B. napus*, *B. nigra*, *B. juncea*, and *B. carinata*, are closely related from an evolutionary standpoint. Their relationships are summarized by U's Triangle (1935), which proposes that three diploid species (*B. rapa*,

AA,  $2n = 20$ ; *B. nigra*, BB,  $2n = 16$ ; *B. oleracea*, CC,  $2n = 18$ ) gave rise, through natural hybridization and chromosome doubling, to three amphiploid species: *B. juncea* (AABB), *B. napus* (AACC), and *B. carinata* (BBCC) (Allender & King, 2010).

Among diploid species, *B. rapa* stands out for its extraordinary morphological, cytogenetic, and molecular variability. Native to Central Asia, where wild populations still exist, this species has a long history of domestication that has led to remarkable genetic and phenotypic diversification. Over time, human selection and adaptation to different agroclimatic environments have generated numerous cultivated subspecies, traditionally classified according to the organ of agronomic interest. East Asia is considered the cradle of leafy types, such as pak choi (*B. rapa* subsp. *chinensis*) and Chinese cabbage (*B. rapa* subsp. *pekinensis*), while Europe is the origin of the oilseed (*B. rapa* subsp. *oleifera*) and root (*B. rapa* subsp. *rapifera*) morphotypes (Sun, 2015). The latter are annual herbaceous plants that develop a thickened hypocotyl and erect, branched stems, adapted to temperate climates with moderate temperatures and high humidity.

In Europe, turnips (*B. rapa* subsp. *rapifera*) are valued not only for their edible roots but also for their aerial parts: in Galicia the tender leaves are known as *nabizas* and the immature floral shoots are called *grelos*. This dual use is particularly notable in northwestern Spain, where *B. rapa* plays a central role in traditional agriculture. Varieties such as “Grelos de Santiago” and “Globo Blanco de Lugo” are registered under the Protected Geographical Indication (PGI) Grelos de Galicia. This designation, established by Commission Regulation (EC) No. 1029/2009, safeguards both commercial varieties and traditional landraces representative of local ecotypes cultivated in authorized areas. Managed by the Galician Agency for Food Quality (AGACAL), the PGI certified 111 tons of product in 2023, generating a market value of €222,000. The registry currently includes 178 producers and 55 hectares of cultivated land, underscoring the growing socioeconomic relevance of this traditional crop.

## **5.2. CAPSICUM ANNUM: ORIGIN, DIVERSITY AND AGRICULTURAL RELEVANCE**

The genus *Capsicum*, belonging to the family Solanaceae, includes around 30 wild and cultivated species native to the American continent, characterized by broad morphological, genetic, and chemical diversity (Bosland & Votava, 2012; Carrizo García et al., 2016). Among them, *Capsicum annum* is the most widely domesticated and

cultivated species worldwide. Its domestication took place approximately six thousand years ago in central and northern Mexico, from wild populations belonging to the *C. annuum* var. *glabriusculum* complex (Pickersgill, 2007; Kraft et al., 2014). Other species, such as *C. baccatum*, *C. chinense*, and *C. frutescens*, were independently domesticated in South America (Perry et al., 2007; Carrizo García et al., 2020).

After its introduction to Europe in the 16th century, peppers and chilis rapidly spread throughout Asia, Africa, and the rest of the world, where they diversified through local selection and ecological adaptation (Andrews, 1995; Ibiza et al., 2012). Today, *C. annuum* holds a prominent place in global agriculture and gastronomy. In 2023, the global production of fresh *Capsicum* fruits reached 38.31 billion kilograms, with China and Mexico as leading producers (FAO, 2025).

The economic importance of *C. annuum* lies in its dual use as a vegetable in sweet varieties and as a spice in hot varieties. Its high content of bioactive compounds has also attracted attention from the pharmaceutical, cosmetic, and food industries (Kim et al., 2014). The species exhibits remarkable phenotypic diversity, with fruits varying in size, shape, color, pericarp thickness, capsaicinoids content, and maturation time (Nimmakayala et al., 2016).

A distinctive feature of the genus *Capsicum* is the presence of capsaicinoids, a group of alkaloids responsible for the characteristic pungency of chili peppers. Synthesized mainly in the fruit placenta through the convergence of the phenylpropanoid and branched-chain fatty acid pathways, capsaicinoids such as capsaicin and dihydrocapsaicin account for over 80% of total content (Suzuki & Iwai, 1984; Kim et al., 2009; Mazourek et al., 2009). These compounds act as defense molecules against herbivores and pathogens while exhibiting pharmacological properties, including analgesic, anti-inflammatory, antioxidant, and antimicrobial effects (Tewksbury & Nabhan, 2001; Reyes-Escogido et al., 2011).

Within the wide diversity of *Capsicum annuum*, the pepper popularly known as “Padrón” has a unique historical origin in the parish of Herbón, in the municipality of Padrón (A Coruña, Spain). According to historical accounts, Franciscan monks introduced seeds from Tabasco (Mexico) in the 17th century, initiating a process of local adaptation that

gave rise to an ecotype closely linked to the physical and cultural environment of the region.

During the 20th century, the commercial expansion of peppers under the name “Padrón,” even by producers outside the original area (Murcia, Almería, Marruecos), led to controversies regarding authenticity. When the name “Padrón” was later registered as a plant variety by a private company, local farmers responded by creating a new Protected Designation of Origin (PDO) under the name *Pemento de Herbón*, officially approved in 2009 through Commission Regulation (EU) No. 700/2010.

The PDO *Pemento de Herbón* currently includes around thirty producers and nine packaging plants, with a total registered area of 22.5 hectares. In 2024, AGACAL certified a production of approximately 72,200 kilos, with an estimated market value of €290.000 (AGACAL, 2023). The pepper is characterized by variability in pungency, a unique agronomic trait, as well as by the size, shape, and color of the fruit, which contributes to its distinctiveness and strong market identity.

Territorial and socioeconomic studies have highlighted the importance of collective action among producers, who have preserved traditional practices such as manual seed selection and intergenerational transmission of landraces. The creation of cooperatives has consolidated certified production, strengthened market positioning, and reinforced the cultural and economic value of *Pemento de Herbón*, making it a paradigmatic example of living agricultural heritage.

Together, *Grelos de Galicia* and *Pementos de Herbón* exemplify the deep interconnection between biodiversity, traditional agriculture, and cultural identity in Galicia. Through quality labels such as PGI and PDO, these crops contribute not only to preserving local genetic resources and traditional practices but also to sustaining the rural economy and promoting recognition of Galician agri-food heritage across Europe.

### **5.3. CURRENT KNOWLEDGE OF ROOT-ASSOCIATED ENDOPHYTES IN *B. RAPA* AND *C.***

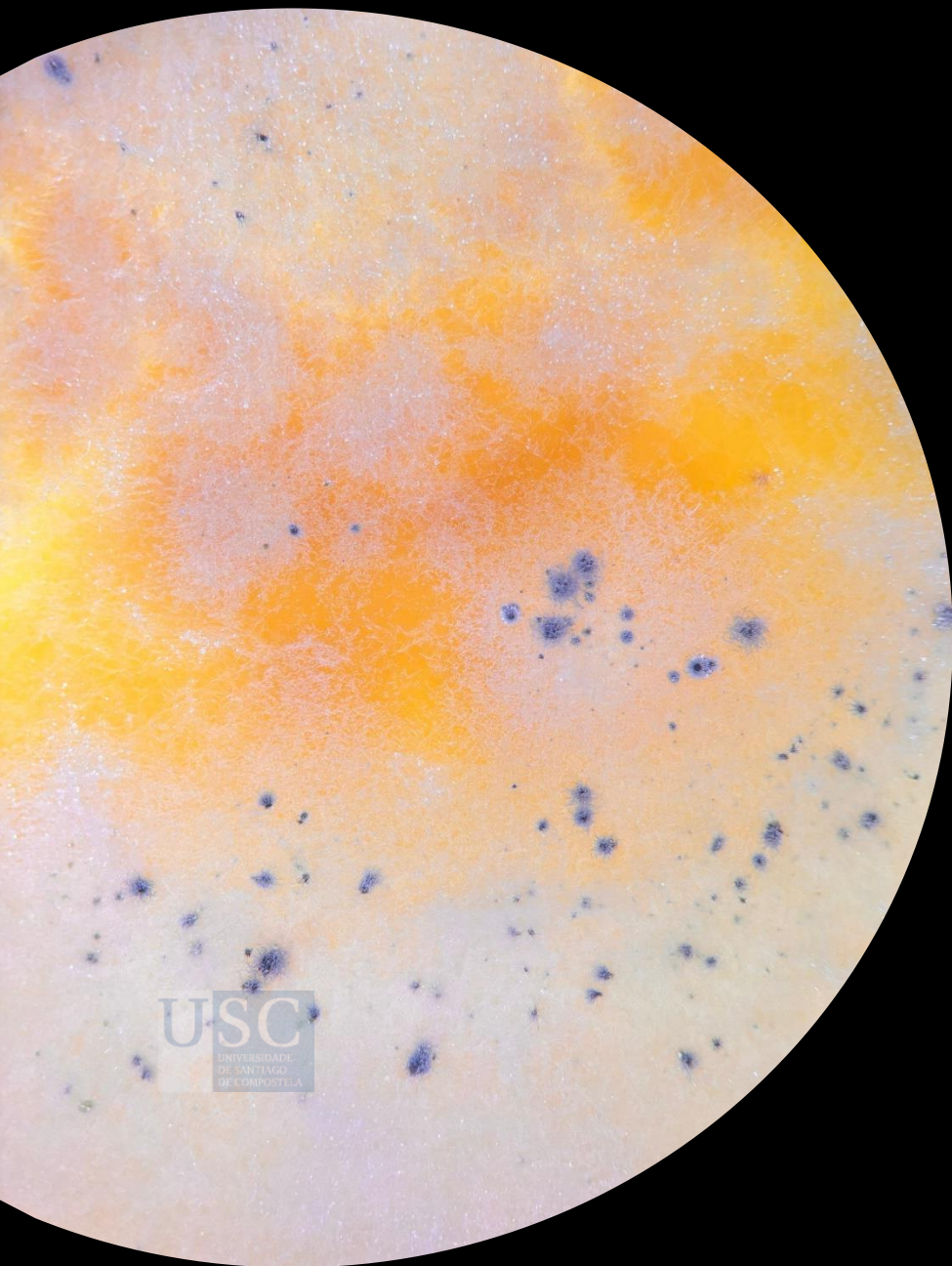
#### *ANNUUM*

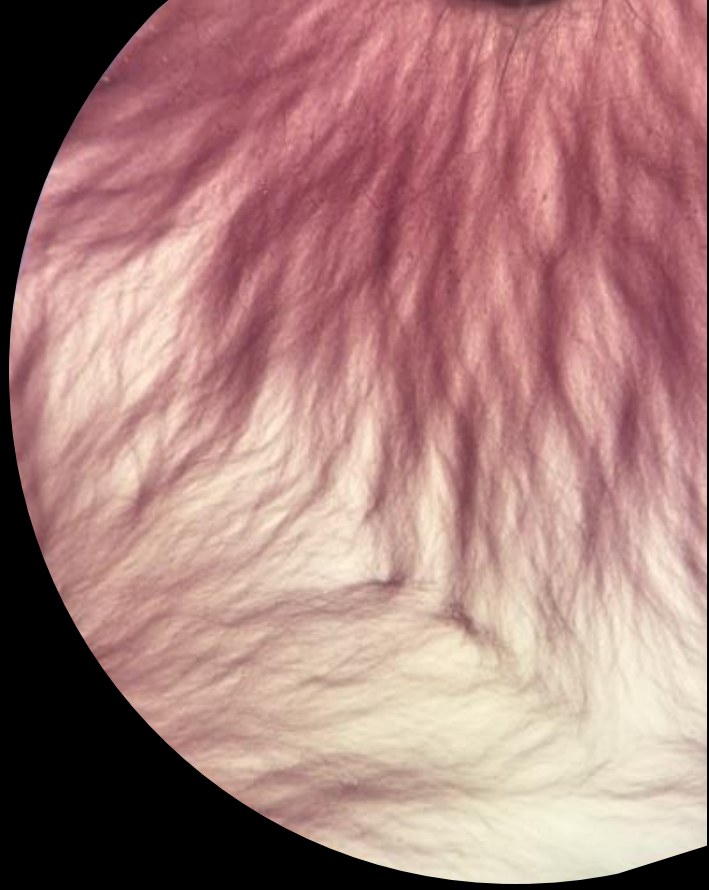
Despite their relevance, the diversity of root-associated endophytic fungi in many horticultural crops, including *B. rapa* (*Grelos de Galicia*, PGI) and *C. annuum* (*Pementos de Herbón*, PDO), remains underexplored. However, the establishment of these symbiotic

associations is complex and imposes specific physiological constraints on the fungal endophytes.

Successful fungal colonization of *Brassica* roots is often contingent on the ability to tolerate or suppress plant defenses, interfere with GSL biosynthesis or hydrolysis, or even degrade GSLs (Poveda et al., 2022). While these chemical barriers may limit colonization, environmental factors such as soil type, climate, and seasonality often play a more prominent role than host genotype in structuring fungal communities (García et al., 2013; Glynou et al., 2016; Thiergart et al., 2020; Urbina et al., 2018). Exposure to Brassicaceae-derived GSLs can reduce soil microbial diversity (Floc'h et al., 2022; Siebers et al., 2018), but in some cases, specific fungal lineages such as members of the order Helotiales are enriched in association with these hosts (Almario et al., 2017; Chen et al., 2020; Maciá-Vicente et al., 2020; Poveda et al., 2020, 2022).

In contrast, the endophytic fungal community of *C. annuum* is less well characterized. While numerous studies have described fungal microbiomes in Solanaceae, comprehensive, multi-environment surveys in *C. annuum* are scarce. Previous research has targeted diverse tissues and developmental stages, including the isolation of endophytic yeasts (Bhuyan et al., 2023), foliar endophytes with protective effects against aphids (Jaber & Alananbeh, 2018), and endophytes in *C. frutescens* contributing to resistance against *Colletotrichum* spp. (Puspitarini & Aji, 2023). In fruits, endophytes have been evaluated for antibacterial and antioxidant activities (Prima et al., 2022), and in roots, stems, and fruits, colonization patterns have been linked to crop management regimes (Halász et al., 2016). Rhizosphere fungal communities have also been characterized (Naziya et al., 2020), and studies in Korea explored tissue-specific assemblages (Paul et al., 2012). Across these reports, genera such as *Colletotrichum*, *Fusarium*, *Alternaria*, *Penicillium*, and *Cladosporium* occur consistently.





# **HYPOTHESIS AND OBJECTIVES**

---



This study, framed within the scope of basic research, is based on the hypothesis that the roots of *Brassica rapa* and *Capsicum annuum* host culturable endophytic fungi capable of positively influencing plant performance and contributing to stress protection, specifically against fungal pathogens and/or drought stress.

The main objective is the identification and preliminary evaluation of fungal strains with biological potential. To achieve this, endophytic fungi were isolated from root samples collected in certified-quality agricultural plots in Galicia. The isolates were identified using molecular techniques, and representative strains were selected for functional assays both *in vitro* and *in planta*.

This integrative approach enables the exploration of the functional diversity of cultivable endophytic fungi associated with these regionally important crops and supports the identification of candidate strains for future studies aimed at validating their application in agricultural contexts. This research approach is summarized in the following objectives:

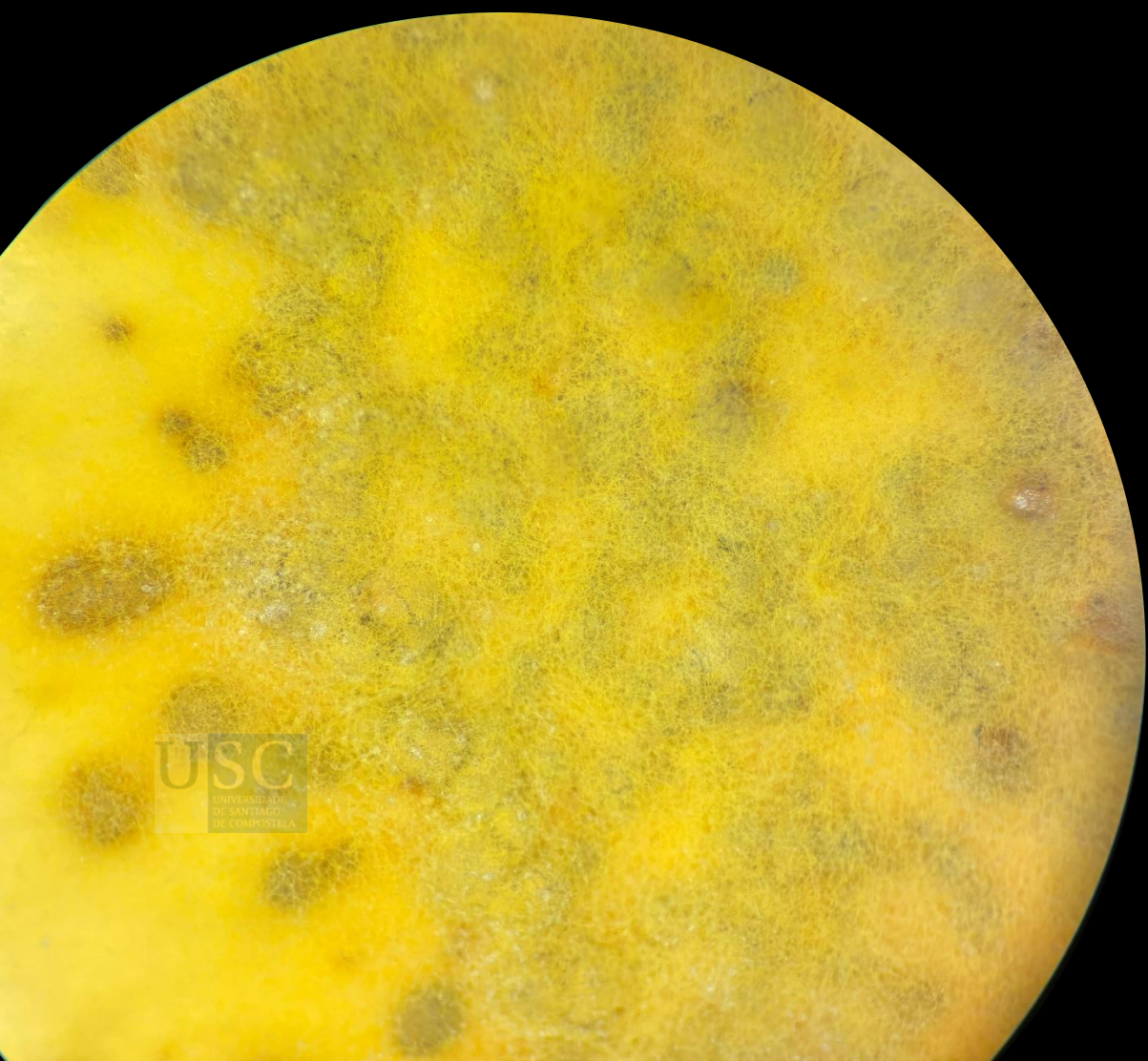
**Objective 1:** To isolate and identify culturable endophytic fungi from the roots of *B. rapa* and *C. annuum*.

**Objective 2:** To identify endophytic fungi with the potential to improve plant performance under biotic and abiotic stress conditions.

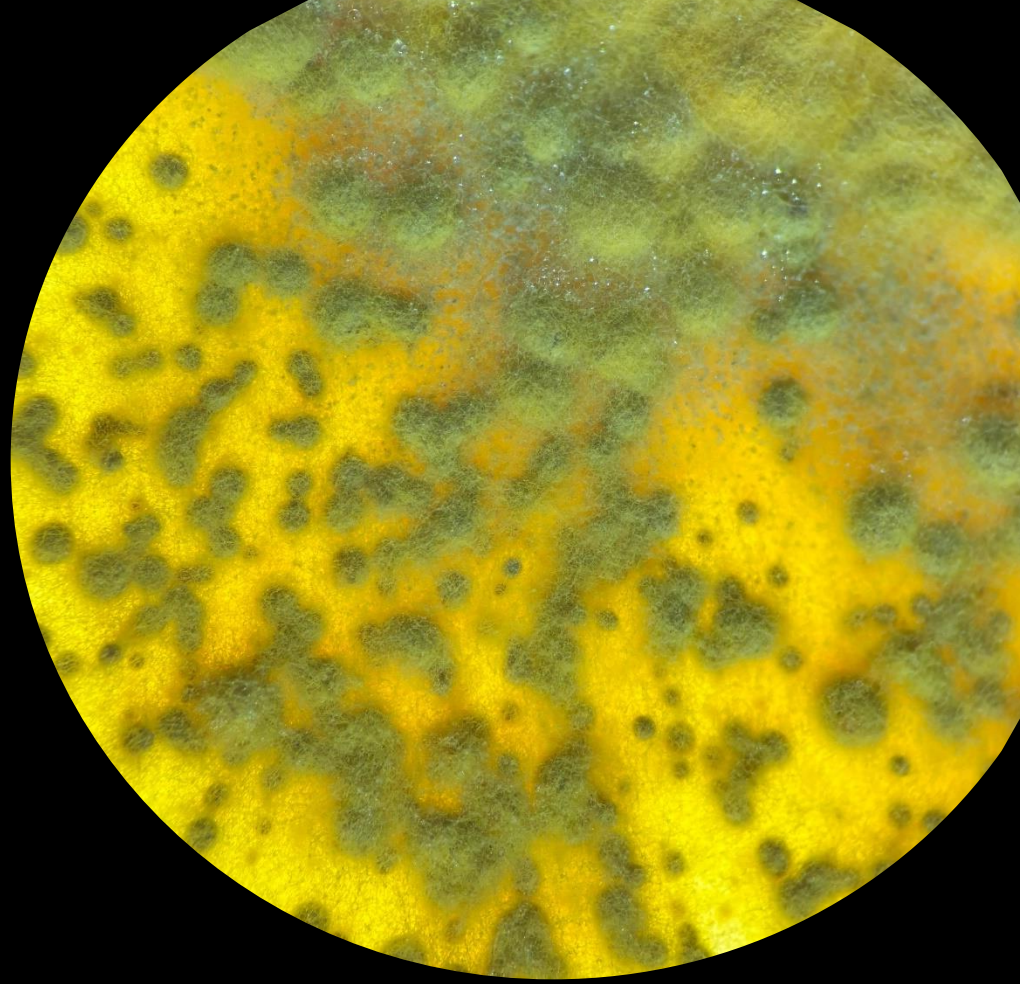
Sub-objective 2.1: *In vitro* evaluation of fungal activity against fungal pathogens and simulated drought conditions.

Sub-objective 2.2: *In planta* evaluation of fungal isolates to assess their effects on plant growth and stress tolerance under controlled conditions.

**Objective 3:** To characterize the antifungal compounds produced by selected endophytic fungi using untargeted metabolomics, aiming to identify metabolites with potential applications in biological control.



USC  
UNIVERSIDADE  
DE SANTIAGO  
DE COMPOSTELA



# GENERAL METHODOLOGY

---

## 1. ESTABLISHMENT OF THE ENDOPHYTIC FUNGI COLLECTION

### 1.1. SAMPLING, ISOLATION AND IDENTIFICATION OF CULTURABLE ENDOPHYTIC FUNGI

Sampling of *B. rapa* and *C. annuum* was conducted in agricultural fields located in northwestern Iberian Peninsula, under two recognized quality schemes: the Protected Geographical Indication (PGI) for *B. rapa* and the Protected Designation of Origin (PDO) for *C. annuum*. Sampling was performed in commercial agricultural fields using conventional agronomic practices. Sites were chosen to reflect environmental heterogeneity within each production area. Six plots were sampled for *B. rapa* across the PGI region, and four for *C. annuum* within the PDO area. Notably, the PGI production zone for *B. rapa* is larger and more diverse than that of *C. annuum*, as illustrated in Figure 3. In addition, key climate and soil variables for each sampling location are summarized in Supplementary Table 1.

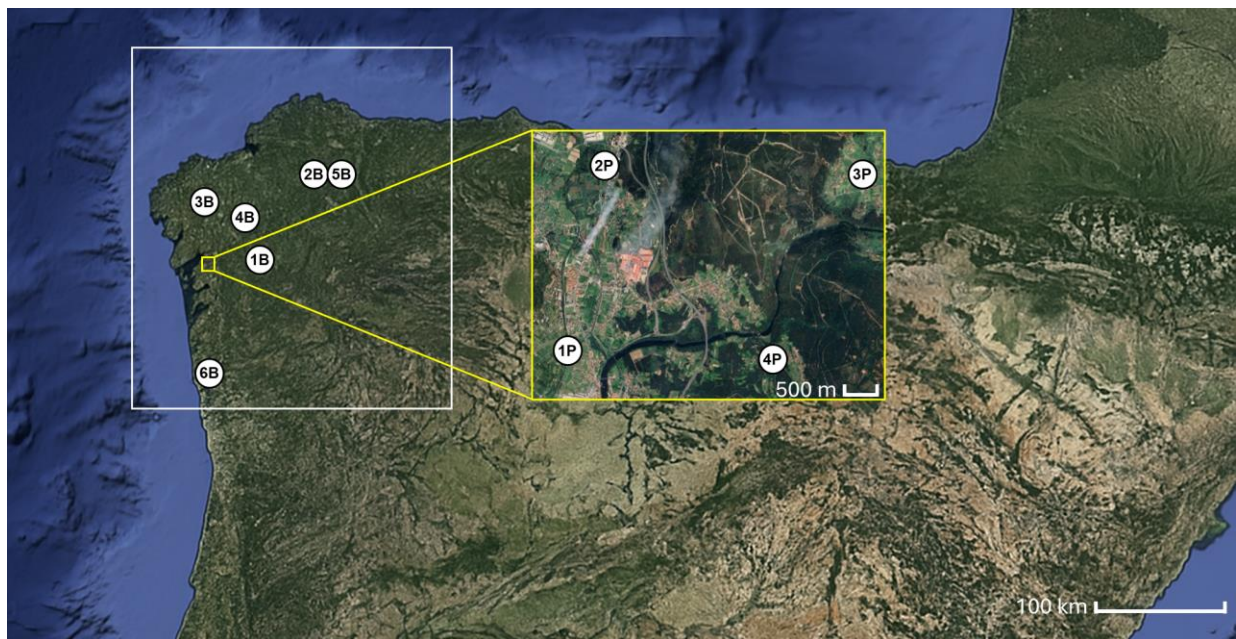


**Figure 3:** Sampling site locations. The plots where *B. rapa* samples were collected are shown within the white rectangle (1B, 2B, 3B, 4B, 5B, and 6B), while the sampling sites for *C. annuum* are indicated within the yellow rectangle (1P, 2P, 3P, and 4P).

To minimize seasonal variation effects on microbial communities (Chen et al., 2020), root sampling was conducted within a narrow time window. Both *B. rapa* and *C. annuum* were sampled during their respective harvest periods *B. rapa* in October–November 2022 (over four weeks), and *C. annuum* in July 2023 (over three weeks). Ten *B. rapa* plants and eight

*C. annuum* plants were randomly selected per plot. Whole plants were manually collected to preserve root integrity, and samples were refrigerated and processed within 24 hours.

Roots were rinsed with tap water, surface-sterilized with 70% ethanol and 5% commercial bleach following Poveda et al. (2020) and air-dried in a laminar flow cabinet. Under aseptic conditions, 30 representative fragments of the complete root system were selected, cut and plated on PDA medium supplemented with 200 mg/L chloramphenicol. Plates were incubated in darkness at room temperature and checked daily. Emerging colonies were sub-cultured by transferring hyphal tips to fresh PDA.

Once established, isolates were grouped into morphotypes based on macroscopic characteristics (colony color, growth rate, sporulation, exudates). One representative per morphotype was selected for molecular identification. Genomic DNA was extracted from PDA-grown mycelia using Extraction (E7526; Sigma-Aldrich Co. LLC, St. Louis, MO, USA) and Dissolution (D5688; Sigma-Aldrich Co. LLC, St. Louis, MO, USA) Solutions, following Avis et al. (2003). The internal transcribed spacer (ITS) region of nuclear rDNA was amplified with primers ITS1 and ITS4 (White et al., 1990) using the Phire Plant Direct PCR Kit (Thermo Fisher Scientific, Waltham, MA, USA). PCR amplifications were carried out using a PTC-100™ Thermal Cycler (MJ Research, Watertown, MA, USA) under the following conditions: an initial denaturation at 98 °C for 5 min, followed by 35 cycles of denaturation at 98 °C for 5 s, annealing at 54 °C for 5 s, and extension at 72 °C for 20 s. A final extension step was performed at 72 °C for 1 min.

PCR products were purified with the E.Z.N.A.® Cycle Pure Kit (Omega) and sequenced at the CACTI Genomics Service (University of Vigo, Spain). Sequences were compared to NCBI database entries via BLAST. Isolates with  $\geq 80\%$  query coverage and  $\geq 97\%$  identity were assigned to genus level following Raja et al. (2017). Sequences below these thresholds were analyzed phylogenetically using the neighbor-joining method.

## 1.2. ANALYSIS OF THE FUNGAL DIVERSITY

Presence/absence data were used to compute alpha and beta diversity metrics using the vegan package in R v4.3.0 (Oksanen et al., 2012).



**Jaccard Index:** The Jaccard index (J) was used to assess the differences in species composition between two communities or samples. Jaccard index is computed

as  $2B/(1+B)$ , where  $B$  is the Bray–Curtis dissimilarity metric. This metric is commonly used in ecological studies to quantify compositional dissimilarity between two samples based on species abundance. It is defined by the equation:

$$BC(A, B) = \frac{\sum_{i=1}^S |A_i - B_i|}{\sum_{i=1}^S |A_i + B_i|},$$
 where  $A_i$  and  $B_i$  represent the abundance of species  $i$  in samples  $A$  and  $B$ , respectively, and  $S$  represents the total number of species in the combined dataset. This index ranges from 0 (indicating identical species composition) to 1 (indicating no shared species).

- **Shannon Diversity Index:** The Shannon–Weaver index ( $H'$ ) is a measure of biodiversity that accounts for both the abundance and evenness of species present in a community. It was calculated to assess the diversity of fungal taxa within each sample as  $H' = -\sum(\pi_i * \ln(\pi_i))$ , where  $\pi_i$  is the proportion of individuals belonging to the  $i$ -th taxa, according to Shannon (1948). Higher  $H'$  values indicate higher diversity, meaning that species are more evenly distributed and there is a greater number of species. The value of  $H'$  typically ranges between 1.5 and 3.5 in most ecological studies but can be higher in very diverse communities.
- **Simpson Diversity Index:** Simpson's index ( $D$ ) was also computed as a complementary measure of alpha diversity, given by:  $D = 1/\sum p_i^2$ . This index estimates the probability that two individuals randomly selected from a sample belong to different species. Unlike the Shannon index, Simpson's index is more influenced by the most abundant taxa and less sensitive to rare species. Values closer to 1 indicate higher diversity.

## 2. FUNGAL ENDOPHYTE EVALUATION AGAINST ABIOTIC STRESS

### 2.1. DROUGHT STRESS TESTING: *IN PLANTA* EVALUATION

#### 2.1.1. PLANT MATERIAL AND GROWTH CONDITIONS

A total of 45 endophytic fungal isolates, representing 36 distinct taxa, were selected for *in planta* evaluation. One representative isolate per genus was included. When the same genus was present in both hosts (*B. rapa* and *C. annuum*), one isolate from each host was retained. For genera comprising multiple morphotypes, the most abundant morphotype was chosen. Taxa that could not be assigned to the genus level were selected if they corresponded to unique morphotypes.

In addition, several isolates from a previously established collection of endophytes obtained from the roots of *B. rapa* (Br) and *B. oleracea* (Bo) were incorporated (Poveda et al., 2020; Díaz-Urbano et al., 2025). A further isolate, *Diaporthe atlantica*, previously reported to confer drought tolerance, was included as a positive control (Toghueo et al., 2022).

Seedlings of *Arabidopsis thaliana* (ecotype Col-0) were used as a model plant due to the small size, rapid cycle and genotypic uniformity. The plants were germinated and grown *in vitro* on ½-strength Murashige and Skoog medium (½ MS) under short-day conditions (8 h light/16 h dark) at 21 °C for 14 days. Two-week-old roots were inoculated by dipping them in fungal suspensions (**¡Error! No se encuentra el origen de la referencia.**). These suspensions were prepared by homogenizing mycelium from three PDA plates in 5 mL phosphate-buffered saline (PBS 1×) using an Ultra-Turrax disperser, following a modified version of the protocol described by Barrio-Duque et al. (2020). Roots were immersed for 30 min, and three plants inoculated with the same fungal suspension were transplanted into 1.5 L pots filled with 750 g of peat-based substrate (Gramoflor GmbH, Germany; 20% initial moisture).

**Figure 4:** Two-week-old *Arabidopsis thaliana* plants being inoculated with endophytic fungal suspensions. Inoculation was performed by submerging the roots into reservoirs containing the fungal solution, allowing direct contact between the root system and the inoculum.



Pots were arranged in a randomized block design to minimize positional effects. Each treatment included four pots, and treatments were organized in sets of eight fungi plus a non-inoculated control. In total, 512 plants were used (**¡Error! No se encuentra el origen de la referencia.**). Following a four-day acclimation with daily irrigation (2 mL H<sub>2</sub>O), water was withheld for four weeks to impose drought stress. Soil moisture decreased from 20% to 0% during this period.

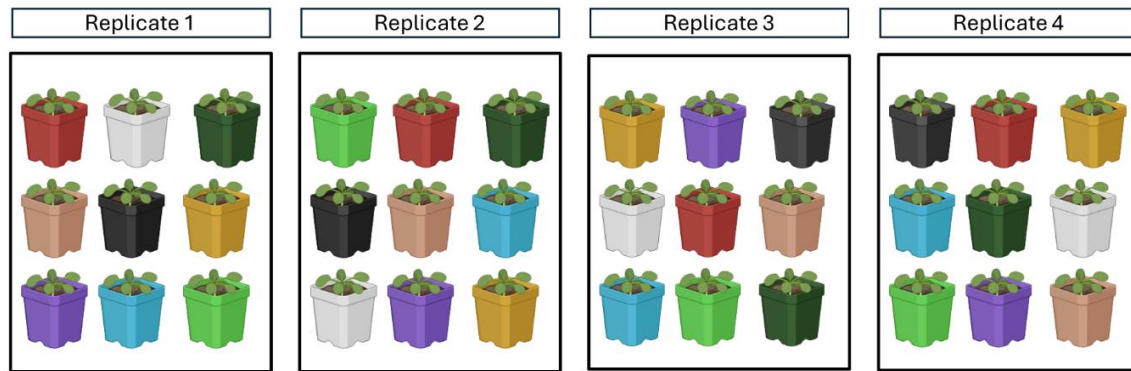


**Figure 5:** Schematic representation of the spatial arrangement of pots within a shelving unit, following a randomized block design. The diagram illustrates a simplified subset of eight treatments plus the control. Each colour corresponds to a different fungal inoculation treatment, while white represents the non-inoculated control. Each pot contained three *Arabidopsis thaliana* plants.

### 2.1.2. PHYSIOLOGICAL MEASUREMENTS

Stomatal conductance and soil moisture were monitored during the drought period to assess plant physiological status. Measurements were taken using a LI-600 Porometer/Fluorometer (LI-COR Biosciences, Lincoln, NE, USA) and a Hydrosense II soil hygrometer (Campbell Scientific, UT, USA), respectively.

After four weeks of drought stress, three fully developed leaves per plant were collected for water content analysis. Fresh weight (FW) was recorded immediately. Leaves were then immersed in distilled water for 24 hours to obtain turgid weight (TW) and subsequently dried at 80 °C for 48 hours to determine dry weight (DW). Relative water content (RWC) was calculated as:  $RWC (\%) = [(FW - DW) / (TW - DW)] \times 100$  (Barrs and Weatherley, 1962). In addition to leaf water content, total fresh and dry biomass of each plant was also recorded.

### 2.1.3. STATISTICAL ANALYSIS

Fresh weight, dry weight, and RWC values from fungal-inoculated plants were normalized using control plants within the same replicate. RWC values were arcsine-transformed to meet normality assumptions (Kasuya, 2004). Fungal-inoculated plants were compared to control plants using one-way analysis of variance (ANOVA) followed

by mean comparison using the least significant difference (LSD) test. All statistical analyses were conducted using SAS software, version 9.4 for Windows.

## 2.2. DROUGHT STRESS TESTING: *IN VITRO* EVALUATION

To evaluate alternative selection methods that are more cost-effective than *in planta* approaches, several *in vitro* systems simulating drought stress were tested. These methods, previously described in the literature, were evaluated using a subset of isolates, including two additional isolates known for conferring drought tolerance: *Diaporthe atlantica* and *Epichloë festucae*, as positive controls (Vázquez-de-Aldana et al., 2013; Pereira et al., 2019; Toghueo et al., 2022). Fungal growth inhibition, colony morphology, and biomass accumulation were recorded as indicators of stress response. All assays were conducted using Potato Dextrose Agar (PDA) or Potato Dextrose Broth (PDB) as basal media (Forchetti et al., 2007; Sandhya et al., 2009; Ripa et al., 2019; Javed et al., 2022). Each treatment was conducted with at least three biological replicates, and additional replicates were included for assays showing low reproducibility or high plate-to-plate variability. Prior to experimentation, isolates were maintained on PDA (Sigma-Aldrich, St. Louis, MO, USA) at 22 °C.

Drought stress was simulated by reducing the osmotic potential of the culture medium through two independent approaches: supplementation with polyethylene glycol (PEG 8000) and increasing agar concentration (“hard agar”, HA). Polyethylene glycol (PEG 8000; Sigma-Aldrich, USA) is a high molecular weight, non-penetrating polymer that decreases the water potential of the medium without altering its nutrient composition or causing toxicity to microorganisms. PEG acts by creating osmotic stress conditions analogous to water deficit. To comprehensively assess its suitability for fungal screening, PEG was tested in three different medium formats: solid, liquid, and semi-solid.

In the second approach, osmotic potential was reduced by increasing the agar concentration, method known as “hard agar” (HA). This technique, previously described for *Arabidopsis* by González et al. (2023), enhances the medium’s tensile strength and limits water availability in a manner comparable to treatments with PEG, mannitol, or NaCl. Importantly, unlike osmotic agents such as mannitol or sorbitol, agar does not interfere with metabolic processes, as it cannot serve as a carbon source for endophytic fungi (Calmes et al., 2013; Dulermo et al., 2010; Vélez et al., 2007).

### 2.2.1. SOLID MEDIA ASSAYS WITH PEG 8000

PEG interferes with agar polymerization and therefore cannot be added directly to solid media. Because of that, PEG was applied using an overlay diffusion method adapted from van der Weele et al. (2000) and Verslues & Bray (2004). PDA plates were prepared and solidified, then overlaid with PEG 8000 solutions (0, 250, 400, 550, and 700 g L<sup>-1</sup>) at a 2:3 solid:liquid volume ratio. After 12 h equilibration, excess solution was removed. Mycelial plugs (5 mm) were placed centrally and incubated at 22 °C. Radial growth was measured every 24 h along two perpendicular axes, and growth inhibition (%) was calculated as  $((A-B)/A) \times 100$ , where *A* and *B* represent colony diameters in control and PEG-treated plates, respectively. Morphological traits (color, density, and sporulation) were qualitatively recorded.

### 2.2.2. LIQUID MEDIA ASSAYS WITH PEG 8000

Liquid media were selected to allow continuous monitoring of fungal growth through optical density (OD) measurements and final biomass quantification via hyphal dry weight. Submerged cultures were prepared in 20 mL of Potato Dextrose Broth (PDB) supplemented with polyethylene glycol 8000 (PEG 8000; 0, 5, 10, 15, and 20% w/v), following the protocols described by Forchetti et al. (2007) and Javed et al. (2022). Cultures were incubated at 22 °C and maintained under agitation (100–120 rpm) for seven days to ensure adequate oxygenation. Fungal biomass was quantified at the end of incubation by measuring fresh and dry mycelial weight after vacuum filtration. Optical density at 600 nm (OD<sub>600</sub>) was measured using a Spectra MR microplate spectrophotometer (Dynex Technologies, USA). Uninoculated PEG–PDB tubes served as negative controls to verify PEG solubility and absence of microbial contamination.

### 2.2.3. CULTURE ON CELLOPHANE MEMBRANES WITH PEG 8000

This method was originally described by Navarro-Ródenas et al. (2011). Cellophane membranes were used to allow fungal growth on a solid surface surrounded by PDB medium supplemented with PEG, enabling continuous monitoring of colony development. Cellophane sheets were pretreated with 1 mM EDTA for 1 h at 100 °C, rinsed thoroughly, autoclaved, and placed on sterile glass beads covering 4 mL of PDB supplemented with PEG (0–30% w/v). Mycelial plugs (5 mm) were inoculated on the

membrane surface and incubated at 22 °C in darkness for two weeks. Colony expansion and morphological traits were recorded periodically.

#### 2.2.4. PDA WITH INCREASED AGAR CONCENTRATION

This method was originally developed to simulate drought stress in plants by reducing the osmotic potential of the medium through an increased agar content. In this study, agar concentration in PDA was elevated to 125–200% of the standard formulation (González et al., 2023). Plates were inoculated, incubated, and measured following the same procedures used for PEG-supplemented media. Colony diameter was recorded daily, and fungal growth inhibition was assessed relative to the standard PDA control.

### 3. FUNGAL ENDOPHYTE EVALUATION AGAINST BIOTIC STRESS

#### 3.1. *IN VITRO* EVALUATION OF ANTIFUNGAL ACTIVITY

A total of 146 isolates (76 from *B. rapa*, 70 from *C. annuum*) were screened against *R. solani* using dual-culture assays on PDA (20 mL in 90 mm plates). A 5 mm plug of endophyte and pathogen were placed at opposite ends of each plate, positioned 1 cm from the edge. Plates were incubated at 26 °C in darkness for 15 days.

Initial screening (non-replicated) identified isolates with either: (i) inhibition halos, or (ii) overgrowth of the pathogen. Selected isolates were subsequently evaluated in triplicate. For each confirmed isolate, nine plates were prepared: three co-cultures with the pathogen, three pathogen-only controls, and three endophyte-only controls. The endophyte-only controls served to compare with dual-culture plates and to verify the growth and morphology of the endophytic fungus. Antagonistic activity was quantified using the formula:  $I\% = ((R1 - R2) / R1) \times 100$  where R1 is radial growth of *R. solani* in control, and R2 in co-culture. Measurements of inhibition halos and radial growth were performed using ImageJ software (Schneider et al., 2012). A quantitative scale was applied to interpret the results: the antagonistic activity was classified as none (0–19%), weak (20–49%), moderate (50–79%), or strong ( $\geq 80\%$ ). Inhibition halos were categorized as none ( $\leq 0.4$  cm), weak (0.45–0.7 cm), moderate (0.75–0.95 cm), or strong ( $\geq 1$  cm), following a modified version of the scale proposed by Duraffourd et al. (1986).

Isolates with confirmed antifungal activity were further evaluated against a panel of fungal pathogens. Isolates from *B. rapa* were tested against *F. oxysporum*, *A. alternata*,

*B. cinerea*, and *S. sclerotiorum*, all of which are major pathogens for this crop. In parallel, isolates from *C. annuum* were tested against *F. solani*, *C. acutatum*, *P. capsici*, *B. cinerea*, and *S. sclerotiorum*, representing key threats to pepper production. The pathogenic fungal strains used in this study were obtained from the Spanish Type Culture Collection (CECT, Valencia, Spain), the Regional Diagnostic Center of Castilla y León (CRD, Salamanca, Spain), and the Areeiro Phytopathology Station (EFA). The strains used included *A. alternata* (Card 41/37/2019 JCYL 965), *F. oxysporum* (CECT 2715), *R. solani* (CRD 207/99 JCYL 957, anastomosis group 3), *S. sclerotiorum* (CRD 345/202), *F. solani*, *C. acutatum*, *P. capsici* (EFA-BH574) and *B. cinerea* (EFA-BH815). All pathogenic strains were routinely maintained on PDA medium prior to experimentation.

### 3.2. IN PLANTA EVALUATION OF ANTIFUNGAL ACTIVITY

#### 3.2.1. PLANT MATERIAL

In this study, plants of *B. oleracea* (MBG-BRS-0468) and *C. annuum* (MBG-PIM-023) were used. The accession MBG-PIM-023 corresponds to the Protected Designation of Origin for *Pemento de Herbón*. MBG-BRS-0468 was selected as a substitute for *B. rapa* because no sufficiently homogeneous varieties of the latter were available for experimental purposes. Given the close genetic relationship between *B. rapa* and *B. oleracea*, MBG-BRS-0468 was chosen for its higher uniformity, ensuring reproducible and consistent experimental conditions. Seeds were sown in germination trays and, after two weeks, seedlings were transplanted into 4 L pots containing peat substrate (Gramoflor GmbH & Co. KG Produktion, Vechta, Germany). Plants were grown in a greenhouse at 21 °C under an 8 h light/16 h dark photoperiod until the four-leaf stage.

#### 3.2.2. ENDOPHYTIC FUNGI INOCULATION

Three endophytic fungal strains: BrT4.01 (*Talaromyces* sp.), P23.03 (*Pseudopyrenochaeta* sp.), and P20.11 (*Trichoderma* sp.) were used in this study. Each strain was grown on Potato Dextrose Agar (PDA) for seven weeks. To prepare hyphal suspensions, mycelia from PDA plates were scraped, suspended in 10 mL of 1× PBS, homogenized using an Ultra-Turrax T25 (Janke & Kunkel, Germany), and adjusted to an optical density of 1.4 at 600 nm.

For inoculation, 5 mL of fungal suspension was applied per plant in two doses of 2.5 mL, delivered at a 1 cm depth in the substrate around the root zone. Inoculated plants were maintained in the greenhouse until pathogen inoculation.

### 3.2.3. PATHOGEN INOCULATION

Pathogenic fungal strains were obtained from the Regional Diagnostic Center of Castilla y León (CRD, Salamanca, Spain) and the Phytopathological Centre of Areiro (EFA, Pontevedra, Spain). The pathogens used were *Sclerotinia sclerotiorum* (CRD 345/202) and *Phytophthora capsici* (EFA-BH574), both routinely maintained on PDA medium. For inoculation, 6 mm<sup>2</sup> agar plugs containing actively growing mycelium were placed on the surface of leaves and covered with plastic bags to maintain high humidity for 48 hours

### 3.2.4. ENDOPHYTE COLONIZATION

Root colonization by endophytic fungi was assessed by re-isolation at the end of the experiment, during plant photography and fresh weight measurement. Roots were washed, surface-sterilized (70% ethanol, 1 min; 5% bleach, 20 min; Poveda, 2020), rinsed with sterile water, and plated on PDA supplemented with chloramphenicol.

For plants inoculated with P23.03, root tissue was flash-frozen in liquid nitrogen, ground, and DNA was extracted using the phenol-chloroform method. Endophyte detection was carried out by nested-PCR following Infantino & Pucci (2005), with an initial amplification using the universal primers ITS4 and ITS5 (White et al., 1990), followed by a second amplification using specific primers P1yc1-F and P1yc1-R targeting the ITS region. The first PCR product was diluted 1:50 with Milli-Q ultrapure water and used as the template for the second reaction. Thermal cycling conditions were: 2 min at 94 °C; 35 cycles of 94 °C for 30 s, 62 °C for 30 s, and 72 °C for 1 min; and a final extension at 72 °C for 7 min. PCR products were separated on 1% agarose gels stained with ethidium bromide, visualized under UV light, and compared against a 100 bp DNA ladder (Thermo Fisher Scientific). Negative controls (no DNA template) were included in all reactions.

### 3.2.5. EXPERIMENTAL DESIGN FOR *IN PLANTA* ASSAYS

Roots were inoculated with the endophytic strains P23.03, P20.11, and BrT4.01. Control plants received 1x PBS. Fifteen days post-inoculation, allowing for endophyte colonization, two leaves per plant were inoculated with *S. sclerotiorum* or *P. capsici*.

After four days, infected leaves were photographed, and lesion area was measured using ImageJ, and the fresh weight of pathogen-inoculated plants was recorded at the time of imaging.

### 3.2.6. INFECTION EVALUATION AND STATISTICAL ANALYSIS

Disease severity was quantified by measuring the necrotic area on infected leaves. The average lesion area from two leaves per plant was used for statistical analysis. Differences between treatments were assessed using two-way t-tests ( $p < 0.05$ ).

### 3.2.7. PLANT GROWTH EVALUATION

Roots were inoculated with the endophytic strains P23.03, P20.11, and BrT4.01. Control plants received  $1\times$  PBS. Plants were maintained under greenhouse conditions and harvested six weeks after inoculation to evaluate potential effects on plant growth.

## 4. FUNCTIONAL AND METABOLOMIC CHARACTERIZATION OF *PSEUDOPYRENOCHAETA* ISOLATES WITH ANTIFUNGAL ACTIVITY

### 4.1. MOLECULAR IDENTIFICATION OF SELECTED FUNGAL ISOLATES

To determine the identity of the isolates (P20.08, P23.10, P23.03, P22.09, P27.24, P24.08, P27.06 and P30.06) within the genus *Pseudopyrenochaeta*, species-specific primers described by Infantino and Pucci (2005) were used, targeting the ITS region of ribosomal DNA. Genomic DNA was extracted from mycelium grown on potato dextrose agar (PDA), following the procedure detailed in Poveda et. al (2020). PCR reactions were prepared using the Phire Plant Direct PCR Kit (Thermo Fisher Scientific, Waltham, MA, USA) with the following primer pairs: Plyc1-F/R (F: 5'-GTAGGATTGCGTGCTTTGGT-3'; R: 5'-AGTTTTCTGACGCTGATTGC-3') for *P. terrestris* (expected amplicon: 147 bp) and Plyc2-F/R (F: 5'-CTGTAACATTGGGGGCTGGT-3'; R: 5'-CGATGCCA GAACCAAGAGAT-3') for *P. lycopersici* (expected amplicon: 209 bp). Cycling conditions were: 94 °C for 2 min; 35 cycles of 94 °C for 30 s, 62 °C for 30 s, 72 °C for 1 min; and a final extension at 72 °C for 7 min. Amplicons were separated by electrophoresis on 1% agarose gels in TBE buffer, stained with ethidium bromide, and visualized under UV illumination (Gel Doc XR+, Bio-Rad, CA, USA). CSL-MDNA-1K Ladder (Clever Scientific) was used as molecular weight marker.

Additional primers reported by Testen et al. (2023) Py1TQ3F/R (F: 5'-CCT GCG GAA GGA TCA TTA ACT-3'; R: 5'-CAA GCC TAC CGA GGA AAC AA-3') and Py2TQ5F/R (F: 5'-CTG CTA CTG CCC ATG TCT TT-3'; R: 5'-AAG GGT TGT AGT GTC CAA TCG-3'), were also evaluated but consistently produced primer–dimers and were therefore excluded from further analyses.

#### 4.2. *IN VITRO* EVALUATION OF SELECTED ENDOPHYTES WITH ANTIFUNGAL ACTIVITY

To explore a potential relationship between antifungal activity and taxonomic classification, the antifungal potential of the eight isolates identified was evaluated.

##### 4.2.1. DUAL-CULTURE ASSAYS

Antagonistic activity against *Rhizoctonia solani* was assessed using dual-culture assays. Petri dishes (90 mm) were filled with 20 mL of PDA Sigma-Aldrich (St. Louis, MO, USA). A 5 mm plug of the endophyte was placed at the center of each plate, while four 5 mm plugs of *R. solani* were symmetrically positioned 1 cm from the edge, forming a square. Plates were incubated at 26 °C in darkness for 15 days. Monocultures of each organism served as controls. All treatments were performed in triplicate.

*Rhizoctonia solani* strain (CRD 207/99 JCYL 957, AG-3) was provided by the Regional Diagnostic Center of Castilla y León (CRD, Salamanca, Spain). Antifungal activity was quantified as the difference in radial growth compared to control plates. Based on inhibition halo diameters, isolates were classified into four activity levels: as none ( $\leq 0.4$  cm), weak (0.45–0.7 cm), moderate (0.75–0.95 cm), or high ( $\geq 1$  cm).

In parallel, to determine whether the observed effects were mediated by volatile compounds produced by isolate P23.03, an assay using modified Petri dishes was performed. These plates, described by Álvarez-García et al. (2021), enabled exposure to volatiles while keeping the culture media physically separated. In this setup, *R. solani* was exposed to volatiles released by P23.03 under both single- and co-culture conditions. The growth of *R. solani* under volatile exposure was then measured and compared with its growth in pure culture without volatile contact. The prototypes were provided by the University Research Group on Engineering and Sustainable Agriculture (GUIIAS) at the University of León.

#### 4.2.2. EXTRACT-BASED INHIBITION ASSAYS (DISC DIFFUSION METHOD)

To verify the production of antifungal compounds secreted by the endophytic fungi, inhibition assays using crude extracts were performed. Mycelial biomass (~0.5 g) was harvested from PDA cultures incubated for 20 days at 26 °C. The biomass was homogenized using a tissue mill (Janke and Kunkel A10; IKA-LabortechnikStaufen, Germany) and sonicated for 5 minutes in Hardy-Hall buffer (Hall & Hardy, 2012). The resulting suspensions were filtered (PTFE, 0.20 µm) and concentrated using a SpeedVac (Savant Instruments, Holbrook, NY, USA). Residues were resuspended in 100 µL of sterile distilled water.

Aliquots (10 µL) were loaded onto sterile 6 mm antibiogram discs and placed on PDA plates freshly inoculated with *R. solani*. Plates were incubated at 26 °C, and inhibition zones were measured after 48–72 h. Water-loaded discs served as negative controls. Antifungal activity was classified using the same halo diameter criteria as in the dual-culture assays.

#### 4.2.3. MEDIUM EFFECT ON ANTIFUNGAL ACTIVITY

To assess the impact of the commercial PDA source on antifungal activity, both dual-culture and extract-based assays were repeated using PDA prepared from dehydrated media supplied by Sigma-Aldrich (St. Louis, MO, USA) and Dinkelberg Analytics (Budapest, Hungary).

Fungi were grown on each PDA type for both direct assays and extract production. The resulting extracts were tested against *R. solani* cultivated on both media types. All other experimental conditions were kept identical to those previously described.

### 4.3. UNTARGETED METABOLOMIC ANALYSIS AND COMPOUND IDENTIFICATION

To investigate the molecular basis underlying the observed antifungal activity, an untargeted metabolomic study was conducted to characterize the metabolic profiles of the fungal isolates under different conditions. The analysis was structured at two comparative levels.



First, the metabolomic profile of *P. terrestris* isolates, which exhibited antifungal activity, were compared with those of *P. lycopersici*, which showed no inhibitory

effect. This interspecific comparison enabled the identification of candidate metabolites whose presence or abundance correlated with antifungal capacity.

- Second, the metabolomic profiles of *P. terrestris* isolates grown on PDA from Sigma-Aldrich (St. Louis, MO, USA), where antifungal activity was preserved, were compared with those grown on PDA from Dinkelberg Analytics (Budapest, Hungary), where activity was lost. This intraspecific comparison allowed the detection of metabolites, potentially influenced by the culture medium.

By integrating both analyses, a dual selection criterion was applied, retaining only those metabolites that showed significant differences in both comparisons. This approach minimized the likelihood of identifying compounds associated solely with species-level variation or medium composition. The resulting set of metabolites was considered as priority candidates for structural identification in the subsequent phase of the study.

#### 4.3.1. SAMPLE PREPARATION AND CHROMATOGRAPHY

In all cases, mycelia were cultivated on PDA for 20 days, homogenized, and extracted following the procedure described in Section 2.2.2 (extract-based inhibition assays, disc diffusion method), with the exception that the solutions were not concentrated. For chromatographic analysis, 200  $\mu$ L of each extract were injected into a Solo 2 C18 column (2.1  $\times$  100 mm, 1.7  $\mu$ m; Bruker, MA, USA).

Chromatographic separation was performed using a binary solvent system consisting of 0.1% formic acid in water (solvent A) and acetonitrile (solvent B). The elution gradient was programmed as follows: 3% B from 0 to 4 min, linearly increasing to 25% B from 4 to 16 min, then to 80% B from 16 to 25 min, followed by 100% B from 25 to 32 min, and returning to 3% B from 33 to 36 min. The flow rate was set at 0.4 mL/min, with an injection volume of 5  $\mu$ L and a column temperature maintained at 35  $^{\circ}$ C (Tortosa et al., 2018).

Metabolomic profiling was first performed on extracts from *P. terrestris* (isolate P23.03) and *P. lycopersici* isolates (P27.06 and P27.24), all grown on PDA prepared with Sigma-Aldrich medium (St. Louis, MO, USA). This initial comparison aimed to identify metabolites potentially associated with antifungal activity by contrasting an active (*P. terrestris*) and inactive (*P. lycopersici*) species.

Subsequently, six *P. terrestris* isolates (P23.03, P30.06, P20.08, P23.10, P22.09, and P24.08) were cultivated on two different PDA formulations: Sigma-Aldrich (St. Louis, MO, USA), in which antifungal activity was retained, and Dinkelberg Analytics (Budapest, Hungary), where antifungal activity was lost. Extracts from these cultures were analysed to determine which metabolites were influenced by the culture medium, allowing the identification of compounds whose production correlated with the preservation or loss of antifungal activity. For each isolate and medium, mycelia were grown on three independent plates.

#### 4.3.2. MASS SPECTROMETRY ACQUISITION

Mass spectrometry was performed in both positive and negative electrospray ionization (ESI) modes across a mass range of 100–1200 m/z. Instrument settings included a gas flow of 9 L/min, nebulizer pressure of 38 psi, dry gas flow of 9 L/min, and dry temperature of 220 °C. The capillary and end plate offset voltages were set at 4500 V and 500 V, respectively. The instrument was externally calibrated using a 1 mM sodium formate/acetate solution in iPrOH/H<sub>2</sub>O (50:50) with 0.2% formic acid. Calibration was performed at the beginning of each run, and all acquired spectra were recalibrated prior to statistical analysis. MS/MS fragmentation was carried out using collision energy ramps ranging from 15 to 50 eV. Fragmentation targets were selected based on accurate mass and retention time (Tortosa et al., 2018).

#### 4.3.3. DATA PROCESSING AND QUALITY CONTROL

Raw LC-MS data were processed using MetaboScape 4.0 (Bruker), applying the T-Rex 3D algorithm for feature detection. Quality control (QC) samples, consisting of pooled extracts from all isolates, were injected every ten runs to monitor instrument stability.

Features absent in more than 50% of QC samples or with a relative standard deviation (RSD) greater than 20% were excluded using a custom script in R (v4.2), ensuring reproducibility and minimizing technical noise.

#### 4.3.4. STATISTICAL ANALYSIS

Datasets from both ionization modes were merged and features present in both ionization modes were combined based on retention time and neutral exact mass. The resulting data matrix (features × samples × intensities) was analyzed using MetaboAnalyst 6.0. Pareto

scaling was applied to normalize the data while preserving its underlying structure. Non-informative variables were filtered using the interquartile range (IQR) method. A Partial Least Squares Discriminant Analysis (PLS-DA) was performed to visualize group separation and identify discriminant metabolites. Model performance was evaluated through cross-validation using  $R^2$  (explained variance) and  $Q^2$  (predictive ability). Features with a Variable Importance in Projection (VIP) score  $\geq 2$  were selected for further annotation. Additionally, univariate analyses were conducted using one-way ANOVA ( $p \leq 0.05$ ) and Volcano Plot analysis, applying thresholds of  $|\log_2FC| \geq 1$  and False Discovery Rate ( $FDR \leq 0.05$ ) to identify significantly differentially accumulated metabolites.

#### 4.3.5. TENTATIVE METABOLITE IDENTIFICATION

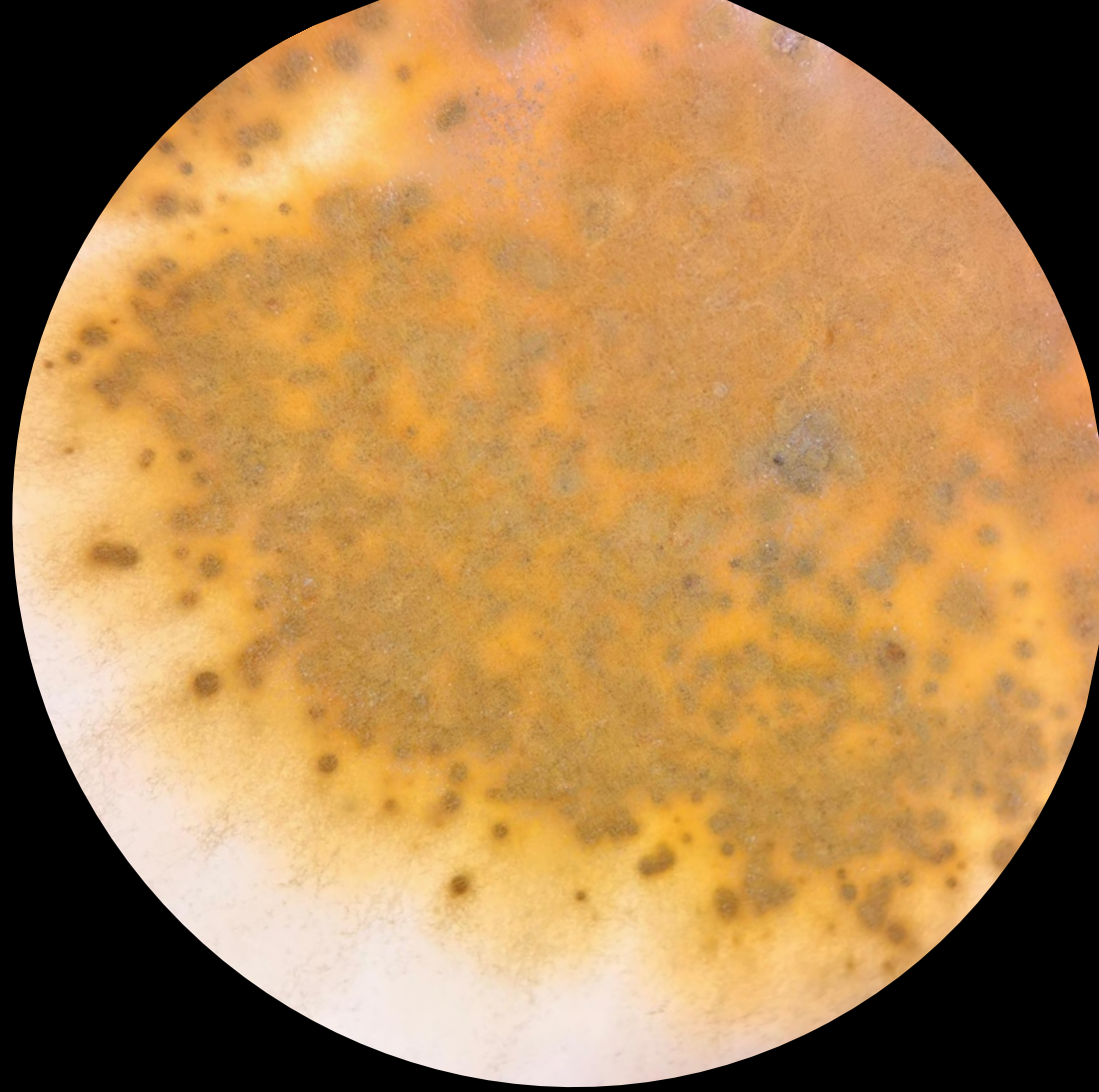
Tentative identification of significant metabolites was performed by matching accurate mass values and MS/MS fragmentation spectra against public databases, including PubChem, ChEBI, HMDB, and the Plant Metabolic Network. Fragmentation patterns were compared with reference spectra from these databases and relevant literature. This approach enabled putative annotation of compounds of interest, without structural confirmation via pure standards.

#### 4.3.6. MOLECULAR FORMULA ASSIGNMENT AND FEATURE CURATION

When needed manual curation of selected features was performed to remove putative in-source fragments. Features co-eluting within a  $\pm 6$ -second retention time window and showing intensity correlation coefficients  $\geq 0.8$  were flagged as likely fragments and investigated. Molecular formulas were assigned using SIRIUS 4.7.0 and MetaboScape, based on exact mass and isotopic patterns. Candidate structures were further evaluated by comparing MS/MS fragmentation spectra with those available in the referenced databases, strengthening the annotation of priority metabolites.



USC  
UNIVERSITY OF  
SOUTH CALIFORNIA



# RESULTS AND DISCUSSION

---

## 1. TAXONOMIC CHARACTERIZATION OF ENDOPHYTIC FUNGI IN *BRASSICA RAPA* AND *CAPSICUM ANNUUM*

This study characterizes the community of culturable endophytic fungi associated with the roots of *B. rapa* and *C. annuum* in northwestern Spain. By integrating molecular identification and diversity metrics, this work offers new insights into the taxonomic composition of root-associated endophytes in two economically relevant crops.

It is important to recognize at the outset that these findings are conditioned by the isolation strategy. The use of potato dextrose agar (PDA) inherently favors fast-growing or saprotrophic taxa capable of developing on excised tissues under artificial conditions. Consequently, the diversity and distribution patterns described here do not represent the total root microbiome, which would include obligate biotrophic or unculturable lineages identifiable only by metabarcoding, but rather the specific subcommunity recoverable under standardized laboratory conditions. Despite these constraints, culture-based studies remain essential for linking taxonomic identity to function and for preserving living isolates for further experimentation.

Within this culturable fraction, a total of 842 fungal isolates were obtained: 203 from 60 *B. rapa* plants (six plots) and 644 from 32 *C. annuum* plants (four plots). These isolates were visually grouped into 72 (*B. rapa*) and 120 (*C. annuum*) distinct morphotypes. ITS sequencing identified 28 taxa in *B. rapa* and 24 in *C. annuum*, spanning 23 and 20 genera, respectively. The identified fungi were distributed across 12 orders in *B. rapa* and 10 in *C. annuum*, with representatives from the phyla Ascomycota, Basidiomycota, and either Mucoromycota (*B. rapa*) or Oomycota (*C. annuum*). Ascomycota was dominant in both hosts, comprising 86% (*B. rapa*) and 99.4% (*C. annuum*) of identified taxa. In *B. rapa*, Basidiomycota and Mucoromycota each represented 7%, while in *C. annuum*, Basidiomycota and Oomycota were marginal (0.28% each). Detailed information on all fungal isolates, including GenBank codes, sequences and taxonomic assignments, is provided in Supplementary Table S2.

Although yeasts were not the main focus of this study, a considerable number of isolates were recovered from the roots of *B. rapa*. These mainly belonged to the genera *Cyberlindnera* (Ascomycota) and *Rhodotorula* (Basidiomycota). This prevalence likely introduced a bias in diversity estimates due to competitive exclusion, as the rapid

proliferation of yeasts in culture media inhibits the emergence of slower-growing filamentous fungi.

Several fungal taxa were common to both hosts, including *Chaetomium*, *Cladosporium*, *Fusarium*, *Penicillium*, *Talaromyces*, and *Trichoderma*. Some Chaetomiaceae isolates could not be confidently assigned to a genus. Further sequencing of additional loci would be required to resolve their identity within closely related genera such as *Dichotomopilus*, *Chaetomidium*, or *Trichocladium*. Isolates failing to meet identity and coverage thresholds were subjected to phylogenetic analyses with type strains to infer their taxonomic placement. Depending on tree topology, sequences were classified to the genus, order, or phylum level.

Nonetheless, the identification process revealed several limitations that impeded the confident classification of a subset of isolates, largely due to technical issues such as contamination, insufficient growth, unsuccessful DNA extraction, low amplification efficiency, or poor sequence quality.

### 1.1. COMPARATIVE ANALYSIS OF FUNGAL COMMUNITY COMPOSITION

The identified fungal taxa were grouped by taxonomic order. Six major orders were shared between both hosts: Hypocreales, Sordariales, Eurotiales, Glomerellales, Pleosporales, and Cladosporiales. The number of taxa per order was comparable between hosts (Figure 6). A comparison of the number of fungal isolates per plant revealed significant differences between hosts (Figure 7).

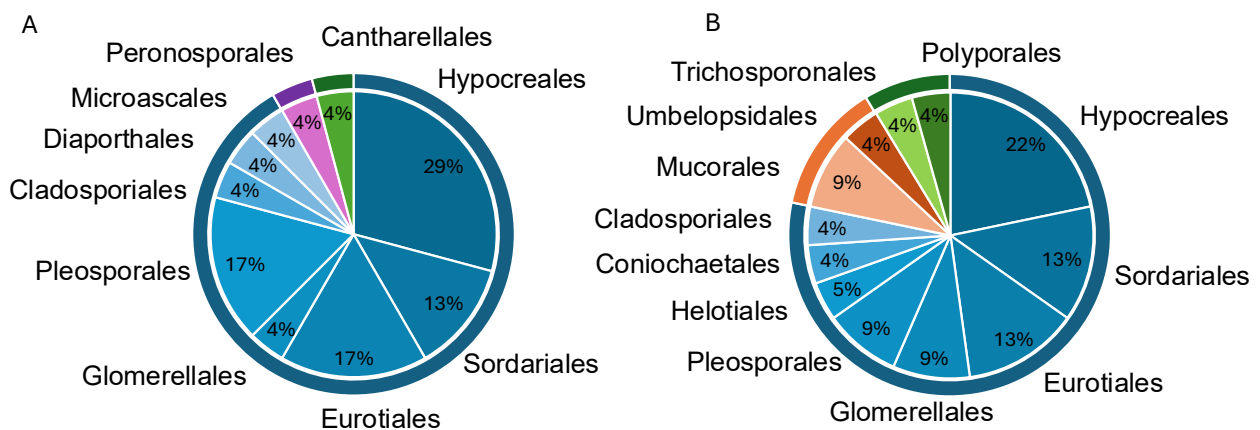


**Figure 6:** Taxonomic distribution of endophytic fungi isolated from *C. annuum* (A) and *B. rapa* (B). Percentages indicate the proportion of distinct genera within each order. The

outer ring represents: Ascomycota (blue), Mucoromycota (orange), Basidiomycota (green), and Oomycota (purple).

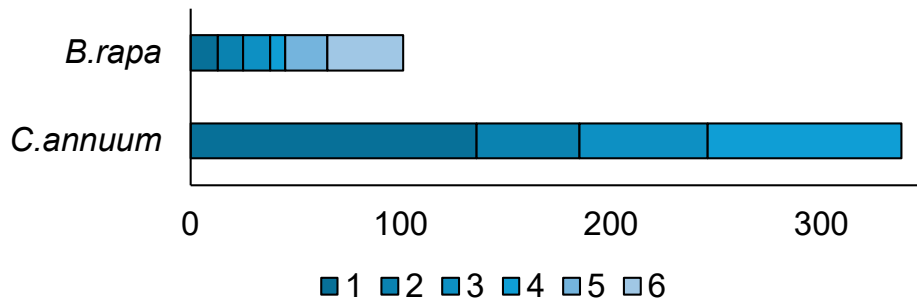


**Figure 7:** Total number of endophytic fungi isolated from *C. annuum* and *B. rapa* across the different sampling spots (1–6).

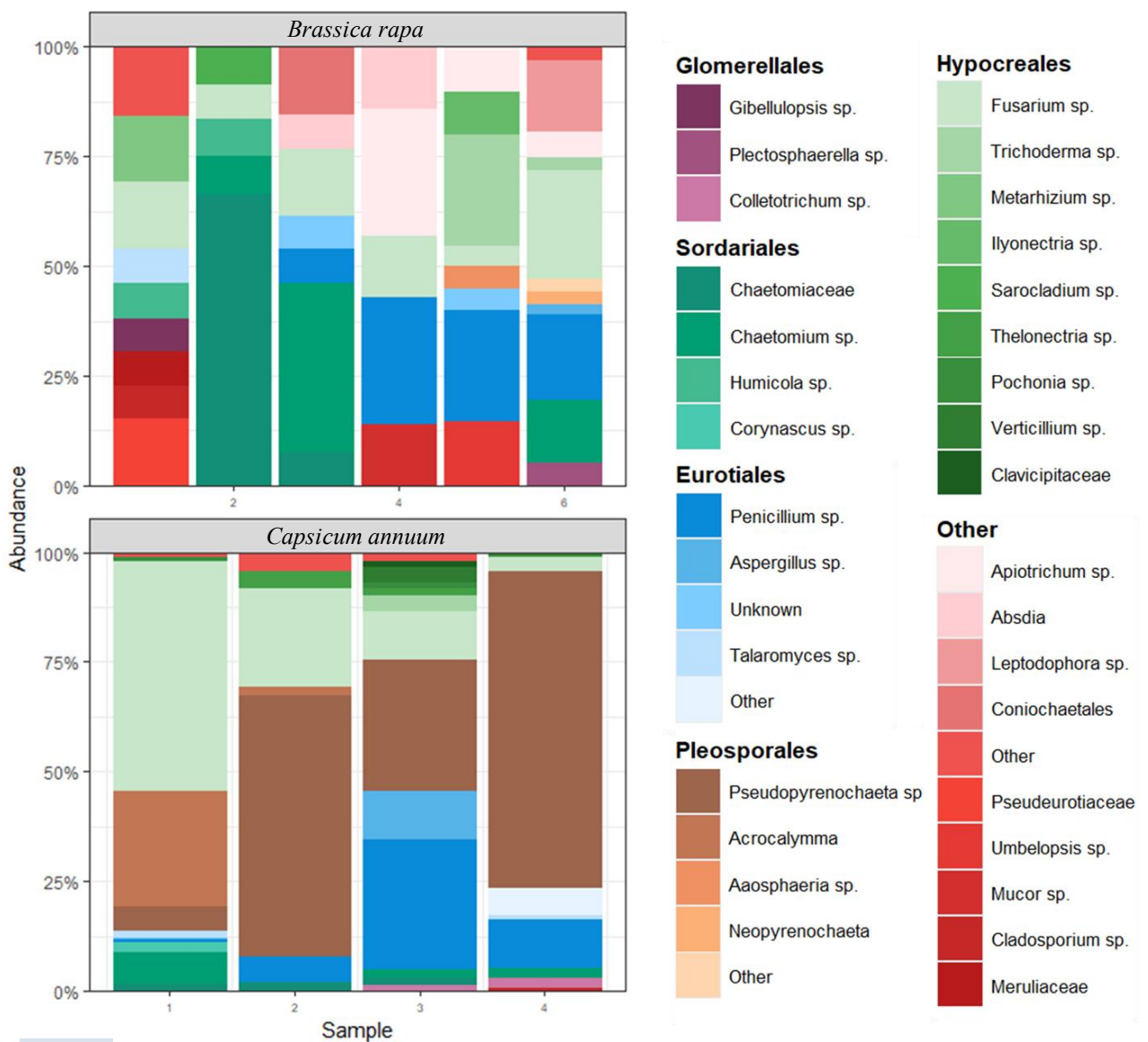


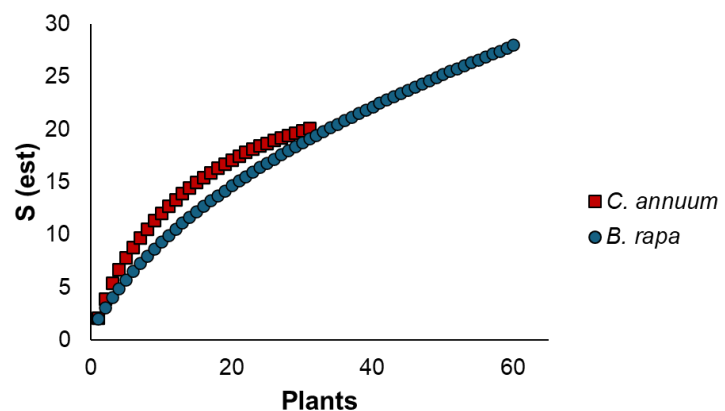
**Figure 8:** Representation of the proportion of identified fungal genera and orders isolated from each sampling event in *B. rapa* and *C. annuum*. Only taxonomically identified isolates are shown.

In *Brassica rapa*, only a small number of filamentous fungal isolates were recovered. For most plants, a single isolate was obtained from the 30 root fragments sampled per plant. Consequently, our data indicate that the majority of *B. rapa* plants hosted only one fungal isolate, with few plants harboring more than three isolates. In contrast, in *Capsicum annuum*, approximately half of the root fragments from a given plant were typically colonized. Accordingly, 60% of *C. annuum* plants contained more than 10 isolates, and 23% exceeded 15 isolates (Figure 7). Despite this high abundance, taxonomic diversity per plant in *C. annuum* was relatively moderate, with most plants hosting between two and five distinct taxa. Furthermore, in *B. rapa*, most fungal taxa occurred as singletons or doubletons (isolated only once or twice across all sampling sites), whereas in *C. annuum*, taxa were more evenly and consistently distributed across sampling events. As illustrated in Figure 8, fungal communities in *C. annuum* were more homogeneous across sampling sites compared to the highly variable composition observed in *B. rapa*.

## 1.2. DIVERSITY PATTERNS AND COMMUNITY ANALYSIS

Rarefaction curves revealed contrasting diversity profiles. The curve for *B. rapa* followed an almost linear trend, suggesting that sampling effort was insufficient to capture total diversity. In contrast, the curve for *C. annuum* approached an asymptote, indicating more complete sampling (**¡Error! No se encuentra el origen de la referencia.**).

**Figure 9:** Rarefaction curves of endophytic fungal isolates from *C. annuum* (red) and *B. rapa* (blue).



Alpha diversity metrics (Shannon: 2.08–2.56; Simpson: 0.87–0.92) confirmed that *C. annuum* had a relatively rich and even fungal community. *B. rapa* showed lower and more variable alpha diversity (Shannon: 1.6–2.3; Simpson: 0.8–0.90), reflecting greater heterogeneity across sites. Beta diversity analysis also highlighted differences: Jaccard distances among *C. annuum* samples ranged from 0.59 to 0.81, whereas those among *B. rapa* samples reached 0.95, indicating greater spatial turnover in the latter (Table 1).

A			B			
	Shannon	Simpson	M1	M2	M3	M4
M1	2.40	0.91	0.00	0.64	0.59	0.63
M2	2.08	0.88		0.00	0.69	0.81
M3	2.56	0.92			0.00	0.59
M4	2.40	0.91				0.00

C			D					
	Shannon	Simpson	M1	M2	M3	M4	M5	M6
M1	2.30	0.90	0.00	0.81	0.93	0.93	0.94	0.95
M2	2.20	0.89		0.00	0.33	0.73	0.86	0.81
M3	1.79	0.83			0.00	0.63	0.82	0.77
M4	1.61	0.80				0.00	0.67	0.85
M5	1.95	0.86					0.00	0.79
M6	2.30	0.90						0.00

**Table 1:** Alpha (Shannon and Simpson) and beta diversity (Jaccard) index of endophytic fungal culturable communities isolated from *C. annuum* (A, B) and *B. rapa* (C, D).

Rarefaction curves suggested that culturable diversity in *B. rapa* may be underestimated, whereas the fungal community of *C. annuum* was more comprehensively captured. This difference is relevant, as the low recovery of isolates in *B. rapa* could bias the results: most fungi appear as singletons (taxa represented by a single isolate) or doubletons (taxa represented by two isolates), likely due to the reduced number of isolates per plant.

### 1.3. ECOLOGICAL DRIVERS OF COMMUNITY STRUCTURE

The lower abundance of endophytic fungi in *B. rapa* could be linked to the presence of glucosinolates (GSL), characteristic Brassicaceae compounds whose derivatives, isothiocyanates (ITC), exhibit strong antimicrobial activity (Bressan et al., 2009; Poveda et al., 2022). It has been demonstrated that the presence of GSL in cruciferous roots, such as those of *A. thaliana*, inhibits root colonization by *Trichoderma*, reducing its ability to enhance plant productivity and tolerance to biotic and abiotic stresses (Poveda, 2021). Other studies report that glucosinolates contribute to resistance against arbuscular mycorrhizal colonization in *Arabidopsis* (Anthony et al., 2020). However, if GSL were the main limiting factor, more defined fungal communities dominated by endophytes specialized in tolerating or degrading these metabolites would be expected. Results do not show that trend: isolates belong to genera which are usually considered generalists, able to colonize multiple crops or soil. The adaptation to GSLs or downstream products might be absent or present for these isolates, and a significant intraspecies variability can be present, but no experiments were conducted to show this. Another factor that may contribute to the lower abundance of endophytic fungi in *B. rapa* is the presence of yeasts, which may outcompete slower-growing filamentous fungi and skew estimates of cultivable richness.

Environmental factors may also explain part of the differences observed between the two crops. The more homogeneous conditions of *C. annuum* may have favored the development of a more uniform fungal community, whereas the greater ecological heterogeneity of the *B. rapa* sites may contribute to high community turnover, as indicated by the elevated Jaccard dissimilarity. This pattern is consistent with previous studies showing that root-associated fungal communities are more strongly influenced by environmental variables than by host identity (Glynou et al., 2016; Thiergart et al., 2020). It also aligns with research showing that the endophytic mycobiome of annual Brassicaceae is dominated by facultative fungi that also occurs in other hosts and non-living substrates (Glynou et al., 2018; Selosse et al., 2018).

Nevertheless, certain host-associated patterns were observed. In *B. rapa*, the orders Hypocreales, Pleosporales, and Helotiales were recurrent, in agreement with other studies on cultivated and wild Brassicaceae (Glynou et al., 2016, 2017; Maciá-Vicente et al., 2020), while Eurotiales and Sordariales also appeared frequently in previous studies (Chen et al., 2020; Poveda et al., 2020).

In contrast, the culturable fungal community of *C. annuum*, although less studied, showed similarities to other Solanaceae hosts. Taxa such as *Colletotrichum*, *Fusarium*, *Alternaria*, *Penicillium*, and *Cladosporium* were consistently detected (Paul et al., 2012; Naziya et al., 2020). Particularly noteworthy is the recurrent detection of *Pseudopyrenochaeta*. Although this genus has been reported as pathogenic in tomato, it was isolated here from asymptomatic plants. This raises important questions about its ecological behaviour. It could function as a latent pathogen, a mutualist under specific conditions, or a context-dependent symbiont. Clarifying its role will require further genomic and functional analyses.

## **2. FUNGAL ENDOPHYTE EVALUATION AGAINST ABIOTIC STRESS**

### **2.1. *IN PLANTA* RESULTS**

#### **2.1.1. RELATIVE WATER CONTENT (RWC)**

The functional evaluation of endophytic fungi as potential agents for drought mitigation presents substantial challenges, particularly when working with taxonomically and physiologically diverse collections. The assessment of relative water content (RWC) and

fresh/dry shoot biomass in *Arabidopsis thaliana* enabled us to evaluate how inoculation with endophytic fungi influenced plant water status and growth performance during prolonged drought.

Overall, plant responses to endophyte inoculation were highly variable. As expected, most inoculated plants did not differ significantly from non-inoculated controls. Of the 45 fungal inoculations tested, only 18 isolates resulted in significant differences in RWC (Figure 10), and 14 isolates produced significant differences in biomass (Figure 11). Notably, no treatment improved both traits simultaneously to a significant degree, aligning with previous observations that enhanced water retention does not necessarily translate into increased vegetative growth under drought (Rodriguez et al., 2009; Naylor et al., 2017).

Regarding water status, plants inoculated with five isolates: *Coniochaeta* sp. (BrT25.01), *Absidia* sp. (BrT40.01), a representative of Pleosporaceae (BrT51.01), *Penicillium* sp. (BrT24.02), and a member of the order Hypocreales (P26.21), exhibited significantly increased RWC (Figure 10). These plants showed improved water status while biomass remained unchanged (except for P26.21, where dry weight decreased), suggesting mechanisms such as enhanced water retention or uptake, osmotic adjustment, or altered stomatal behavior (Marulanda et al., 2009; Lata et al., 2018).

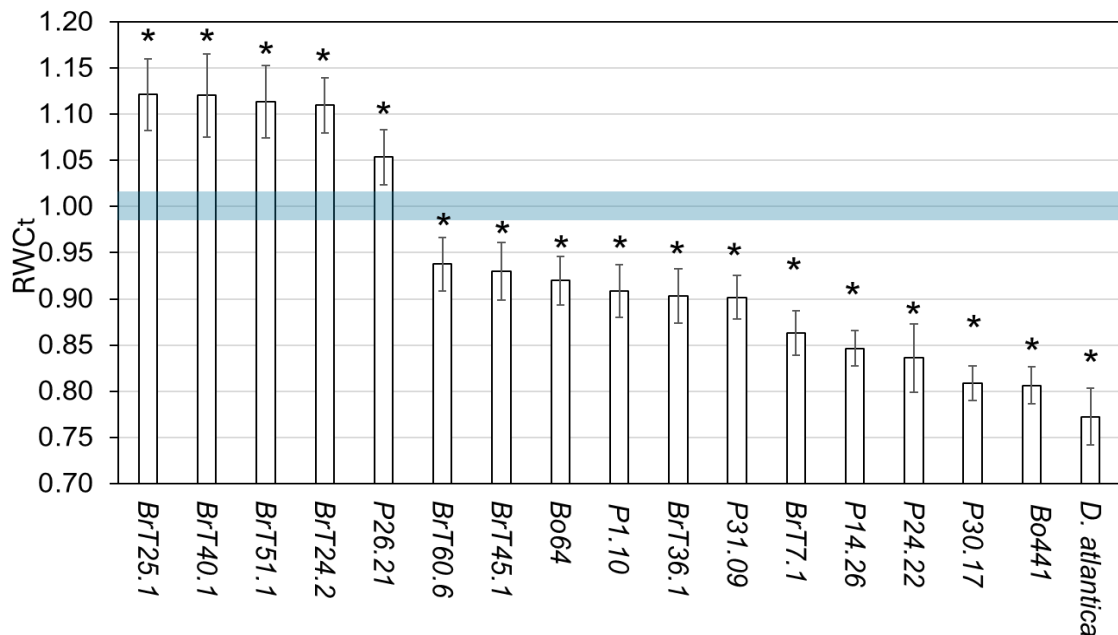


**Figure 10:** Relative water content (RWC) in *A. thaliana* inoculated with endophytic fungi under drought stress. Only the 18 treatments that showed significant differences from the uninoculated control ( $p < 0.05$ ; ANOVA) are displayed, with data normalized

and arcsine-transformed. Bars show mean RWC per treatment, ranked from highest to lowest. The horizontal line indicates the mean control value (1), blue shading represents the control's standard error. Error bars show standard error per treatment.

In contrast, 13 isolates showed a significant reduction in RWC, indicating neutral or potentially detrimental responses under water deficit. Notably, plants inoculated with *D. atlantica*, despite its expected role as a positive control, displayed the lowest RWC values among all treatments. However, *D. atlantica* was among the eight isolates that significantly increased dry biomass, alongside *Pochonia* sp. (P31.09), *Cladosporium* spp. (P30.17, BrT7.01), *P. gallaeciana*, *Fusarium* sp. (P14.26), *Humicola* sp. (BrT3.03), and a member of Pseudeurotiaceae (BrT6.01) (Figure 11).

This decoupling of growth and water status is particularly evident in the group showing increased biomass but lower or unchanged RWC. These responses suggest that increased growth may have raised water demand or reduced water-use efficiency during drought (Khan et al., 2016; Sharma et al., 2021). The observed patterns may also be influenced by the experimental design, which subjected plants to a progressive drought regime. Early moderate stress may have allowed plants inoculated with isolates like *Pochonia* sp., *D. atlantica*, *Cladosporium* spp., *P. gallaeciana*, or *Fusarium* sp. to grow more vigorously than the control, but as drought intensified, these larger plants likely struggled to maintain adequate water status.

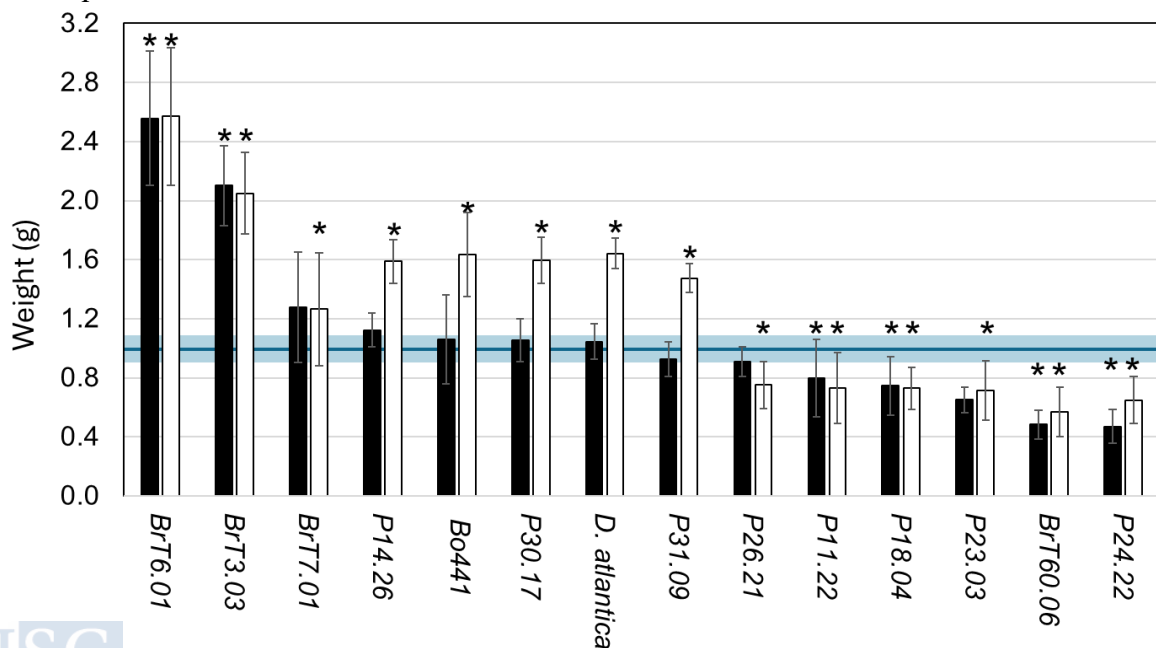


**Figure 11:** Fresh (black bars) and dry (white bars) biomass of *A. thaliana* inoculated with endophytic fungi under drought stress. Only the 14 treatments with significant differences

from the control ( $p < 0.05$ ; ANOVA) are shown. Bars represent the normalized mean biomass per treatment, ranked by fresh weight. The horizontal line marks the mean control value (normalized to 1), blue shading indicates control standard error. Error bars indicate standard error for each treatment.

A distinct response pattern was observed for plants inoculated with *Humicola* sp. and BrT6.01 (Pseudeurotiaceae). These isolates significantly enhanced dry biomass and uniquely, also fresh biomass, while maintaining RWC values comparable to, or slightly higher than, the control. This indicates a more sustained physiological adjustment to drought (Redman et al., 2011; Sadeghi et al., 2020). Although not statistically significant, plants inoculated with *Sarocladium* sp. and *Metarhizium* sp. showed similar trends, exhibiting consistently higher fresh and dry weight and slightly higher RWC.

Conversely, some interactions appeared detrimental. Plants inoculated with *Verticillium* sp. (P24.22), *Aspergillus* sp. (BrT60.6), *Phomopsis* sp. (P18.04), and *Corynascus* sp. (P11.22) exhibited significantly lower fresh and dry biomass than controls. Additionally, *Pseudopyrenochaeta terrestris* (P23.03) and the Hypocreales isolate P26.21 caused reductions exclusively in dry biomass.

In conclusion, the contrasting effects on growth and water status indicate that endophytic fungi can influence plant responses to water deficit through diverse mechanisms: some strains may enhance water retention and conservation, while others stimulate growth processes that indirectly mitigate stress effects. In this context, isolates belonging to *Humicola* sp. and *Pseudeurotiaceae* proved particularly promising, as they promoted both water content and biomass accumulation, suggesting potential applicability under prolonged drought.

Several methodological limitations must also be considered. Symbiosis establishment could not be confirmed, and limited colonization or poor sporulation may have restricted the observed effects. Additionally, the use of *Arabidopsis thaliana* as a model system, while advantageous for reproducibility, might have influenced the outcomes: isolates naturally adapted to pepper roots may not recognize *Arabidopsis* as a compatible host, whereas those derived from *B. rapa* could have been favored due to closer phylogenetic affinity. Verifying colonization success through microscopy, qPCR, or molecular

markers, and validating these functional effects in the original crop species under both controlled and field conditions, should therefore be a priority for future work.

## **2.2. *IN VITRO* RESULTS**

To identify a simple, reproducible, and predictive screening system useful for characterizing fungal isolates, a set of *in vitro* methodologies commonly used to simulate osmotic stress were assessed.

Initially, solid media supplemented with Polyethylene Glycol (PEG) were evaluated. Fungal growth decreased progressively as PEG concentration increased, with marked inhibition at concentrations above 600 g L<sup>-1</sup>. At intermediate levels (400–550 g L<sup>-1</sup>), several isolates maintained or even exceeded the growth observed in control plates, suggesting differential tolerance to osmotic stress among taxa.

To identify the most informative parameters, detailed assays were conducted at 400 and 550 g L<sup>-1</sup> using four isolates with five replicates each. Growth measurements were recorded at multiple time points to capture the temporal dynamics of fungal response (Figure 12). The results revealed that growth measurements were most informative at longer incubation times (t<sub>3</sub>), when colonies had occupied more than half of the plate surface. At early time points (t<sub>1</sub> and t<sub>2</sub>), most isolates grew as well as or better than the control, whereas at later time points, growth generally decreased relative to non-stressed cultures. However, biological variation complicated interpretation; for instance, isolate Bo441 showed comparable growth to controls at early time points but significantly lower growth at t<sub>3</sub>, while isolate Bo690 grew better than the control at t<sub>1</sub> under both PEG concentrations, showed reduced growth at both t<sub>2</sub> and t<sub>3</sub>.

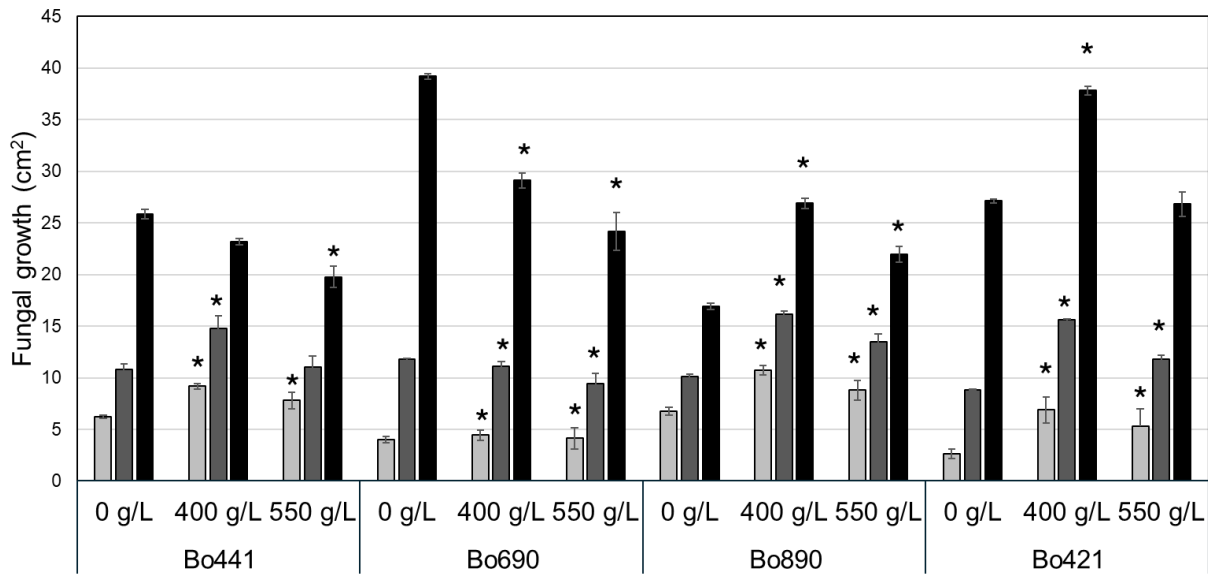


**Figure 12:** Average growth of the endophytic fungi Bo441, Bo690, Bo890 and Bo421 at three time points ( $t_1$ : light gray,  $t_2$ : dark gray, and  $t_3$ : black) and under three PEG concentrations (0, 400, and 550 g/L). Asterisks indicate statistically significant differences compared to the control (0g/L).

Despite the biological variation observed among isolates, PEG-based assays on solid media presented several significant practical limitations that compromised their utility as a screening tool. Because PEG is heat-sensitive and degrades at high temperatures, it cannot be autoclaved and must instead be sterilized by filtration, a process complicated by the high viscosity of concentrated solutions. The subsequent steps of mixing sterile PEG with the medium, allowing adequate equilibration time, and carefully removing excess PEG were time-consuming and frequently led to contamination. Moreover, treatments showed high variability and low reproducibility across replicate plates, making it difficult to draw consistent conclusions about isolate performance

Liquid cultures were subsequently tested to enable direct biomass quantification (dry weight or optical density), theoretically minimizing errors associated with radial expansion. However, this approach introduced new and significant technical challenges.

Under agitation, fungi tended to grow as compact spherical aggregates rather than dispersed mycelia (Figure 13), which made it impossible to obtain consistent OD readings throughout the incubation period. To measure  $OD_{600}$  reliably, the aggregates had to be homogenized using an Ultra-Turrax T25 homogenizer (Janke & Kunkel, Germany). However, since this procedure fragments the hyphae and disrupts the normal development

of the mycelium, it prevents reliable measurements of growth kinetics over time from the same culture.

To enable temporal measurements, experiments were designed with a high number of replicates ( $n = 10$ ), allowing sequential sampling at different time points. At each time point a subset of replicates was homogenized and measured. This approach required numerous repetitions to identify the most appropriate sampling time and to compare fungal growth relative to the control.

At low PEG concentrations (10–20% w/v), most fungal isolates showed no significant differences in dry weight or OD across time points, suggesting either insufficient osmotic stress or limited sensitivity of the method. However, at concentrations above 20%, PEG precipitation occurred in the culture medium, compromising the reliability of the assay.



**Figure 13:** Left: Eight membranes containing fungal hyphae retained after filtration of cultures grown under different PEG concentrations. The top four membranes correspond to *Trichoderma* isolate, while the bottom four correspond to *Fusarium*. Right: Three tubes showing the formation of compact spherical aggregates by different fungal isolates grown in liquid media supplemented with PEG.

A semi-solid setup using cellophane membranes over liquid PEG medium was also implemented where fungal colonies grew on the membrane surface placed over liquid medium supplemented with PEG (0–20% w/v). This configuration was expected to combine the quantitative advantages of radial growth measurements with the controlled osmotic stress delivery of liquid media.

Growth inhibition was evident at higher PEG concentrations, confirming that osmotic stress was being transmitted through the membrane. However, the method proved applicable to only a limited subset of isolates. Fast-growing, highly sporulating species

such as *Trichoderma* sp. formed irregular and fragmented colonies that were difficult to quantify accurately (Figure 14). Other isolates exhibited patchy or uneven growth patterns, with substantial variation even among replicate plates of the same isolate (Figure 14, first row). Consequently, PEG-based methods were deemed inconsistent and unsuitable for reliable screening.

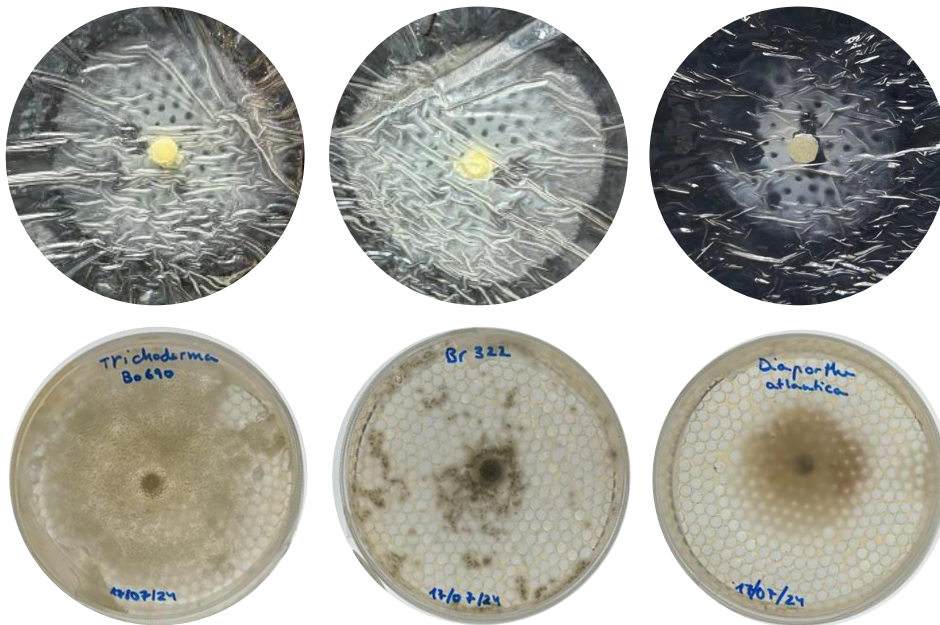


**Figure 14:** The first row shows cellophane membranes on a black background, each corresponding to one of three replicates of the same fungal isolate. In the first two replicates, growth appears homogeneous and circular, whereas in the third, the fungus exhibits irregular development. The second row displays three different fungal isolates growing on cellophane membranes.

In contrast to PEG-based assays, the agar-based approach showed greater stability and produced interpretable and repeatable outcomes across isolates. This method, adopted here as a novel application for fungal screening, simulated drought conditions by increasing the agar concentration in the growth medium. At intermediate levels (125–200% of the standard concentration), most isolates exhibited a clear inverse relationship between agar content and colony expansion.

Comparisons between standard conditions (100% agar) and high-agar media (HA; 125% agar) revealed distinct responses: while *D. atlantica* grew better under standard conditions, *E. festucae* showed no significant differences between control and drought-mimicking conditions. Additional assays using smaller increments (105–120%) yielded

similar results (data not shown). Consequently, the screening was extended to the remaining isolates using 125% agar as the standard screening concentration. Replicated experiments confirmed these patterns, showing significant growth reductions in nearly all isolates (Figure 15). This method proved promising due to its simplicity and low variability; with three replicates per fungal isolate, growth remained consistent, allowing reproducible measurements at multiple time points.

Given its stability, the predictive capacity of the agar-based assay was evaluated by screening a set of fungal isolates previously characterized *in planta*. This enabled a direct comparison between their performance under simulated drought and their actual ability to confer drought tolerance. Isolates that showed no significant growth reduction compared to the control were considered theoretically drought-tolerant. According to this criterion, isolates *E. festucae*, P24.02, P11.07, BrT3.03, and P24.22 met the requirements. Notably, a single isolate, P31.09 (*Pochonia* sp.), even exhibited enhanced growth under drought conditions.

However, the predictive power of this trial was limited. While the method identified several promising strains, three additional isolates known to be beneficial *in planta* would not have been detected using this approach. Overall, the method correctly classified eight strains and misclassified four, successfully identifying only half of the beneficial isolates. These findings indicate limited sensitivity and highlight the need to optimize assay conditions to improve discriminatory capacity.

Despite these limitations in sensitivity, the simplicity, low cost, and scalability of the agar-based assay make it a practical tool for initial screening. Unlike PEG-based media, which proved inconsistent and difficult to handle, the agar-concentration system offers a practical balance between stability and reproducibility, serving as an efficient first filter within a tiered selection strategy. However, it is crucial to acknowledge that any *in vitro* assay represents a simplified model of the complex soil–plant–microbe interface. Consequently, these outcomes should be interpreted as preliminary indicators rather than definitive measures of drought tolerance, requiring subsequent validation to estimate the true proportion of beneficial isolates.

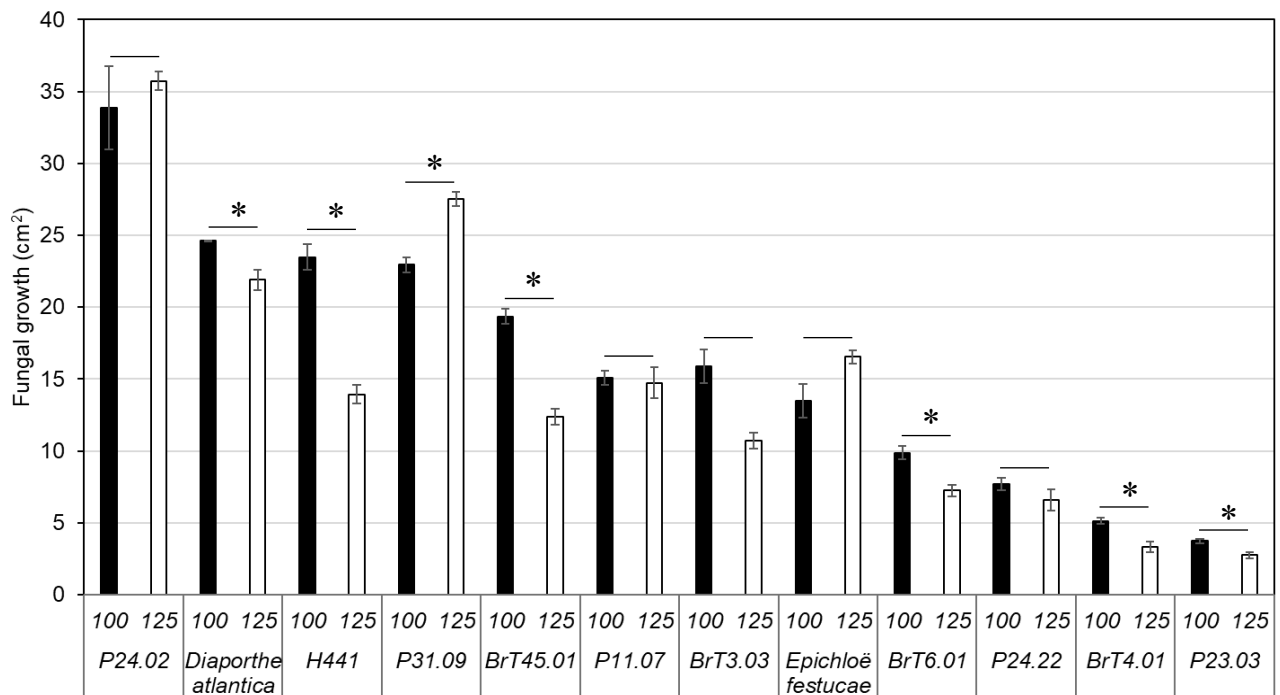


**Figure 15:** Growth area of endophytic fungi on control medium (100% agar; black bars) and drought-simulating medium (125% agar; white bars), based on three replicate plates per isolate. Asterisks indicate statistically significant differences ( $P < 0.05$ ). Error bars represent standard error.

Across all *in vitro* approaches, several morphological differences were observed between control and stress treatments, including alterations in pigmentation, mycelial density, and colony texture (Figure 16). These qualitative changes, although indicative of stress responses, were highly variable among isolates and difficult to quantify.

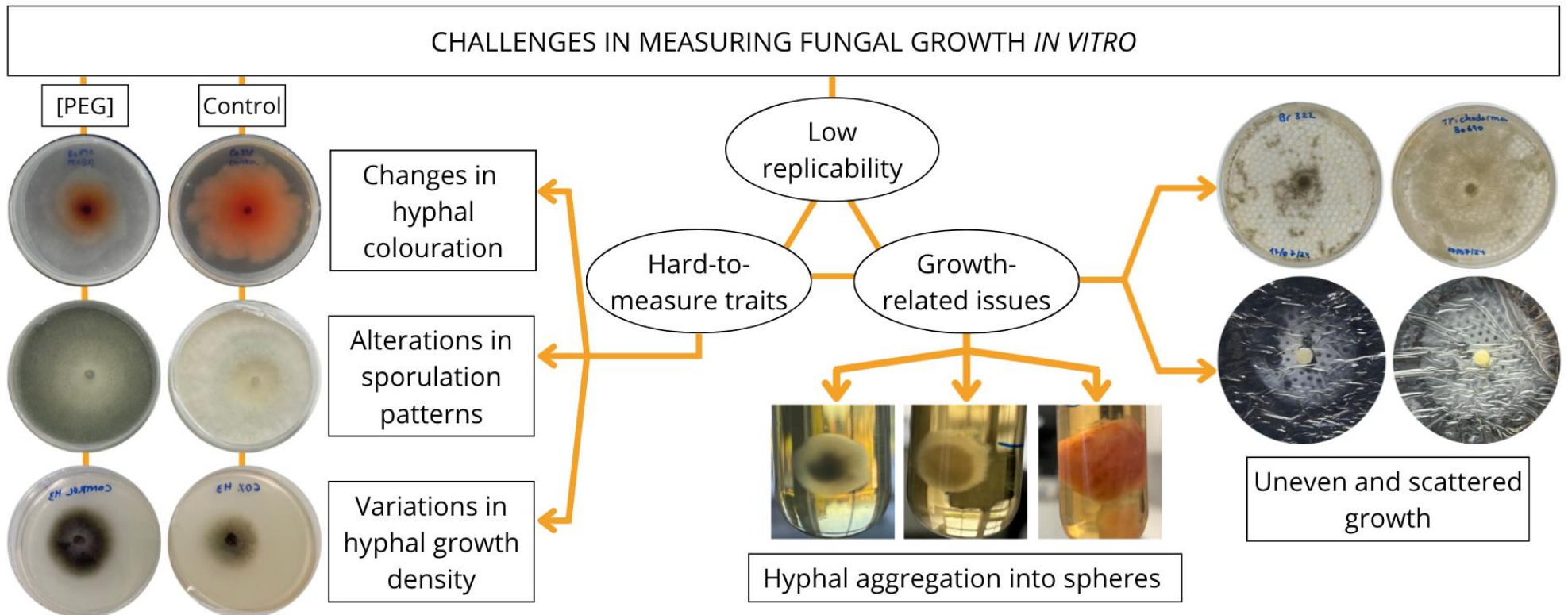


**Figure 16:** Infographic illustrating the challenges associated with *in vitro* drought stress testing.

### 3. FUNGAL ENDOPHYTE EVALUATION AGAINST BIOTIC STRESS

#### 3.1. *IN VITRO* ANTAGONISTIC ACTIVITY AGAINST *RHIZOCTONIA SOLANI*

Of the 146 endophytes screened against *R. solani*, 34 isolates showed visible inhibition or overgrowth in preliminary assays and were selected for quantitative evaluation. Eleven isolates with consistent activity were tested against additional phytopathogens. Data on inhibition percentages and halo sizes are detailed in Supplementary Table S3; representative results are shown in Figure 17 and 18.

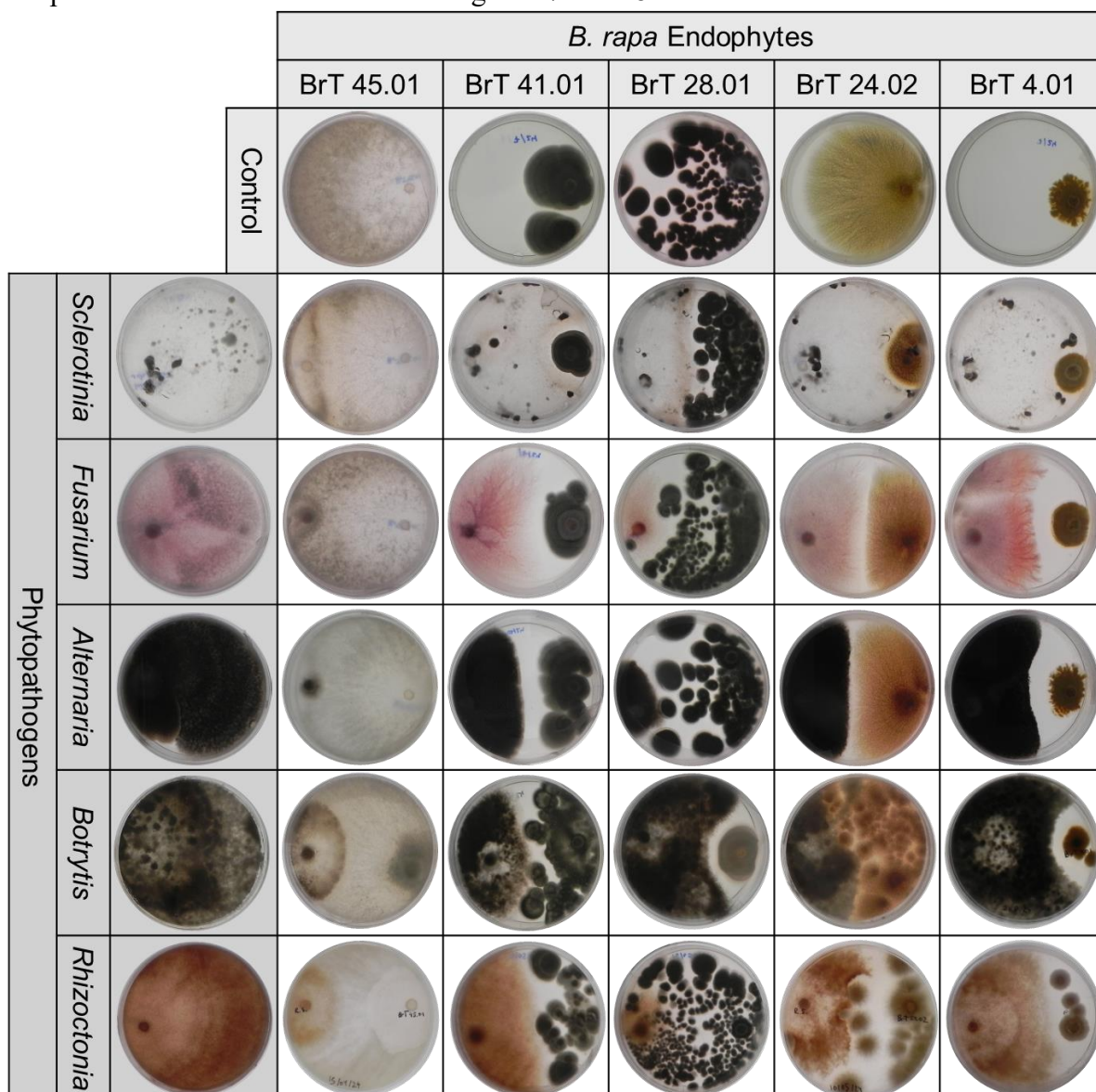


**Figure 17:** Dual culture assays on PDA plates showing antagonistic interactions between endophytic fungi isolated from *B. rapa* and phytopathogens. The top row shows individual growth of endophytic fungi, the left column displays individual growth of

phytopathogens, and the central panel shows dual confrontations between each pathogen and endophyte 15 days after inoculation.

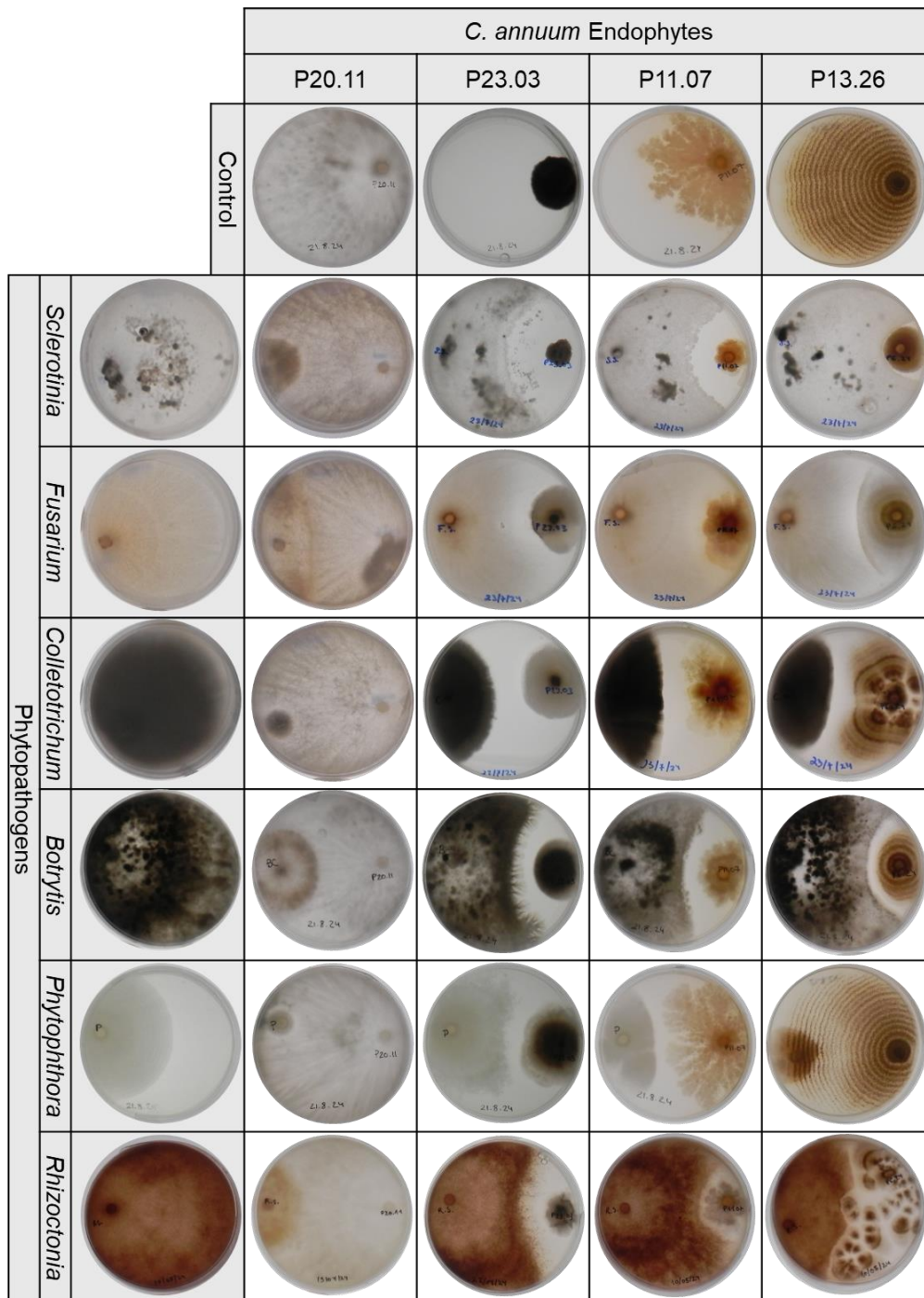


**Figure 18:** Dual culture assays on PDA plates showing antagonistic interactions between endophytic fungi isolated from *C. annuum* and phytopathogens. The top row shows individual growth of endophytic fungi, the left column displays individual growth of phytopathogens, and the central panel shows dual confrontations between each pathogen and endophyte 15 days after inoculation.



Functional screening revealed a spectrum of antagonistic behaviors among the isolates. While some fungi showed narrow-spectrum inhibition, others displayed broad-spectrum activity across multiple pathogens, a trait highly desirable in IPM programs. Furthermore, two primary modes of action were observed: rapid spatial exclusion and the production of diffusible antifungal compounds, evidenced by consistent inhibition halos (Figure 19).

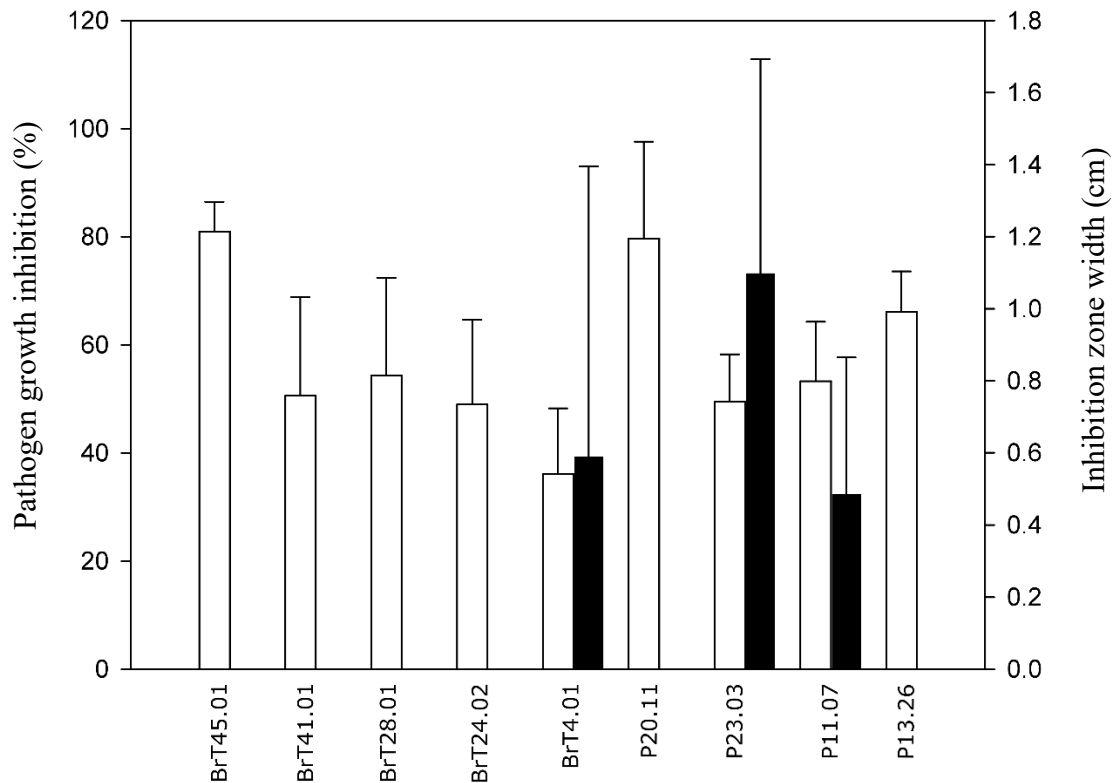


**Figure 19:** Summary of antibiosis effect represented by the mean percentage of inhibition for all pathogens (left y-axis, shown as white bars). The right y-axis (black bars) shows the mean inhibition halo radius in centimeters, averaged across all pathogens. The x-axis displays the different endophytic isolates selected. Error bars represent the standard error.

Specific genera demonstrated distinct strategies. Notably, *Trichoderma* isolates from both hosts, such as BrT45.01 (from *B. rapa*) and P20.11 (from *C. annuum*), stood out for their potent broad-spectrum inhibition driven by rapid overgrowth rather than halo formation. BrT45.01 strongly suppressed all tested pathogens, and P20.11 displayed similar efficacy without producing inhibition zones. These findings align with the well-established profile of the genus *Trichoderma*, which is renowned for mechanisms including mycoparasitism, competition for space and nutrients, antibiosis, and the induction of systemic resistance (Alfiky & Weisskopf, 2021; Asad, 2022). The existence of commercial formulations such as Trianum-P, TUSAL, and Trichotropic WP reflects its recognized biocontrol potential

(Koppert, 2022; Timac Agro, 2022; Invesa, 2020), and the identification of these native strains with high antagonistic capacity further strengthens the case for their integration into sustainable crop protection strategies. Other isolates, such as BrT41.01 and BrT28.01, exhibited moderate inhibitory effects consistent with this competitive model, with BrT41.01 proving particularly effective against *Botrytis cinerea*.

In contrast to the spatial competition observed in *Trichoderma*, other isolates appeared to rely on the production of diffusible antifungal compounds, as evidenced by consistent inhibition halos. For instance, BrT4.01 (*Talaromyces* sp.) consistently produced distinct halos against *F. oxysporum* and *A. alternata*, despite being less effective in spatial displacement. This genus has emerged as a promising biocontrol agent due to its production of antimicrobial compounds, mycoparasitic ability, and growth-promoting effects (Nicoletti et al., 2023). Its efficacy against pathogens such as *B. cinerea* and *S. sclerotiorum* has been previously documented, with reported yield improvements in crops like rice (Abbas et al., 2025), supporting the potential inclusion of BrT4.01 in IPM strategies. Similarly, isolate P11.07 (*Chaetomium* sp.) showed reproducible inhibitory activity with distinct halos. *Chaetomium* spp. are known for producing a wide array of antifungal and antioxidant compounds (Abdel-Azeem, 2020), and extracts from species like *C. cochliodes* have been shown to reduce phytopathogen spore production by more than 70% (Thiep & Soyong, 2015). This suggests that P11.07 may serve as a strong candidate for biofungicide development, pending further chemical characterization.

Finally, the strongest inhibitory effect among all tested isolates was exhibited by P23.03 (*Pseudopyrenochaeta* sp.), which produced well-defined halos against all tested pathogens. Although *Pseudopyrenochaeta* has been previously described as a pathogen, this strain was isolated from asymptomatic hosts and showed consistent antagonistic activity, suggesting a potentially broader ecological role. It is possible that P23.03 functions as a latent, low-virulence endophyte capable of inhibiting more aggressive pathogens. However, to assess its suitability as a biocontrol agent, future studies must address its pathogenicity, metabolite profile, and performance *in planta*. Comprehensive characterization through metabolomics, whole-genome analysis, and greenhouse validation will be essential to confirm the efficacy and safety of these promising isolates

for agricultural applications.

### 3.2. *IN PLANTA* EVALUATION OF ANTIFUNGAL ACTIVITY

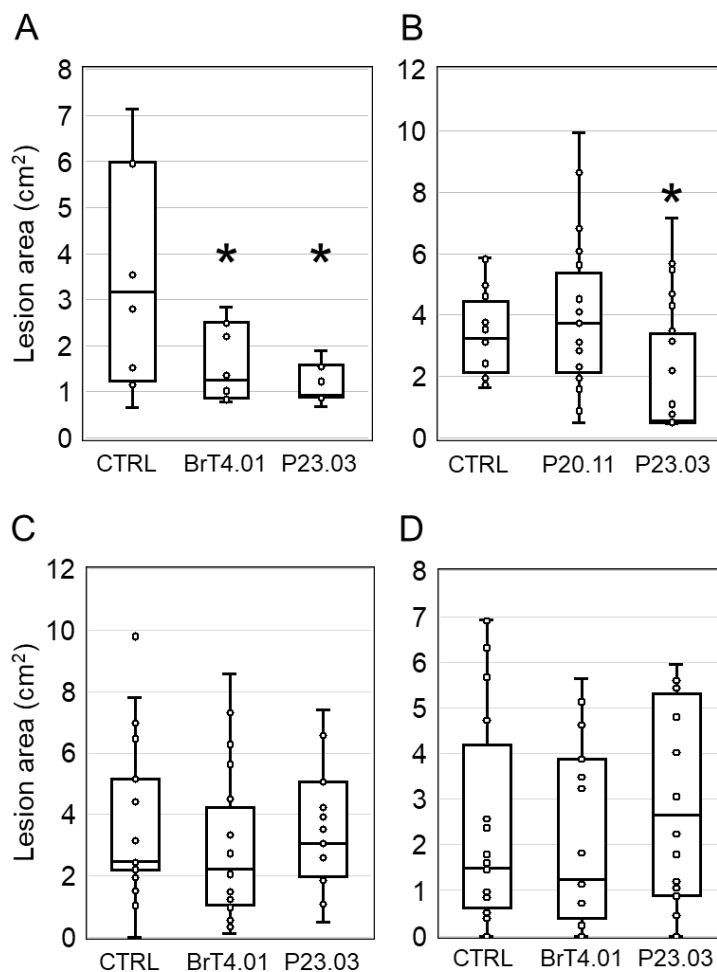
Following the *in vitro* screening, isolates P23.03, P20.11, and BrT4.01 were selected for their strong antagonistic activity and evaluated *in planta* to assess their efficacy in reducing disease severity caused by *S. sclerotiorum*. The pathogenicity assay was conducted under controlled conditions and subsequently repeated to confirm reproducibility. Furthermore, *P. capsici* was included as a target pathogen in the *C. annuum* trials.

The three endophytes were tested on two host species, *C. annuum* and *B. oleracea*. In the first assay, plants pre-inoculated with P23.03 and later infected with *S. sclerotiorum* exhibited a significant reduction in necrotic leaf area compared to non-inoculated controls, regardless of the host species. Similarly, *B. oleracea* plants inoculated with BrT4.01 showed a marked decrease in disease symptoms. In contrast, *C. annuum* plants treated with P20.11 did not differ significantly from the control group (Figure 20, A and B). However, these protective effects were not consistently reproduced in the repeated assay, where no statistically significant differences were observed across treatments, host species (*C. annuum* or *B. oleracea*), or pathogens (*S. sclerotiorum* or *P. capsici*) (Figure 20, C and D).

In both assays, attempts to re-isolate the inoculated endophytes using culture-dependent methods were unsuccessful due to the overgrowth of a fast-growing contaminant. Consequently, PCR-based detection was employed in the second assay to assess colonization by P23.03. Molecular analysis confirmed the presence of this strain in all tested plants, including non-inoculated controls of both species, suggesting background contamination or natural environmental occurrence.

Taken together, the initial results suggest that these endophytes may act *in planta*, potentially by secreting antifungal compounds or activating host defense responses (Lan and Wu, 2020; Harman et al., 2004). However, the lack of reproducibility between assays underscores the context-dependent nature of endophyte-mediated biocontrol and highlights the critical importance of replication when assessing microbial inoculants.

**Figure 20:** Boxplots representing the lesion area caused by *S. sclerotiorum* in plants pre-inoculated with endophytic fungi (BrT4.01, P20.11, P23.03) or with PBS 1× (control; CTRL). Panels A and C correspond to *C. annuum*, and panels B and D to *B. rapa*. Panels A and B show results from the first experiment, while panels C and D present data from the second experiment. Statistically significant differences ( $p < 0.05$ ) are indicated with an asterisk.



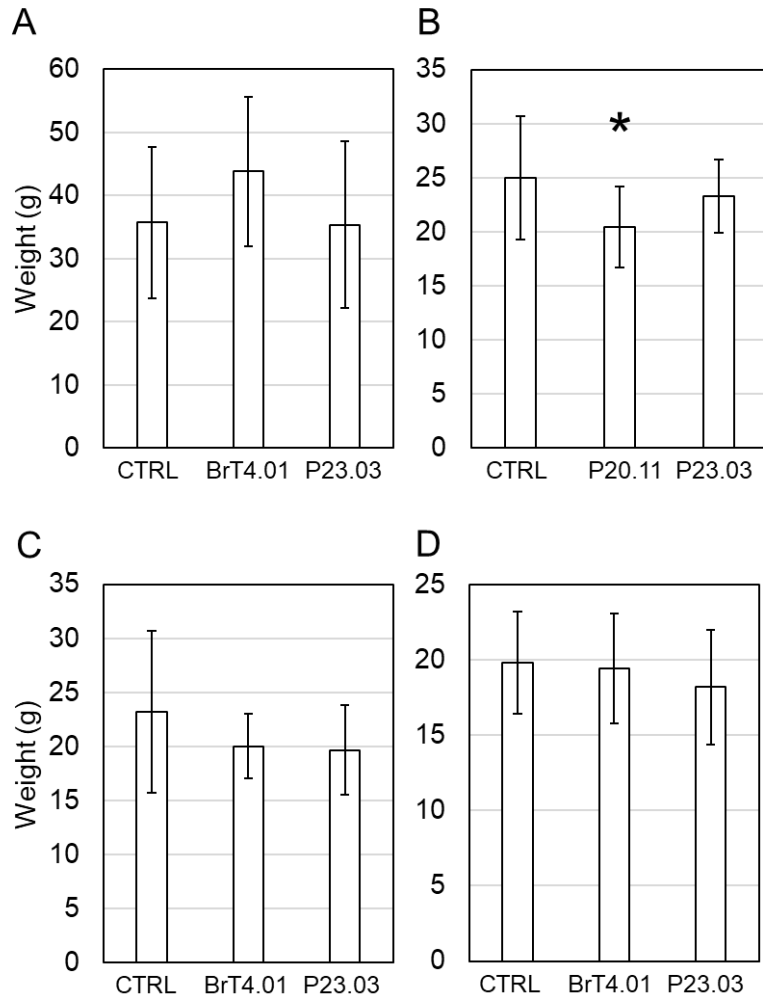
### 3.3. EFFECT OF ENDOPHYTIC FUNGI ON PLANT GROWTH AND PHYSIOLOGY

To assess whether endophyte inoculation had any detrimental effect on plant development, the fresh weight of all plants inoculated with endophytes and pathogens was measured. Additionally, a subset of *C. annuum* and *B. oleracea* plants inoculated with endophytes was maintained for an extra two weeks to evaluate biomass and physiological parameters using a LI-600 Porometer/Fluorometer (LI-COR Biosciences).

In all tested species, plants inoculated with P23.03 and BrT4.01 showed no significant differences in fresh weight or stomatal conductance compared to control plants (Figure 21). However, strain P20.11 proved to be an exception, causing a significant reduction in *C. annuum* biomass. These results suggest that, under the tested conditions, these fungi are generally not detrimental to host plant physiology, a crucial prerequisite for their potential agricultural application. Nevertheless, the growth reduction observed with

P20.11 aligns with previous reports indicating that endophyte–host interactions may involve trade-offs or detrimental effects depending on the environmental or physiological context (Schulz & Boyle, 2005).

**Figure 21:** Bar chart showing the fresh weight of plants inoculated with different endophytic fungi (BrT4.01, P20.11, P23.03) or with PBS 1× (control; CTRL). Error bars represent the standard error. Panels A and C correspond to *C. annuum* plants, and panels B and D to *B. rapa* plants. Panels A and B show data from the first experiment, while panels C and D show data from the second experiment. Statistically significant differences ( $p < 0.05$ ) are indicated with an asterisk.



Altogether, these results emphasize both the promise and the complexity of using endophytic fungi as biocontrol agents. On one hand, several isolates showed strong antifungal activity *in vitro* and potential to reduce disease symptoms *in planta*; on the other hand, the variability of outcomes and methodological limitations (such as the inability to confirm colonization and the potential for unintended contamination) highlight key obstacles to practical application. These findings reinforce the need for rigorous, replicated experiments and improved methodological approaches, including optimized colonization protocols, reliable molecular tools for detection, and functional assays of fungi metabolites synthesis.

## 4. FUNCTIONAL AND METABOLOMIC CHARACTERIZATION OF *PSEUDOPYRENOCHAETA* ISOLATES WITH ANTIFUNGAL ACTIVITY

### 4.1. MOLECULAR IDENTIFICATION OF FUNGAL ISOLATES

To characterize the *Pseudopyrenochaeta* isolates at the species level, two sets of specific primers were employed: Plyc1-F/R, designed to amplify a 147-bp fragment in *P. terrestris* and Plyc2-F/R, which targets a 209-bp fragment in *P. lycopersici*.

The molecular analysis confirmed the identity of isolates P27.06 and P27.24 as *P. lycopersici*, as both yielded amplicons of the expected 209-bp size with the Plyc2-F/R primer set. Although faint non-specific bands of approximately 500 bp were occasionally observed with Plyc1-F/R in these isolates, their size deviation from the target amplicon allowed for clear discrimination, ensuring they did not compromise the diagnostic accuracy of the assay.

In contrast, isolates P20.08, P22.09, P23.10, P23.03, P30.06, and P24.08 showed specific amplification exclusively with Plyc1-F/R, consistent with the expected 147-bp fragment. The absence of amplification with Plyc2-F/R in these samples supports their classification as *P. terrestris* and highlights the high specificity of the primer sets for distinguishing between these closely related species. The reliability of the assay was further validated by the negative controls, which showed no amplification (Figure 22), confirming the absence of contamination and the robustness of the identification method.

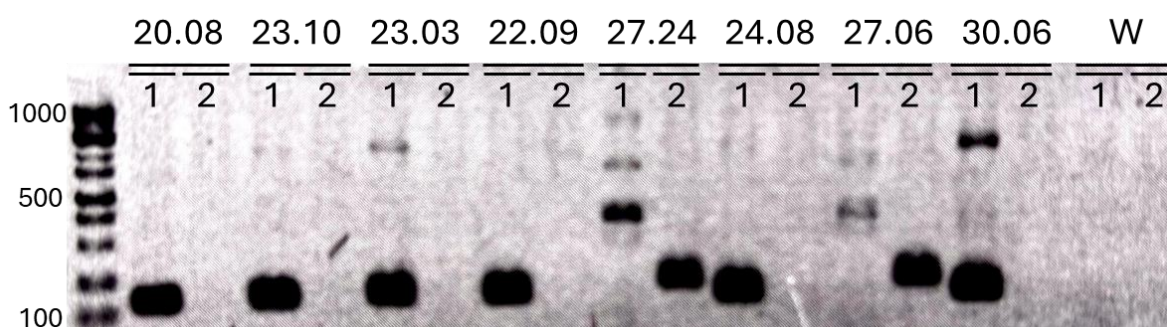


**Figure 22:** Agarose gel electrophoresis showing PCR amplification of fungal isolates P20.08, P23.10, P23.03, P22.09, P27.24, P24.08, P27.06, and P30.06 using species-specific primers Plyc1-F/R (lane 1) and Plyc2-F/R (lane 2). Isolates were classified as *P. terrestris* or *P. lycopersici* based on the presence of a ~147 bp band in lane 1 or a 209 bp

band in lane 2, respectively. A 100 bp DNA ladder (Thermo Fisher Scientific) was included as a molecular size reference. The final lane shows the negative controls.

## 4.2. *IN VITRO* EVALUATION OF ANTIFUNGAL ACTIVITY

### 4.2.1. DUAL-CULTURE ASSAYS

A total of eight fungal isolates (P20.08, P23.10, P23.03, P22.09, P27.24, P24.08, P27.06 and P30.06), all belonging to the *Pseudopyrenochaeta* morphotype, were evaluated for antifungal activity against *R. solani* using dual-culture assays on PDA prepared with Sigma-Aldrich medium (St. Louis, MO, USA). Based on the diameter of the inhibition halos, isolates were classified into three categories:

- **High activity:** P23.03 and P30.06 produced strong inhibition halos ( $\geq 1.0$  cm), significantly reducing the radial growth of *R. solani*.
- **Moderate activity:** P20.08, P23.10, and P22.09 generated halos ranging from 0.75 to 0.95 cm, significantly reducing the radial growth of *R. solani*.
- **Weak (0.45–0.7 cm) or no activity ( $\leq 0.4$  cm):** P24.08, 27.24 and P27.06, showed inhibition halos  $\leq 0.4$  cm, with *R. solani* growth comparable to control plates (Figure 23).

When high or moderate antifungal activity was observed, the mycelia of the antagonistic isolates and *R. solani* did not establish direct contact, suggesting that growth inhibition was likely mediated by diffusible extracellular metabolites. To verify this, a modified Petri dish assay (Álvarez-García et al., 2021) was simultaneously employed to determine whether the observed effects could be attributed to volatile compounds produced by the most active isolate, P23.03. The results indicated that volatile-mediated interaction was negligible, as exposure of *R. solani* to volatiles emitted either by P23.03 alone or by its co-culture with the pathogen did not reduce or alter growth. These findings support the hypothesis that the antifungal activity of P23.03 is primarily driven by non-volatile metabolites, thereby justifying the subsequent use of extract-based assays and LC-QTOF analysis for their chemical characterization.

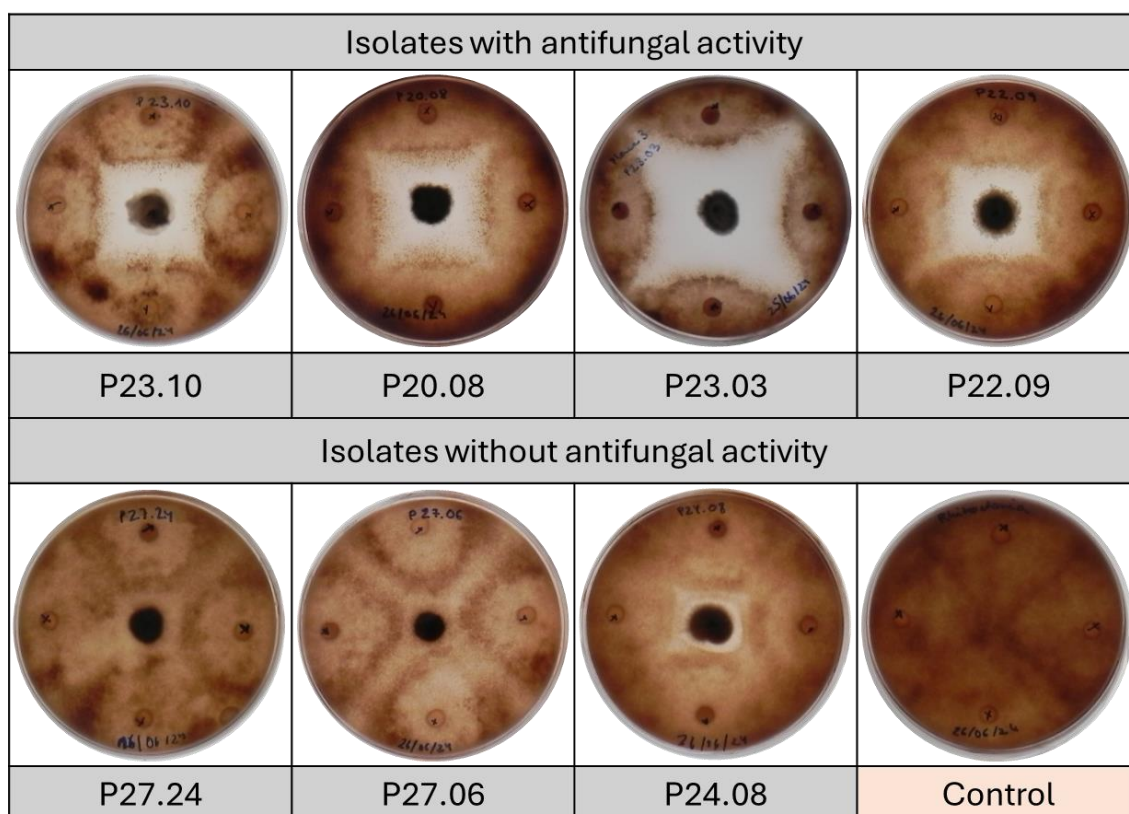


**Figure 23:** Representative replicate of dual-culture assays between *Pseudopyrenochaeta* isolates and *R. solani* on PDA Sigma-Aldrich medium (St. Louis, MO, USA), 15 days post-inoculation (dpi). Each plate shows the antagonist inoculated at the center and *R. solani* as four plugs arranged in a square.

#### 4.2.2. EXTRACT-BASED INHIBITION ASSAYS (DISC DIFFUSION METHOD)

To confirm the involvement of bioactive secondary metabolites, extract-based assays were performed. Extracts obtained from all *P. terrestris* isolates (P23.10, P24.08, P20.08, P22.09, P30.06, and P23.03) displayed high or moderate inhibitory activity against *R. solani*. In contrast, extracts from the *P. lycopersici* isolates P27.06 and P27.24 exhibited no detectable inhibition. The inhibitory effect was highly consistent across biological replicates (Figure 24).

Within this framework, a clear relationship was observed between taxonomic identity and antagonistic activity: all isolates exhibiting moderate to high inhibitory capacity were identified as *P. terrestris*, whereas inactive isolates corresponded to *P. lycopersici*. This pattern suggests that antagonistic capacity is not a general trait of the genus, but rather a species-specific characteristic, likely linked to differences in the biosynthesis or regulation of secondary metabolites.

The case of isolate P24.08 is particularly noteworthy. Although this isolate did not exhibit antifungal activity in previous dual-culture assays, its extract produced clear and well-defined inhibition halos, suggesting the synthesis of antifungal metabolites that may not be expressed or detectable under direct confrontation conditions

Nevertheless, even among the *P. terrestris* isolates, not all showed the same level of inhibition. This functional heterogeneity could be explained by genetic differences, epigenetic mechanisms, or differential regulation of biosynthetic pathways in response to environmental cues. In many fungal genera, secondary metabolite production is strain-specific and depends on the activation or silencing of Biosynthetic Gene Clusters (BGCs) (Brakhage, 2012; Westphal et al., 2021). Therefore, the limited number of isolates analyzed in this study prevents us from stating with certainty whether the observed association between *P. terrestris* and antifungal activity represents a general trait of the species or a phenomenon specific to the studied populations. Broader geographic sampling and multilocus analyses will be required to determine whether these observed functional differences reflect evolutionary divergence, intraspecific variability, or local adaptation processes.

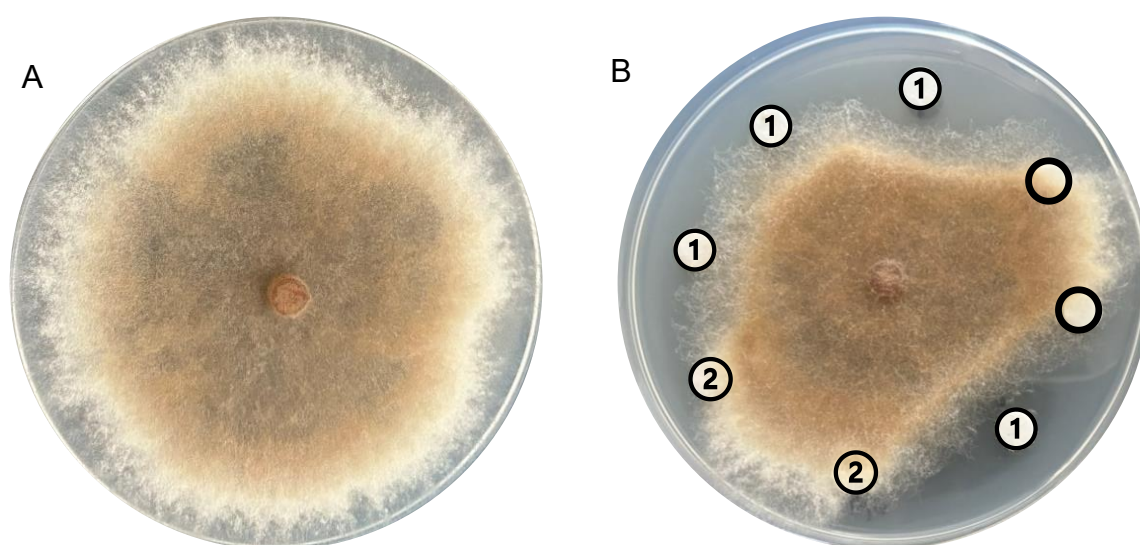


**Figure 24:** Disc diffusion assays assessing the effect of species identity on antifungal activity against *R. solani*. Each PDA Sigma-Aldrich (St. Louis, MO, USA) plate was inoculated with *R. solani* at the center and surrounded by eight cotton discs containing fungal culture extracts. (A) *R. solani* without extracts; (B) extracts from *P. terrestris* (1) and *P. lycopersici* (2) grown on PDA Sigma-Aldrich (St. Louis, MO, USA). Unnumbered discs are negative controls.

#### 4.2.3. MEDIUM EFFECT ON ANTIFUNGAL ACTIVITY

The composition of the culture medium significantly influenced both the morphology of *P. terrestris* and its antagonistic interaction with *R. solani*. Isolates grown on PDA Dinkelberg Analytics (Budapest, Hungary) exhibited minimal or no inhibitory effect against *R. solani* (inhibition halos  $\leq 0.4$  cm). In contrast, when cultivated on PDA from Sigma-Aldrich (St. Louis, MO, USA) under identical conditions, the same isolates displayed clear antagonistic activity (Figure 25). These differences became more pronounced with extended incubation periods.

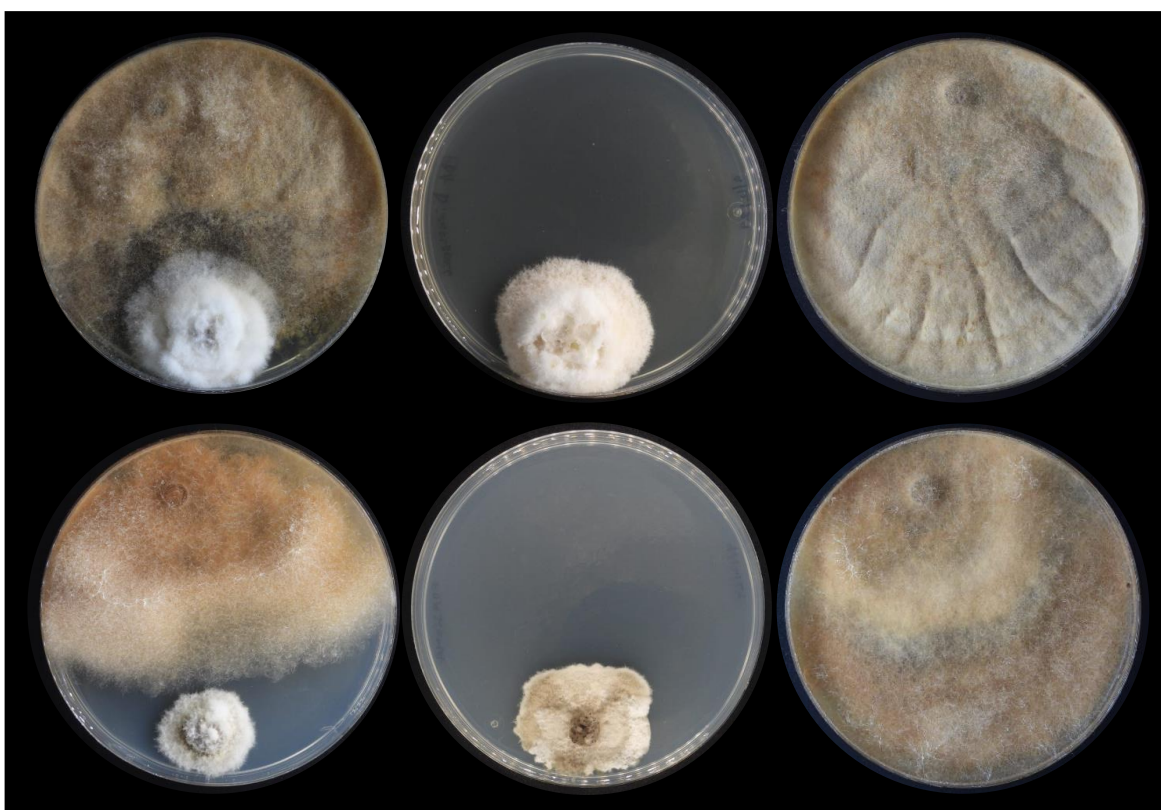


**Figure 25:** Comparative growth of *P. terrestris* and *R. solani* on PDA prepared with the two commercial media. The top row shows plates containing PDA from Dinkelberg Analytics (Budapest, Hungary), while the bottom row corresponds to PDA from Sigma-Aldrich (St. Louis, MO, USA). Within each row: column 1 shows dual-culture assays, column 2 shows *P. terrestris* in monoculture, and column 3 shows *R. solani* alone. The images highlight how fungal morphology and inhibitory capacity vary depending on the culture medium, after six weeks of incubation.

This medium-dependent variation was not limited to direct physical interactions but also affected the production of bioactive compounds. Extract-based assays revealed that the

antifungal activity of extracellular metabolites was strictly dependent on the cultivation medium. Extracts obtained from isolates grown on PDA Dinkelberg Analytics failed to inhibit *R. solani*, regardless of whether the pathogen was tested on PDA Sigma-Aldrich or PDA Dinkelberg Analytics. Conversely, extracts from the same isolates cultivated on PDA Sigma-Aldrich consistently produced distinct inhibition halos (Figure 26).

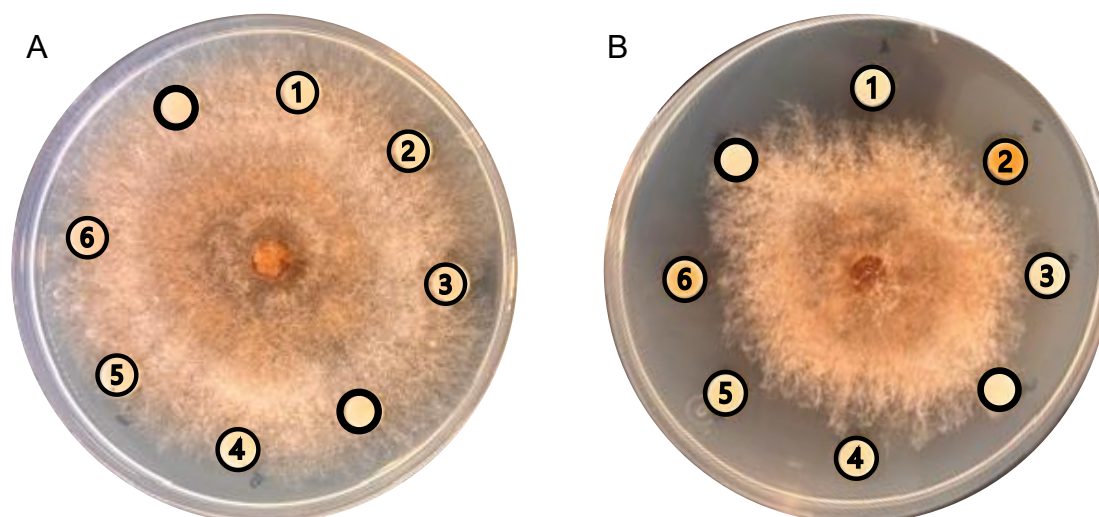


**Figure 26:** Disc diffusion assays evaluating the effect of culture medium on antifungal activity against *R. solani*, after four weeks of incubation. Each PDA Sigma-Aldrich (St. Louis, MO, USA) plate was inoculated with *R. solani* at the center and surrounded by eight cotton discs containing *P. terrestris* fungal extracts: (A) extracts from isolates grown on PDA Dinkelberg Analytics (Budapest, Hungary); (B) extracts from the same isolates grown on PDA Sigma-Aldrich (St. Louis, MO, USA). Numbers correspond to isolates: 1 = P23.10, 2 = P24.08, 3 = P20.08, 4 = P22.09, 5 = P30.06, 6 = P23.03. Unnumbered discs represent negative controls.

These results indicate that external cultivation conditions are decisive in regulating the expression of antifungal activity. Specifically, isolates grown on Sigma-Aldrich medium exhibited strong inhibition, whereas those cultivated on Dinkelberg Analytics medium suppressed such activity. This behavior aligns with previous observations indicating that undefined media, such as PDA, can exhibit considerable variability in chemical composition depending on the manufacturer or batch, particularly regarding micronutrient content (Griffith et al., 2007; Westphal et al., 2021). Such differences are sufficient to alter the expression of Biosynthetic Gene Clusters (BGCs) and redirect metabolic fluxes, leading to profound differences in the abundance and diversity of secondary metabolites. Consequently, these findings underscore the high sensitivity of

fungal secondary metabolism to environmental cues and highlight the critical need to standardize culture media in comparative and bioprospecting studies to ensure reproducibility.

### 4.3. UNTARGETED METABOLOMIC ANALYSIS AND COMPOUND IDENTIFICATION

To investigate the metabolic basis of the antifungal activity observed in *Pseudopyrenochaeta* isolates, untargeted metabolomic profiling was performed. Given that preliminary assays indicated this activity depends on both taxonomic identity and culture conditions, two comparative analyses were conducted. The first addressed the species effect, contrasting the highly active *P. terrestris* (isolate P23.03) with the inactive *P. lycopersici* (isolates P27.06 and P27.24). The second examined the medium effect, comparing six *P. terrestris* isolates grown on PDA prepared with media from Sigma-Aldrich (St. Louis, MO, USA), where extracts retained strong antifungal activity, versus Dinkelberg Analytics (Budapest, Hungary), where extracts were inactive.

Prior to statistical analysis, the dataset underwent strict quality control (QC) filtering to ensure reproducibility. QC samples, prepared as representative mixtures of all study samples, were used to monitor instrument stability. Features absent in more than 50% of QC samples or exhibiting high variability (RSD > 20%) were removed to eliminate noise and unstable peaks. This rigorous filtering yielded a robust dataset, retaining 303 out of 702 high-quality features for the species comparison, and 1,230 out of 3,475 for the medium comparison.

Statistical analysis combined two complementary approaches. Univariate analysis using Volcano plots identified features significantly different between groups ( $|\log_2FC| \geq 1$ ;  $FDR \leq 0.05$ ), while multivariate analysis using Partial Least Squares Discriminant Analysis (PLS-DA) captured global metabolic differences and highlighted features with high importance in projection ( $VIP \geq 2$ ). Together, these methods provided a rigorous framework for prioritizing candidate metabolites.

In the species comparison, PLS-DA revealed a clear separation between *P. terrestris* and *P. lycopersici*, demonstrating strong model performance ( $R^2 = 0.92$ ;  $Q^2 = 0.68$ ). Analysis identified 44 features with high importance in projection ( $VIP \geq 2$ ), five of which were significantly enriched in *P. terrestris* according to Volcano plot criteria, representing candidates potentially linked to its specific antifungal phenotype.

Similarly, the medium comparison (Sigma-Aldrich (St. Louis, MO, USA) and Dinkelberg Analytics (Budapest, Hungary)) showed robust discrimination between cultivation conditions ( $R^2 = 0.97$ ;  $Q^2 = 0.94$ ). Forty-nine features had  $VIP \geq 2$ , and 364 were significantly more abundant in Sigma-Aldrich (St. Louis, MO, USA) extracts, suggesting that many antifungal metabolites are downregulated or absent under Dinkelberg Analytics (Budapest, Hungary) conditions (Figure 27).

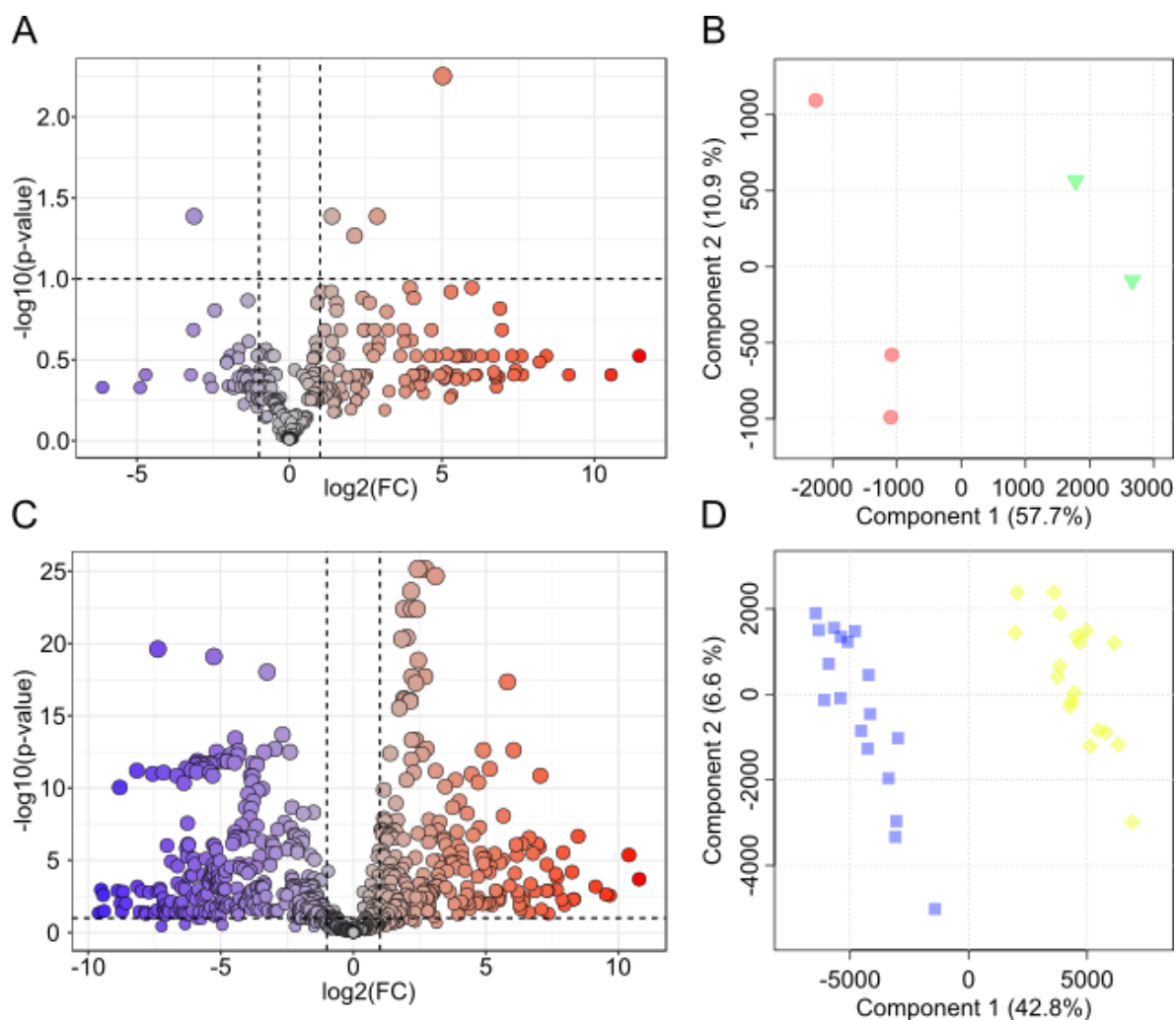


**Figure 27:** Volcano plots (A and C; FDR = 0.1) showing differences in the metabolomic profiles between the compared groups. A: Comparison between *P. terrestris* (isolate P23.03) and *P. lycopersici* (P27.24 and P27.06). C: Comparison of endophytic fungi grown on PDA medium from two different suppliers (Dinkelberg Analytics (Budapest, Hungary) and Sigma-Aldrich (St. Louis, MO, USA)). B and D: PLS-DA Score plots illustrate the separation between groups corresponding to the comparisons shown in A and C, respectively. In the plots, green triangles represent *P. lycopersici*, red circles correspond to *P. terrestris* (P23.03), blue squares indicate isolates grown on Dinkelberg

Analytics (Budapest, Hungary) PDA (P23.03, P30.06, P20.08, P23.10, P22.09, and P24.08), and yellow diamonds represent the same isolates grown on Sigma-Aldrich (St. Louis, MO, USA) PDA.

By integrating the differential analyses from both comparisons, nine features emerged as high-priority candidates. These metabolites were consistently more abundant in *P. terrestris* relative to *P. lycopersici* and were simultaneously enriched under the permissive Sigma-Aldrich conditions compared to the restrictive Dinkelberg medium. These overlapping features, supported by at least one statistical criterion in each comparison, represent the most robust candidates likely responsible for the observed antifungal activity (Table 2).

#### 4.3.1. TENTATIVE IDENTIFICATION AND ANNOTATION

To facilitate interpretation, the nine features identified were grouped according to shared chromatographic and spectral characteristics. The first group comprised features 1 and 2, which coeluted (identical retention time) and shared two diagnostic fragments ( $m/z$  60.081 and 85.028). The second group included three features with overlapping fragmentation patterns: features 3 and 4 coeluted, and the major ion of feature 4 matched the precursor mass of feature 3, while features 3 and 5 shared common fragments. The third group consisted of features with identical retention time and a unique fragment at  $m/z$  329.21. Finally, groups 4 and 5 contained individual features that did not cluster with others and were therefore analyzed independently.

Subsequent tentative identification was performed using tandem mass spectrometry (MS/MS). Accurate masses and fragmentation spectra were compared against multiple public databases, including METLIN, KEGG, PubChem, HMDB, ChEBI, and the Plant Metabolic Network. In addition, SIRIUS (version 6.2.2) and MetaboAnalyst (Xia et al., 2009) were employed to predict molecular formulas based on exact mass and isotopic patterns, providing complementary evidence for structural annotation.

G	F	m/z	RT	I	Fragments of greater intensity (m/z)	Chemical formula	Putative identification [M]	References
1	F1	162.113	1.01	[M+H] <sup>+</sup>	45.057, 57.034, 58.066, 59.073, 60.081, 69.033, 85.028, 102.092, 103.039	C <sub>7</sub> H <sub>15</sub> NO <sub>3</sub>	Carnitine	MassBank <sup>1</sup>
	F2	204.123	1.01	[M+H] <sup>+</sup>	60.081, 145.050, 85.028	C <sub>9</sub> H <sub>17</sub> NO <sub>4</sub>	Acetylcarnitine	MassBank <sup>2</sup>
2	F3	513.099	17.19	[M+H] <sup>+</sup>	283.094, 155.046, 139.051, 167.046, 265.082, 485.105	C <sub>21</sub> H <sub>24</sub> N <sub>2</sub> O <sub>9</sub> S <sub>2</sub>	Thiodiketopiperazine alkaloids	-
	F4	283.092	17.18	[M+H] <sup>+</sup>	45.035, 114.092, 166.058	C <sub>12</sub> H <sub>14</sub> N <sub>2</sub> O <sub>6</sub>		
	F5	495.088	21.40	[M+H] <sup>+</sup>	109.029, 139.050, 81.034, 155.045, 231.015, 265.083	C <sub>21</sub> H <sub>22</sub> N <sub>2</sub> O <sub>8</sub> S <sub>2</sub>		
3	F6	659.430	24.73	[2M-H] <sup>-</sup>	329.212	C <sub>21</sub> H <sub>30</sub> O <sub>3</sub>	Hydroxyretinoic acid methyl ester	Human Metabolome Database <sup>12</sup>
	F7	681.411	24.76	[2M-2H+Na] <sup>-</sup>	329.212			
4	F8	565.170	24.08	[M-H] <sup>-</sup>	273.075, 257.081, 279.231, 547.158, 529.148, 503.169, 183.029, 291.086, 165.018, 167.034, 149.023, 139.039, 123.044	C <sub>30</sub> H <sub>30</sub> O <sub>11</sub>	Polyphenol	-
5	F9	365.067	20.27	[M-H] <sup>-</sup>	175.040, 189.019, 161.024, 145.029, 117.035, 133.029, 205.014, 301.053, 319.063, 329.046, 348.065	C <sub>20</sub> H <sub>14</sub> O <sub>7</sub>	Pentahydroxyflavone +R1	-

**Table 2:** Summary of the 9 key metabolic features (F) consistently overrepresented in *P. terrestris* and Sigma-Aldrich (St. Louis, MO, USA) medium extracts. The table includes the group in which they are classified (G), exact mass (M), ionization mode (I), retention time (RT, minutes), the fragments with highest intensity, the putative chemical formula, the putative compound identification and the references where the main fragments can be found.

MassBank 1: [https://massbank.jp/MassBank/RecordDisplay?id=MSBNK-Antwerp\\_Univ-METOX\\_P100201\\_EF88](https://massbank.jp/MassBank/RecordDisplay?id=MSBNK-Antwerp_Univ-METOX_P100201_EF88)

MassBank 2: [https://massbank.jp/MassBank/RecordDisplay?id=MSBNK-SMB\\_Measured-HSA001P0204000](https://massbank.jp/MassBank/RecordDisplay?id=MSBNK-SMB_Measured-HSA001P0204000)

Human Metabolome Database 1: <https://hmdb.ca/metabolites/HMDB0035185#spectra>

Human Metabolome Database 2: <https://hmdb.ca/metabolites/HMDB0012452#spectra>

#### 4.3.1.1. GROUP 1: FEATURES 1 Y 2 – TENTATIVE ANNOTATION AND FRAGMENTATION ANALYSIS

Group 1 comprises features 1 and 2, detected at  $m/z$  162.1126 and 204.1230 ( $[M+H]^+$ ), respectively. These features were grouped based on their coelution (retention time = 1.01 min) and the presence of two diagnostic fragment ions in their MS/MS spectra:  $m/z$  60.081 ( $C_3H_{10}N^+$ ,  $\Delta = 3.3$  ppm) and  $m/z$  85.028 ( $C_4H_5O_2^+$ ,  $\Delta = 1.2$  ppm). These ions are widely recognized as characteristics of carnitine derivatives, corresponding to the trimethylammonium group and the propenylcarboxylate moiety, respectively.

Feature 1 ( $m/z$  162.1126) exhibited additional fragment ions at  $m/z$  69.034, 102.092 ( $C_5H_{12}NO^+$ ), 58.066, 59.073, 57.034, and 45.058 (Figure 28), all previously reported in carnitine fragmentation patterns (Airaksinen, 2018; MassBank). The calculated neutral molecular mass ( $C_7H_{15}NO_3$ , 161.105 Da) is consistent with that of carnitine.

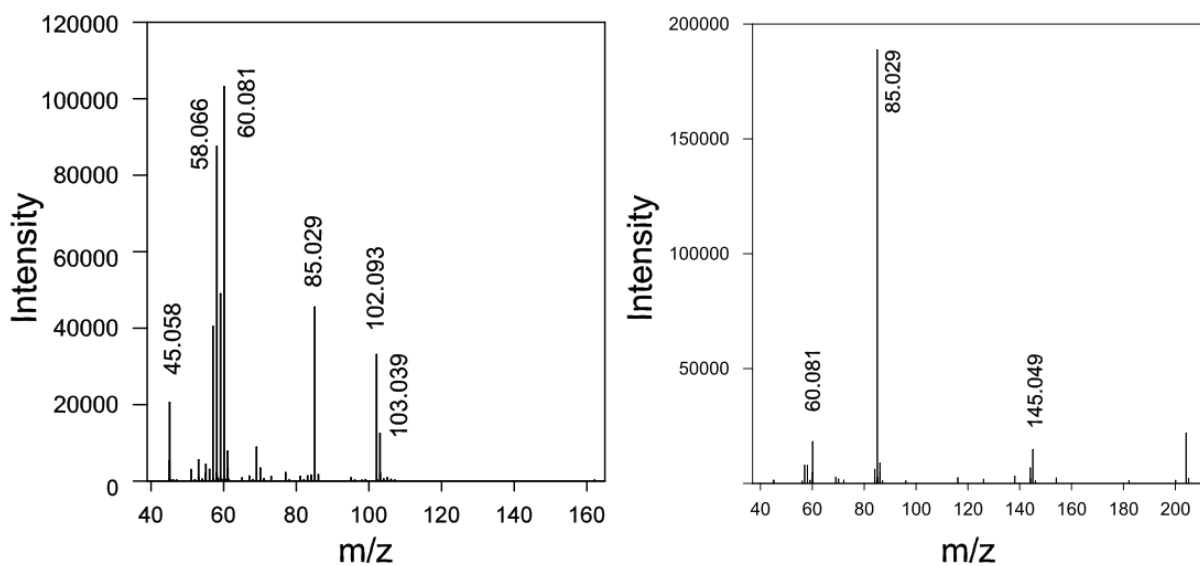


**Figure 28:** MS/MS spectrum showing the fragmentation pattern of feature 1 (left) and feature 2 (right), with a precursor ion at  $m/z$  162.113 and  $m/z$  204.123, respectively.

Feature 2 ( $m/z$  204.1230,  $\Delta = 0$  ppm) displayed the diagnostic ion  $m/z$  145.050, which is characteristic of acetylcarnitine ( $C_9H_{17}NO_4$ , 203.115 Da). The molecular formula also matches acetylcarnitine.

Taken together, the fragmentation data support the tentative annotation of Group 1 as carnitine and its acetylated derivative, acetylcarnitine, corresponding to MSI level 2 confidence. The relationship between fragment ions and proposed structures is illustrated

in Figure 29, which highlights neutral losses, chemical formulas of each ion, and the mass accuracy ( $\Delta m/z$ ) between theoretical and observed values.

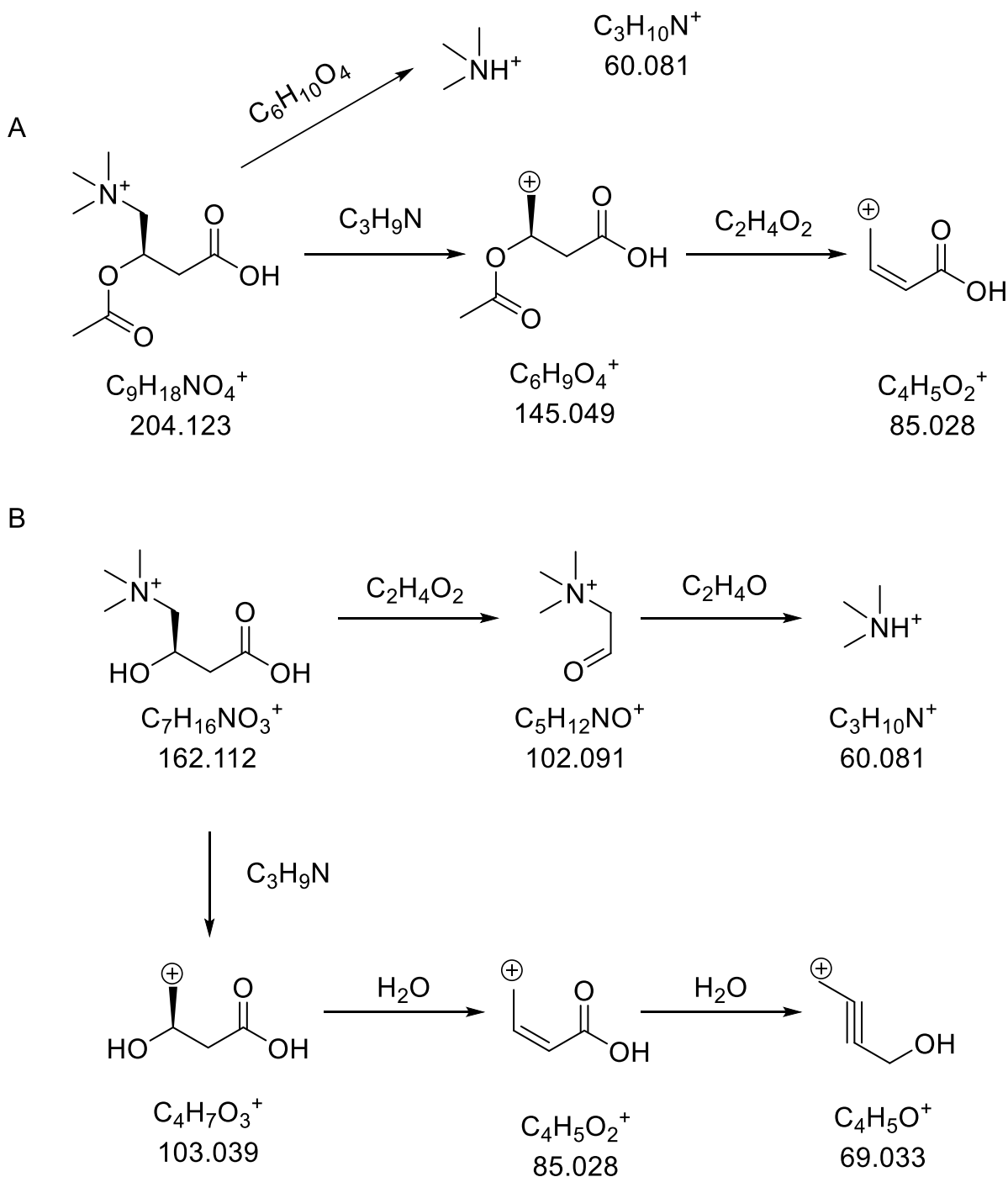


**Figure 29:** Proposed fragmentation scheme for features 1 (A, m/z 162.113,  $[M+H]^+$ ) and 2 (B, m/z 204.123,  $[M+H]^+$ ), tentatively annotated as carnitine and acetylcarnitine, respectively. The main MS/MS fragment ions are shown, with their corresponding chemical formulas, theoretical m/z values (to three decimal places). Arrows indicate inferred neutral losses between fragments.

Biologically, although a direct antifungal role for these compounds appears unlikely, their accumulation may indicate increased  $\beta$ -oxidation and mitochondrial activity, processes typically intensified during secondary metabolite synthesis or under oxidative stress conditions (Calvo et al., 2002).

#### 4.3.1.2. GROUP 2: FEATURES 3, 4 Y 5. TENTATIVE ANNOTATION AND FRAGMENTATION ANALYSIS

Group 2, detected in positive ionization mode ( $[M+H]^+$ ), comprises three features with  $m/z$  513.099 (F3), 283.092 (F4), and 495.088 (F5), eluting at 17.19, 17.18, and 21.40 min, respectively (Table 2). Features F3 and F4 coeluted, and examination of the MS/MS spectrum of F3 (Figure 30B) shows that its largest fragment (283.094) matches the  $m/z$  value of feature F4 (283.092). This suggests that F3 undergoes fragmentation and that F4 may correspond to one of its in-source fragments. Correlation analysis in MetaboScape ( $r = 0.991$ ) further supports this interpretation, indicating that F4 likely represents an in-source fragment of F3 (Figure 31).

Fragmentation spectra showed that F3 ( $m/z$  513.099) generated a predominant fragment at  $m/z$  283.094, along with lower-intensity ions at  $m/z$  155.046, 265.083, 139.051, 167.046, and 485.101 (Figure 30B). In the case of F5 ( $m/z$  495.088), the major fragment was  $m/z$  265.083, followed by  $m/z$  155.045 and 231.015 (Figure 30C). Both compounds shared several fragments, including the aforementioned  $m/z$  155.046, 485.101, and 231.015, as well as  $m/z$  139.050, 81.034, 109.029, 111.055, 150.055, 160.040, 167.046, 202.074, and 219.077 suggesting a structural or biosynthetic relationship between them (Figure 31).

The fact that F5 lacks the fragment at  $m/z$  283.090, but contains the fragment at  $m/z$  265.085, indicates that the  $m/z$  283.090 species has undergone a neutral loss of  $H_2O$  ( $-18.010$  Da). In other words,  $m/z$  265.085 corresponds to the dehydrated form of the  $m/z$  283.09 molecule ( $C_{12}H_{14}N_2O_6 \rightarrow C_{12}H_{13}N_2O_5$ ). Similarly, the mass difference between F3 ( $m/z$  513.099) and F5 ( $m/z$  495.088) also corresponds to  $-18.010$  Da, supporting a direct chemical relationship between these species. In F3, an additional fragment at  $m/z$  485.101 differs by 27.99 Da from the precursor, which may indicate the loss of a carbonyl group ( $-C=O$ ). This observation suggests that  $m/z$  485.101 could represent the core structure, while  $m/z$  513.099 corresponds to a carbonylated form (Figure 31).

Correlation analysis in MetaboScape also revealed an additional precursor at  $m/z$  530.126 that coeluted with F3 and F4 (TR = 17.18 min,  $r = 0.972$ ). The mass difference of 17.026 Da relative to  $m/z$  513.099 is consistent with the loss of  $\text{NH}_3$ . The proposed molecular formula for this precursor is  $\text{C}_{21}\text{H}_{27}\text{N}_3\text{O}_9\text{S}_2$ . Its fragmentation pattern showed intense signals at  $m/z$  283.092, 513.095, 265.084 and 155.045 (Figure 30A), indicating that these compounds are chemically related (Figure 31).

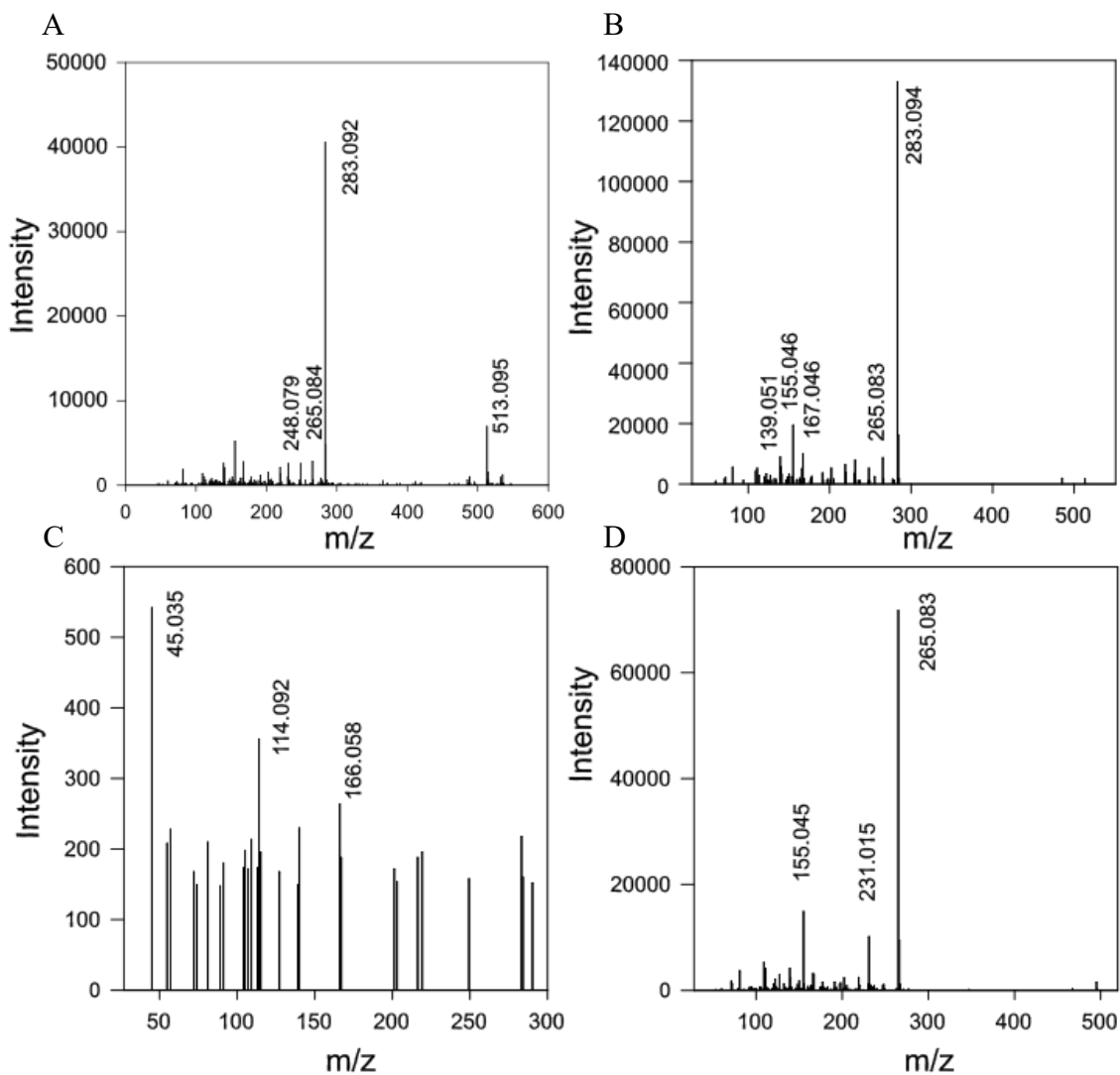


**Figure 30:** MS/MS spectra displaying the fragmentation patterns of: (A) the correlated feature at  $m/z$  530.12; (B) feature 3 with  $m/z$  513.099; (C) feature 4 with  $m/z$  283.093; and (D) feature 5 with  $m/z$  495.089.

Based on accurate mass and isotopic patterns, the following molecular formulas were proposed:

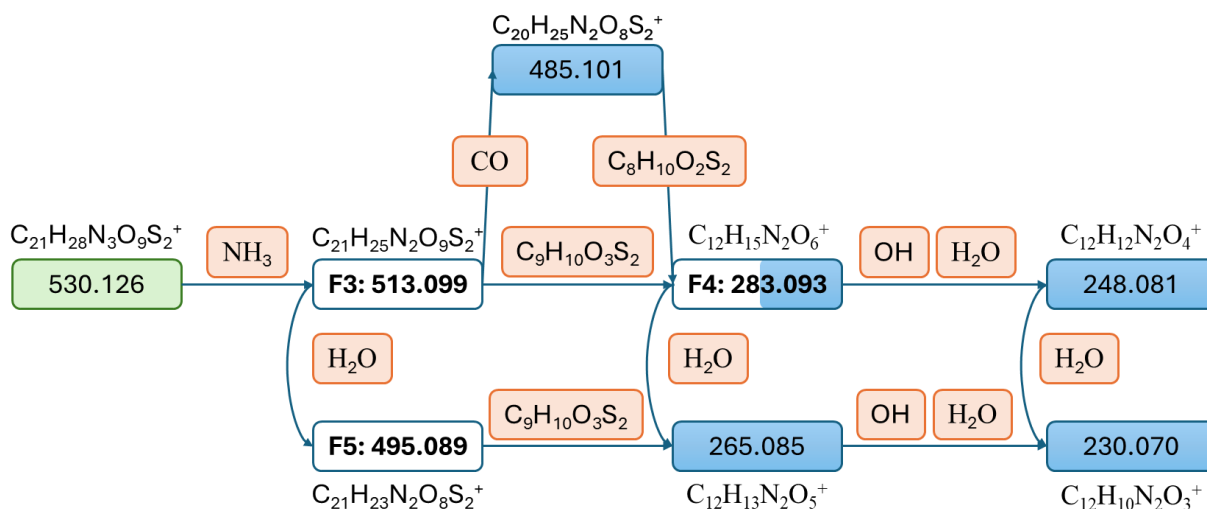


**Figure 31:** Proposed fragmentation scheme, highlighting the precursor ions (white boxes), major fragments (blue), and neutral losses (orange). The ion  $m/z$  283.09 appears both as the precursor of F4 and as a fragment of F3. The correlated precursor  $m/z$  530.12 is indicated in green. Arrows represent proposed relationships between features and their main fragments, and molecular formulas are shown for each species.

Database searches for characteristic fragments ( $m/z$  155.046, 265.083, 283.094, 513.099, and 530.126) did not yield conclusive matches. The ion  $m/z$  283.09 coincides with the mass of guanosine (Zhou et al., 2025) and has been reported, together with  $m/z$  265.08, in degradation products of magnoflorine (Xue et al., 2015) and fragments of trepibutone (Sun et al., 2019), but none of these compounds matched the fragmentation pattern or molecular formula of the features (F3, F4 or F5). The precursor  $m/z$  530.126 corresponds to the mass of lumefantrine, although its structure is inconsistent with the observed fragments. For the highest-mass feature ( $C_{21}H_{27}N_3O_9S_2$ ,  $m/z$  530.126), PubChem returned six hits; five were incompatible with the fragmentation pattern, while one compound (CID: 163586631) could explain the loss of  $NH_3$  leading to F3 ( $m/z$  513.099) and subsequent fragments  $m/z$  485.101 and 495.094. However, the presence of two sulfonic acid groups in this structure conflicts with the formula assigned to  $m/z$  283.092 ( $C_{12}H_{15}N_2O_6$ ), which contains six oxygens but no sulfur. These inconsistencies suggest that the core structure may correspond to  $C_{21}H_{24}N_2O_9S_2$  ( $m/z$  513.099). A PubChem

search for this formula returned 47 entries, among which several candidates share structural features compatible with the proposed fragmentation pathway.

Analysis of the most intense fragments supports a sequential loss pattern:  $C_{21}H_{24}N_2O_9S_2$  ( $m/z$  513.099) loses CO to yield  $C_{20}H_{25}N_2O_8S_2$  ( $m/z$  485.101), then loses  $C_8H_{10}O_2S_2$  to form  $C_{12}H_{15}N_2O_6$  ( $m/z$  283.092), followed by OH losses generating  $C_{12}H_{13}N_2O_5$  ( $m/z$  265.085) and  $C_{12}H_{12}N_2O_4$  ( $m/z$  248.081), and finally the loss of  $C_6H_5O$  to produce  $C_6H_7N_2O_3$  ( $m/z$  155.046). These observations indicate that oxygen groups are likely present as hydroxyls rather than sulfonyl moieties, and that the disulfide bridge may be cleaved early, while both nitrogen atoms remain in all major fragments, suggesting they form part of the molecular core. Among the remaining candidates after structural filtering, nine share features consistent with thiodiketopiperazine alkaloids (TDKPs), which fit the proposed fragmentation scheme and include a central heterocycle with two nitrogen atoms and a disulfide bridge (Figure 32).

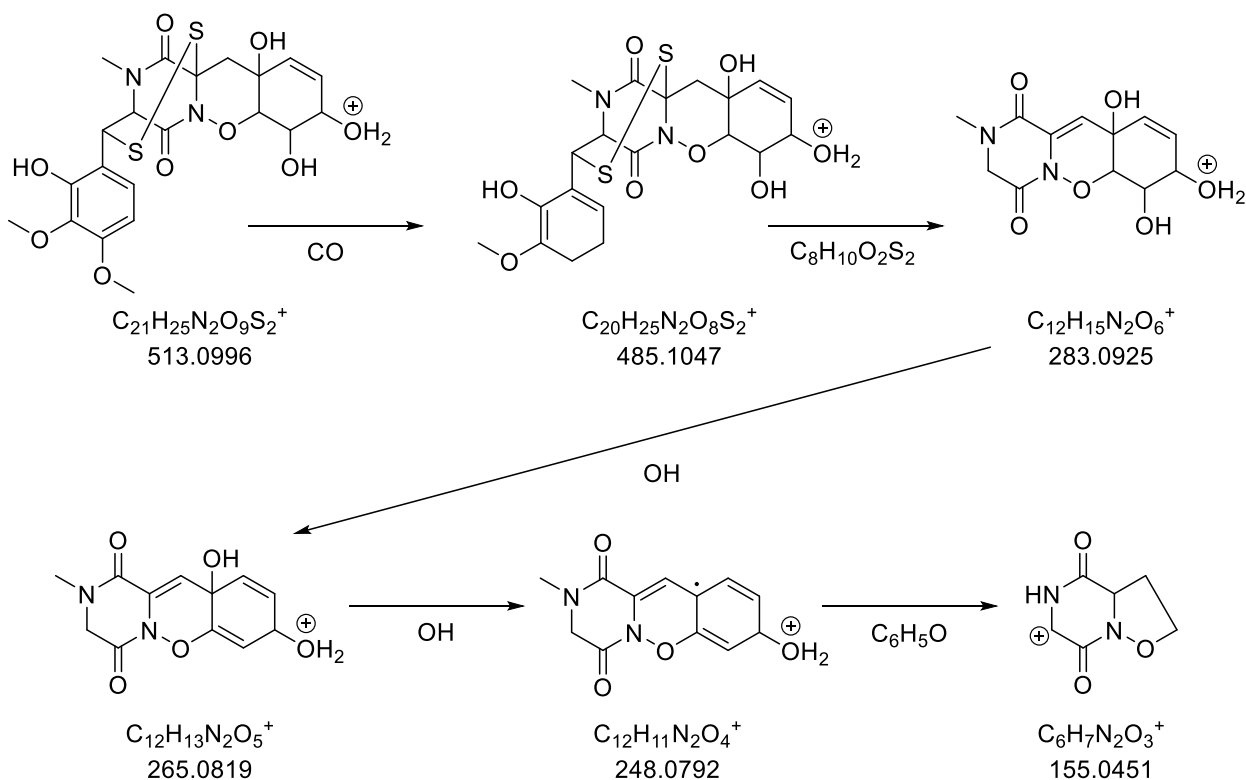


**Figure 32:** Proposed fragmentation scheme for features 3, 4, and 5 ( $[M+H]^+$ ), tentatively annotated as thiodiketopiperazine alkaloids. The diagram displays the main MS/MS fragment ions, along with their corresponding chemical formulas, theoretical  $m/z$  values (to three decimal places). Arrows indicate inferred neutral losses between fragments.

Based on these structural insights, features F3–F5 were tentatively annotated as TDKPs. This class of sulfur-containing cyclic dipeptides widely distributed in filamentous fungi, and exhibit substantial structural and functional diversity, with cytotoxic and antifungal activities being among their most notable biological properties. TDKPs containing a piperazine ring bridged by polysulfide linkages have demonstrated strong bioactivity, and structure–activity relationship studies have shown that the sulfur bridge is a key determinant of these effects (Ma et al., 2016). Given their broad spectrum of bioactivities and the recognized efficacy of their analogues against fungal phytopathogens (such as sporidesmins and chetocins), TDKPs are the most plausible and promising candidates to explain the antagonism observed against *R. solani*.

#### 4.3.1.3. GROUP 3: FEATURES 6 Y 7 (M/Z , RT MIN) – TENTATIVE ANNOTATION AND FRAGMENTATION ANALYSIS

Features 6 (m/z 659.429) and 7 (m/z 681.413) were detected in negative ionization mode, coeluting at 24.7 min and both producing a single fragment at m/z 329.212. Feature 6 corresponds to the dimer of this fragment ( $[2M-H]^-$ ), as its mass is twice that of m/z 329.212. Feature 7 differs by +22.98 Da, consistent with the formation of a sodium adduct ( $[2M-2H+Na]^-$ ), a phenomenon previously described for aromatic acids in negative ESI-MS (Schug & McNair, 2003). These observations suggest that F6 and F7 are likely dimerization products formed in the ion source (Figure 33).

$[M - H]^-$	$[2M - H]^-$	$[2M - 2H + Na]^-$
329.212	<b>F6: 659.429</b>	<b>F7: 681.413</b>
$C_{21}H_{29}O_3^-$	$C_{42}H_{59}O_6^-$	$(C_{42}H_{58}O_6)^{-2} + Na^+$

**Figure 33:** Summary of the detected molecular features. The molecular formula and molecular weight of the compound are shown. The image includes three ion species observed: (i) the deprotonated ion ( $[M-H]^-$ ), (ii) the deprotonated dimer ( $[2M-H]^-$ ), and (iii) the doubly deprotonated dimer with a sodium adduct ( $[2M-2H+Na]^-$ ).

Putative molecular formulas were assigned as  $C_{42}H_{59}O_6$  for F6 and  $C_{44}H_{57}O_6$  for F7, although SIRIUS did not return any associated structures. This further supports the hypothesis that F6 and F7 may correspond to *in-source* dimerization products. Based on

these findings, MS/MS analysis focused on the fragment  $m/z$  329.213 (TR = 24.7 min), attributed to the formula  $C_{21}H_{30}O_3$ .

The loss of a carboxyl group explains the transition from  $m/z$  329.213 ( $C_{21}H_{30}O_3$ ) to  $m/z$  285.224 ( $C_{20}H_{30}O$ ), while the loss of a hydroxyl group generates the ion at  $m/z$  267.217 ( $C_{20}H_{28}$ ). The fragments at  $m/z$  229.197 ( $C_{17}H_{26}$ ), 147.118 ( $C_{11}H_{16}$ ), 121.103 ( $C_9H_{14}$ ), 107.087 ( $C_8H_{12}$ ), and 67.055 ( $C_5H_8$ ) reflect a series of neutral losses composed primarily of carbon and hydrogen. The associated losses would be, respectively:  $C_3H_2$ ,  $C_6H_{10}$ ,  $C_2H_2$ ,  $CH_2$ , and  $C_3H_4$ . It should be noted that, although these losses are represented sequentially in the Figure 35 and 36, this is only for interpretative purposes, fragmentations may occur at different positions, producing ions with coincident masses. This could explain the high relative intensity of fragments at  $m/z$  67.055, 107.087, and 121.103, which are likely generated through multiple fragmentation pathways (Figure 34).

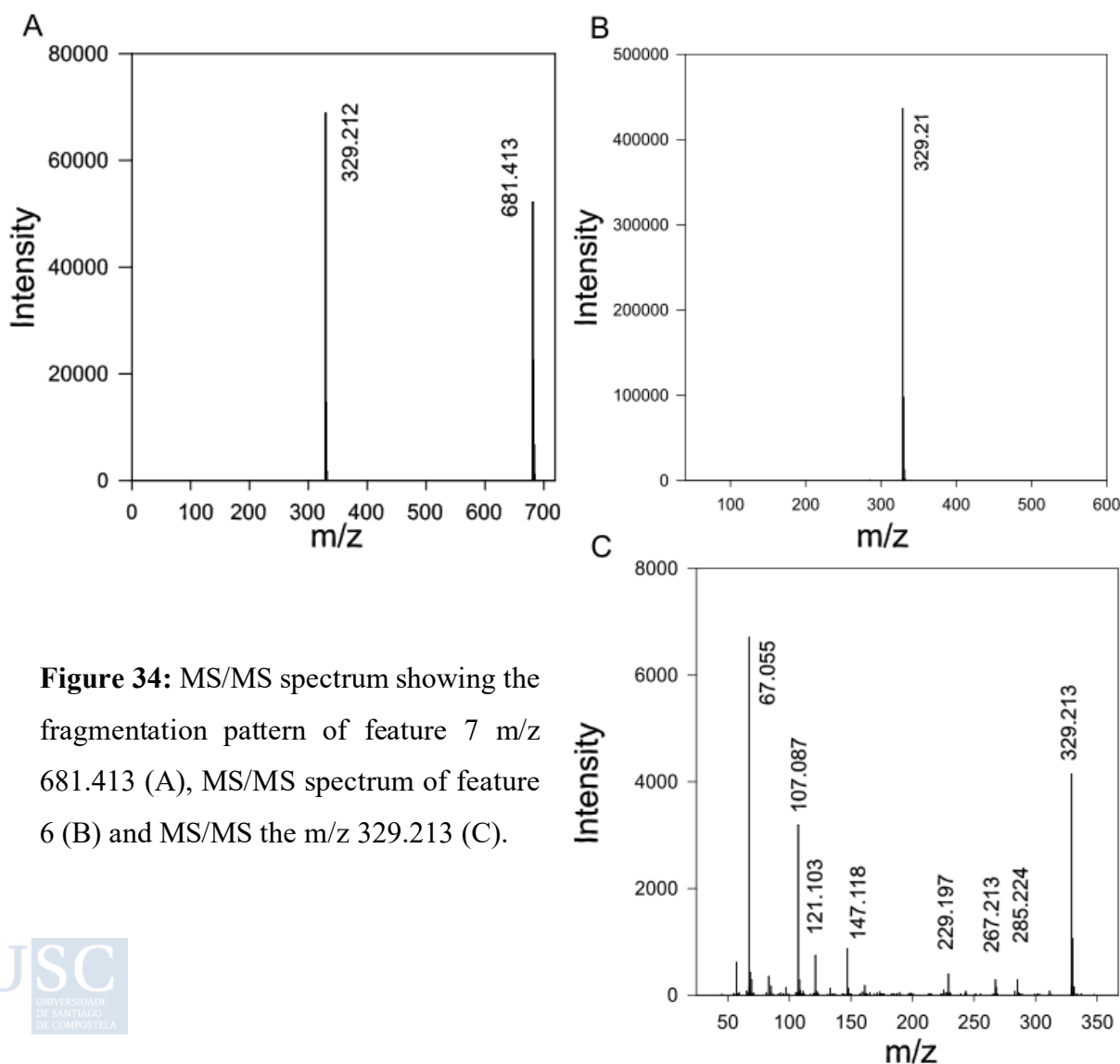


**Figure 34:** MS/MS spectrum showing the fragmentation pattern of feature 7  $m/z$  681.413 (A), MS/MS spectrum of feature 6 (B) and MS/MS the  $m/z$  329.213 (C).

The fragmentation pattern obtained did not include diagnostic ions that would allow unequivocal identification. Nevertheless, the molecular formula  $C_{21}H_{30}O_3$  is consistent with lipid-like metabolites, including oxygenated fatty acids and steroids (Macián, 2016). Several fragments provide additional context:  $m/z$  67.055 and 107.087 have previously been reported as characteristic of terpenoids (Masi et al., 2017) and oxygenated fatty acids. Similarly, fragments at  $m/z$  147.118 and 267.217 have been associated with resolvins (PubChem CID 71665428) and other bioactive lipids (Herzog et al., 2012; Kliman et al., 2010; NCBI, 2025c). In addition, the fragment at  $m/z$  121.103 has been linked to 8-Methyl-4-(phenylamino)quinoline-3-carboxamide (Crocetti et al., 2024). However, none of these fragments provide definitive evidence for structural elucidation.

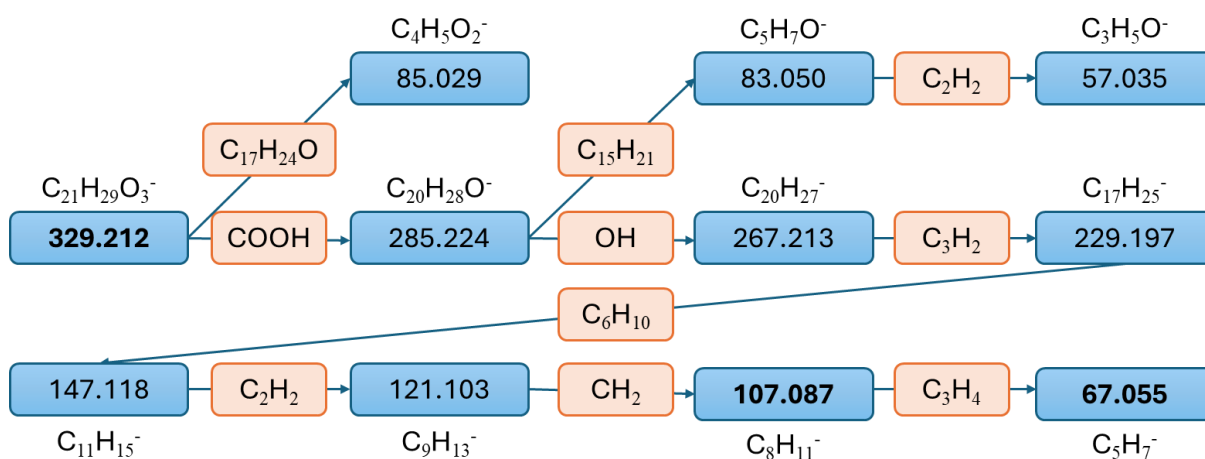


**Figure 35:** Proposed fragmentation scheme for the ion at  $m/z$  329.212. The diagram shows the  $m/z$  values and the proposed molecular formulas of the fragments detected by MS/MS (in blue). Arrows indicate the relationships between fragments, and neutral losses are represented in orange.

Considering the overall fragmentation pattern, the presence of a sterol structure appears unlikely. Sterols typically generate large fragments corresponding to the molecular backbone, whereas in our spectrum, the most intense fragments are  $m/z$  67.055 and 107.087. This observation suggests that the feature under study may possess an alternative structural framework.

To further explore this possibility, a literature search for the molecular formula  $C_{21}H_{30}O_3$  in PubChem indicated that these features may correspond to hydroxyretinoic acid methyl ester (PubChem CID 11174913). Although experimental spectra for this compound are

not available, *in silico* predictions provided by The Human Metabolome Database (HMDB) for related molecules (such as retinol acetate (C<sub>22</sub>H<sub>32</sub>O<sub>2</sub>), all-trans-18-hydroxyretinoic acid (C<sub>20</sub>H<sub>28</sub>O<sub>3</sub>), and retinyl ester (C<sub>20</sub>H<sub>30</sub>O<sub>2</sub>)) showed notable similarities. These predicted spectra include fragments at m/z 285.22, 267.21, 147.10, 121.10, 107.08, 85.05, and 67.05, which coincide with those observed in our analysis. Consequently, despite the need for additional experimental evidence, the convergence of spectral data supports the tentative annotation of Features F6–F7 as oxygenated lipids, likely derived from retinoids or apocarotenoids-lipophilic compounds.

From a functional perspective, these lipophilic compounds are of significant interest. Although the biosynthetic pathway of retinoic acid has not been described in fungi, this compound has demonstrated antifungal activity (Campione et al., 2021; Cosio et al., 2025), suggesting that structurally related analogs may play a similar role. Among these are metabolites synthesized by fungi and yeasts, such as torularhodin, produced by *Rhodotorula* spp., which exhibits antimicrobial and antioxidant activity (Kot et al., 2018), and neurosporaxanthin, an acidic carotenoid synthesized by *Neurospora crassa* and *Fusarium fujikuroi*, known for its antioxidant properties. The presence of structurally related compounds in *P. terrestris* suggests a potential role in redox balance modulation or indirect defense mechanisms against other microorganisms.

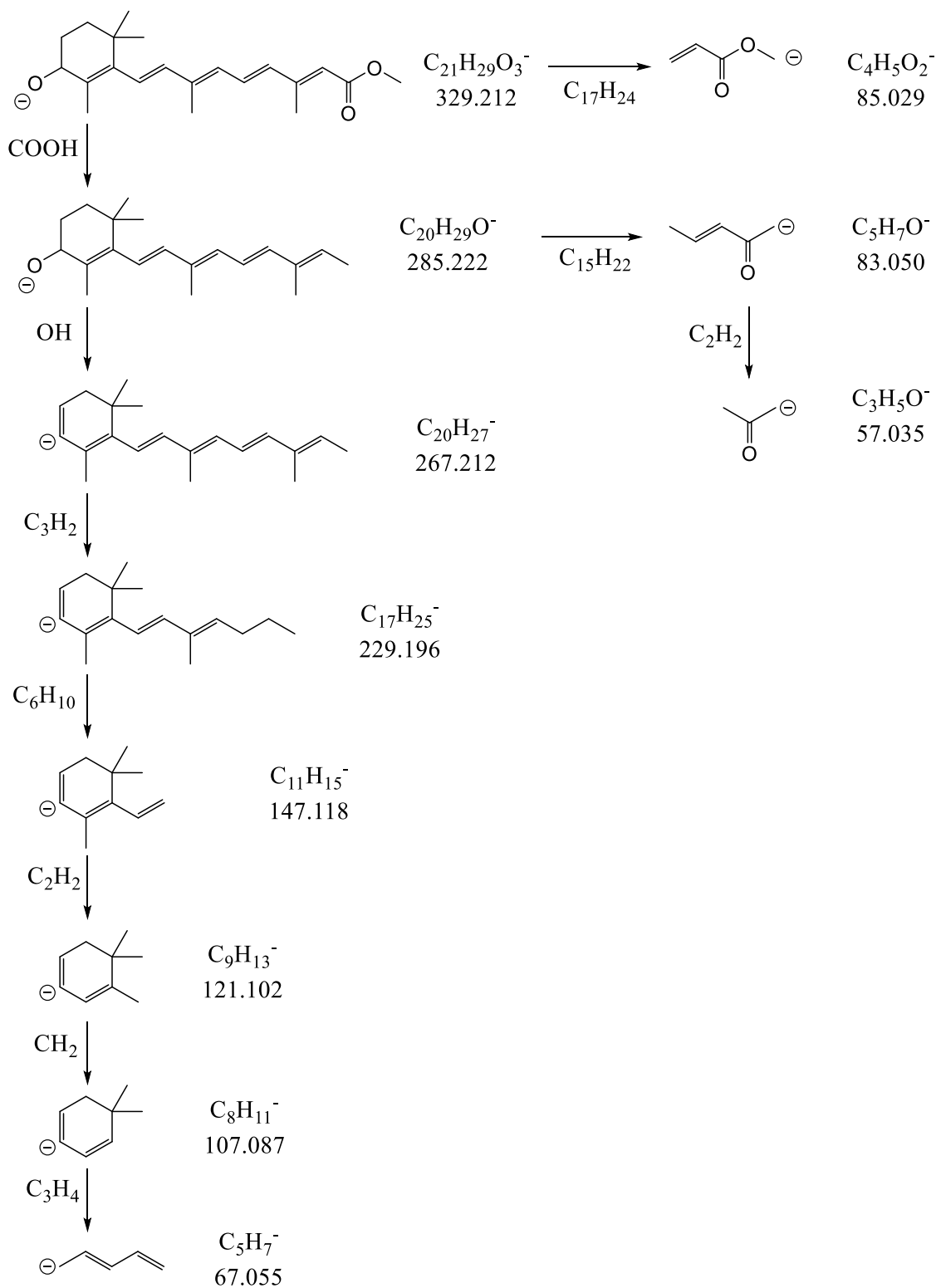
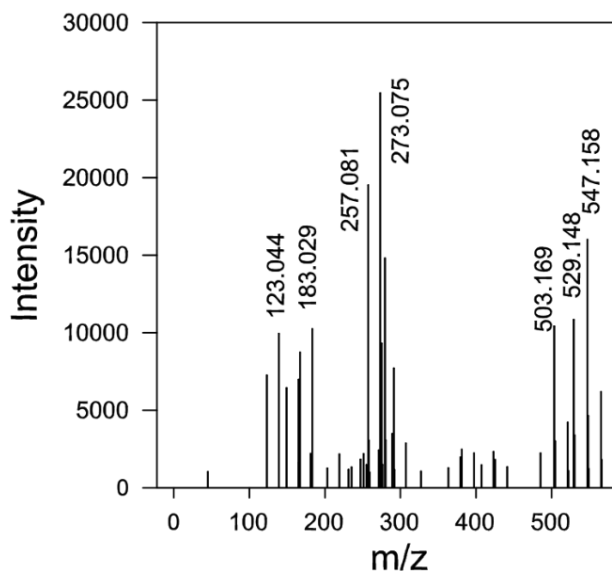


**Figure 36:** Proposed fragmentation scheme for the ion at  $m/z$  329.212 ( $[\text{M}-\text{H}]^-$ ), tentatively annotated as hydroxyretinoic acid methyl ester. The diagram displays the fragments detected by MS/MS, indicating for each its chemical formula, theoretical  $m/z$  value (to three decimal places). Arrows represent inferred neutral losses between fragments.

#### 4.3.1.4. FEATURE 8 (M/Z 565.1703, RT 24.08 MIN) – TENTATIVE ANNOTATION AND FRAGMENTATION ANALYSIS

Feature 8 exhibited a m/z 565.1703 and a RT 24.08 min in negative ionization mode. Accurate mass measurement suggested a molecular formula of C<sub>30</sub>H<sub>30</sub>O<sub>11</sub> for the [M–H]<sup>–</sup> ion, with a mass error of –1.22 mDa, indicating a highly oxygenated structure consistent with complex polyphenolic compounds.

**Figure 37:** MS/MS spectrum showing the fragmentation pattern of feature 8, m/z 565.1703.



MS/MS fragmentation analysis based on accurate mass and isotopic patterns (analyzed with SIRIUS and MetaboScape), revealed a series of fragments with mass errors within acceptable limits ( $\pm 10$  ppm), represented in figures 37 and 38.

Sequential neutral losses of 18 Da (H<sub>2</sub>O) were observed, suggesting the presence of multiple hydroxyl groups, which aligns with the high oxygen content of the proposed molecular formula. These progressive dehydrations are evident in transitions such as 565.170  $\rightarrow$  547.158  $\rightarrow$  529.148, 521.178  $\rightarrow$  503.169, 183.028  $\rightarrow$  165.018, and 291.086  $\rightarrow$  273.075.

Initial database searches indicated a possible match with schaftoside (C<sub>26</sub>H<sub>28</sub>O<sub>14</sub>); however, key diagnostic fragments (m/z 473, 443, 383 and saccharide fragments) were either absent or of minimal intensity, and the measured mass differed by +2.03 Da from the theoretical value. Similarly, comparison with reference spectra of C-glycosylated flavones (derived from apigenin and chrysin) showed partial matches (e.g., m/z 503.17)

but failed to reproduce the full diagnostic pattern expected for schaftoside or isoschaftoside.

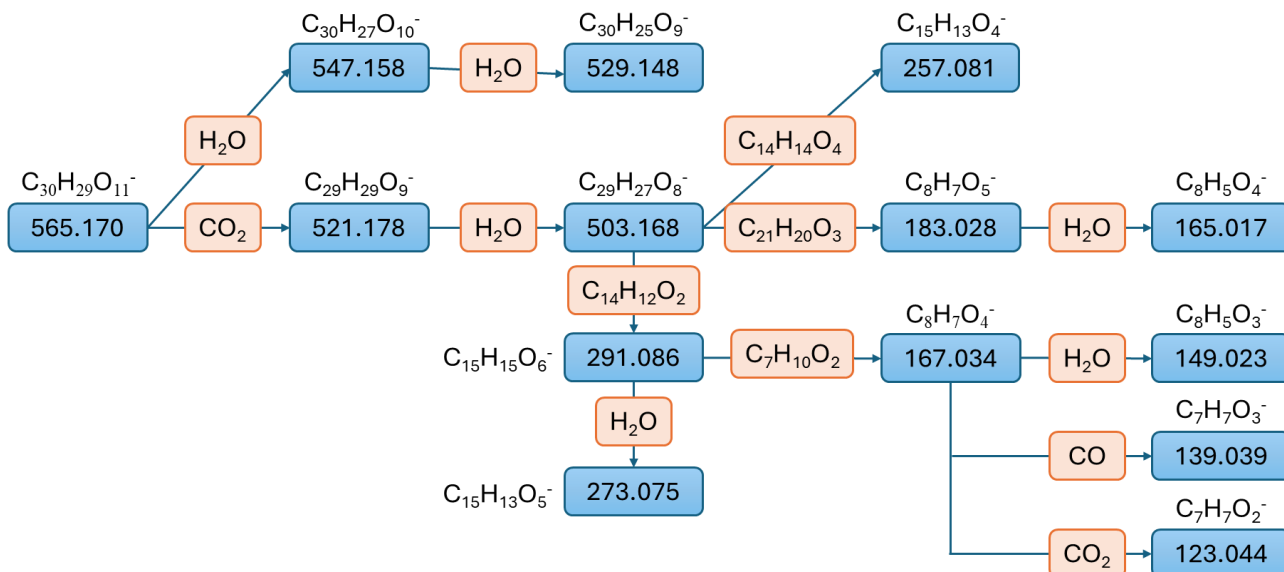


**Figure 38:** Proposed fragmentation scheme for the ion at m/z 565.17. The diagram shows the m/z values and the proposed molecular formulas of the fragments detected by MS/MS (in blue). Arrows indicate the relationships between fragments, and neutral losses are represented in orange.

In contrast, a low-mass fragment series (m/z 183.029 → 167.034 → 149.023 → 139.040 → 123.045) was identified, consistent with methyl trihydroxybenzoate or methyl galloyl units previously described in the literature (Gevrenova et al., 2024; Sheng et al., 2021). Additionally, fragments at m/z 273.075 and 257.080, separated by a neutral loss of H<sub>2</sub>O, correspond to ions previously reported for tetrahydrogenistein (C<sub>15</sub>H<sub>13</sub>O<sub>5</sub><sup>-</sup>, 273.0768 Da) and liquiritigenin (C<sub>15</sub>H<sub>13</sub>O<sub>4</sub><sup>-</sup>, 257.0819 Da), supporting the presence of an (iso)flavonoid-type core.

Notably, the fragment at m/z 279.231 could not be assigned to a coherent molecular formula and does not conform to typical flavonoid fragmentation patterns. This ion has been associated with anions derived from unsaturated fatty acids (C<sub>18</sub>:2), suggesting the possible presence of a lipidic or hybrid structure (Okazaki et al., 2013; Piszcz et al., 2016; Prasain et al., 2017). This observation, combined with the absence of typical disaccharide fragments, points to a compound potentially conjugated to a low-mass lipidic moiety rather than a canonical glycosyl group.

Taken together, the data suggests that feature 8 corresponds to a moderately hydrophobic compound of (iso)flavonoid or polyphenolic nature, possibly bearing a galloyl or methyl galloyl substituent and maybe conjugated to a lipidic fragment that contributes to its structural complexity (Figure 39). Despite partial matches with known compounds, no database entry fully reproduces the observed MS/MS fragmentation pattern, indicating that this may be a previously unreported or poorly characterized structure.

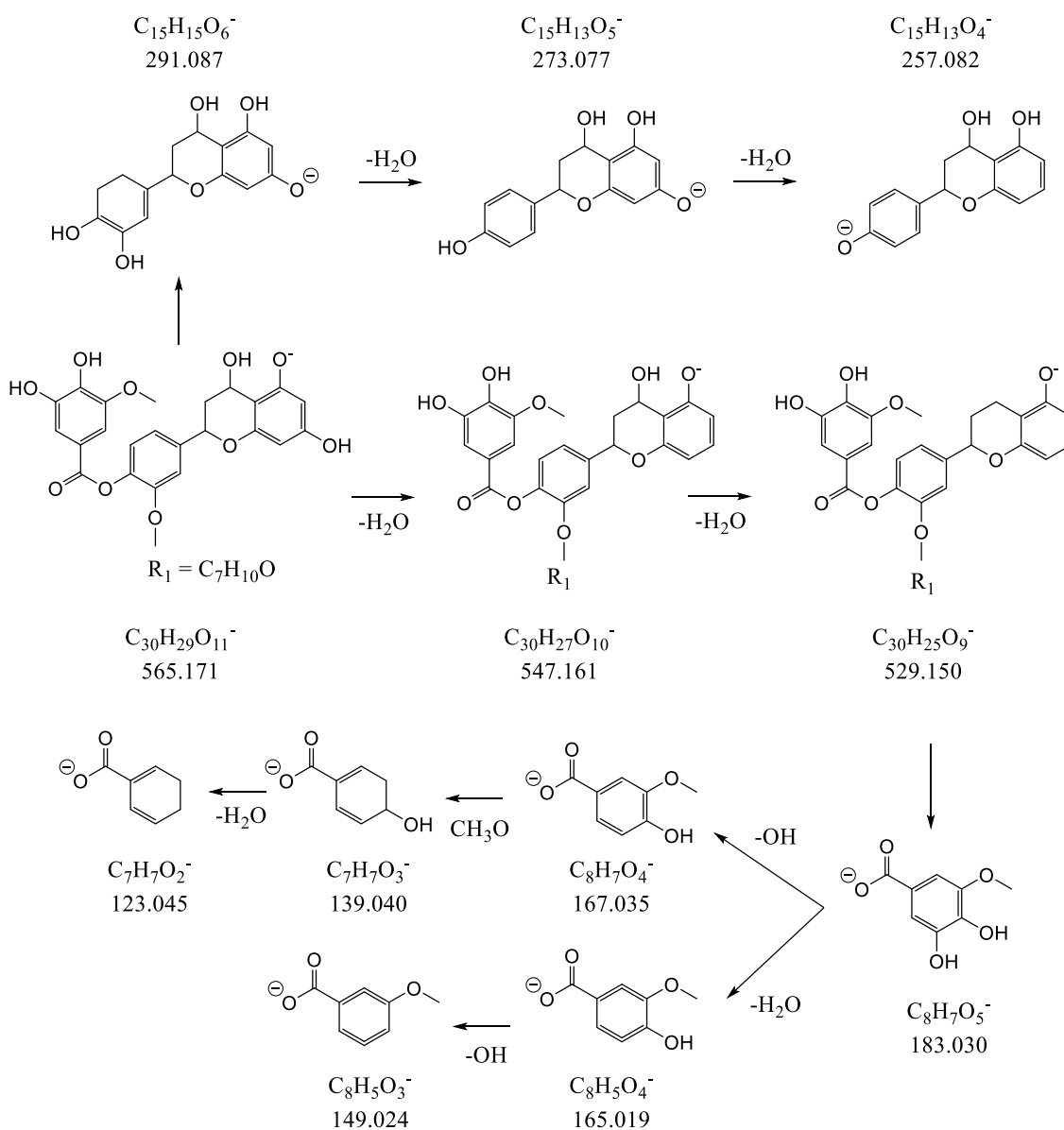


**Figure 39:** Proposed fragmentation scheme for the feature 8 at  $m/z$  565.171 ( $[M-H]^-$ ), tentatively annotated as polyphenol. The diagram displays the fragments detected by MS/MS, indicating for each its chemical formula, theoretical  $m/z$  value (to three decimal places). Arrows represent inferred neutral losses between fragments.

#### 4.3.1.5. FEATURE 9 (M/Z 365.067, RT 20.27 MIN) – TENTATIVE ANNOTATION AND FRAGMENTATION ANALYSIS

Negative-mode mass spectrometry analysis enabled the identification of feature 9 with  $m/z$  365.067 ( $[M-H]^-$ ) and a retention time of 20.27 minutes, to which the molecular formula  $C_{20}H_{14}O_7$  was tentatively assigned, with a mass error of 2.227 ppm. This formula suggests a high degree of unsaturation, consistent with polycyclic aromatic structures. The assignment was supported by isotopic pattern analysis using SIRIUS and MetaboScape, which confirmed the validity of the formula within an acceptable error margin ( $<10$  ppm).

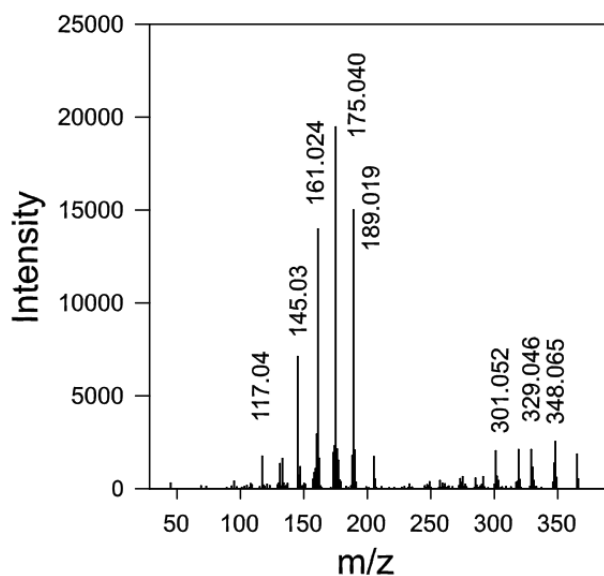


**Figure 40:** MS/MS spectrum showing the fragmentation pattern of feature 8,  $m/z$  565.1703.

The MS/MS fragmentation spectrum revealed a series of fragment ions that provide insight into the possible structure of the compound (Figure 40). The presence of these fragments suggests a structure rich in phenolic groups and possibly derived from a flavonoid core. Initially, the compound was considered to belong to the perylenequinone class, given that its exact mass matches that of the metabolite Alterlosin I ( $C_{20}H_{14}O_7$ ,  $m/z$  365.0667). However, the lack of published fragmentation data for Alterlosin I prevents a direct comparison that could confirm this hypothesis. In light of this limitation, an alternative structural possibility was explored based on the nature of the observed fragments.

Several of the detected ions have been previously reported in the literature as derivatives of flavonoids and related compounds. For instance, the fragment  $m/z$  145.0296 ( $C_9H_6O_2$ ) corresponds to the coumarin core, a basic structure found in many flavonoids. From this, the fragment  $m/z$  161.0243 ( $C_9H_6O_3$ ) can be interpreted as the addition of a hydroxyl

group, while  $m/z$  133.0293 ( $C_8H_6O_2$ ) may result from the loss of CO from 161.0243. Likewise,  $m/z$  117.0336 ( $C_8H_6O$ ) could derive from the loss of a hydroxyl group from 133.0293.

Other fragments, such as  $m/z$  175.040, 145.0296, 161.0243, and 205.0141, have been associated in previous studies with the presence of feruloyl groups, as seen in the compound Tenuifoliside, an ester-type oligosaccharide composed of sugars linked to phenolic groups via ester bonds (Ling et al., 2013a; Li et al., 2021), and in flavonols bearing feruloyl substituents (Poveda et al., 2021). It is important to note, however, that the fragments associated with feruloyl groups could also be explained as originating from the aromatic structure of the compound itself. The fragment  $m/z$  145.0296 has also been linked to flavones such as luteolin and rhoifolin (Li et al., 2021). Nevertheless, no signals indicative of sugar moieties were detected in the spectrum, suggesting that the feature does not contain monosaccharide substituents.

Additionally, the fragments  $m/z$  161.024 and 189.019 may arise from a Retro-Diels–Alder (RDA) reaction occurring at the C-ring of a flavonoid, a fragmentation pathway commonly described for this class of compounds (Hettiarachchi & Grassian, 2024; De Brito et al., 2021). This mechanism provides further evidence supporting the presence of a flavonoid core in the structure of the feature.

Considering the proposed molecular formula, the absence of sugars, and the nature of the observed fragments, it is hypothesized that the compound corresponds to a pentahydroxyflavone-type flavonoid, possibly substituted with an unsaturated side chain containing oxygen as a heteroatom. This configuration would account for the observed mass and justify the detected fragmentation patterns. Figure 41 presents the proposed fragmentation scheme, indicating the chemical formulas and theoretical  $m/z$  values along with inferred neutral losses between fragments.

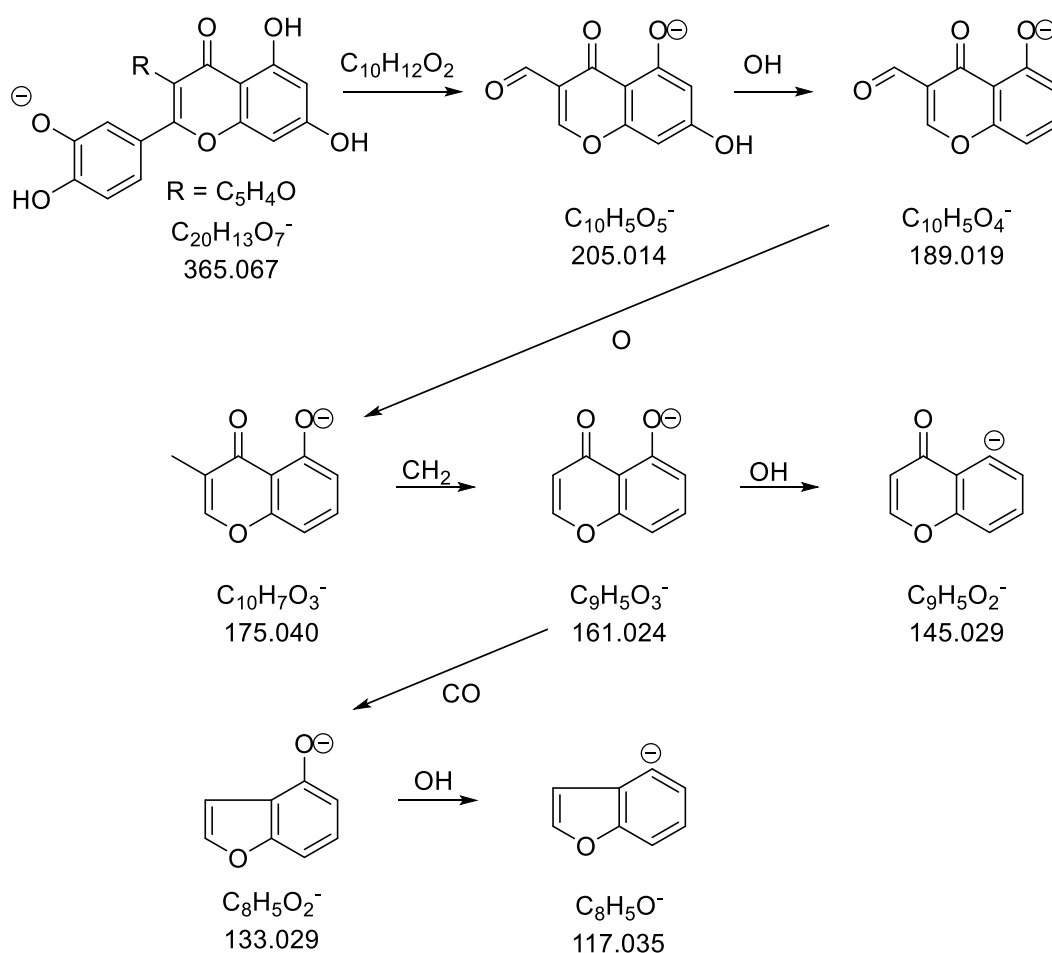


**Figure 41:** Proposed fragmentation scheme for the feature 9,  $m/z$  365.067 ( $[\text{M}-\text{H}]^-$ ), tentatively annotated as a pentahydroxyflavone. The diagram displays the fragments detected by MS/MS, indicating for each its chemical formula, theoretical  $m/z$  value (to three decimal places). Arrows represent inferred neutral losses between fragments.

Collectively, features F8 and F9 were associated with polyphenolic or flavonoid-like compounds. These metabolites may contribute complementarily to the fungus's antioxidant and protective capacity. However, their structure and function require further investigation before a definitive link to the observed antifungal activity can be established.

In summary, this study demonstrates that *P. terrestris* possesses notable antifungal potential, driven by the production of secondary metabolites whose expression is critically dependent on nutritional and environmental contexts. The integration of functional and metabolomic data established a clear relationship between taxonomic identity, cultivation conditions, and the chemical phenotype of the isolates. This chemical diversity not only helps explain the observed antifungal activity but also provides insights

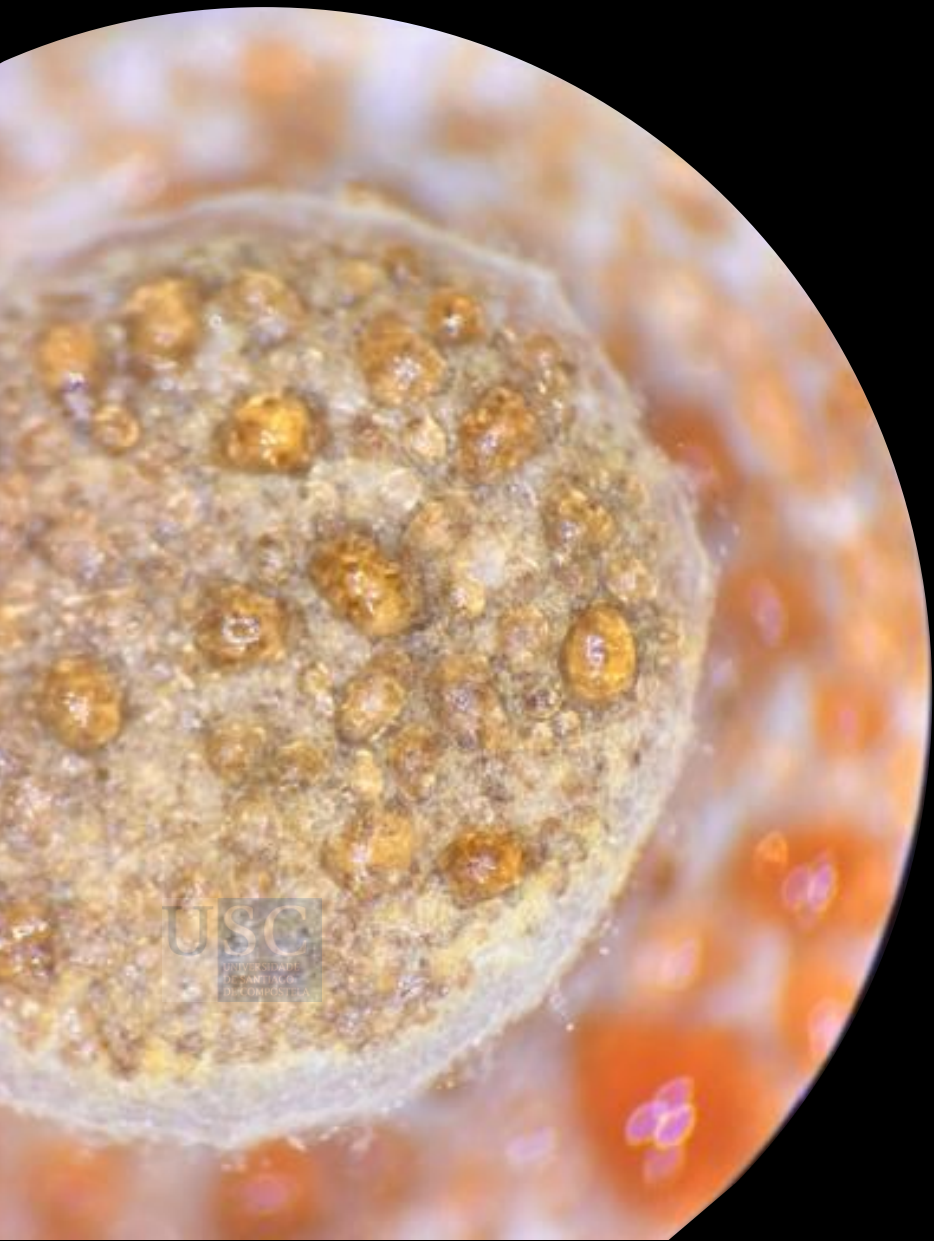
into the ecological role of the fungus. Specifically, the production of antifungal metabolites by *P. terrestris* may represent a competitive strategy that limits colonization by phytopathogens, thereby contributing to the maintenance of its endophytic niche within the roots of *C. annuum*.

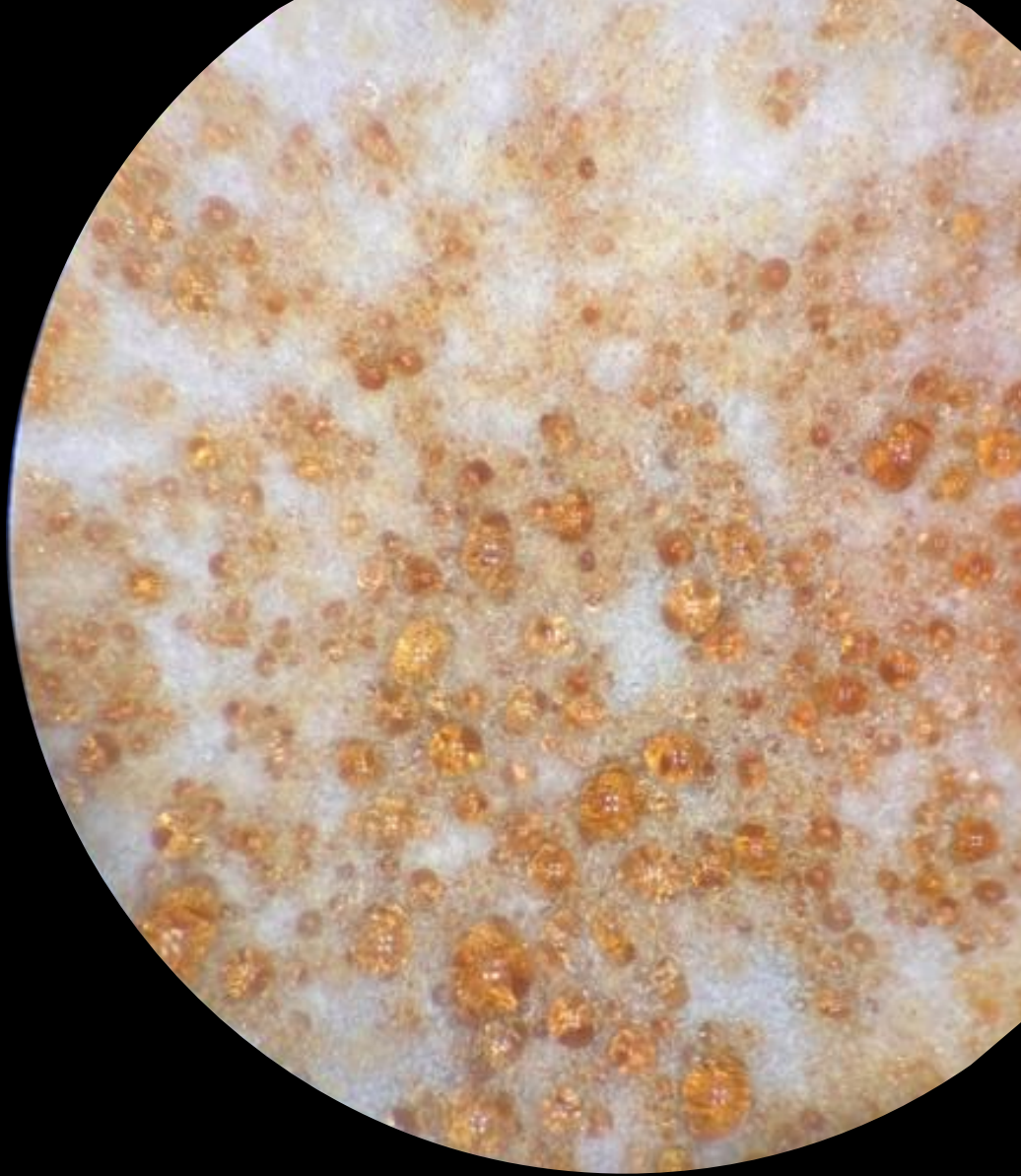
This ecological interpretation aligns with recent studies documenting the beneficial roles of *Pseudopyrenochaeta* isolates, such as conferring cadmium tolerance in *Pinus* (Zhou et al., 2024) and antagonizing *Phytophthora infestans* in potato (El-Hasan et al., 2022). Collectively, these findings expand the repertoire of fungal genera with potential for biocontrol applications. Nevertheless, the reduction in *Arabidopsis* dry weight observed under drought conditions in our trials should be taken into account. This negative impact on plant biomass suggests that the symbiotic outcome of *P. terrestris* may be context-dependent. Therefore, further *in planta* experiments are needed to determine the specific conditions under which colonization shifts from beneficial to detrimental, ensuring that its application does not come at a fitness cost in situations of water scarcity.

Furthermore, the observation that culture medium composition varies across manufacturers in ways that can silence or activate the production of key metabolites highlights the remarkable metabolic plasticity of these fungi. This finding strongly reinforces the rationale behind the “One Strain, Many Compounds” (OSMAC) approach to maximize detectable chemical diversity (Bode et al., 2002). Controlled manipulation of nutritional factors, such as the use of specific media or the addition of elicitors, represents an effective strategy to induce or enhance the synthesis of bioactive compounds in *Pseudopyrenochaeta*.

Among the detected metabolites, the thiodiketopiperazine (TDKP) alkaloids are particularly promising. However, since their current identification remains tentative (MSI levels 2–3), future research must prioritize their purification and structural confirmation. Subsequent studies should focus on evaluating their individual bioactivities to fully elucidate their biocontrol mechanisms. Additionally, genomic analysis of *Pseudopyrenochaeta* will be essential to identify the Biosynthetic Gene Clusters (BGCs) responsible for TDKP synthesis, which will provide a deeper understanding of the species- and strain-specific regulatory mechanisms governing this valuable chemical







# GENERAL CONCLUSIONS

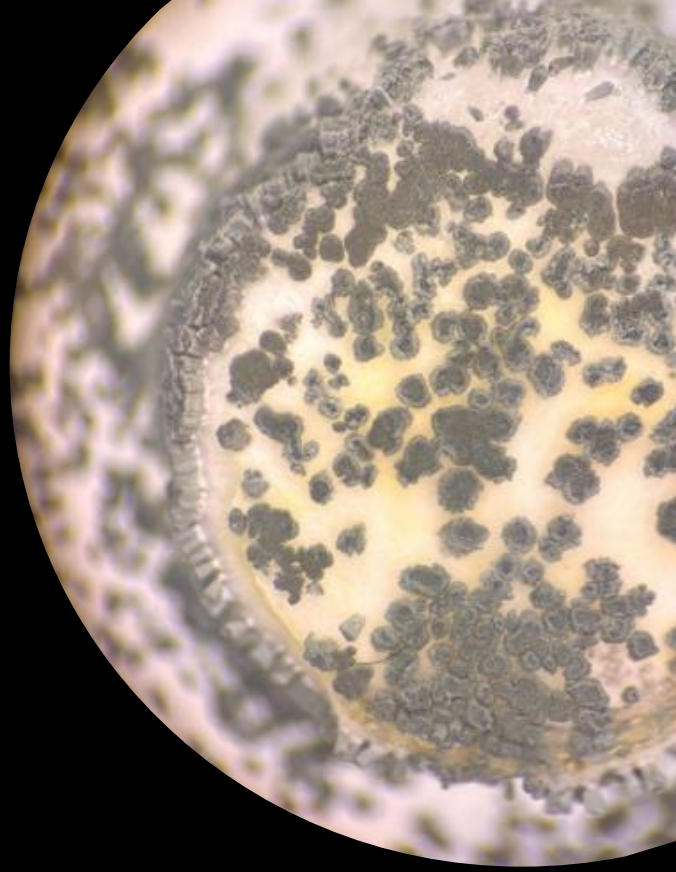
---



- I. The roots of *Brassica rapa* and *Capsicum annuum* in Galicia host culturable endophytic communities taxonomically dominated by Ascomycota, with marked spatial heterogeneity, particularly in *B. rapa*. The identification of over 36 taxa represents a valuable source of microbial strains potentially adapted to local agroecological conditions.
- II. Several isolates belonging to the genera *Trichoderma*, *Talaromyces*, *Chaetomium* and *Pseudopyrenochaeta*, showed antifungal activity against a range of phytopathogens.
- III. Drought experiments demonstrated that *in vitro* methodologies are promising tools for evaluating fungal tolerance to water deficit. Two isolates, belonging to *Humicola* sp. and the *Pseudeurotiaceae* family, were particularly effective, enhancing both plant water content and biomass accumulation.
- IV. Functional and metabolomic analyses showed that antifungal *Pseudopyrenochaeta* isolates correspond to *Pseudopyrenochaeta terrestris* and produce multiple metabolites, linked to the inhibition of *Rhizoctonia solani*.

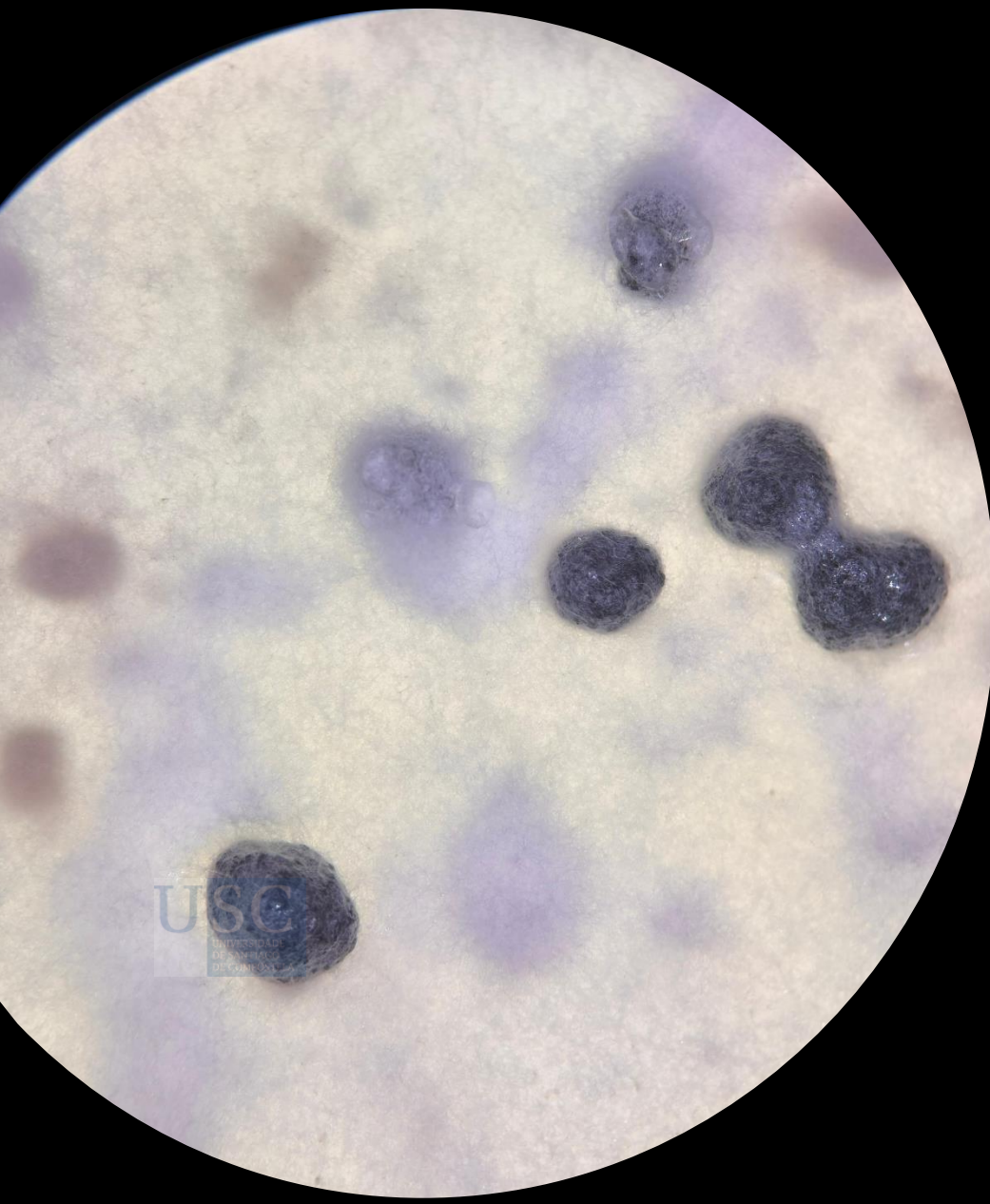






# FUTURE PERSPECTIVES

---

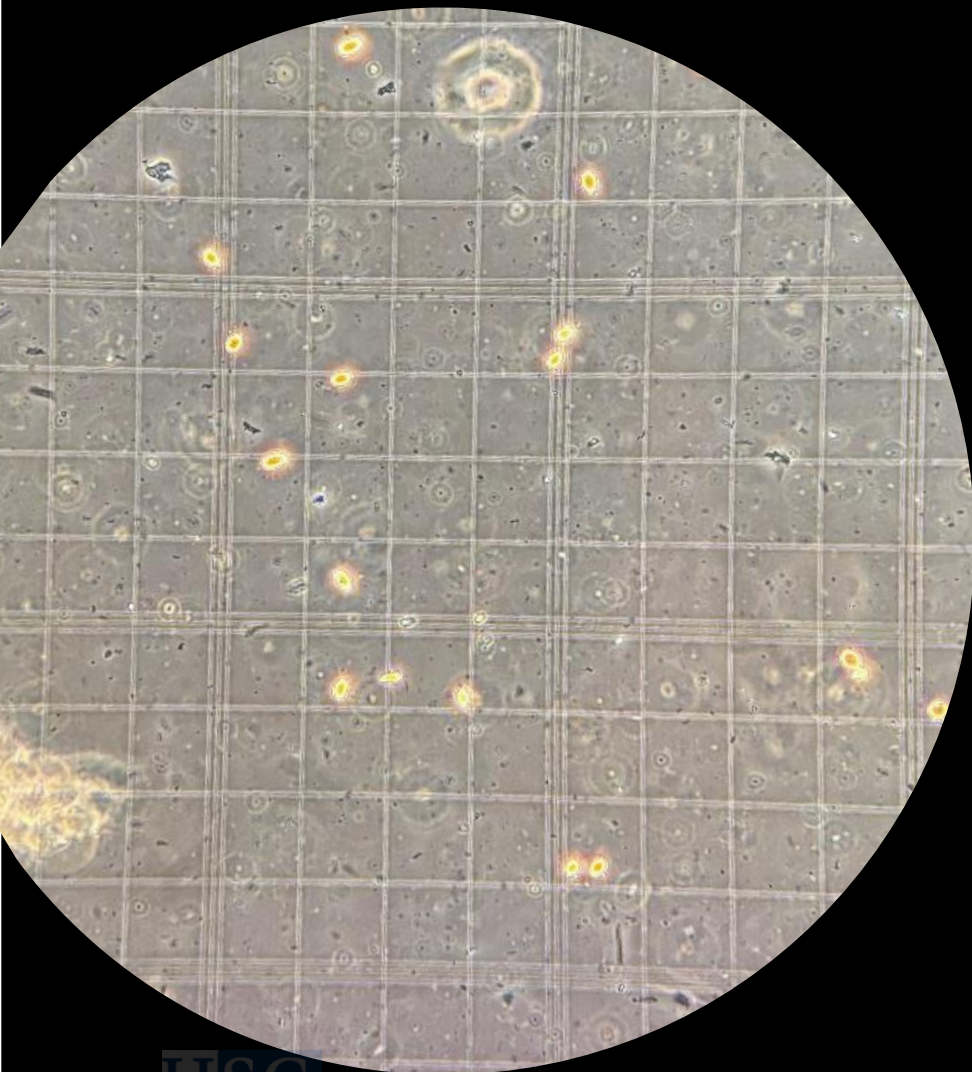


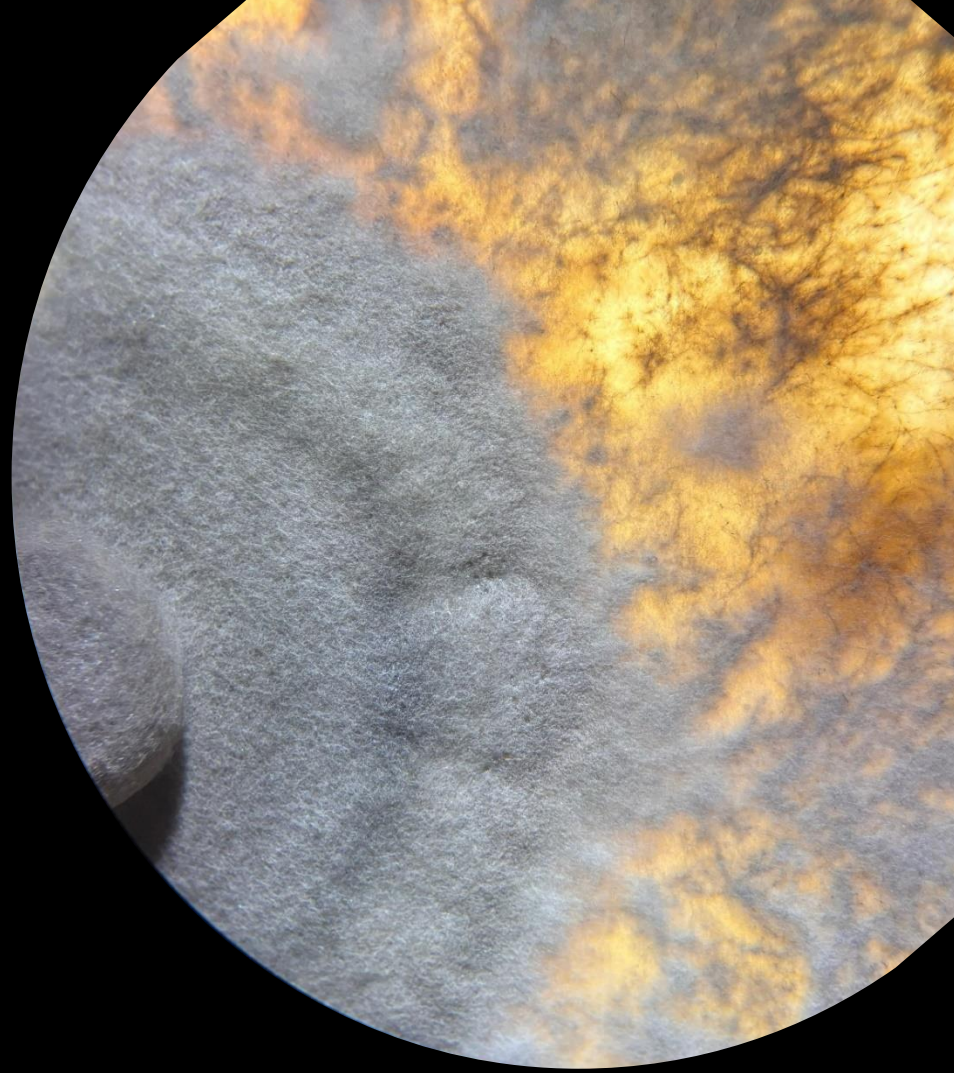
Building on the results and limitations discussed above, several research directions can be proposed:

- **Methodological innovation in endophyte research.** Developing isolation methods targeting living tissues and integrating culture-independent sequencing will minimize biases and provide a more accurate picture of active endophytic populations. Integrating multi-omics analyses with physiological assays will further deepen our understanding of how endophytes influence plant performance.
- **Temporal and environmental dynamics.** Repeated sampling across different years and environmental contexts, particularly under drought episodes, will help determine the stability of endophytic communities and identify strains consistently associated with plant resilience.
- **Development of improved inoculation systems.** The use of carrier-based inoculants could enhance the viability, persistence, and distribution of fungal propagules in soil. Tailoring inoculation protocols to specific endophytes will be essential to achieve consistent colonization and plant responses.
- **Verification of colonization and plant responses.** Future studies should focus on quantifying fungal colonization within plant tissues using molecular markers, microscopy, or qPCR detection.
- **Comparative genomics and molecular mechanisms.** Closely related isolates that differ in functional behavior represent valuable models to explore the molecular basis of antifungal activity and plant interaction. Whole genome sequencing and proteomic analysis could reveal key genes and regulatory pathways involved in symbiosis and metabolite production.
- **Optimization of culture-based methods for metabolite production.** Systematic evaluation of culture conditions including media composition, nutrient ratios, salinity, pH, and co-culture strategies could maximize the production of bioactive metabolites by endophytic fungi.

- **Expansion to original host crops and field conditions.** Functional assays should be extended to *B. rapa* and *C. annuum* to confirm whether drought tolerance and biocontrol effects observed in model systems are transferable to agronomically relevant hosts. Field and greenhouse trials will be critical to evaluate performance under realistic conditions.
- **Design of synthetic communities of endophytic fungi.** Constructing synthetic consortia that combine strains with complementary functions could harness metabolic cooperation and niche partitioning among isolates, leading to more stable and self-sustaining systems capable of enhancing plant growth and stress resilience more effectively than single inoculants.

This thesis provides a framework for future exploration of plant–endophyte systems. By refining inoculation methods, validating colonization, and linking functional outcomes with molecular and ecological data, it will be possible to move toward the rational design of microbial inoculants that enhance crop resilience in a sustainable and environmentally compatible manner.





# REFERENCES

---

- Abbas, A., Ali, S., Mubeen, M., Hussain, A., Gutumsary, K. A., Hussain, B., & Chen, T. (2025). *Talaromyces* spp. are promising biocontrol agents for sustainable agriculture Aqleem. In A. Kumar & M. K. Solanki (Eds.), *Microbial biocontrol techniques* (pp. 245–280). Springer Nature Singapore Pte Ltd. [https://doi.org/10.1007/978-981-97-8739-5\\_13](https://doi.org/10.1007/978-981-97-8739-5_13)
- Abbas, A., Fu, Y., & Qu, Z. (2021). Isolation and evaluation of the biocontrol potential of *Talaromyces* spp. against rice sheath blight guided by soil microbiome. *Environmental Microbiology*, 23, 5946–5961. <https://doi.org/10.1111/1462-2920.15596>
- Abdel-azeem, A., Nada, A. A., Donovan, A. O., & Thakur, V. K. (2020). Mycogenic silver nanoparticles from endophytic *Trichoderma atroviride* with antimicrobial activity. *Journal of Renewable Materials*. <https://doi.org/10.32604/jrm.2020.08960>
- Adeleke, B. S., Ayilara, M. S., Akinola, S. A., & Babalola, O. O. (2022). Biocontrol mechanisms of endophytic microorganisms. *Egyptian Journal of Biological Pest Control*, 32, 1–339. <https://doi.org/10.1016/C2020-0-02202-4>
- Alfiky, A., & Weisskopf, L. (2021). Deciphering *Trichoderma*–plant–pathogen interactions for better development of biocontrol applications. *Journal of Fungi*, 7(1), 1–18. <https://doi.org/10.3390/jof7010061>
- Allwood, J. W., Williams, A., Uthe, H., van Dam, N. M., Luis, L. A. J., Grant, M. R., & Pétriacq, P. (2021). Unravelling plant responses to stress—the importance of targeted and untargeted metabolomics. *Metabolites*, 11(8), Article 558. <https://doi.org/10.3390/metabo11080558>
- Almario, J., Jeena, G., Wunder, J., et al. (2017). Root-associated fungal microbiota of nonmycorrhizal *Arabidopsis thaliana* and its contribution to plant phosphorus nutrition. *Proceedings of the National Academy of Sciences of the United States of America*, 114, E9403–E9412. <https://doi.org/10.1073/pnas.1710455114>
- Álvarez-García, S., Mayo-Prieto, S., Carro-Huerga, G., Rodríguez-González, Á., González-López, O., Gutiérrez, S., & Casquero, P. A. (2021). Volatile Organic Compound Chamber: A novel technology for microbiological volatile interaction assays. *Journal of Fungi*, 7, 248. <https://doi.org/10.3390/jof7040248>
- Andrews, J. (1995). *Peppers: The domesticated capsicums*. University of Texas Press.
- Anthony, M. A., Celenza, J. L., Armstrong, A., & Frey, S. D. (2020). Indolic glucosinolate pathway provides resistance to mycorrhizal fungal colonization in a non-host Brassicaceae. *Ecosphere*, 11(4), e03100. <https://doi.org/10.1002/ECS2.3100>
- Aragona, M., Minio, A., Ferrarini, A., Valente, M. T., Bagnaresi, P., Orrù, L., Tononi, P., Zamperin, G., Infantino, A., Valè, G., Cattivelli, L., & Delledonne, M. (2014). De novo genome assembly of the soil-borne fungus and tomato pathogen *Pyrenochaeta lycopersici*. *BMC Genomics*, 15, Article 313. <https://doi.org/10.1186/1471-2164-15-313>
- Asad, S. A. (2022). Mechanisms of action and biocontrol potential of *Trichoderma* against fungal plant diseases: A review. *Ecological Complexity*, 49, 100978. <https://doi.org/10.1016/j.ecocom.2021.100978>
- Avis, P. G., McLaughlin, D. J., Dentinger, B. C., & Reich, P. B. (2003). Long-term increase in nitrogen supply alters above- and below-ground ectomycorrhizal communities and increases the dominance of *Russula* spp. in a temperate oak savanna. *New Phytologist*, 160, 239–253. <https://doi.org/10.1046/j.1469-8137.2003.00865.x>

- Barrs, H. D., & Weatherley, P. E. (1962). A re-examination of the relative turgidity technique for estimating water deficits in leaves. *Australian Journal of Biological Sciences*, *15*, 413–428. <http://dx.doi.org/10.1071/BI9620413>
- Bills, G. F., & Gloer, J. B. (2017). Biologically active secondary metabolites from the fungi. In *The fungal kingdom* (pp. 1087–1119). <https://doi.org/10.1128/9781555819583.ch54>
- Biswas, D., Chakraborty, A., Haque, S. M., & Ghosh, B. (2023). Endophytic fungal diversity in solanaceous medicinal plants and their beneficial impact. In M. Jha & S. Halder (Eds.), *Medicinal plants: Biodiversity, biotechnology and conservation*. Springer. [https://doi.org/10.1007/978-981-19-9936-9\\_30](https://doi.org/10.1007/978-981-19-9936-9_30)
- Bode, H. B., Bethe, B., Höfs, R., & Zeeck, A. (2002). Big effects from small changes: Possible ways to explore nature's chemical diversity. *ChemBioChem*, *3*, 619–627. [https://doi.org/10.1002/1439-7633\(20020703\)3](https://doi.org/10.1002/1439-7633(20020703)3)
- Bosland, P., & Votava, W. (2012). *Peppers: Vegetable and spice capsicums*. (Vol. 22) CABI.
- Botha, A. (2006). Yeasts in soil. In *Biodiversity and ecophysiology of yeasts* (pp. 221–240). Berlin, Heidelberg: Springer Berlin Heidelberg.
- Botha, A. (2011). The importance and ecology of yeasts in soil. *Soil Biology and Biochemistry*, *43*, 1–8. <https://doi.org/10.1016/j.soilbio.2010.10.001>
- Brakhage, A. A. (2012). Secondary metabolism. *Nature Reviews Microbiology*, *11*(1), 21–32. <https://doi.org/10.1038/nrmicro2916>
- Bressan, M., Roncato, M. A., Bellvert, F., et al. (2009). Exogenous glucosinolate produced by *Arabidopsis thaliana* has an impact on microbes in the rhizosphere and plant roots. *The ISME Journal*, *3*, 1243–1257. <https://doi.org/10.1038/ismej.2009.68>
- Calmes, B., Guillemette, T., Teyssier, L., Siegler, B., Pigné, S., Landreau, A., Iacomi, B., Lemoine, R., Richomme, P., & Simoneau, P. (2013). Role of mannitol metabolism in the pathogenicity of the necrotrophic fungus *Alternaria brassicicola*. *Frontiers in Plant Science*, *4*, 131. <https://doi.org/10.3389/fpls.2013.00131>
- Calvo, A. M., Wilson, R. A., Bok, J. W., & Keller, N. P. (2002). Relationship between secondary metabolism and fungal development. *Microbiology and Molecular Biology Reviews*, *66*(3), 447–459. <https://doi.org/10.1128/MMBR.66.3.447>
- Campione, E., Gaziano, R., Doldo, E., Marino, D., Falconi, M., Iacovelli, F., Tagliaferri, D., Pacello, L., Bianchi, L., Lanna, C., Aurisicchio, L., Centofanti, F., Di Francesco, P., Del Principe, I., Del Bufalo, F., Locatelli, F., Pistoia, E. S., Marra, E., & Orlandi, A. (2021). Antifungal effect of all-trans retinoic acid against *Aspergillus fumigatus* *in vitro* and in a pulmonary aspergillosis *in vivo* model. *Antimicrobial Agents and Chemotherapy*, *65*(3), e01874-20. <https://doi.org/10.1128/AAC.01874-20>
- Chen, J., Akutse, K. S., Saqib, H. S. A., et al. (2020). Fungal endophyte communities of crucifer crops are seasonally dynamic and structured by plant identity, plant tissue and environmental factors. *Frontiers in Microbiology*, *11*, 1519. <https://doi.org/10.3389/fmicb.2020.01519>
- Cheng, X. F., Xie, M. M., Li, Y., Liu, B. Y., Liu, C. Y., Wu, Q. S., & Kuča, K. (2022). Effects of field inoculation with arbuscular mycorrhizal fungi and endophytic fungi on fruit quality and soil properties of Newhall navel orange. *Applied Soil Ecology*, *170*, 104308. <https://doi.org/10.1016/j.apsoil.2021.104308>
- Clergeot, P.-H., Schuler, H., Mørtz, E., Brus, M., Vintila, S., & Ekengren, S. (2012). The corky root rot pathogen *Pyrenochaeta lycopersici* secretes a proteinaceous inducer of cell death affecting host plants differentially. *Phytopathology*. <https://doi.org/10.1094/phyto-01-12-0004.r3>

- Cosio, T., Romeo, A., Pistoia, E. S., Pica, F., Freni, C., Iacovelli, F., Orlandi, A., Falconi, M., Campione, E., & Gaziano, R. (2025). Retinoids as alternative antifungal agents against *Candida albicans*: *In vitro* and in silico evidence. *Microorganisms*, *13*(2), 237. <https://doi.org/10.3390/microorganisms13020237>
- Cramer, W., Holten, J. I., Kaczmarek, Z., Martens, P., Nicholls, R. J., Öquist, M., Rounsevell, M. D. A., & Szolgay, J. (2022). *IPCC - Climate change 2001: Impacts, adaptation and vulnerability (Ch. 13 Europe)* (pp. 643–692).
- Crocetti, L., Giovannoni, M. P., Vergelli, C., Guerrini, G., Melani, F., & Cilibrizzi, A. (2024). New quinoline-based PDE4 inhibitors through GSK-256066 fragment-based elaboration. *Journal of Molecular Structure*, *1295*, 136719. <https://doi.org/10.1016/j.molstruc.2023.136719>
- Dastogeer, K. M. G., & Wylie, S. J. (2017). Plant-fungi association: Role of fungal endophytes in improving plant tolerance to water stress. In *Plant-microbe interactions in agro-ecological perspectives* (Vol. 1, pp. 161–176). Springer. [https://doi.org/10.1007/978-981-10-5813-4\\_8](https://doi.org/10.1007/978-981-10-5813-4_8)
- De Brito, J. A. G., Pinto, L. D. S., Chaves, C. F., Da Silva, A. J. R., Da Silva, M. F. D. G. F., & Cotinguiba, F. (2021). Chemophenetic significance of *Anomalocalyx uleanus* metabolites are revealed by dereplication using molecular networking tools. *Molecules*, *26*(4), 0925. <https://doi.org/10.3390/molecules26040925>
- de Gruyter, H., Woudenberg, J. H. C., Aveskamp, M. M., Verkley, G. J. M., Groenewald, J. Z., & Crous, P. W. (2013). Redisposition of phoma-like anamorphs in Pleosporales. *Studies in Mycology*, *75*, 1–36. <https://doi.org/10.3114/sim0004>
- de Gruyter, J., Woudenberg, J. H. C., Aveskamp, M. M., Verkley, G. J. M., Groenewald, J. Z., & Crous, P. W. (2010). Systematic reappraisal of species in *Phoma* section *Paraphoma*, *Pyrenochaeta* and *Pleurophoma*. *Mycologia*, *102*(5), 1066–1081. <https://doi.org/10.3852/09-240>
- De Silva, N. I., Lumyong, S., Hyde, K. D., Bulgakov, T., Phillips, A. J. L., & Yan, J. Y. (2016). Mycosphere essays 9: Defining biotrophs and hemibiotrophs. *Mycosphere*, *7*(5), 545–559. <https://doi.org/10.5943/mycosphere/7/5/2>
- del Barrio-Duque, A., Samad, A., Nybroe, O., Antonielli, L., Sessitsch, A., & Compant, S. (2020). Interaction between endophytic Proteobacteria strains and *Serendipita indica* enhances biocontrol activity against fungal pathogens. *Plant and Soil*, *451*(1–2), 277–305. <https://doi.org/10.1007/s11104-020-04512-5>
- Derbyshire, M. C., & Denton-Giles, M. (2016). The control of sclerotinia stem rot on oilseed rape (*Brassica napus*): Current practices and future opportunities. *Plant Pathology*, *65*, 859–877. <https://doi.org/10.1111/ppa.12517>
- Díaz-Urbano, M., Velasco, P., Abilleira, R., et al. (2025). Diversity and biological activity of culturable endophytic fungi isolated from turnip (*Brassica rapa* subsp. *rapa*) roots. *Scientia Horticulturae*, *339*, 113861. <https://doi.org/10.1016/j.scienta.2024.113861>
- Díaz-Urbano, M., Velasco, P., Rodríguez, V.M. (2025). Fungal Metabolites as Inductors of Plant Abiotic Stresses Tolerance in Crops. In: Poveda, J., Santamaría, Ó., Martín-García, J. (eds) *Fungal Metabolites for Agricultural Applications*. Fungal Biology. (pp. 85–104). Springer Nature Switzerland. [https://doi.org/10.1007/978-3-031-76587-2\\_5](https://doi.org/10.1007/978-3-031-76587-2_5)
- Druzhinina, I., Seidl-Seiboth, V., Herrera-Estrella, A., et al. (2011). *Trichoderma*: The genomics of opportunistic success. *Nature Reviews Microbiology*, *9*, 749–759. <https://doi.org/10.1038/nrmicro2637>

- Dulermo, T., Rasche, C., Billon-Grand, G., Gout, E., Bligny, R., & Cotton, P. (2010). Novel insights into mannitol metabolism in the fungal plant pathogen *Botrytis cinerea*. *Biochemical Journal*, 427(2), 323–332. <https://doi.org/10.1042/BJ20091813>
- Duraffourd, D'Hervicourt, L., & Lapraz, J. (1987). *Clinical phytotherapy notebooks* (Vol. 4). Versión castellana de A. Alzina. Masson.
- EFEAGRO. (2024, February 12). *Climate change and the lack of producers reduces the harvest of grelos in Galicia*. EFEAGRO. Retrieved November 12, 2025, from <https://efeagro.com/cambio-climatico-cosecha-grelos/>
- El-Hasan, A., Ngatia, G., Link, T. I., & Voegelé, R. T. (2022). Isolation, identification, and biocontrol potential of root fungal endophytes associated with solanaceous plants against potato late blight (*Phytophthora infestans*). *Plants*, 11(12), 1605. <https://doi.org/10.3390/plants11121605>
- Eydoux, L., & Farrer, E. C. (2020). Does salinity affect lifestyle switching in the plant pathogen *Fusarium solani*? *Access Microbiology*, 2(7), 1–5. <https://doi.org/10.1099/acmi.0.000114>
- Ferus, P., Barta, M., & Konôpková, J. (2019). Endophytic fungus *Beauveria bassiana* can enhance drought tolerance in red oak seedlings. *Trees*, 33(4), 1179–1186. <https://doi.org/10.1007/s00468-019-01854-1>
- Fite, T., Kebede, E., Tefera, T., & Bekeko, Z. (2023). Endophytic fungi: Versatile partners for pest biocontrol, growth promotion, and climate change resilience in plants. *Frontiers in Sustainable Food Systems*, 7, 1322861. <https://doi.org/10.3389/fsufs.2023.1322861>
- Floc'h, J. B., Hamel, C., Lateralrière, M., Michaud, J., & Hijri, M. (2022). Long-term persistence of arbuscular mycorrhizal fungi in the rhizosphere and bulk soils of non-host *Brassica napus* and their networks of co-occurring microbes. *Frontiers in Plant Science*, 13, 828145. <https://doi.org/10.3389/fpls.2022.828145>
- Fontana, D. C., de Paula, S., Torres, A. G., de Souza, V. H. M., Pascholati, S. F., Schmidt, D., & Neto, D. D. (2021). Endophytic fungi: Biological control and induced resistance to phytopathogens and abiotic stresses. *Pathogens*, 10(5), 570. <https://doi.org/10.3390/pathogens10050570>
- Food and Agriculture Organization of the United Nations (FAO). (2025). *Crops primary Chillies and peppers (Capsicum spp.)*. FAOSTAT database. Retrieved August 1, 2025, from <http://www.fao.org/faostat/>
- Forchetti, G., Masciarelli, O., Alemanno, S., Alvarez, D., & Abdala, G. (2007). Endophytic bacteria in sunflower (*Helianthus annuus* L.): Isolation, characterization, and production of jasmonates and abscisic acid in culture medium. *Applied Microbiology and Biotechnology*, 76(5), 1145–1152. <https://doi.org/10.1007/s00253-007-1077-7>
- Gao, L., Kantar, M. B., Moxley, D., Ortiz-Barrientos, D., & Rieseberg, L. H. (2023). Crop adaptation to climate change: An evolutionary perspective. *Molecular Plant*, 16(10), 1518–1546. <https://doi.org/10.1016/j.molp.2023.07.011>
- Carrizo García, C., Barfuss, M. H., Sehr, E. M., Barboza, G. E., Samuel, R., Moscone, E. A., & Ehrendorfer, F. (2016). Phylogenetic relationships, diversification and expansion of chili peppers (*Capsicum*, Solanaceae). *Annals of Botany*, 118(1), 35–51. <https://doi.org/10.1093/aob/mcw079>
- Gevrenova, R., Zengin, G., Balabanova, V., Szakiel, A., & Zheleva-Dimitrova, D. (2024). *Pelargonium graveolens*: Towards in-depth metabolite profiling, antioxidant and enzyme-inhibitory potential. *Plants*, 13(18), 1–19. <https://doi.org/10.3390/plants13182612>

- Gonzalez, S., Swift, J., Yaaran, A., Xu, J., Miller, C., Illouz-Eliaz, N., Nery, J. R., Busch, W., Zait, Y., & Ecker, J. R. (2023). *Arabidopsis* transcriptome responses to low water potential using high-throughput plate assays. *eLife*, *12*, 1–12. <https://doi.org/10.7554/eLife.84747>
- Glynou, K., Ali, T., Buch, A. K., et al. (2016). The local environment determines the assembly of root endophytic fungi at a continental scale. *Environmental Microbiology*, *18*, 2418–2434. <https://doi.org/10.1111/1462-2920.13112>
- Glynou, K., Ali, T., Kia, S. H., Thines, M., & Maciá-Vicente, J. G. (2017). Genotypic diversity in root-endophytic fungi reflects efficient dispersal and environmental adaptation. *Molecular Ecology*, *26*, 4618–4630. <https://doi.org/10.1111/mec.14231>
- Glynou, K., Nam, B., Thines, M., & Maciá-Vicente, J. G. (2018). Facultative root-colonizing fungi dominate endophytic assemblages in roots of nonmycorrhizal *Microthlaspi* species. *New Phytologist*, *217*, 1190–1202. <https://doi.org/10.1111/nph.14873>
- Glynou, K., Thines, M., & Maciá-Vicente, J. G. (2018). Host species identity in annual Brassicaceae has a limited effect on the assembly of root-endophytic fungal communities. *Plant Ecology & Diversity*, *11*, 569–580. <https://doi.org/10.1080/17550874.2018.1504332>
- Griffith, G. W., Easton, G. L., Detheridge, A., Roderick, K., Edwards, A., Worgan, H. J., Nicholson, J., & Perkins, W. T. (2007). Copper deficiency in potato dextrose agar causes reduced pigmentation in cultures of various fungi. *FEMS Microbiology Letters*, *276*(2), 165–171. <https://doi.org/10.1111/j.1574-6968.2007.00923.x>
- Grove, G. G., & Campbell, R. N. (1987). Host range and survival in soil of *Pyrenochaeta lycopersici*. *Plant Disease*, *71*(9), 806–809. <https://doi.org/10.1094/PD-71-0806>
- Guzmán-Guzmán, P., Kumar, A., de los Santos-Villalobos, S., et al. (2023). *Trichoderma* species: Our best fungal allies in the biocontrol of plant diseases – A review. *Plants*, *12*, 432. <https://doi.org/10.3390/plants12030432>
- Hall, R. D., & Hardy, N. W. (2012). Practical applications of metabolomics in plant biology. In *Methods in Molecular Biology* (Vol. 860). [https://doi.org/10.1007/978-1-61779-594-7\\_1](https://doi.org/10.1007/978-1-61779-594-7_1)
- Hardoim, P. R., van Overbeek, L. S., Berg, G., Pirttilä, A. M., Compant, S., Campisano, A., Döring, M., & Sessitsch, A. (2015). The hidden world within plants: Ecological and evolutionary considerations for defining functioning of microbial endophytes. *Microbiology and Molecular Biology Reviews*, *79*(3), 293–320. <https://doi.org/10.1128/mnbr.00050-14>
- Harman, G. E., Howell, C. R., Viterbo, A., Chet, I., & Lorito, M. (2004). *Trichoderma* species—opportunistic, avirulent plant symbionts. *Nature Reviews Microbiology*, *2*(1), 43–56. <https://doi.org/10.1038/nrmicro797>
- Herzog, R., Schuhmann, K., Schwudke, D., Sampaio, J. L., Bornstein, S. R., Schroeder, M., & Shevchenko, A. (2012). LipidXplorer: A software for consensual cross-platform lipidomics. *PLoS ONE*, *7*(1), e29851. <https://doi.org/10.1371/journal.pone.0029851>
- Hettiarachchi, E., & Grassian, V. H. (2024). Heterogeneous reactions of phenol on different components of mineral dust aerosol: Formation of oxidized organic and nitro-phenolic compounds. *ACS ES&T Air*, *1*(4), 259–272. <https://doi.org/10.1021/acsestair.3c00042>
- Hossain, M., Sultana, F., Mostafa, M., Ferdus, H., & Rahman, M. (2024). Plant disease dynamics in a changing climate: Impacts, molecular mechanisms, and climate-informed strategies for sustainable management. In *Discover Agriculture*. Springer International Publishing. <https://doi.org/10.1007/s44279-024-00144-w>

- Hou, S., & Tsuda, K. (2022). Salicylic acid and jasmonic acid crosstalk in plant immunity. *Essays in Biochemistry*, 66(5), 647–656. <https://doi.org/10.1042/EBC20210090>
- Ibiza, V. P., Blanca, J., Cañizares, J., & Nuez, F. (2012). Taxonomy and genetic diversity of domesticated Capsicum species in the Andean region. Genetic resources and crop evolution, 59(6), 1077-1088. <https://doi.org/10.1007/s10722-011-9744-z>
- Ibrahim, A., Shahid, A. A., Shafiq, M., & Haider, M. S. (2012). Management of root knot nematodes on the turnip plant (*Brassica rapa*) by using fungus (*Trichoderma harzianum*) and neem (*Azadirachta indica*) and effect on the growth rate. *Pakistan Journal of Phytopathology*, 24(2). <https://doi/full/10.5555/20133055326>
- Infantino, A., Aragona, M., Brunetti, A., Lahoz, E., Oliva, A., & Porta-Puglia, A. (2003). Molecular and physiological characterization of Italian isolates of *Pyrenochaeta lycopersici*. *Mycological Research*, 107(6), 707-716. <https://doi.org/10.1017/S0953756203007962>
- Infantino, A., & Pucci, N. (2005). A PCR-based assay for the detection and identification of *Pyrenochaeta lycopersici*. *European Journal of Plant Pathology*, 112(4), 337–347. <https://doi.org/10.1007/s10658-005-6605-7>
- Infantino, A., Pucci, N., Aragona, M., de Felice, S., & Rau, D. (2015). Genetic structure of Italian populations of *Pyrenochaeta lycopersici*, the causal agent of corky root rot of tomato. *Plant Pathology*, 64(4), 941–950. <https://doi.org/10.1111/ppa.12326>
- Invesa. (2020). *Trichotropico WP: Trichoderma harzianum & T. koningii*. Industrias Veterinarias S.A. Retrieved November 12, 2025, from <https://www.invesa.com/product/trichotropico-wp/>
- IPCC. (2023). *Climate Change 2023: Synthesis Report. Contribution of Working Groups I, II and III to the Sixth Assessment Report of the Intergovernmental Panel on Climate Change* (Core Writing Team, H. Lee & J. Romero, Eds., pp. 35–115). Geneva, Switzerland: IPCC. <https://doi.org/10.59327/IPCC/AR6-9789291691647>
- Isaeva, O. V., Glushakova, A. M., Garbuz, S. A., Kachalkin, A. V., & Chernov, I. Y. (2010). Endophytic yeast fungi in plant storage tissues. *Biology bulletin*, 37(1), 26-34. <https://doi.org/10.1134/S1062359010010048>
- Ishimoto, H., Fukushi, Y., Yoshida, T., & Tahara, S. (2000). *Rhizopus* and *Fusarium* are selected as dominant fungal genera in rhizospheres of Brassicaceae. *Journal of Chemical Ecology*, 26, 2387–2391. <https://doi.org/10.1023/A:1005583012561>
- Jaber, L. R., & Alananbeh, K. M. (2018). Fungal entomopathogens as endophytes reduce several species of *Fusarium* causing crown and root rot in sweet pepper (*Capsicum annuum* L.). *Biological Control*, 126, 117–126. <https://doi.org/10.1016/j.biocontrol.2018.08.007>
- Javed, J., Rauf, M., Arif, M., Hamayun, M., Gul, H., Ud-Din, A., Ud-Din, J., Sohail, M., Rahman, M. M., & Lee, I. J. (2022). Endophytic fungal consortia enhance basal drought-tolerance in *Moringa oleifera* by upregulating the antioxidant enzyme (APX) through heat shock factors. *Antioxidants*, 11(9). <https://doi.org/10.3390/antiox11091669>
- Johnson, J. M., Alex, T., & Oelmüller, R. (2014). *Piriformospora indica*: The versatile and multifunctional root endophytic fungus for enhanced yield and tolerance to biotic and abiotic stress in crop plants. *Journal of Tropical Agriculture*, 52(2), 103–122. <https://jtropag.kau.in/index.php/ojs2/article/view/311>
- Joubert, P. M., & Doty, S. L. (2018). Endophytic yeasts: Biology, ecology and applications. *Endophytes of Forest Trees: Biology and Applications*, 3-14.
- Kasuya, E. (2004). Angular transformation—Another effect of different sample sizes. *Ecological Research*, 19(2), 165–167. <https://doi.org/10.1111/j.1440-1703.2003.00620.x>

- Khan, A., Hamayun, M., Kang, S. M., Kim, Y. H., Jung, H. Y., Lee, J. H., & Lee, I. J. (2012). Endophytic fungal association via gibberellins and indole acetic acid can improve plant growth under abiotic stress: An example of *Paecilomyces formosus* LHL10. *BMC Microbiology*, *12*, 3. <https://doi.org/10.1186/1471-2180-12-3>
- Khan, A. L., Hussain, J., Al-Harrasi, A., Al-Rawahi, A., & Lee, I. J. (2013). Endophytic fungi: Resource for gibberellins and crop abiotic stress resistance. *Critical Reviews in Biotechnology*, *35*(1), 62–74. <https://doi.org/10.3109/07388551.2013.800018>
- Khan, A. L., Waqas, M., Hamayun, M., Al-Harrasi, A., Al-Rawahi, A., & Lee, I. J. (2013). Co-synergism of endophyte *Penicillium resedanum* LK6 with salicylic acid helped *Capsicum annuum* in biomass recovery and osmotic stress mitigation. *BMC Microbiology*, *13*, 51. <https://doi.org/10.1186/1471-2180-13-51>
- Khruengchai, S., Pripdeevech, P., Tanapichatsakul, C., Srisuwannapa, C., D'Souza, P. E., & Panuwet, P. (2021). Antifungal properties of volatile organic compounds produced by *Daldinia eschscholtzii* MFLUCC 19-0493 isolated from *Barleria prionitis* leaves against *Colletotrichum acutatum* and its postharvest infections on strawberry fruits. *PeerJ*, *9*, e11242. <https://doi.org/10.7717/peerj.11242>
- Kim, W. R., Kim, E. O., Kang, K., Oidovsambuu, S., Jung, S. H., Kim, B. S. & Um, B. H. (2014). Antioxidant activity of phenolics in leaves of three red pepper (*Capsicum annuum*) cultivars. *Journal of Agricultural and Food Chemistry*, *62*(4), 850-859. [dx.doi.org/10.1021/jf403006c](https://doi.org/10.1021/jf403006c)
- Kim, C. G., Kim, D. I., Kim, H. J., Park, J. E., Lee, B., Park, K. W. & Kim, H. M. (2009). Assessment of gene flow from genetically modified anthracnose-resistant chili pepper (*Capsicum annuum* L.) to a conventional crop. *Journal of Plant Biology*, *52*(3), 251-258. <https://doi.org/10.1007/s12374-009-9025-y>
- Kliman, M., Vijayakrishnan, N., Wang, L., Tapp, J. T., Broadie, K., & McLean, J. A. (2010). Structural mass spectrometry analysis of lipid changes in a *Drosophila* epilepsy model brain. *Molecular BioSystems*, *6*(6), 958–966. <https://doi.org/10.1039/b927494d>
- Klopper, J. W., Ryu, C., & Zhang, S. (2004). Induced systemic resistance and promotion of plant growth by *Bacillus* spp. *Phytopathology*, *94*(11), 1259–1266.
- Koppert. (2022). *Trianum-P: Prevent and control soil-borne diseases*. Koppert Biological Systems. Retrieved November 12, 2025, from <https://www.koppert.com/trianum-p/>
- Kot, A. M., Błazejak, S., Gientka, I., Kieliszek, M., & Bryś, J. (2018). Torulene and torularhodin: “New” fungal carotenoids for industry? *Microbial Cell Factories*, *17*(1), 1–14. <https://doi.org/10.1186/s12934-018-0893-z>
- Kraft, K. H., Brown, C. H., Nabhan, G. P., Luedeling, E., Jesús, J. De, & Ruiz, L. (2014). Multiple lines of evidence for the origin of domesticated chili pepper, *Capsicum annuum*, in Mexico. *Proceedings of the National Academy of Sciences*, *111*(17), 6165–6170. <https://doi.org/10.1073/pnas.1308933111>
- Kumar, V., Sarma, M. V. R. K., Saharan, K., Srivastava, R., Kumar, L., Sahai, V., Bisaria, V. S., & Sharma, A. K. (2012). Effect of formulated root endophytic fungus *Piriformospora indica* and plant growth promoting rhizobacteria fluorescent pseudomonads R62 and R81 on *Vigna mungo*. *World Journal of Microbiology and Biotechnology*, *28*, 595–603. <https://doi.org/10.1007/s11274-011-0852-x>
- Lamour, K. H., Stam, R., Jupe, J., Huitema, E., Programme, P. P., Road, E., & Dd, D. (2012). Pathogen profile: The oomycete broad-host-range pathogen *Phytophthora capsici*. *Molecular Plant Pathology*, *13*, 329–337. <https://doi.org/10.1111/j.1364-3703.2011.00754.x>

- Lan, D., & Wu, B. (2020). Chemistry and bioactivities of secondary metabolites from the genus *Talaromyces*. *Chemistry & Biodiversity*, 17(8), e2000229. <https://doi.org/10.1002/cbdv.202000229>
- Latz, M. A. C., Jensen, B., Collinge, D. B., & Jørgensen, H. J. L. (2018). Endophytic fungi as biocontrol agents: Elucidating mechanisms in disease suppression. In *Plant Ecology and Diversity* (Vol. 11, Issues 5–6, pp. 555–567). Taylor & Francis. <https://doi.org/10.1080/17550874.2018.1534146>
- Li, J., Chen, B., Zhang, X., Hao, Z., Zhang, X., & Zhu, Y. (2021). Arsenic transformation and volatilization by arbuscular mycorrhizal symbiosis under axenic conditions. *Journal of Hazardous Materials*, 413, 125390. <https://doi.org/10.1016/j.jhazmat.2021.125390>
- Liao, C., Doilom, M., Jeewon, R., Hyde, K. D., Manawasinghe, I. S., Chethana, K. W. T., Balasuriya, A., Thakshila, S. A. D., Luo, M., Mapook, A., Htet, Z. H., Koodalugodaarachchi, V., Wijekoon, N., Saxena, R. K., Senanayake, I. C., Kularathnage, N. D., Alrefaei, A. F., & Dong, W. (2025). Challenges and update on fungal endophytes: Classification, definition, diversity, ecology, evolution and functions. In *Fungal Diversity* (Vol. 131, Issue 1). Springer Netherlands. <https://doi.org/10.1007/s13225-025-00550-5>
- Liarzi, O., Bar, E., Lewinsohn, E., & Ezra, D. (2016). Use of the endophytic fungus *Daldinia cf. concentrica* and its volatiles as bio-control agents. *PLoS ONE*, 11(12), e0168242. <https://doi.org/10.1371/journal.pone.0168242>
- Ling, Y., Li, Z., Chen, M., Sun, Z., Fan, M., & Huang, C. (2013). Analysis and detection of the chemical constituents of *Radix Polygalae* and their metabolites in rats after oral administration by ultra high-performance liquid chromatography coupled with electrospray ionization. *Journal of Pharmaceutical and Biomedical Analysis*, 85, 1–13. <https://doi.org/10.1016/j.jpba.2013.06.011>
- Lugtenberg, B. J. J., Caradus, J. R., & Johnson, L. J. (2016). Fungal endophytes for sustainable crop production. *FEMS Microbiology Ecology*, 92(12), fiw194. <https://doi.org/10.1093/femsec/fiw194>
- Ma, Y. M., Liang, X. A., Kong, Y., & Jia, B. (2016). Structural diversity and biological activities of indole diketopiperazine alkaloids from fungi. *Journal of Agricultural and Food Chemistry*, 64(35), 6659–6671. <https://doi.org/10.1021/acs.jafc.6b01772>
- Raro Macián, M. (2016). *Evaluación de nuevas herramientas analíticas para mejorar la capacidad de detección en el control del dopaje* (Tesis doctoral). Universitat Jaume I, Departamento de Química Física y Analítica, Instituto Universitario de Plaguicidas y Aguas. <http://hdl.handle.net/10803/379308>
- Macías-Rubalcava, M. L., Sánchez-Fernández, R. E., Roque-Flores, G., Lappe-Oliveras, P., & Medina-Romero, Y. M. (2018). Volatile organic compounds from *Hypoxylon anthochroum* endophytic strains as postharvest mycofumigation alternative for cherry tomatoes. *Food Microbiology*, 76, 363–373. <https://doi.org/10.1016/j.fm.2018.06.014>
- Maciá-Vicente, J. G., Nam, B., & Thines, M. (2020). Root filtering, rather than host identity or age, determines the composition of root-associated fungi and oomycetes in three naturally co-occurring Brassicaceae. *Soil Biology and Biochemistry*, 146, 107806. <https://doi.org/10.1016/j.soilbio.2020.107806>
- Madbouly, A. K., Abo Elyousr, K. A. M., & Ismail, I. M. (2020). Biocontrol of *Monilinia fructigena*, causal agent of brown rot of apple fruit, by using endophytic yeasts. *Biological Control*, 144, 104239. <https://doi.org/10.1016/j.biocontrol.2020.104239>

- Mandal, A., Sarkar, B., Mandal, S., et al. (2020). Impact of agrochemicals on soil health. In M. N. V. Prasad (Ed.), *Agrochemicals: Detection, treatment and remediation* (pp. 161–187). Oxford: Butterworth-Heinemann. <https://doi.org/10.1016/B978-0-08-103017-2.00007-6>
- Mari, M., Di Francesco, A., & Bertolini, P. (2014). Control of fruit postharvest diseases: Old issues and innovative approaches. *Stewart Postharvest Review*, 10(1). <https://doi.org/10.2212/spr.2014.1.1>
- Masi, E., Caparrotta, S., Taiti, C., Ieri, F., Fiume, P., Moselhy, N., Mancuso, S., & Romani, A. (2017). Characterization of volatile compounds in *Mentha spicata* L. dried leaves. *Advances in Horticultural Science*, 31(2), 89–95. <https://doi.org/10.13128/ahs-20588>
- Mazourek, M., Pujar, A., Borovsky, Y., Paran, I., Mueller, L., & Jahn, M. M. (2009). A dynamic interface for capsaicinoid systems biology. *Plant Physiology*, 150(4), 1806-1821. <https://doi.org/10.1104/pp.109.136549>
- Ministry of Agriculture, Fisheries and Food. (2023). *Statistical yearbook 2023: Part 3, Chapter 7, Group 4 [Statistical data on industrial crop areas and production]*. <https://www.mapa.gob.es/es/estadistica/temas/publicaciones/anuario-de-estadistica/2023?parte=3&capitulo=7&grupo=4> (accessed 1 August 2025)
- Mousa, W. K., & Raizada, M. N. (2013). The diversity of anti-microbial secondary metabolites produced by fungal endophytes: An interdisciplinary perspective. *Frontiers in Microbiology*, 4, 65. <https://doi.org/10.3389/fmicb.2013.00065>
- Nagaharu, U. J. J. B., & Nagaharu, N. J. J. B. (1935). Genome analysis in Brassica with special reference to the experimental formation of *B. napus* and peculiar mode of fertilization. *Japanese Journal of Botany*, 7(7), 389-452.
- Navarro-Ródenas, A., Lozano-Carrillo, M. C., Pérez-Gilabert, M., & Morte, A. (2011). Effect of water stress on *in vitro* mycelium cultures of two mycorrhizal desert truffles. *Mycorrhiza*, 21(4), 247–253. <https://doi.org/10.1007/s00572-010-0329-z>
- Naziya, B., Murali, M., & Amruthesh, K. N. (2019). Plant growth-promoting fungi (PGPF) instigate plant growth and induce disease resistance in *Capsicum annuum* L. upon infection with *Colletotrichum capsici* (Syd.) Butler & Bisby. *Biomolecules*, 10(1), 41. <https://doi.org/10.3390/biom10010041>
- NCBI. (2025). *NCBI*. <https://pubchem.ncbi.nlm.nih.gov/compound/5283162>
- Nelson, A., Vandegrift, R., Carroll, G. C., & Roy, B. A. (2020). Double lives: transfer of fungal endophytes from leaves to woody substrates. *PeerJ*, 8, e9341. <https://doi.org/10.7717/peerj.9341>
- Nicoletti, R., Andolfi, A., & Salvatore, M. M. (2023). Endophytic fungi of the genus *Talaromyces* and plant health. In *Microbial Endophytes and Plant Growth*. INC. <https://doi.org/10.1016/b978-0-323-90620-3.00004-0>
- Nimmakayala, P., Abburi, V. L., Saminathan, T., Tonapi, K., Yadav, L., Malkaram, S., Vajja, G., & Hankins, G. (2016). Genome-wide diversity and association mapping for capsaicinoids and fruit weight in *Capsicum annuum* L. *Scientific Reports*, 6, 38081. <https://doi.org/10.1038/srep38081>
- Okazaki, Y., Otsuki, H., Narisawa, T., Kobayashi, M., Sawai, S., Kamide, Y., Kusano, M., Aoki, T., Hirai, M. Y., & Saito, K. (2013). A new class of plant lipid is essential for protection against phosphorus depletion. *Nature Communications*, 4, 2512. <https://doi.org/10.1038/ncomms2512>
- Oksanen, J., Blanchet, F. G., Friendly, M., Kindt, R., Legendre, P., McGlinn, D., Minchin, P. R., O'Hara, R. B., Simpson, G. L., Solymos, P., Stevens, M. H. H., Szöcs, E., & Wagner, H. (2023). *vegan: Community Ecology Package* (R package version 2.6-4). <https://CRAN.R-project.org/package=vegan>

- Parrón, T., Requena, M., Hernández, A. F., & Alarcón, R. (2014). Environmental exposure to pesticides and cancer risk in multiple human organ systems. *Toxicology Letters*, 230(2), 157–165. <https://doi.org/10.1016/j.toxlet.2013.11.009>
- Paul, N. C., Deng, J. X., Sang, H. K., Choi, Y. P., & Yu, S. H. (2012). Distribution and antifungal activity of endophytic fungi in different growth stages of chili pepper (*Capsicum annuum* L.) in Korea. *Plant Pathology Journal*, 28(1), 10–19. <https://doi.org/10.5423/PPJ.OA.07.2011.0126>
- Pelaez, F., Cabello, A., Platas, G., Díez, M. T., Del Val, A. G., Basilio, A., Martán, I., Vicente, F., Bills, G. F., Giacobbe, R. A., Schwartz, R. E., Onishi, J. C., Meinz, M. S., Abruzzo, G. K., Flattery, A. M., Kong, L., & Kurtz, M. B. (2000). The discovery of enfumafungin, a novel antifungal compound produced by an endophytic *Hormonema* species: Biological activity and taxonomy of the producing organisms. *Systematic and Applied Microbiology*, 23(3), 333–343. [https://doi.org/10.1016/S0723-2020\(00\)80062-4](https://doi.org/10.1016/S0723-2020(00)80062-4)
- Pereira, E. C., Zabalgoageazcoa, I., Arellano, J. B., Ugalde, U., & Vázquez de Aldana, B. R. (2023). *Diaporthe atlantica* enhances tomato drought tolerance by improving photosynthesis, nutrient uptake and enzymatic antioxidant response. *Frontiers in Plant Science*, 14, 1118698. <https://doi.org/10.3389/fpls.2023.1118698>
- Pereira, E., Vázquez De Aldana, B. R., Emeterio, L. S., & Zabalgoageazcoa, I. (2019). A survey of culturable fungal endophytes from *Festuca rubra* subsp. *pruinosa*, a grass from marine cliffs, reveals a core microbiome. *Frontiers in Microbiology*, 10, 3321. <https://doi.org/10.3389/fmicb.2018.03321>
- Perry, L., Dickau, R., Zarrillo, S., Holst, I., Pearsall, D. M., Piperno, D. R., ... & Zeidler, J. A. (2007). Starch fossils and the domestication and dispersal of chili peppers (*Capsicum* spp. L.) in the Americas. *Science*, 315(5814), 986–988. <https://doi.org/10.1126/science.1136914>
- Pickersgill, B. (2007). Domestication of plants in the Americas: Insights from Mendelian and molecular genetics. *Annals of Botany*, 100(5), 925–940. <https://doi.org/10.1093/aob/mcm193>
- Piszczyk, J., Armitage, E. G., Ferrarini, A., Rupérez, F. J., Kulczynska, A., Bolkun, L., Kloczko, J., Kretowski, A., Urbanowicz, A., Ciborowski, M., & Barbas, C. (2016). To treat or not to treat: Metabolomics reveals biomarkers for treatment indication in chronic lymphocytic leukaemia patients. *Oncotarget*, 7(16), 22324–22338. <https://doi.org/10.18632/oncotarget.8078>
- Plaszko, T., Szűcs, Z., & Vasas, G. (2021). Effects of glucosinolate-derived isothiocyanates on fungi: A comprehensive review on direct effects, mechanisms, structure–activity relationship data and possible agricultural applications. *Journal of Fungi*, 7, 539. <https://doi.org/10.3390/jof7070539>
- Plaszko, T., Szűcs, Z., Cziáky, Z., Ács-Szabó, L., Csoma, H., Géczi, L. & Gonda, S. (2022). Correlations between the metabolome and the endophytic fungal metagenome suggests importance of various metabolite classes in community assembly in horseradish (*Armoracia rusticana*, Brassicaceae) roots. *Frontiers in Plant Science*, 13, 921008. <https://doi.org/10.3389/fpls.2022.932288>
- Poveda, J. (2021). Glucosinolates profile of *Arabidopsis thaliana* modified root colonization of *Trichoderma* species. *Biological Control*, 155, 104522. <https://doi.org/10.1016/j.biocontrol.2020.104522>
- Poveda, J., Díaz-González, S., Díaz-Urbano, M., et al. (2022). Fungal endophytes of Brassicaceae: Molecular interactions and crop benefits. *Frontiers in Plant Science*, 13, 932288. <https://doi.org/10.3389/fpls.2022.932288>

- Poveda, J., Eugui, D., Abril-Urías, P., & Velasco, P. (2021). Endophytic fungi as direct plant growth promoters for sustainable agricultural production. *Symbiosis*, 85(1), 1–19. <https://doi.org/10.1007/s13199-021-00789-x>
- Poveda, J., Zabalgogea, I., Soengas, P., et al. (2020). *Brassica oleracea* var. *acephala* (kale) improvement by biological activity of root endophytic fungi. *Scientific Reports*, 10, 77215. <https://doi.org/10.1038/s41598-020-77215-7>
- Pozo, M. J., Zabalgogea, I., Vazquez de Aldana, B. R., & Martinez-Medina, A. (2021). Untapping the potential of plant mycobiomes for applications in agriculture. *Current Opinion in Plant Biology*, 60, 102034. <https://doi.org/10.1016/j.pbi.2021.102034>
- Prasain, J. K., Wilson, L. S., Arabshahi, A., Grubbs, C., & Barnes, S. (2017). Mass spectrometric evidence for the modification of small molecules in a cobalt-60 irradiated rodent diet. *Physiology & Behavior*, 176(3), 139–148. <https://doi.org/10.1002/jms.3950.Mass>
- Pratap, D., Harikesh, S., Singh, B., & Prabha, R. (2016). Microbial inoculants in sustainable agricultural productivity (Vol. 2). Springer. <https://doi.org/10.1007/978-81-322-2644-4>
- Promptutha, I., & Miller, A. N. (2010). Three new species of *Acanthostigma* (Tubeufiaceae, Dothideomycetes) from Great Smoky Mountains National Park. *Mycologia*, 102(3), 574–587. <https://doi.org/10.3852/09-051>
- Qiang, X., Ding, J., Lin, W., Li, Q., Xu, C., Zheng, Q., & Li, Y. (2019). Alleviation of the detrimental effect of water deficit on wheat (*Triticum aestivum* L.) growth by an indole acetic acid-producing endophytic fungus. *Plant and Soil*, 439(1–2), 373–391. <https://doi.org/10.1007/s11104-019-04028-7>
- Qin, J., Lyu, A., Zhang, Q. H., et al. (2019). Strain identification and metabolites isolation of *Aspergillus capensis* CanS-34A from *Brassica napus*. *Molecular Biology Reports*, 46, 3451–3460. <https://doi.org/10.1007/s11033-019-04808-5>
- Raja, H. A., Miller, A. N., Pearce, C. J., & Oberlies, N. H. (2017). Fungal identification using molecular tools: A primer for the natural products research community. *Journal of Natural Products*, 80, 756–770. <https://doi.org/10.1021/acs.jnatprod.6b01085>
- Raza, W., & Shen, Q. (2020). Volatile organic compounds mediated plant–microbe interactions in soil. In *Molecular Aspects of Plant Beneficial Microbes in Agriculture*. INC. <https://doi.org/10.1016/b978-0-12-818469-1.00018-3>
- Redkar, A., Sabale, M., Zuccaro, A., & Di Pietro, A. (2022). Determinants of endophytic and pathogenic lifestyle in root colonizing fungi. *Current Opinion in Plant Biology*, 67, 102226. <https://doi.org/10.1016/j.pbi.2022.102226>
- Redman, R. S., Kim, Y. O., Woodward, C. J. D. A., Greer, C., Espino, L., Doty, S. L., & Rodriguez, R. J. (2011). Increased fitness of rice plants to abiotic stress via habitat adapted symbiosis: A strategy for mitigating impacts of climate change. *PLoS ONE*, 6(7), e14823. <https://doi.org/10.1371/journal.pone.0014823>
- Reyes-Escogido, M. D. L., Gonzalez-Mondragon, E. G., & Vazquez-Tzompantzi, E. (2011). Chemical and pharmacological aspects of capsaicin. *Molecules*, 16(2), 1253–1270. <https://doi.org/10.3390/molecules16021253>
- Ghaffari, M. R., Mirzaei, M., Ghabooli, M., Khatabi, B., Wu, Y., Zabet-Moghaddam, M., & Salekdeh, G. H. (2019). Root endophytic fungus *Piriformospora indica* improves drought stress adaptation in barley by metabolic and proteomic reprogramming. *Environmental and experimental botany*, 157, 197–210. <https://doi.org/10.1016/j.envexpbot.2018.10.002>

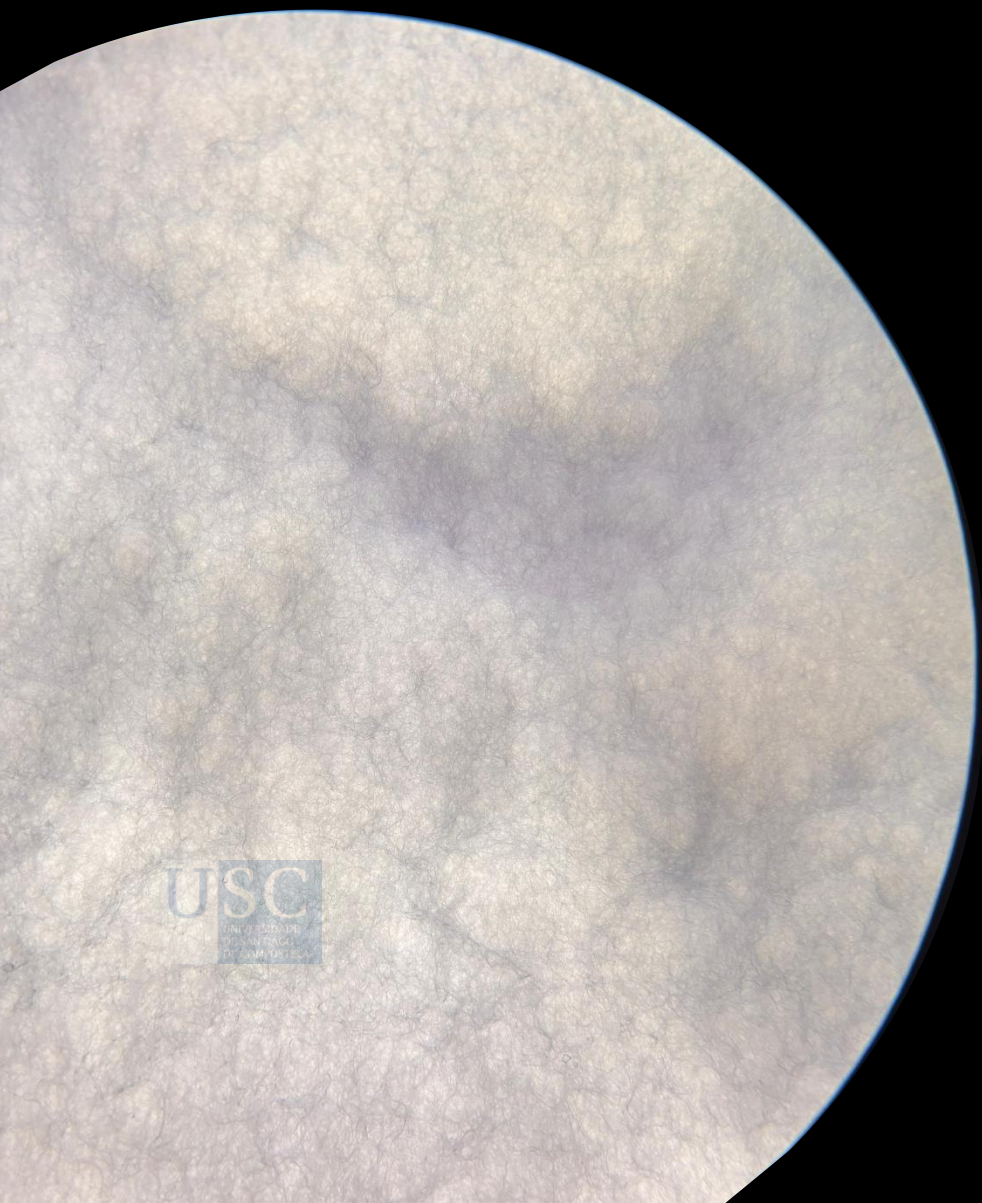
- Ripa, F. A., Cao, W. D., Tong, S., & Sun, J. G. (2019). Assessment of plant growth promoting and abiotic stress tolerance properties of wheat endophytic fungi. *BioMed Research International*, 2019(1), 6105865. <https://doi.org/10.1155/2019/6105865>
- Rodriguez, R. J., White, J. F., Arnold, A. E., & Redman, R. S. (2009). Fungal endophytes: Diversity and functional roles. *New Phytologist*, 182(2), 314–330. <https://doi.org/10.1111/j.1469-8137.2009.02773.x>
- Sadeghi, F., Samsampour, D., Askari Seyahooei, M., Bagheri, A., & Soltani, J. (2020). Fungal endophytes alleviate drought-induced oxidative stress in mandarin (*Citrus reticulata* L.): Toward regulating the ascorbate–glutathione cycle. *Scientia Horticulturae*, 261, 108991. <https://doi.org/10.1016/j.scienta.2019.108991>
- Sánchez-Fernández, R. E., Sánchez-Ortiz, B. L., Monserrat Sandoval-Espinosa, Y. K., Ulloa-Benítez, Á., Armendáriz-Guillén, B., García-Méndez, C., & Macías-Rubalcava, L. (2013). Hongos endófitos: Fuente potencial de metabolitos secundarios bioactivos con utilidad en agricultura y medicina. *TIP*, 16(2), 132–146. [https://doi.org/10.1016/s1405-888x\(13\)72084-9](https://doi.org/10.1016/s1405-888x(13)72084-9)
- Sandhya, V., A. S., Grover, M., Reddy, G., & Venkateswarlu, B. (2009). Alleviation of drought stress effects in sunflower seedlings by the exopolysaccharides producing *Pseudomonas putida* strain GAP-p45. *Biology and Fertility of Soils*, 46(1), 17–26. <https://doi.org/10.1007/s00374-009-0401-z>
- Schneider, C. A., Rasband, W. S., & Eliceiri, K. W. (2012). NIH Image to ImageJ: 25 years of image analysis. *Nature Methods*, 9, 671–675. <https://doi.org/10.1038/nmeth.2089>
- Schug, K., & McNair, H. M. (2003). Adduct formation in electrospray ionization mass spectrometry: II. Benzoic acid derivatives. *Journal of Chromatography A*, 985(1–2), 531–539. [https://doi.org/10.1016/S0021-9673\(02\)01732-6](https://doi.org/10.1016/S0021-9673(02)01732-6)
- Schulz, B., & Boyle, C. (2005). The endophytic continuum. *Mycological Research*, 109(6), 661–686. <https://doi.org/10.1017/S095375620500273X>
- Selosse, M. A., Schneider-Maunoury, L., & Martos, F. (2018). Time to re-think fungal ecology? Fungal ecological niches are often prejudged. *New Phytologist*, 217, 968–972. <https://doi.org/10.1111/nph.14983>
- Shahzad, R., Waqas, M., Khan, A. L., Asaf, S., Khan, M. A., Kang, S. M., Yun, B. W., & Lee, I. J. (2016). Seed-borne endophytic *Bacillus amyloliquefaciens* RWL-1 produces gibberellins and regulates endogenous phytohormones of *Oryza sativa*. *Plant Physiology and Biochemistry*, 106, 236–243. <https://doi.org/10.1016/j.plaphy.2016.05.006>
- Sharma, H., Rai, A. K., Dahiya, D., Chettri, R., Nigam, P. S. (2021). Exploring endophytes for *in vitro* synthesis of bioactive compounds similar to metabolites produced *in vivo* by host plants. *AIMS Microbiology*, 7(2), 175–199. <https://doi.org/10.3934/microbiol.2021012>
- Sharma, P., & Singh, S. P. (2021). Role of the endogenous fungal metabolites in the plant growth improvement and stress tolerance. In *Fungi Bio-prospects in Sustainable Agriculture, Environment and Nano-technology: Volume 3: Fungal Metabolites, Functional Genomics and Nano-technology*. INC. <https://doi.org/10.1016/b978-0-12-821734-4.00002-2>
- Sheng, F., Hu, B., Jin, Q., Wang, J., Wu, C., & Luo, Z. (2021). The analysis of phenolic compounds in walnut husk and pellicle by UPLC-Q-Orbitrap HRMS and HPLC. *Molecules*, 26(10), 3013. <https://doi.org/10.3390/molecules26103013>

- Sherameti, I., Shahollari, B., Venus, Y., Altschmied, L., Varma, A., & Oelmüller, R. (2005). The endophytic fungus *Piriformospora indica* stimulates the expression of nitrate reductase and the starch-degrading enzyme glucan-water dikinase in tobacco and *Arabidopsis* roots through a homeodomain transcription factor that binds to a conserved motif in their promoters. *Journal of Biological Chemistry*, 280(28), 26241–26247. <https://doi.org/10.1074/jbc.M500447200>
- Shoresh, M., Yedidia, I., & Chet, I. (2007). Involvement of jasmonic acid/ethylene signaling pathway in the systemic resistance induced in cucumber by *Trichoderma asperellum* T203. *Phytopathology*, 95(1), 76–84. <https://doi.org/10.1094/PHYTO-95-0076>
- Siebers, M., Rohr, T., Ventura, M., et al. (2018). Disruption of microbial community composition and identification of plant growth promoting microorganisms after exposure of soil to rapeseed-derived glucosinolates. *PLoS ONE*, 13(e0200160). <https://doi.org/10.1371/journal.pone.0200160>
- Stone, J. K., Bacon, C. W., & White Jr, J. F. (2000). An overview of endophytic microbes: endophytism defined. *Microbial endophytes*, 17-44.
- Sugiura, T., Horinouchi, H., Taguchi, Y., & Hyahamachi, M. (2003, February). Two types of *Pyrenochaeta lycopersici*, causal pathogen of corky root of tomato. In *Proceedings of the 8th International Congress of Plant Pathology, Christchurch, New Zealand* (pp. 2-7).
- Sun, C., Johnson, J. M., Cai, D., Sherameti, I., Oelmüller, R., & Lou, B. (2010). *Piriformospora indica* confers drought tolerance in Chinese cabbage leaves by stimulating antioxidant enzymes, the expression of drought-related genes and the plastid-localized CAS protein. *Journal of Plant Physiology*, 167(12), 1009–1017. <https://doi.org/10.1016/j.jplph.2010.02.013>
- Sun, R. (2015). Economic/academic importance of *Brassica rapa*. In *The Brassica rapa Genome* (pp. 1–15). Springer Berlin Heidelberg. [https://doi.org/10.1007/978-3-662-47901-8\\_1](https://doi.org/10.1007/978-3-662-47901-8_1)
- Suzuki, T., & Iwai, K. (1984). Constituents of red pepper species: Chemistry, biochemistry, pharmacology, and food science of the pungent principle of *Capsicum* species. In *The Alkaloids: Chemistry and Pharmacology* (pp. 227–299). [https://doi.org/10.1016/S0099-9598\(08\)60072-3](https://doi.org/10.1016/S0099-9598(08)60072-3)
- Szűcs, Z., Plaszkó, T., Cziáky, Z., et al. (2018). Endophytic fungi from the roots of horseradish (*Armoracia rusticana*) and their interactions with the defensive metabolites of the glucosinolate–myrosinase–isothiocyanate system. *BMC Plant Biology*, 18, 95. <https://doi.org/10.1186/s12870-018-1295-4>
- Taylor, J. W. (2011). One fungus = one name: DNA and fungal nomenclature twenty years after PCR. *IMA Fungus*, 2(2), 113–120. <https://doi.org/10.5598/ima fungus.2011.02.02.01>
- Testen, A. L., Shaw, R. S., Rotondo, F., Moodispaw, M. R., & Miller, S. A. (2023). A quantitative PCR method to detect the tomato corky root rot pathogens, *Pseudopyrenochaeta lycopersici* and *P. terrestris*. *Plant Disease*, 107(9), 2673–2678. <https://doi.org/10.1094/PDIS-08-22-2009-RE>
- Tewksbury, J. J., & Nabhan, G. P. (2001). Directed deterrence by capsaicin in chillies. *Nature*, 412(6845), 403-404. <https://doi.org/10.1038/35086653>
- Thiergart, T., Durán, P., Ellis, T., Vannier, N., Garrido-Oter, R., Kemen, E., ... & Hacquard, S. (2020). Root microbiota assembly and adaptive differentiation among European *Arabidopsis* populations. *Nature ecology & evolution*, 4(1), 122-131. <https://doi.org/10.1038/s41559-019-1063-3>

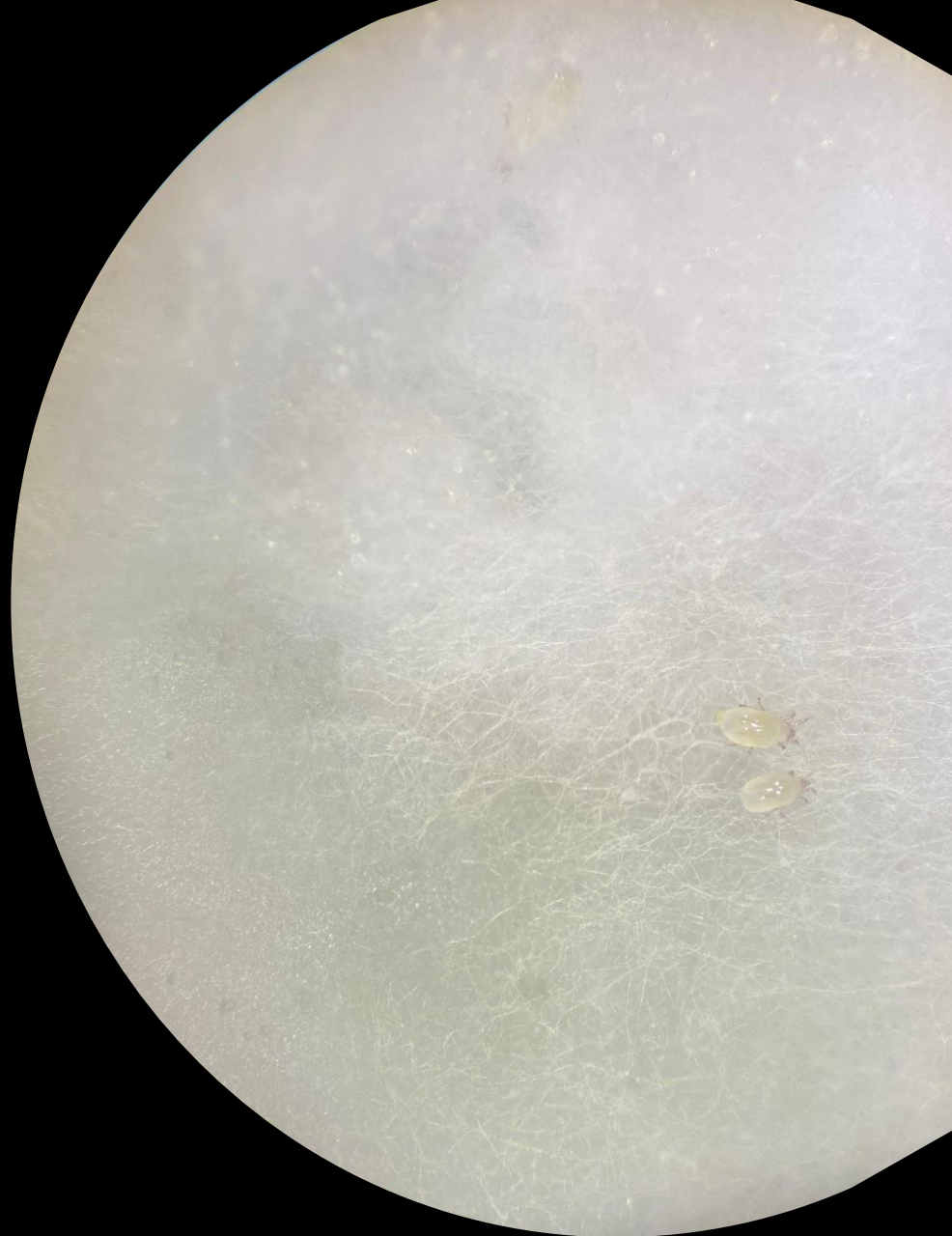
- Thiep, N. V., & Soyong, K. (2015). *Chaetomium* spp. as biocontrol potential to control tea and coffee pathogens in Vietnam. *International Journal of Agricultural Technology*, *11*(6), 1381–1392.
- Timac Agro. (2022). TUSAL: Fungicida biológico / Soluciones de nutrición del suelo. Timac Agro España. Retrieved November 12, 2025, from <https://es.timacagro.com/soluciones/nutricion-del-suelo/fungicida-biologico/tusal/>
- Toghueo, R. M. K., Zabalgoeazcoa, I., Pereira, E. C., & Vázquez de Aldana, B. R. (2022). A *Diaporthe* fungal endophyte from a wild grass improves growth and salinity tolerance of Tritordeum and perennial ryegrass. *Frontiers in Plant Science*, *13*, 896755. <https://doi.org/10.3389/fpls.2022.896755>
- Urbina, H., Breed, M. F., Zhao, W., et al. (2018). Specificity in *Arabidopsis thaliana* recruitment of root fungal communities from soil and rhizosphere. *Fungal Biology*, *122*, 231–240. <https://doi.org/10.1016/j.funbio.2017.12.013>
- Valenzuela-López, N., Cano-Lira, J. F., Guarro, J., Sutton, D. A., Wiederhold, N., Crous, P. W., & Stchigel, A. M. (2018). Coelomycetous Dothideomycetes with emphasis on the families Cucurbitariaceae and Didymellaceae. *Studies in Mycology*, *90*, 1–69. <https://doi.org/10.1016/j.simyco.2017.11.003>
- Van Der Weele, C. M., Spollen, W. G., Sharp, R. E., & Baskin, T. I. (2000). Growth of *Arabidopsis thaliana* seedlings under water deficit studied by control of water potential in nutrient-agar media. *Journal of experimental botany*, *51*(350), 1555–1562. <https://doi.org/10.1093/jexbot/51.350.1555>
- Vázquez-de-Aldana, B. R., García-Ciudad, A., García-Criado, B., Vicente-Tavera, S., & Zabalgoeazcoa, I. (2013). Fungal endophyte (*Epichloë festucae*) alters the nutrient content of *Festuca rubra* regardless of water availability. *PLoS ONE*, *8*(12), e84539. <https://doi.org/10.1371/journal.pone.0084539>
- Véléz, H., Glassbrook, N. J., & Daub, M. E. (2007). Mannitol metabolism in the phytopathogenic fungus *Alternaria alternata*. *Fungal Genetics and Biology*, *44*(4), 258–268. <https://doi.org/10.1016/j.fgb.2006.09.008>
- Verslues, P. E., & Bray, E. A. (2004). LWR1 and LWR2 are required for osmoregulation and osmotic adjustment in *Arabidopsis*. *Plant physiology*, *136*(1), 2831–2842. <https://doi.org/10.1104/pp.104.045856>
- Waller, F., Achatz, B., Baltruschat, H., Fodor, J., Becker, K., Fischer, M., ... Kogel, K. H. (2005). The endophytic fungus *Piriformospora indica* reprograms barley to salt-stress tolerance, disease resistance, and higher yield. *Proceedings of the National Academy of Sciences*, *102*(38), 13386–13391. <https://doi.org/10.1073/pnas.0504423102>
- Wanasinghe, D. N., Phookamsak, R., Jeewon, R., Li, W. J., Hyde, K. D., Jones, E. B. G., Camporesi, E., & Promputtha, I. (2017). A family-level rDNA-based phylogeny of Cucurbitariaceae and Fenestellaceae with descriptions of new *Fenestella* species and *Neocucurbitaria* gen. nov. *Mycosphere*, *8*(4), 397–414. <https://doi.org/10.5943/mycosphere/8/4/2>
- Waqas, M., Khan, A. L., Kamran, M., Hamayun, M., Kang, S. M., Kim, Y. H., & Lee, I. J. (2012). Endophytic fungi produce gibberellins and indoleacetic acid and promote host-plant growth during stress. *Molecules*, *17*(9), 10754–10773. <https://doi.org/10.3390/molecules170910754>
- Warwick, S. I. (2011). Genetics and genomics of the Brassicaceae. In *Genetics and Genomics of the Brassicaceae*. <https://doi.org/10.1007/978-1-4419-7118-0>

- Westphal, K. R., Heidelbach, S., Zeuner, E. J., Riisgaard-Jensen, M., Nielsen, M. E., Vestergaard, S. Z., Søndergaard, T. E. (2021). The effects of different potato dextrose agar media on secondary metabolite production in *Fusarium*. *International Journal of Food Microbiology*, 347, 109171. <https://doi.org/10.1016/j.ijfoodmicro.2021.109171>
- White, T. J., Bruns, T. D., Lee, S. B., & Taylor, J. W. (1990). Amplification and direct sequencing of fungal ribosomal RNA genes for phylogenetics. In M. A. Innis, D. H. Gelfand, J. J. Sninsky, & T. J. White (Eds.), *PCR protocols: A guide to methods and applications* (pp. 315–322). Academic Press.
- Wilson, D. (1995). Endophyte: The evolution of a term, and clarification of its use and definition. *Oikos*, 73(2), 274–276. <https://doi.org/10.2307/3545919>
- Woo, S. L., Ruocco, M., Vinale, F., Nigro, M., Marra, R., Lombardi, N., Pascale, A., Lanzuise, S., & Manganiello, G. (2014). Trichoderma-based products and their widespread use in agriculture. *The Open Mycology Journal*, 8, 71–126. <https://doi.org/10.2174/1874437001408010071>
- Wu, Q., Patocka, J., Nepovimova, E., & Kuca, K. (2018). A review on the synthesis and bioactivity aspects of beauvericin, a *Fusarium* mycotoxin. *Frontiers in Pharmacology*, 9, 1338. <https://doi.org/10.3389/fphar.2018.01338>
- Axencia Galega da Calidade Alimentaria (AGACAL). (2023). *Publications*. Retrieved November 2, 2024, Xunta de Galicia. <https://agacal.xunta.gal/es/publicaciones>
- Yan, L., Zhu, J., Zhao, X., Shi, J., Jiang, C., & Shao, D. (2019). Beneficial effects of endophytic fungi colonization on plants. *Applied Microbiology and Biotechnology*, 103(8), 3327–3340. <https://doi.org/10.1007/s00253-019-09713-2>
- Zaid, R., Koren, R., Kligun, E., Gupta, R., Leibman-Markus, M., Mukherjee, P. K., ... & Horwitz, B. A. (2022). Gliotoxin, an immunosuppressive fungal metabolite, primes plant immunity: evidence from *Trichoderma virens*-tomato interaction. *MBio*, 13(4), e00389-22. <https://doi.org/10.1128/mbio.00389-22>
- Zhang, H., Zhu, J., Gong, Z., & Zhu, J.-K. (2022). Abiotic stress responses in plants. *Nature Reviews Genetics*, 23(2), 104–119. <https://doi.org/10.1038/s41576-021-00413-0>
- Zhang, Q., Zhang, J., Yang, L., et al. (2014). Diversity and biocontrol potential of endophytic fungi in *Brassica napus*. *Biological Control*, 72, 98–108. <https://doi.org/10.1016/j.biocontrol.2014.02.018>
- Zhou, Y., Zheng, Y., Li, P., Xu, L., & Fu, Q. (2024). Ectomycorrhizal fungi and dark septate endophyte inoculation improve growth and tolerance of *Pinus tabulaeformis* under cadmium stress. *Pedosphere*, 34(2), 473–483. <https://doi.org/10.1016/j.pedsph.2023.09.003>





USC  
UNIVERSITY OF SOUTHERN CALIFORNIA  
LIBRARY



# APPENDIX

---

**Supplementary Table 1:** Climate variables and soil characteristics at sampling points. The soil section includes pH, organic matter content (%), and texture class. The climate section includes annual averages for temperature (MAT, °C) and precipitation (MAP, mm). Data retrieved from the RGIS portal (<http://rgis.cesga.es/>).

Samplig spot	Location	Coordinates	pH	Organic matter (%)	Texture (soil taxonomy)	MAT (°C)	MAP (mm)
<b>1B</b>	Silleda (Pontevedra)	42°43'19.2"N 8°14'32.4"W	5.20	9.00	Loam	12.67	1286.47
<b>2B</b>	Villalva (Lugo)	43°18'23.3"N 7°43'51.1"W	5.11	11.70	Loam	11.50	1230.08
<b>3B</b>	Anxeriz (A Coruña)	43°05'55.8"N 8°46'01.3"W	5.63	14.20	Loam	11.86	1508.98
<b>4B</b>	Oroso (A Coruña)	43°01'09.0"N 8°26'28.9"W	5.18	10.30	Loam	12.47	1298.88
<b>5B</b>	Villalva (Lugo)	43°18'23.3"N 7°43'51.1"W	5.11	11.70	Loam	11.50	1230.08
<b>6B</b>	O Rosal (Pontevedra)	41°55'05.4"N 8°49'36.2"W	5.33	11.00	Sandy Loam	14.56	1328.61
<b>1P</b>	Padrón (A Coruña)	42°43'39.0"N 8°39'43.5"W	5.29	12.40	Sandy Loam	14.49	1449.40
<b>2P</b>	Padrón (A Coruña)	42°43'31.7"N 8°37'35.5"W	4.96	14.10	Sandy Loam	14.27	1502.60
<b>3P</b>	Padrón (A Coruña)	42°45'03.6"N 8°36'34.1"W	4.97	13.00	Sandy Loam	14.24	1506.62
<b>4P</b>	Padrón (A Coruña)	42°45'09.1"N 8°39'16.2"W	5.34	11.80	Sandy Loam	14.44	1458.93

**Supplementary Table 2:** Table showing the GenBank accession codes of the fungal isolates, the internal code assigned in this thesis (isolate), and the name given to each isolate (organism). The table also includes the closest match obtained using the BLAST tool, the query cover (QC, %), percentage identity (PI, %), and the phylogenetic classification at the phylum, order, family, and genus levels.

GenBank Code	Isolate	Organism	Closest_match	Qc	PI	Phylum	Order	Family	Genus
PV892087	BrT1.01	<i>Gibellulopsis</i>	<i>Gibellulopsis simonii</i>	100	97.86	Ascomycota	Glomerellales	Plectosphaerellaceae	<i>Gibellulopsis</i>
PV892088	BrT1.02	<i>Fusarium</i>	<i>Fusarium foetens</i>	91	98.94	Ascomycota	Hypocreales	Nectriaceae	<i>Fusarium</i>
PV892089	BrT3.02	Mucorales	<i>Absidia edaphica</i>	75	83.26	Mucoromycota	Mucorales	Cunninghamellaceae	<i>Absidia</i>
PV892090	BrT3.03	<i>Humicola</i>	<i>Humicola fuscogrisea</i>	100	99.37	Ascomycota	Sordariales	Chaetomiaceae	<i>Humicola</i>
PV892091	BrT3.04	<i>Pseudeurotium</i>	<i>Pseudeurotium bakeri</i>	97	99.35	Ascomycota	-	Pseudeurotiaceae	<i>Pseudeurotium</i>
PV892092	BrT4.01	<i>Talaromyces</i>	<i>Talaromyces wortmannii</i>	100	99.03	Ascomycota	Eurotiales	Trichocomaceae	<i>Talaromyces</i>
PV892093	BrT4.02	<i>Metarhizium</i>	<i>Metarhizium robertsii</i>	100	100.00	Ascomycota	Hypocreales	Clavicipitaceae	<i>Metarhizium</i>
PV892094	BrT4.03	<i>Ceriporiopsis</i>	<i>Ceriporiopsis kunmingensis</i>	98	90.70	Basidiomycota	Polyporales	Meruliaceae	<i>Ceriporiopsis</i>
PV892095	BrT6.01	<i>Pseudeurotium</i>	<i>Pseudeurotium bakeri</i>	96	99.78	Ascomycota	<i>Pseudeurotium</i>	Pseudeurotiaceae	<i>Pseudeurotium</i>
PV892096	BrT7.01	<i>Cladosporium</i>	<i>Cladosporium subuliforme</i>	100	99.58	Ascomycota	Cladosporiales	Cladosporiaceae	<i>Cladosporium</i>
PV892097	BrT13.01	<i>Chaetomium</i>	<i>Chaetomium graminiforme</i>	100	100.00	Ascomycota	Sordariales	Chaetomiaceae	<i>Chaetomium</i>
PV892098	BrT14.01	<i>Fusarium</i>	<i>Fusarium foetens</i>	95	99.77	Ascomycota	Hypocreales	Nectriaceae	<i>Fusarium</i>
PV892099	BrT15.02	Chaetomiaceae	<i>Chaetomium/Dichotomopilus funicola</i>	99	92.94	Ascomycota	Sordariales	Chaetomiaceae	<i>Dichotomopilus</i>

<b>PV892100</b>	BrT15.03	<i>Sarocladium</i>	<i>Sarocladium kiliense</i>	95	98.35	Ascomycota	Hypocreales	Sarocladiaceae	<i>Sarocladium</i>
<b>PV892101</b>	BrT15.04	Chaetomiaceae	<i>Trichocladium arxii/Dichotomopilus funicola</i>	100	99.79	Ascomycota	Sordariales	Chaetomiaceae	-
<b>PV892102</b>	BrT16.02	Chaetomiaceae	<i>Dichotomopilus indi</i>	98	99.79	Ascomycota	Sordariales	Chaetomiaceae	<i>Dichotomopilus</i>
<b>PV892103</b>	BrT17.01	Chaetomiaceae	<i>Trichocladium arxii/Dichotomopilus funicola</i>	100	99.55	Ascomycota	Sordariales	Chaetomiaceae	<i>Trichocladium</i>
<b>PV892104</b>	BrT18.02	Chaetomiaceae	<i>Trichocladium arxii/Dichotomopilus funicola</i>	100	100.00	Ascomycota	Sordariales	Chaetomiaceae	-
<b>PV892105</b>	BrT18.03	<i>Humicola</i>	<i>Humicola fuscogrisea</i>	100	99.33	Ascomycota	Sordariales	Chaetomiaceae	<i>Humicola</i>
<b>PV892106</b>	BrT18.05	<i>Metarhizium</i>	<i>Metarhizium robertsii</i>	100	99.75	Ascomycota	Hypocreales	Clavicipitaceae	<i>Metarhizium</i>
<b>PV892107</b>	BrT23.03	<i>Chaetomium</i>	<i>Chaetomium afropilosum</i>	100	99.77	Ascomycota	Sordariales	Chaetomiaceae	<i>Chaetomium</i>
<b>PV892108</b>	BrT23.05	<i>Chaetomium</i>	<i>Chaetomium afropilosum</i>	99	99.74	Ascomycota	Sordariales	Chaetomiaceae	<i>Chaetomium</i>
<b>PV892109</b>	BrT24.03	Cunninghamellaceae	<i>Absidia cuneospora</i>	100	97.18	Mucoromycota	Mucorales	Cunninghamellaceae	<i>Absidia</i>
<b>PV892110</b>	BrT25.01	Coniochaetales	<i>Coniochaeta gigantospora</i>	91	93.88	Ascomycota	Coniochaetales	Coniochaetaceae	<i>Coniochaeta</i>
<b>PV892111</b>	BrT25.02	<i>Penicillium</i>	<i>Penicillium onobense</i>	99	99.80	Ascomycota	Eurotiales	Aspergillaceae	<i>Penicillium</i>
<b>PV892112</b>	BrT25.04	Chaetomiaceae	<i>Chaetomidium/Trichocladium arxii</i>	94	99.01	Ascomycota	Sordariales	Chaetomiaceae	<i>Trichocladium</i>
<b>PV892113</b>	BrT31.01	<i>Apiotrichum</i>	<i>Apiotrichum dulciturum</i>	99	98.95	Basidiomycota	Trichosporonales	Trichosporonaceae	<i>Apiotrichum</i>

<b>PV892114</b>	BrT35.01	<i>Mucor</i>	<i>Mucor moelleri</i>	97	98.30	Mucoromycota	Mucorales	Mucoraceae	<i>Mucor</i>
<b>PV892115</b>	BrT36.01	<i>Fusarium</i>	<i>Fusarium foetens</i>	100	100.00	Ascomycota	Hypocreales	Nectriaceae	<i>Fusarium</i>
<b>PV892116</b>	BrT38.01	<i>Penicillium</i>	<i>Penicillium soli</i>	100	100.00	Ascomycota	Eurotiales	Aspergillaceae	<i>Penicillium</i>
<b>PV892117</b>	BrT40.01	Cunninghamellaceae	<i>Absidia cuneospora</i>	100	97.29	Mucoromycota	Mucorales	Cunninghamellaceae	<i>Absidia</i>
<b>PV892118</b>	BrT41.03	<i>Penicillium</i>	<i>Penicillium soli</i>	96	100.00	Ascomycota	Eurotiales	Aspergillaceae	<i>Penicillium</i>
<b>PV892119</b>	BrT43.01	<i>Ilyonectria</i>	<i>Ilyonectria liliigena</i>	100	99.36	Ascomycota	Hypocreales	Nectriaceae	<i>Ilyonectria</i>
<b>PV892120</b>	BrT43.02	<i>Ilyonectria</i>	<i>Ilyonectria liliigena</i>	96	99.33	Ascomycota	Hypocreales	Nectriaceae	<i>Ilyonectria</i>
<b>PV892121</b>	BrT43.03	<i>Penicillium</i>	<i>Penicillium soli</i>	100	100.00	Ascomycota	Eurotiales	Aspergillaceae	<i>Penicillium</i>
<b>PV892122</b>	BrT45.01	<i>Trichoderma</i>	<i>Trichoderma gamsii</i>	99	100.00	Ascomycota	Hypocreales	Hypocreaceae	<i>Trichoderma</i>
<b>PV892123</b>	BrT46.07	<i>Umbelopsis</i>	<i>Umbelopsis vinacea</i>	100	99.06	Mucoromycota	Umbelopsidales	Umbelopsidaceae	<i>Umbelopsis</i>
<b>PV892124</b>	BrT47.01	<i>Apiotrichum</i>	<i>Apiotrichum akiyoshidainum</i>	100	100.00	Basidiomycota	Trichosporonales	Trichosporonaceae	<i>Apiotrichum</i>
<b>PV892125</b>	BrT49.02	<i>Aaosphaeria</i>	<i>Aaosphaeria arxii</i>	96	98.50	Ascomycota	Pleosporales	Pleosporales incertae sedis	<i>Aaosphaeria</i>
<b>PV892126</b>	BrT49.04	<i>Penicillium</i>	<i>Penicillium pancosmium</i>	100	99.22	Ascomycota	Eurotiales	Aspergillaceae	<i>Penicillium</i>
<b>PV892127</b>	BrT49.05	<i>Penicillium</i>	<i>Penicillium pancosmium</i>	100	99.55	Ascomycota	Eurotiales	Aspergillaceae	<i>Penicillium</i>
<b>PV892128</b>	BrT51.01	Pleosporales	<i>Pyrenophora nisikadoi</i>	97	93.25	Ascomycota	Pleosporales	Pleosporaceae	<i>Pyrenophora</i>
<b>PV892129</b>	BrT51.03	Helotiales	<i>Mollisia asteliae</i>	96	96.73	Ascomycota	Helotiales	Mollisiaceae	<i>Mollisia</i>
<b>PV892130</b>	BrT51.05	<i>Leptodophora</i>	<i>Leptodophora echinata</i>	100	100.00	Ascomycota	Helotiales	Helotiales incertae sedis	<i>Leptodophora</i>
<b>PV892131</b>	BrT51.06	<i>Neopyrenochaeta</i>	<i>Neopyrenochaeta acicola</i>	99	94.90	Ascomycota	Pleosporales	Neopyrenochaetaceae	<i>Neopyrenochaeta</i>

<b>PV892132</b>	BrT53.01	<i>Trichoderma</i>	<i>Trichoderma hamatum</i>	100	100.00	Ascomycota	Hypocreales	Hypocreaceae	<i>Trichoderma</i>
<b>PV892133</b>	BrT53.03	<i>Penicillium</i>	<i>Penicillium pancosmium</i>	100	99.43	Ascomycota	Eurotiales	Aspergillaceae	<i>Penicillium</i>
<b>PV892134</b>	BrT53.06	<i>Aaosphaeria</i>	<i>Aaosphaeria arxii</i>	100	99.96	Ascomycota	Pleosporales	Pleosporales incertae sedis	<i>Aaosphaeria</i>
<b>PV892135</b>	BrT53.07	<i>Plectosphaerella</i>	<i>Plectosphaerella niemeijerorum</i>	99	98.55	Ascomycota	Glomerellales	Plectosphaerellaceae	<i>Plectosphaerella</i>
<b>PV892136</b>	BrT54.01	<i>Chaetomium</i>	<i>Chaetomium afropilosum</i>	100	100.00	Ascomycota	Sordariales	Chaetomiaceae	<i>Chaetomium</i>
<b>PV892137</b>	BrT54.02	<i>Fusarium</i>	<i>Fusarium foetens</i>	100	100.00	Ascomycota	Hypocreales	Nectriaceae	<i>Fusarium</i>
<b>PV892138</b>	BrT55.02	<i>Leptodophora</i>	<i>Leptodophora echinata</i>	99	95.29	Ascomycota	Helotiales	Helotiales incertae sedis	<i>Leptodophora</i>
<b>PV892139</b>	BrT55.04	<i>Leptodophora</i>	<i>Leptodophora echinata</i>	100	100.00	Ascomycota	Helotiales	Helotiales incertae sedis	<i>Leptodophora</i>
<b>PV892140</b>	BrT55.06	<i>Leptodophora</i>	<i>Leptodophora orchidicola</i>	100	99.61	Ascomycota	Helotiales	Helotiales incertae sedis	<i>Leptodophora</i>
<b>PV892141</b>	BrT55.08	<i>Penicillium</i>	<i>Penicillium soli</i>	98	99.79	Ascomycota	Eurotiales	Aspergillaceae	<i>Penicillium</i>
<b>PV892142</b>	BrT55.09	<i>Leptodophora</i>	<i>Leptodophora orchidicola</i>	100	100.00	Ascomycota	Helotiales	Helotiales incertae sedis	<i>Leptodophora</i>
<b>PV892143</b>	BrT56.02	<i>Chaetomium</i>	<i>Chaetomium pseudocochliodes</i>	100	99.77	Ascomycota	Sordariales	Chaetomiaceae	<i>Chaetomium</i>
<b>PV892144</b>	BrT56.04	<i>Chaetomium</i>	<i>Chaetomium sacchari</i>	100	100.00	Ascomycota	Sordariales	Chaetomiaceae	<i>Chaetomium</i>
<b>PV892145</b>	BrT56.05	<i>Leptodophora</i>	<i>Leptodophora orchidicola</i>	97	99.81	Ascomycota	Helotiales	Helotiales incertae sedis	<i>Leptodophora</i>

<b>PV892146</b>	BrT56.06	<i>Chaetomium</i>	<i>Chaetomium graminiforme</i>	100	99.97	Ascomycota	Sordariales	Chaetomiaceae	<i>Chaetomium</i>
<b>PV892147</b>	BrT56.07	<i>Penicillium</i>	<i>Penicillium infrabuccalum</i>	98	94.05	Ascomycota	Eurotiales	Aspergillaceae	<i>Penicillium</i>
<b>PV892148</b>	BrT57.02	<i>Fusarium</i>	<i>Fusarium foetens</i>	97	100.00	Ascomycota	Hypocreales	Nectriaceae	<i>Fusarium</i>
<b>PV892149</b>	BrT58.01	<i>Penicillium</i>	<i>Penicillium soli</i>	100	99.40	Ascomycota	Eurotiales	Aspergillaceae	<i>Penicillium</i>
<b>PV892150</b>	BrT60.06	<i>Aspergillus</i>	<i>Aspergillus insuetus</i>	100	100.00	Ascomycota	Eurotiales	Aspergillaceae	<i>Aspergillus</i>
<b>PV892151</b>	BrT63.02	<i>Fusarium</i>	<i>Fusarium foetens</i>	99	99.79	Ascomycota	Hypocreales	Nectriaceae	<i>Fusarium</i>
<b>PV892152</b>	BrT66.01	<i>Apiotrichum</i>	<i>Apiotrichum xylopi</i>	100	99.74	Basidiomycota	Trichosporonales	Trichosporonaceae	<i>Apiotrichum</i>
<b>PV892153</b>	BrT67.03	<i>Penicillium</i>	<i>Penicillium camponotum</i>	92	96.82	Ascomycota	Eurotiales	Aspergillaceae	<i>Penicillium</i>
<b>PV892154</b>	BrT69.05	<i>Fusarium</i>	<i>Fusarium foetens</i>	100	100.00	Ascomycota	Hypocreales	Nectriaceae	<i>Fusarium</i>
<b>PV892155</b>	BrT69.06	<i>Penicillium</i>	<i>Penicillium soli</i>	100	100.00	Ascomycota	Eurotiales	Aspergillaceae	<i>Penicillium</i>
<b>PV892156</b>	P1.03	<i>Fusarium</i>	<i>Fusarium foetens</i>	100	99.57	Ascomycota	Hypocreales	Nectriaceae	<i>Fusarium</i>
<b>PV892157</b>	P1.10	<i>Acrocalymma</i>	<i>Acrocalymma ampeli</i>	97	95.73	Ascomycota	Pleosporales	Morosphaeriaceae	<i>Acrocalymma</i>
<b>PV892158</b>	P1.18	<i>Acrocalymma</i>	<i>Acrocalymma ampeli</i>	99	96.02	Ascomycota	Pleosporales	Morosphaeriaceae	<i>Acrocalymma</i>
<b>PV892159</b>	P2.04	<i>Chaetomium</i>	<i>Chaetomium contagiosum</i>	99	93.87	Ascomycota	Sordariales	Chaetomiaceae	<i>Chaetomium</i>
<b>PV892160</b>	P2.09	<i>Fusarium</i>	<i>Fusarium martii</i>	100	100.00	Ascomycota	Hypocreales	Nectriaceae	<i>Fusarium</i>
<b>PV892161</b>	P2.18	<i>Pochonia</i>	<i>Pochonia chlamydosporia</i>	100	98.28	Ascomycota	Hypocreales	Clavicipitaceae	<i>Pochonia</i>
<b>PV892162</b>	P2.23	<i>Fusarium</i>	<i>Fusarium pseudocircinatum</i>	95	98.29	Ascomycota	Hypocreales	Nectriaceae	<i>Fusarium</i>

<b>PV892163</b>	P2.25	<i>Pochonia</i>	<i>Pochonia chlamydosporia</i>	99	97.66	Ascomycota	Hypocreales	Clavicipitaceae	<i>Pochonia</i>
<b>PV892164</b>	P3.01	<i>Fusarium</i>	<i>Fusarium croci</i>	100	99.57	Ascomycota	Hypocreales	Nectriaceae	<i>Fusarium</i>
<b>PV892165</b>	P3.02	<i>Fusarium</i>	<i>Fusarium foetens</i>	99	99.97	Ascomycota	Hypocreales	Nectriaceae	<i>Fusarium</i>
<b>PV892166</b>	P3.03	<i>Fusarium</i>	<i>Fusarium foetens</i>	96	99.77	Ascomycota	Hypocreales	Nectriaceae	<i>Fusarium</i>
<b>PV892167</b>	P3.06	<i>Fusarium</i>	<i>Fusarium pseudocircinatum</i>	98	98.58	Ascomycota	Hypocreales	Nectriaceae	<i>Fusarium</i>
<b>PV892168</b>	P4.01	<i>Fusarium</i>	<i>Fusarium pseudocircinatum</i>	99	99.77	Ascomycota	Hypocreales	Nectriaceae	<i>Fusarium</i>
<b>PV892169</b>	P4.13	<i>Fusarium</i>	<i>Fusarium foetens</i>	96	99.77	Ascomycota	Hypocreales	Nectriaceae	<i>Fusarium</i>
<b>PV892170</b>	P6.24	<i>Aspergillus</i>	<i>Aspergillus westerdijkiae</i>	100	99.60	Ascomycota	Eurotiales	Aspergillaceae	<i>Aspergillus</i>
<b>PV892171</b>	P6.28	<i>Acrocalymma</i>	<i>Acrocalymma ampeli</i>	97	96.04	Ascomycota	Pleosporales	Morosphaeriaceae	<i>Acrocalymma</i>
<b>PV892172</b>	P7.15	<i>Penicillium</i>	<i>Penicillium roseopurpureum</i>	100	95.91	Ascomycota	Eurotiales	Aspergillaceae	<i>Penicillium</i>
<b>PV892173</b>	P8.01	<i>Fusarium</i>	<i>Fusarium foetens</i>	93	99.57	Ascomycota	Hypocreales	Nectriaceae	<i>Fusarium</i>
<b>PV892174</b>	P8.02	<i>Chaetomium</i>	<i>Chaetomium interruptum</i>	99	92.47	Ascomycota	Sordariales	Chaetomiaceae	<i>Chaetomium</i>
<b>PV892175</b>	P8.09	<i>Corynascus</i>	<i>Corynascus novoguineensis</i>	100	99.56	Ascomycota	Sordariales	Chaetomiaceae	<i>Corynascus</i>
<b>PV892176</b>	P8.10	Chaetomiaceae	<i>Corynascus novoguineensis</i>	99	85.08	Ascomycota	Sordariales	Chaetomiaceae	<i>Corynascus</i>
<b>PV892177</b>	P8.17	<i>Fusarium</i>	<i>Fusarium noneumartii</i>	100	99.80	Ascomycota	Hypocreales	Nectriaceae	<i>Fusarium</i>
<b>PV892178</b>	P8.20	<i>Talaromyces</i>	<i>Talaromyces brevis</i>	99	100.00	Ascomycota	Eurotiales	Trichocomaceae	<i>Talaromyces</i>

<b>PV892179</b>	P8.22	<i>Talaromyces</i>	<i>Talaromyces brevis</i>	100	99.79	Ascomycota	Eurotiales	Trichocomaceae	<i>Talaromyces</i>
<b>PV892180</b>	P8.23	<i>Scedosporium</i>	<i>Scedosporium apiospermum</i>	100	100.00	Ascomycota	Microascales	Microascaceae	<i>Scedosporium</i>
<b>PV892181</b>	P8.25	<i>Fusarium</i>	<i>Fusarium noneumartii</i>	100	99.79	Ascomycota	Hypocreales	Nectriaceae	<i>Fusarium</i>
<b>PV892182</b>	P9.10	<i>Fusarium</i>	<i>Fusarium foetens</i>	100	99.55	Ascomycota	Hypocreales	Nectriaceae	<i>Fusarium</i>
<b>PV892183</b>	P9.12	<i>Fusarium</i>	<i>Fusarium foetens</i>	95	99.55	Ascomycota	Hypocreales	Nectriaceae	<i>Fusarium</i>
<b>PV892184</b>	P10.05	<i>Fusarium</i>	<i>Fusarium foetens</i>	96	98.77	Ascomycota	Hypocreales	Nectriaceae	<i>Fusarium</i>
<b>PV892185</b>	P11.03	<i>Fusarium</i>	<i>Fusarium martii</i>	100	100.00	Ascomycota	Hypocreales	Nectriaceae	<i>Fusarium</i>
<b>PV892186</b>	P11.07	<i>Chaetomium</i>	<i>Chaetomium spiculipilium</i>	100	99.79	Ascomycota	Sordariales	Chaetomiaceae	<i>Chaetomium</i>
<b>PV892187</b>	P11.11	<i>Fusarium</i>	<i>Fusarium croci</i>	100	99.80	Ascomycota	Hypocreales	Nectriaceae	<i>Fusarium</i>
<b>PV892188</b>	P11.17	<i>Fusarium</i>	<i>Fusarium foetens</i>	99	99.77	Ascomycota	Hypocreales	Nectriaceae	<i>Fusarium</i>
<b>PV892189</b>	P11.22	<i>Corynascus</i>	<i>Corynascus novoguineensis</i>	100	99.57	Ascomycota	Sordariales	Chaetomiaceae	<i>Corynascus</i>
<b>PV892190</b>	P12.1	<i>Pseudopyrenochaeta</i>	<i>Pseudopyrenochaeta terrestris</i>	100	100.00	Ascomycota	Pleosporales	Pseudo-pyrenochaetaceae	<i>Pseudo-pyrenochaeta</i>
<b>PV892191</b>	P13.13	<i>Penicillium</i>	<i>Penicillium roseopurpureum</i>	99	97.71	Ascomycota	Eurotiales	Aspergillaceae	<i>Penicillium</i>
<b>PV892192</b>	P13.26	<i>Penicillium</i>	<i>Penicillium subrubescens</i>	100	96.77	Ascomycota	Eurotiales	Aspergillaceae	<i>Penicillium</i>
<b>PV892193</b>	P13.27	<i>Pseudopyrenochaeta</i>	<i>Pseudopyrenochaeta terrestris</i>	100	100.00	Ascomycota	Pleosporales	Pseudo-pyrenochaetaceae	<i>Pseudo-pyrenochaeta</i>
<b>PV892194</b>	P13.29	<i>Fusarium</i>	<i>Fusarium noneumartii</i>	100	100.00	Ascomycota	Hypocreales	Nectriaceae	<i>Fusarium</i>
<b>PV892195</b>	P14.01	<i>Fusarium</i>	<i>Fusarium foetens</i>	92	98.98	Ascomycota	Hypocreales	Nectriaceae	<i>Fusarium</i>

<b>PV892196</b>	P14.05	Nectriaceae	<i>Theλονectria blackeriella</i>	95	96.27	Ascomycota	Hypocreales	Nectriaceae	<i>Theλονectria</i>
<b>PV892197</b>	P14.15	<i>Pochonia</i>	<i>Pochonia chlamydosporia</i>	100	98.29	Ascomycota	Hypocreales	Clavicipitaceae	<i>Pochonia</i>
<b>PV892198</b>	P14.26	<i>Fusarium</i>	<i>Fusarium tonkinense</i>	100	100.00	Ascomycota	Hypocreales	Nectriaceae	<i>Fusarium</i>
<b>PV892199</b>	P14.27	<i>Pseudopyrenochaeta</i>	<i>Pseudopyrenochaeta terrestris</i>	100	99.58	Ascomycota	Pleosporales	Pseudo-pyrenochaetaceae	<i>Pseudo-pyrenochaeta</i>
<b>PV892200</b>	P15.16	<i>Pseudopyrenochaeta</i>	<i>Pseudopyrenochaeta terrestris</i>	<u>100</u>	99.80	Ascomycota	Pleosporales	Pseudo-pyrenochaetaceae	<i>Pseudo-pyrenochaeta</i>
<b>PV892201</b>	P16.19	<i>Pseudopyrenochaeta</i>	<i>Pseudopyrenochaeta terrestris</i>	100	100.00	Ascomycota	Pleosporales	Pseudo-pyrenochaetaceae	<i>Pseudo-pyrenochaeta</i>
<b>PV892202</b>	P16.27	<i>Pseudopyrenochaeta</i>	<i>Pseudopyrenochaeta terrestris</i>	100	99.56	Ascomycota	Pleosporales	Pseudo-pyrenochaetaceae	<i>Pseudo-pyrenochaeta</i>
<b>PV892203</b>	P17.01	<i>Phytophthora</i>	<i>Phytophthora nicotianae</i>	100	94.66	Oomycota	Peronosporales	Peronosporaceae	<i>Phytophthora</i>
<b>PV892204</b>	P18.04	<i>Phomopsis</i>	<i>Phomopsis tuberivora</i>	100	99.08	Ascomycota	Diaporthales	Valsaceae	<i>Phomopsis</i>
<b>PV892205</b>	P19.25	<i>Fusarium</i>	<i>Fusarium foetens</i>	100	99.54	Ascomycota	Hypocreales	Nectriaceae	<i>Fusarium</i>
<b>PV892206</b>	P20.04	<i>Trichoderma</i>	<i>Trichoderma hamatum</i>	99	100.00	Ascomycota	Hypocreales	Hypocreaceae	<i>Trichoderma</i>
<b>PV892207</b>	P20.08	<i>Pseudopyrenochaeta terrestris</i>	<i>Pseudopyrenochaeta terrestris</i>	100	100.00	Ascomycota	Pleosporales	Pseudo-pyrenochaetaceae	<i>Pseudo-pyrenochaeta</i>
<b>PV892208</b>	P20.11	<i>Trichoderma</i>	<i>Trichoderma hamatum</i>	100	98.54	Ascomycota	Hypocreales	Hypocreaceae	<i>Trichoderma</i>
<b>PV892209</b>	P20.21	<i>Pseudopyrenochaeta</i>	<i>Pseudopyrenochaeta terrestris</i>	100	99.41	Ascomycota	Pleosporales	Pseudo-pyrenochaetaceae	<i>Pseudo-pyrenochaeta</i>
<b>PV892210</b>	P20.23	<i>Aspergillus</i>	<i>Aspergillus elongatus</i>	100	99.75	Ascomycota	Eurotiales	Aspergillaceae	<i>Aspergillus</i>

<b>PV892211</b>	P21.04	<i>Colletotrichum</i>	<i>Colletotrichum nigrum</i>	100	99.80	Ascomycota	Glomerellales	Glomerellaceae	<i>Colletotrichum</i>
<b>PV892212</b>	P21.05	<i>Thelonectria</i>	<i>Thelonectria blackeriella</i>	95	96.67	Ascomycota	Hypocreales	Nectriaceae	<i>Thelonectria</i>
<b>PV892213</b>	P21.11	<i>Pochonia</i>	<i>Pochonia chlamydosporia</i>	100	98.36	Ascomycota	Hypocreales	Clavicipitaceae	<i>Pochonia</i>
<b>PV892214</b>	P22.03	<i>Fusarium</i>	<i>Fusarium foetens</i>	96	100.00	Ascomycota	Hypocreales	Nectriaceae	<i>Fusarium</i>
<b>PV892215</b>	P22.05	<i>Fusarium</i>	<i>Fusarium foetens</i>	98	99.78	Ascomycota	Hypocreales	Nectriaceae	<i>Fusarium</i>
<b>PV892216</b>	P22.09	<i>Pseudopyrenochaeta terrestris</i>	<i>Pseudopyrenochaeta terrestris</i>	100	99.80	Ascomycota	Pleosporales	Pseudo-pyrenochaetaceae	<i>Pseudo-pyrenochaeta</i>
<b>PV892217</b>	P23.03	<i>Pseudopyrenochaeta terrestris</i>	<i>Pseudopyrenochaeta terrestris</i>	100	99.60	Ascomycota	Pleosporales	Pseudo-pyrenochaetaceae	<i>Pseudo-pyrenochaeta</i>
<b>PV892218</b>	P23.06	<i>Pseudopyrenochaeta</i>	<i>Pseudopyrenochaeta lycopersici</i>	100	98.62	Ascomycota	Pleosporales	Pseudo-pyrenochaetaceae	<i>Pseudo-pyrenochaeta</i>
<b>PV892219</b>	P23.10	<i>Pseudopyrenochaeta terrestris</i>	<i>Pseudopyrenochaeta terrestris</i>	100	100.00	Ascomycota	Pleosporales	Pseudo-pyrenochaetaceae	<i>Pseudo-pyrenochaeta</i>
<b>PV892220</b>	P23.19	<i>Pseudopyrenochaeta</i>	<i>Pseudopyrenochaeta terrestris</i>	100	100.00	Ascomycota	Pleosporales	Pseudo-pyrenochaetaceae	<i>Pseudo-pyrenochaeta</i>
<b>PV892221</b>	P23.22	<i>Pseudopyrenochaeta</i>	<i>Pseudopyrenochaeta lycopersici</i>	100	98.38	Ascomycota	Pleosporales	Pseudo-pyrenochaetaceae	<i>Pseudo-pyrenochaeta</i>
<b>PV892222</b>	P24.01	<i>Ceratobasidium</i>	<i>Ceratobasidium praxillae</i>	98	97.35	Ascomycota	Cantharellales	Ceratobasidiaceae	<i>Ceratobasidium</i>
<b>PV892223</b>	P24.02	<i>Pseudopyrenochaeta</i>	<i>Pseudopyrenochaeta terrestris</i>	98	99.03	Ascomycota	Pleosporales	Pseudo-pyrenochaetaceae	<i>Pseudo-pyrenochaeta</i>
<b>PV892224</b>	P24.06	<i>Fusarium</i>	<i>Fusarium foetens</i>	96	98.75	Ascomycota	Hypocreales	Nectriaceae	<i>Fusarium</i>

<b>PV892225</b>	P24.07	<i>Penicillium</i>	<i>Penicillium subrubescens</i>	100	99.40	Ascomycota	Eurotiales	Aspergillaceae	<i>Penicillium</i>
<b>PV892226</b>	P24.08	<i>Pseudopyrenochaeta terrestris</i>	<i>Pseudopyrenochaeta terrestris</i>	100	99.80	Ascomycota	Pleosporales	Pseudo-pyrenochaetaceae	<i>Pseudo-pyrenochaeta</i>
<b>PV892227</b>	P24.11	<i>Fusarium</i>	<i>Fusarium foetens</i>	100	100.00	Ascomycota	Hypocreales	Nectriaceae	<i>Fusarium</i>
<b>PV892228</b>	P24.12	<i>Pseudopyrenochaeta</i>	<i>Pseudopyrenochaeta terrestris</i>	99	100.00	Ascomycota	Pleosporales	Pseudo-pyrenochaetaceae	<i>Pseudo-pyrenochaeta</i>
<b>PV892229</b>	P24.16	<i>Chaetomium</i>	<i>Chaetomium concavisporum</i>	100	99.79	Ascomycota	Sordariales	Chaetomiaceae	<i>Chaetomium</i>
<b>PV892230</b>	P24.22	<i>Verticillium</i>	<i>Verticillium longisporum</i>	99	99.78	Ascomycota	Glomerellales	Plectosphaerellaceae	<i>Verticillium</i>
<b>PV892231</b>	P25.03	<i>Penicillium</i>	<i>Penicillium roseopurpureum</i>	98	99.18	Ascomycota	Eurotiales	Aspergillaceae	<i>Penicillium</i>
<b>PV892232</b>	P25.07	<i>Fusarium</i>	<i>Fusarium foetens</i>	99	100.00	Ascomycota	Hypocreales	Nectriaceae	<i>Fusarium</i>
<b>PV892233</b>	P25.14	<i>Pochonia</i>	<i>Pochonia chlamydosporia</i>	100	98.02	Ascomycota	Hypocreales	Clavicipitaceae	<i>Pochonia</i>
<b>PV892234</b>	P25.16	<i>Pseudopyrenochaeta</i>	<i>Pseudopyrenochaeta lycopersici</i>	100	99.10	Ascomycota	Pleosporales	Pseudo-pyrenochaetaceae	<i>Pseudo-pyrenochaeta</i>
<b>PV892235</b>	P25.22	<i>Penicillium</i>	<i>Penicillium subrubescens</i>	98	99.98	Ascomycota	Eurotiales	Aspergillaceae	<i>Penicillium</i>
<b>PV892236</b>	P26.01	<i>Pseudopyrenochaeta</i>	<i>Pseudopyrenochaeta terrestris</i>	97	99.61	Ascomycota	Pleosporales	Pseudo-pyrenochaetaceae	<i>Pseudo-pyrenochaeta</i>
<b>PV892237</b>	P26.12	<i>Pseudopyrenochaeta</i>	<i>Pseudopyrenochaeta terrestris</i>	99	99.58	Ascomycota	Pleosporales	Pseudo-pyrenochaetaceae	<i>Pseudo-pyrenochaeta</i>

<b>PV892238</b>	P26.14	<i>Pseudopyrenochaeta</i>	<i>Pseudopyrenochaeta terrestris</i>	100	100.00	Ascomycota	Pleosporales	Pseudo-pyrenochaetaceae	<i>Pseudo-pyrenochaeta</i>
<b>PV892239</b>	P26.20	<i>Talaromyces</i>	<i>Talaromyces brevis</i>	100	99.60	Ascomycota	Eurotiales	Trichocomaceae	<i>Talaromyces</i>
<b>PV892240</b>	P26.21	Pochonia	<i>Pochonia chlamydosporia</i>	100	98.24	Ascomycota	Hypocreales	Clavicipitaceae	<i>Pochonia</i>
<b>PV892241</b>	P27.06	<i>Pseudopyrenochaeta lycopersici</i>	<i>Pseudopyrenochaeta lycopersici</i>	100	98.39	Ascomycota	Pleosporales	Pseudo-pyrenochaetaceae	<i>Pseudo-pyrenochaeta</i>
<b>PV892242</b>	P27.10	Pleosporales	<i>Edenia gomezpompae</i>	97	93.79	Ascomycota	Pleosporales	Pleosporaceae	-
<b>PV892243</b>	P27.14	<i>Edenia</i>	<i>Edenia gomezpompae</i>	99	94.57	Ascomycota	Pleosporales	Pleosporaceae	<i>Edenia</i>
<b>PV892244</b>	P27.22	<i>Pseudopyrenochaeta</i>	<i>Pseudopyrenochaeta lycopersici</i>	100	99.22	Ascomycota	Pleosporales	Pseudo-pyrenochaetaceae	<i>Pseudo-pyrenochaeta</i>
<b>PV892245</b>	P27.24	<i>Pseudopyrenochaeta lycopersici</i>	<i>Pseudopyrenochaeta lycopersici</i>	100	99.10	Ascomycota	Pleosporales	Pseudo-pyrenochaetaceae	<i>Pseudo-pyrenochaeta</i>
<b>PV892246</b>	P27.25	<i>Pseudopyrenochaeta</i>	<i>Pseudopyrenochaeta terrestris</i>	95	99.80	Ascomycota	Pleosporales	Pseudo-pyrenochaetaceae	<i>Pseudo-pyrenochaeta</i>
<b>PV892247</b>	P27.28	<i>Pseudopyrenochaeta</i>	<i>Pseudopyrenochaeta terrestris</i>	100	100.00	Ascomycota	Pleosporales	Pseudo-pyrenochaetaceae	<i>Pseudo-pyrenochaeta</i>
<b>PV892248</b>	P28.03	<i>Fusarium</i>	<i>Fusarium phyllophilum</i>	100	99.53	Ascomycota	Hypocreales	Nectriaceae	<i>Fusarium</i>
<b>PV892249</b>	P28.16	<i>Chaetomium</i>	<i>Chaetomium graminiforme</i>	100	100.00	Ascomycota	Sordariales	Chaetomiaceae	<i>Chaetomium</i>
<b>PV892250</b>	P28.17	<i>Edenia</i>	<i>Edenia gomezpompae</i>	97	94.90	Ascomycota	Pleosporales	Pleosporaceae	<i>Edenia</i>
<b>PV892251</b>	P29.07	Pochonia	<i>Pochonia chlamydosporia</i>	100	98.08	Ascomycota	Hypocreales	Clavicipitaceae	<i>Pochonia</i>
<b>PV892252</b>	P29.09	<i>Edenia</i>	<i>Edenia gomezpompae</i>	98	93.32	Ascomycota	Pleosporales	Pleosporaceae	<i>Edenia</i>

<b>PV892253</b>	P29.11	<i>Colletotrichum</i>	<i>Colletotrichum nigrum</i>	100	99.61	Ascomycota	Glomerellales	Glomerellaceae	<i>Colletotrichum</i>
<b>PV892254</b>	P30.02	<i>Pseudo-pyrenochaeta</i>	<i>Pseudopyrenochaeta terrestris</i>	99	100.00	Ascomycota	Pleosporales	Pseudo-pyrenochaetaceae	<i>Pseudo-pyrenochaeta</i>
<b>PV892255</b>	P30.04	<i>Edenia</i>	<i>Edenia gomezpompae</i>	98	93.05	Ascomycota	Pleosporales	Pleosporaceae	<i>Edenia</i>
<b>PV892256</b>	P30.05	<i>Edenia</i>	<i>Edenia gomezpompae</i>	98	93.32	Ascomycota	Pleosporales	Pleosporaceae	<i>Edenia</i>
<b>PV892257</b>	P30.14	<i>Edenia</i>	<i>Edenia gomezpompae</i>	99	93.32	Ascomycota	Pleosporales	Pleosporaceae	<i>Edenia</i>
<b>PV892258</b>	P30.17	<i>Cladosporium</i>	<i>Cladosporium puris</i>	100	99.79	Ascomycota	Cladosporiales	Cladosporiaceae	<i>Cladosporium</i>
<b>PV892259</b>	P31.09	<i>Pochonia</i>	<i>Pochonia chlamydosporia</i>	100	97.98	Ascomycota	Hypocreales	Clavicipitaceae	<i>Pochonia</i>
<b>PV892260</b>	P31.10	<i>Colletotrichum</i>	<i>Colletotrichum nigrum</i>	100	99.80	Ascomycota	Glomerellales	Glomerellaceae	<i>Colletotrichum</i>
<b>PV892261</b>	P31.14	<i>Chaetomium</i>	<i>Chaetomium novozelandicum</i>	98	99.59	Ascomycota	Sordariales	Chaetomiaceae	<i>Chaetomium</i>

**Supplementary Table 3:** table showing the percentage of pathogen inhibition during *in vitro* co-cultivation with endophytes, as well as the inhibition halo (cm) generated with the corresponding standard deviations.

Endophyte	Pathogen	Inhibition %	Standard deviation	Halo width	Standard deviation
<b>BrT45.01</b>	<i>R. solani</i>	73.41	2.45	0.00	0.00
	<i>S. sclerotiorum</i>	83.50	3.51	0.00	0.00
	<i>F. oxysporum</i>	85.27	4.72	0.00	0.00
	<i>B. cinerea</i>	77.32	2.82	0.00	0.00
	Alternaria	85.72	6.95	0.00	0.00
<b>BrT41.01</b>	<i>R. solani</i>	47.90	7.39	0.40	0.16
	<i>S. sclerotiorum</i>	31.64	3.75	0.00	0.00
	<i>F. oxysporum</i>	39.16	8.85	0.35	0.35
	<i>B. cinerea</i>	79.12	4.69	0.00	0.00
	Alternaria	55.33	2.71	0.00	0.00
<b>BrT28.01</b>	<i>R. solani</i>	64.32	20.32	0.00	0.00
	<i>S. sclerotiorum</i>	54.79	16.13	0.00	0.00
	<i>F. oxysporum</i>	78.43	9.43	0.00	0.00
	<i>B. cinerea</i>	33.07	4.63	0.28	0.26
	Alternaria	41.40	29.11	0.22	0.10
<b>BrT24.02</b>	<i>R. solani</i>	59.57	14.38	0.18	0.30
	<i>S. sclerotiorum</i>	26.22	4.29	0.00	0.00
	<i>F. oxysporum</i>	50.79	4.34	0.35	0.26
	<i>B. cinerea</i>	66.33	11.17	0.00	0.00
	Alternaria	42.01	18.51	0.00	0.00
<b>BrT4.01</b>	<i>R. solani</i>	40.66	6.60	0.25	0.11
	<i>S. sclerotiorum</i>	22.43	1.86	0.00	0.00
	<i>F. oxysporum</i>	37.86	6.94	0.76	0.08
	<i>B. cinerea</i>	53.08	2.21	0.62	0.27
	Alternaria	26.73	24.57	1.55	0.09
<b>P20.11</b>	<i>R. solani</i>	65.29	1.41	0.00	0.00
	<i>S. sclerotiorum</i>	89.96	0.78	0.00	0.00
	<i>F. solani</i>	85.07	3.16	0.00	0.00
	<i>B. cinerea</i>	78.54	2.54	0.00	0.00
	<i>C. acutatum</i>	92.38	1.13	0.00	0.00
	<i>P. capsici</i>	87.98	0.98	0.00	0.00
<b>P23.03</b>	<i>R. solani</i>	36.87	5.70	1.31	0.20
	<i>S. sclerotiorum</i>	57.97	5.02	1.64	0.22
	<i>F. solani</i>	56.22	3.21	0.00	0.00

	<i>B. cinerea</i>	45.43	5.23	1.04	0.15
	<i>C. acutatum</i>	56.96	4.69	1.57	0.08
	<i>P. capsici</i>	43.59	4.89	1.02	0.19
<b>P11.07</b>	<i>R. solani</i>	44.52	4.51	0.00	0.00
	<i>S. sclerotiorum</i>	63.38	2.17	0.76	0.16
	<i>F. solani</i>	58.25	0.74	0.00	0.00
	<i>B. cinerea</i>	44.39	5.88	0.83	0.28
	<i>C. acutatum</i>	67.23	1.09	0.70	0.35
	<i>P. capsici</i>	42.01	15.30	0.61	0.12
<b>P13.26</b>	<i>R. solani</i>	59.98	14.80	0.00	0.00
	<i>S. sclerotiorum</i>	63.72	10.16	0.00	0.00
	<i>F. solani</i>	70.44	7.58	0.00	0.00
	<i>B. cinerea</i>	55.87	4.00	0.00	0.00
	<i>C. acutatum</i>	73.88	8.15	0.00	0.00
	<i>P. capsici</i>	73.16	8.11	0.00	0.00
<b>P8.20</b>	<i>R. solani</i>	44.57	11.38	0.55	0.03
	<i>S. sclerotiorum</i>	42.50	7.02	0.00	0.00
	<i>F. solani</i>	60.64	4.35	0.67	0.04
	<i>B. cinerea</i>	49.72	4.39	0.00	0.00
	<i>C. acutatum</i>	59.00	1.86	0.69	0.60
	<i>P. capsici</i>	49.02	8.78	0.00	0.00
<b>P6.24</b>	<i>R. solani</i>	51.47	8.02	0.22	0.09
	<i>S. sclerotiorum</i>	35.88	10.56	0.00	0.00
	<i>F. solani</i>	60.84	8.20	0.00	0.00
	<i>B. cinerea</i>	32.08	6.08	0.28	0.11
	<i>C. acutatum</i>	58.23	5.31	0.75	0.27
	<i>P. capsici</i>	51.10	11.02	0.00	0.00

This thesis investigates culturable endophytic fungi in the roots of *Brassica rapa* and *Capsicum annuum*, two emblematic Galician crops certified under European quality schemes. The study characterized fungal diversity and evaluated its potential to enhance plant health through biocontrol and drought tolerance assays. Fungi from the genus *Pseudopyrenochaeta* exhibited strain specific and culture dependent antifungal activity, while other fungal isolates improved water retention capacity and plant biomass under water-stress conditions. Overall, the findings underscore the endophytic diversity of Galician crops as a promising resource for developing microbial inoculants that strengthen plant resilience, sustain productivity, and help preserve Galicia's agrifood heritage.